(975)

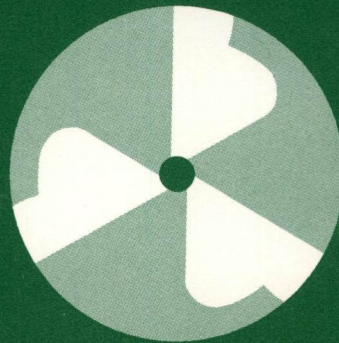# Annual Report

## 1971-72

# Cyclotron Laboratory

# Michigan State University

## DISCLAIMER

This report was prepared as an account of work sponsored by an agency of the United States Government. Neither the United States Government nor any agency Thereof, nor any of their employees, makes any warranty, express or implied, or assumes any legal liability or responsibility for the accuracy, completeness, or usefulness of any information, apparatus, product, or process disclosed, or represents that its use would not infringe privately owned rights. Reference herein to any specific commercial product, process, or service by trade name, trademark, manufacturer, or otherwise does not necessarily constitute or imply its endorsement, recommendation, or favoring by the United States Government or any agency thereof. The views and opinions of authors expressed herein do not necessarily state or reflect those of the United States Government or any agency thereof.

# DISCLAIMER

**Portions of this document may be illegible in electronic image products. Images are produced from the best available original document.**

ANNUAL REPORT

of the

MICHIGAN STATE UNIVERSITY

CYCLOTRON LABORATORY*

for the period

July 1, 1971 to July 1, 1972

By

Project Staff

November 1972

East Lansing, Michigan

# Preface

As initiated last year, this Annual Report is a combined report submitted to all of the funding agencies supporting programs at the MSU Cyclotron Laboratory. The National Science Foundation was responsible for construction of the Laboratory and supplies the major grant that supports the experimental nuclear physics program. The other research programs, in making use of the NSF-supplied facilities, are by this fact also supported substantially by the NSF. These other agencies and contracts include the following: (a) the Atomic Energy Commission supports the nuclear chemistry group, (b) theoretical nuclear physics was shifted from AEC to NSF support midway through the year and is now supported under a separate NSF grant, and (c) the Office of Naval Research has provided funds for neutron research. The specific grants or contracts and their relative contributions to the financial support of the Laboratory are listed in Table I. In Table II we list the faculty, research associates, and graduate students in the Laboratory together with the grants or contracts to which they are attached.

The primary motivation for a combined annual report comes from the close collaboration of the various groups. Indeed, the interplay between and among these groups, be they physics or chemistry, experimental or theoretical, is in our view one of the real strong points of the Laboratory; complex problems can be attacked from many sides and the understanding and progress which results is almost always greatly enhanced by the collaboration.

In our annual report this year, we continue with the brief writeups on Current Research in Progress, which we initiated in last year's Annual Report. These writeups, although often incomplete, give an up-to-date presentation of latest scientific information. We also include abstracts of papers delivered at meetings and of papers submitted to journals but not yet in print. Regretfully, it is necessary this year to discontinue our past practice of including reprints of papers published during the year. (This would have led to an Annual Report of more than 650 pages.) As a partial measure we include the first page of each journal article, which gives at least part of the introduction and indicates the reference. Readers interested in the full article can then refer to the appropriate journal or contact the authors for reprints. We would appreciate comments from readers as to the usefulness of this new arrangement. Finally I will repeat the annual reminder that we welcome colloborators from other laboratories—if you have an experiment for which our facilities would be particularly appropriate please let us know.

Henry Blosser

slb

Table I.   Sources of support for the MSU Cyclotron Laboratory for the fiscal year 1971-72

| Institution or Agency | | Per Cent of Total |
|---|---|---|
| National Science Foundation | Grant GP 27483 (experimental nuclear physics) | 60.0 |
| Atomic Energy Commission | Contract AT(11-1)-1779 (nuclear chemistry) | 8.8 |
| National Science Foundation | Grant GP 31265X (theoretical nuclear physics) | 3.2 |
| Atomic Energy Commission | Contract AT(11-1)-1051 (theoretical nuclear physics) | 2.6 |
| Office of Naval Research | Contract N00014-68-A-0109-0008 | 3.4 |
| Michigan State University | | 22.0 |

Table II. List of faculty, research associates, and graduate students working at the MSU Cyclotron Laboratory during 1971-72 and principal sources of support.

| Professors | supported by | present address |
|---|---|---|
| Sam M. Austin | NSF-exp, MSU | |
| Henry G. Blosser | NSF-exp, MSU | |
| Aaron I. Galonsky | NSF-exp, ONR, MSU | |
| Morton M. Gordon | NSF-exp, NASA, MSU | (on sabbatical leave to CERN, Geneva, 1971-72) |
| Edwin Kashy | NSF-exp, MSU | |
| Wm. H. Kelly | NSF-exp, MSU | |
| Wm. C. McHarris | AEC-chem, MSU | (on sabbatical leave to Lawrence Berkeley Lab., 1971-72) |
| Hugh McManus | NSF-theor, AEC-theor, MSU | |
| B.H. Wildenthal | NSF-exp, MSU | |

| Associate Professors | | |
|---|---|---|
| Walter Benenson | NSF-exp, MSU | |
| George F. Bertsch | NSF-theor, MSU | |
| Jerzy R. Borysowicz | NSF-theor, AEC-theor, MSU | |
| Gerard M. Crawley | NSF-exp, MSU | |
| Sven Maripuu | NSF-exp, MSU | (visiting Associate Professor, 1972) |
| Jerry A. Nolen, Jr. | NSF-exp, MSU | |

| Assistant Professors | | |
|---|---|---|
| Thelma Arnette | NSF-exp, MSU | |
| Fred M. Bernthal | AEC-chem, MSU | |
| Ray Warner | AEC-chem, MSU | (research assistant professor) |

| Research Associates | supported by | present address |
|---|---|---|
| John S. Boyno | NSF-exp, AEC-chem | |
| Maria Dworzecka | AEC-theor | University of Mass. |
| Ronald W. Goles | AEC-chem, MSU | Battelle Northwest Lab. |
| Paul S. Hauge | NSF-theor | |
| Roger A. Hinrichs | NSF-exp | SUNY, Oswego |
| Teng Lek Khoo | NSF-exp, AEC-chem | |
| Wm.A. Lanford | NSF-exp | |
| Peter S. Miller | NSF-exp | |
| Donald Patterson | ONR | |
| Fred Petrovich | NSF-theor | Lawrence Berkeley Lab. |
| R.G.H. Robertson | NSF-exp | |
| Richard R. Todd | NAS-NIRA | Western Michigan Univ. |

| Graduate Students | supported by | present address |
|---|---|---|
| Thomas Amos | NSF-exp, ONR | |
| Jerry N. Black | AEC-chem, NSF-exp | Mound Laboratories |
| Paul Brinza | NSF-exp | |
| Wm.B. Chaffee | MSU, NSF-exp | |
| Wilton Chung | NSF-exp | |
| John C. Collins | NSF-exp, ONR | |
| Robert R. Doering | NSF-exp | |
| Carol L. Dors | AEC-chem, NSF-exp | |
| Steven C. Ewald | NSF-exp, ONR | |
| Richard B. Firestone | AEC-chem, NSF-exp | |
| Stanley H. Fox | NSF-exp | Children's Hospital Cincinnati |
| Greg. C. Giesler | AEC-chem, NSF-exp | Los Alamos Scientific Laboratories |
| Jean Guile | NSF-exp | |
| Greg Hamilton | NSF-exp | |
| G. Richard Hammerstein | AEC-theor, NSF-theor | |
| Robert Howard (Computer Sci.) | AEC-chem | |
| Richard Howell | NSF-exp, ONR | Lawrence Livermore Laboratories |
| Kenneth L. Kosanke | AEC-chem, NSF-exp | |
| Duane C. Larson | NSF-exp | Oak Ridge Natl. Lab. |
| Nancy Larson | NSF-theor | Oak Ridge Natl. Lab. |
| Clare B. Morgan | NSF-exp | |
| Leroy B.C. Moy | NSF-exp | |
| Lolo M. Pannggabean | NSF-exp | |
| David Perry | NSF-theor, AEC-theor | |
| Ivan D. Proctor | NSF-exp | Lawrence Livermore Laboratory |
| James A. Rice | NSF-exp | |
| Lawrence Samuelson | NSF-exp | Nuclear Information Reserach Associate, MSU |
| David L. Show | NSF-exp | |
| Wm.F. Steele | NSF-exp | |
| Richard Trilling | AEC-theor | University of Abidjan Ivory Coast |
| Wm. Wagner | NSF-exp | |
| Herman White | NSF-exp | |

CONTENTS

I. Research in Progress

## II.   Abstracts of Talks at Meetings
(July 1971-June 1972)

### Tuscon APS Meeting - November 1971

### San Francisco APS Meeting - January 1972

### South Carolina APS Meeting - March 1972

### Washington APS Meeting - April 1972

Section I

RESEARCH IN PROGRESS

# Structure of the A=6-14 Nuclei Calculated with an Effective Interaction

Paul S. Hauge and S. Maripuu

Numerous properties of the normal parity states for all 0p shell nuclei are being calculated with the shell model computer codes of French, Halbert, McGrory and Wong.[1] The Hamiltonian is diagonalized in the full 0p basis, and the effective two-body interaction used in the calculation is computed directly from the relative Sussex matrix elements.[2] Corrections to the two-body matrix elements (2BME's) involving intermediate states up to 2$\hbar\omega$ in excitation energy are computed to second order in the perturbation theory. As seen in Table I, the second order corrections change the 2BME's significantly and are definitely needed, if one is to obtain satisfactory agreement between experiment and theory. The effective 2BME's shown in the last column are found to be similar to those determined from the least squares fittings of Cohen and Kurath[3] and of Goldhammer and coworkers.[4]

The only two parameters that one could possibly consider in the present calculation are the harmonic oscillator size parameter (b), and the energy separation between the $p_{3/2}$ and $p_{1/2}$ single particle states ($\epsilon$). Recent experimental data has shown (somewhat surprisingly) that all 0p shell nuclei have approximately the same rms radius.[5] We therefore choose to fix b at a value of 1.7 fm for all nuclei, and not vary this parameter. On the other hand, the average potential well depth should increase considerably as one proceeds from mass A=6 to A=14, and this should affect the energy separation of the single particle orbits. Consequently, we allow $\epsilon$ to vary from mass number to mass number.

A comparison of calculated with experimental energy spectra is very encouraging, and much better than one might expect for a one-parameter theory. Two minor, but noticable discrepancies between the theoretical and experimental spectra were the following:

1. We calculate the three lowest states in $^8$Be around 2.0 MeV too high. Also, two low-lying states in $^{12}$C (at 7.66 and 10.1 MeV) are observed much lower than theoretically predicted.

2. The lowest $J^\pi T=0^+1$ states in masses A=6, 10, and 14 are predicted about 2.0 MeV too low.

The first discrepancy is not serious, since the five experimental states involved have high reduced $\alpha$ decay widths, and are known to be collective states of highly deformed $\alpha$-structures.[6] In order to accurately describe these states in the shell model, we would need a larger configuration basis for constructing the Hamiltonian. The second discrepancy is a common problem that arises in many calculations with realistic 2BME's.[7] It could presumably be rectified by

(1) introducing an attractive monopole shift into the effective diagonal T=0 2BME's, or (2) including higher order corrections into the perturbation calculation.

Table II shows the values of $\epsilon$ that yield the best agreement with the experimental levels for each mass number considered. The number shown for mass A=5 is an experimental number.[8]
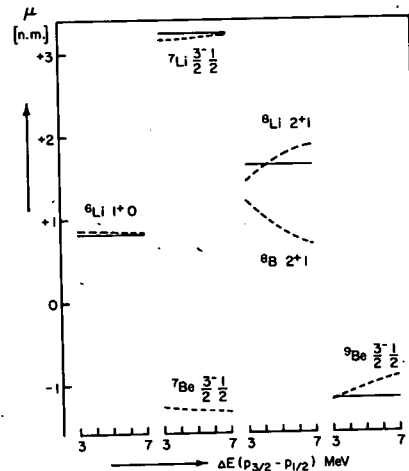


Fig. 1 Magnetic moments for $6 \leq A \leq 9$. Solid lines denote experimental numbers, and the dashed lines show how the theoretical moments vary with $\epsilon$.
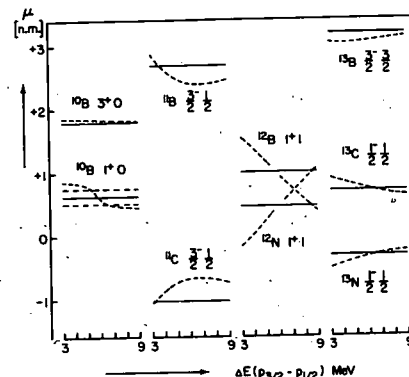


Fig. 2 Magnetic moments for $10 \leq A \leq 13$.

Using the eigenvectors found from the energy-level fitting, we computed magnetic dipole moments, M1 transition strengths, $\beta$-decay matrix elements, and single nucleon spectroscopic factors. Most results are in good agreement with experiment. Typical results are shown in Figs. 1 and 2, where we show how the magnetic moments vary with increasing $\epsilon$. In a few nuclei, it was found that some observables agreed with the experimental numbers at slightly different values of $\epsilon$. An example of such a variance is shown in Fig. 3 for the mass A=13 nuclei. Most observables are predicted best at $\epsilon$=6.8 MeV, but the $\beta$-decay rates favor a value of $\epsilon \approx 5.0$ MeV
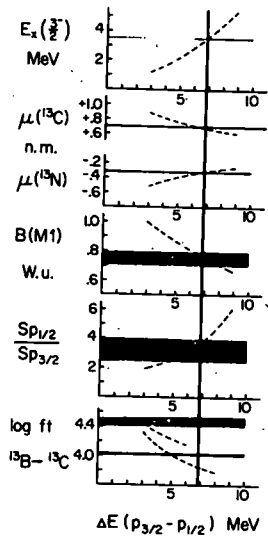
Fig. 3 Various observables for the mass A=13 nuclei. Horizontal solid lines denote measured quantities, their width implying experimental uncertainty. Dashed lines show how theoretical values vary with ε.

We find it encouraging, indeed, that our calculation, essentially without parameters and derived from first principles, does just as well as those works[3,4] which deduce the effective 2BME's from a least-squares fitting and which have upwards of thirteen free parameters.

References

1. J.B. French, E.C. Halbert, J.B. McGrory, and S.S.M. Wong, in Advances in Nuclear Physics, Vol. 3, edited by M. Baranger and E. Vogt (plenum Press, New York, 1969), pp. 193-257.

2. J.P. Elliott, A.D. Jackson, H.A. Mavromatis, E.A. Sanderson, and B. Singh, Nucl. Phys. A121, 241(1968).

3. S. Cohen and D. Kurath, Nucl. Phys. 73, 1(1965).

4. P. Goldhammer, J.R. Hill, and J. Nachamkin, Nucl. Phys. A106, 62(1968); J.L. Norton and P. Goldhammer, Nucl. Phys. A165, 33(1971).

5. D.H. Wilkinson and M.E. Mafethe, Nucl. Phys. 85, 97(1966).

6. T. Kanellopoulos and K. Wildermuth, Nucl. Phys. 14, 349(1960); H. Morinaga, Phys. Letters 21, 78(1966).

7. M. Dworzecka and H. McManus, BAPS 17, 554(1972).

8. P. Fessenden and D.R. Maxson, Phys. Rev. 133, B71(1964).

TABLE I

The 2BME's, in the form $<ab;JT|V|cd;JT>$, are shown for the 0p shell along with their most important perturbative corrections. The quantum numbers abcd represent $2J_a$, $2J_b$, $2J_c$, and $2J_d$ respectively. All matrix elements are expressed in MeV's.

| Quantum Numbers a b c d - J T | Second-Order Corrections | | | | |
|---|---|---|---|---|---|
| | $<V>$ | $<V_{3p-1h}>$ | $<V_{4p-2h}>$ | $<V_{2p}>$ | $<V_{eff}>$ |
| 3 3 3 3 - 1 0 | -1.541 | -0.055 | -0.112 | -0.838 | -2.546 |
| - 3 0 | -4.060 | -0.158 | – | -0.764 | -4.982 |
| - 0 1 | -3.020 | -0.276 | -0.303 | -0.414 | -4.013 |
| - 2 1 | -1.453 | +0.315 | – | -0.170 | -1.308 |
| 3 3 3 1 - 1 0 | +3.528 | +0.059 | +0.316 | +0.562 | +4.465 |
| - 2 1 | -1.539 | -0.276 | – | -0.127 | -1.942 |
| 3 3 1 1 - 1 0 | +1.676 | +0.026 | -0.138 | +0.437 | +2.001 |
| - 0 1 | -3.606 | -0.643 | -0.214 | -0.176 | -4.639 |
| 3 1 3 1 - 1 0 | -4.770 | +0.196 | -0.888 | -0.923 | -6.385 |
| - 2 0 | -5.350 | +0.156 | – | -1.255 | -6.449 |
| - 1 1 | -0.728 | +0.544 | – | -0.051 | -0.235 |
| - 2 1 | -2.542 | +0.522 | – | -0.261 | -2.281 |
| 3 1 1 1 - 1 0 | +0.942 | +0.256 | +0.389 | -0.174 | +1.413 |
| 1 1 1 1 - 1 0 | -1.843 | +0.065 | -0.170 | -0.722 | -2.670 |
| - 0 1 | -0.470 | +0.264 | -0.152 | -0.289 | -0.647 |

TABLE II

Values of the Separation Energy, ε, which yield Optimum Agreement with the Experimental Energy Levels for each Mass Number in the Region $5 \leq A \leq 14$.

| A | 5 | 6 | 7 | 8 | 9 | 10 | 11 | 12 | 13 | 14 |
|---|---|---|---|---|---|---|---|---|---|---|
| ε(MeV) | $2.6^+_-0.4$ | 3.0 | 3.0 | 4.8 | 4.0 | 7.0 | 7.0 | 7.0 | 6.5 | 7.0 |

# Proton Capture by $^7$Be, and the Solar Neutrino Problem

R.G.H. Robertson

The recent experiments of Davis[1] have set an upper limit of 1.0 SNU on the neutrino flux from the sun (1 SNU=$10^{-36}$ captures per target atom per sec.), in sharp disagreement with the theoretical prediction of 9 SNU, calculated by Bahcall and Ulrich.[2] The rare termination of the p-p chain $^7$Be(p,$\gamma$)$^8$B(e$^+\nu$)2$\alpha$ results in energetic neutrinos and is calculated to contribute 7.3 SNU. It is therefore important to have an accurate estimate of the rate of this reaction in the solar interior. Very detailed measurements of the cross-section for $^7$Be(p,$\gamma$)$^8$B have been carried out by Kavanagh et al.[3,4] at laboratory energies $E_p$=0.165 to 10.0 MeV. A theoretical extrapolation to lower energies based on a calculation by Tombrello[5] yielded a zero-energy cross-section factor[6] S(0) of 0.034 keV-b, where, if $\sigma$ is the cross section and $E_p$ the lab proton energy in MeV,

$$S(E_p)=0.87441\sigma E_p \exp(3.9734\ E_p^{-1/2})$$

for the $^7$Be(p,$\gamma$)$^8$B reaction. A calculation by Aurdal[7] similar to that of Tombrello gave S(0)= 0.044 keV-b, but the new data of Kavanagh et al. were not used in that extrapolation. The value S(0)=0.030 keV-b actually adopted by Bahcall and Ulrich[2] is lower than either of these, and is presumably the result of an empirical extrapolation.

Proton capture by $^7$Be involves the radiative transition of a proton in a continuum state to the $2^+$ ground state of $^8$B, bound by 137.2 keV. Only dipole radiation is of importance at the energies considered here. Because the spin and parity of $^7$Be are $\frac{3}{2}^-$, capture from the s and d partial waves leads to El radiation, and from the p wave, M1. Higher partial waves cannot contribute to dipole

radiation. The calculations of Tombrello[5] and Aurdal[7] assumed that only s wave capture was significant. Re-examination of the $^7$Be(p,$\gamma$)$^8$B reaction shows that while this is approximately true in the solar environment ($E_p \gtrsim 20$ keV), it is not the case at laboratory energies, even as low as 150 keV. The small binding energy of $^8$B results in a spatially extended wave function, enhancing capture from the p and d partial waves.

Detailed calculation (Fig. 1), in which particular attention was paid to the choice of s wave potential and to the influence of nearby p wave resonances, has yielded a revised cross-section factor at $E_p$=0.02 MeV of

$$S(.02)=.031 \text{ keV-b}.$$

This value is lower than the previous theoretical results,[5,7] and very close to the empirical value actually used by Bahcall and Ulrich.[2] Thus there is no appreciable change in the predicted $^8$B neutrino flux from the sun.

## References

1. R. Davis, Jr., BAPS 17, 527(1972).

2. J.N. Bahcall and R.K. Ulrich, Astrophys. J. 170, 593(1971).

3. R.W. Kavanagh, T.A. Tombrello, J.M. Mosher, and D.R. Goosman, BAPS 14, 209(1969).

4. C.A. Barnes, in "Advances in Nuclear Physics" ed. M. Baranger and E. Vogt (Plenum Press 1971) Vol. 4, p. 133.

5. T.A. Tombrello, Nucl. Phys. 71, 459(1965).

6. W.A. Fowler, G.R. Caughlan, and B.A. Zimmerman, Ann. Rev. Astron. Astrophys. 5, 525(1967).

7. A. Aurdal, Nucl. Phys. A146, 385(1970).
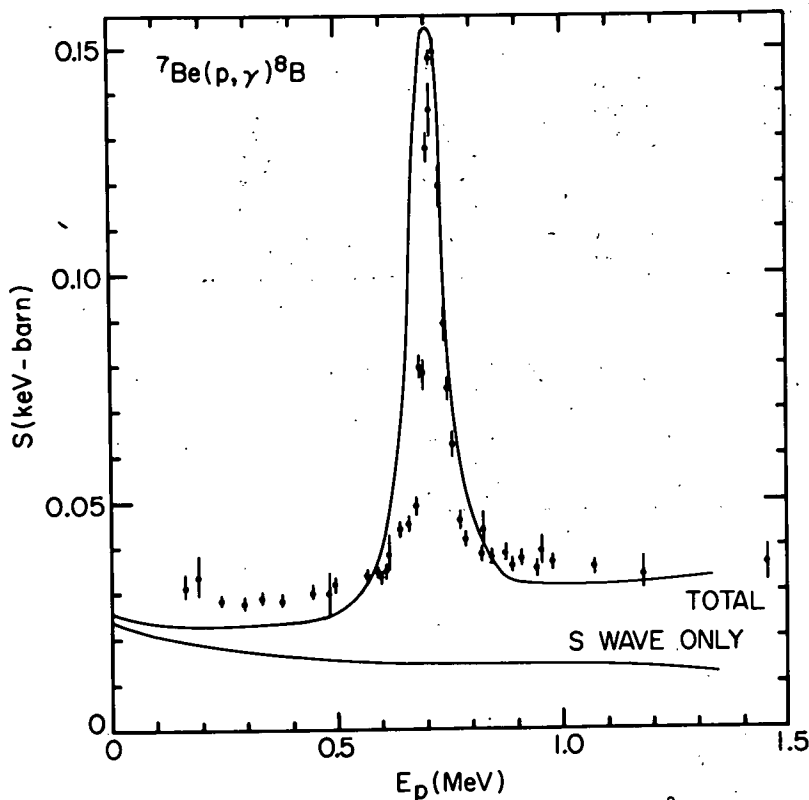
Fig. 1 Comparison between the experimental measurements of the $^7$Be(p,$\gamma$)$^8$B cross-section by Kavanagh et al. and the theoretical calculation (smooth curves). The calculation is shown here in absolute form, without normalization to the data. The abscissa is the lab proton energy. The sharp resonance at 720 keV is M1 capture through an unbound $1^+$ state in $^8$B.

# A Survey of the ($^3$He,$^7$Be) Reaction

W.F. Steele, G.M. Crawley, and S. Maripuu

During the past year, work has continued[1] on the α-pickup reaction, ($^3$He,$^7$Be). To date, the effort has been directed primarily toward developing an effective, reliable position sensitive gas proportional counter system[2] for the focal plane of the laboratory's split-pole broad range magnetic spectrograph. The basic counter employs a gas chamber 25x1x1 cm with an axial nichrome wire 10μ in diameter. Because $^7$Li$^{3+}$ and $^7$Be$^{4+}$ ions have similar differential energy loss for a given momentum, a ΔE signal from the counter provides insufficient information for unambiguous particle identification. Consequently, a plastic scintillator photomultiplier detector is used behind the proportional counter. The scintillator yields both a total energy signal and a signal proportional to the time-of-flight in the spectrometer. Using the ΔE, E, and time-of-flight information, excellent particle identification is routinely achieved.

So far, spectra have been obtained at several angles for $^{12}$C, $^{16}$O, $^{24}$Mg, $^{26}$Mg, $^{40}$Ca, and $^{48}$Ca targets using a 70 MeV incident $^3$He beam. Spectra from the $^{24}$Mg target at 10° and 40° are displayed in Figs. 1 and 2. The doublet structure of each $^{20}$Ne level, which is caused by the 432 keV first excited state of $^7$Be, is clearly resolved. At all angles, the dominant level in $^{20}$Ne is the 5.62 MeV 3$^-$. This result is rather surprising if the reaction goes predominantly by α-pickup. The 10° spectrum shows the 4.97 MeV 2$^-$ to be weakly excited. It is essentially absent at larger angles. The 0$^+$ ground state is somewhat weaker than the 1.63 2$^+$, 4.25 4$^+$, and 5.62 3$^-$. Around 7 MeV, there is a cluster of unresolved states. However, it appears from the preliminary energy calibration, that neither the 6.72 nor 7.17 MeV 0$^+$ states are strongly excited as the peak energy is 7.01 MeV. Higher lying states are not clearly resolved. As the resolution is target thickness limited, further work will be undertaken with a thinner target to resolve more states. In addition the survey will be extended to heavier targets in coming months.

## References

1. G.M. Crawley et al., A Survey of the ($^3$He,$^7$Be) Reaction, Annual Report 1970-71, Cyclotron Laboratory, Dept. of Physics, Michigan State University.

2. W.A. Lanford et al., A Charge Division Position Sensitive Proportional Counter System, Abstract submitted for the Seattle Meeting of the APS, Nov. 2-4, 1972.

FIG. 1 — $^{24}$Mg($^3$He,$^7$Be)$^{20}$Ne, 10°



FIG. 2 — 40°

COUNTS PER CHANNEL vs CHANNEL NUMBER
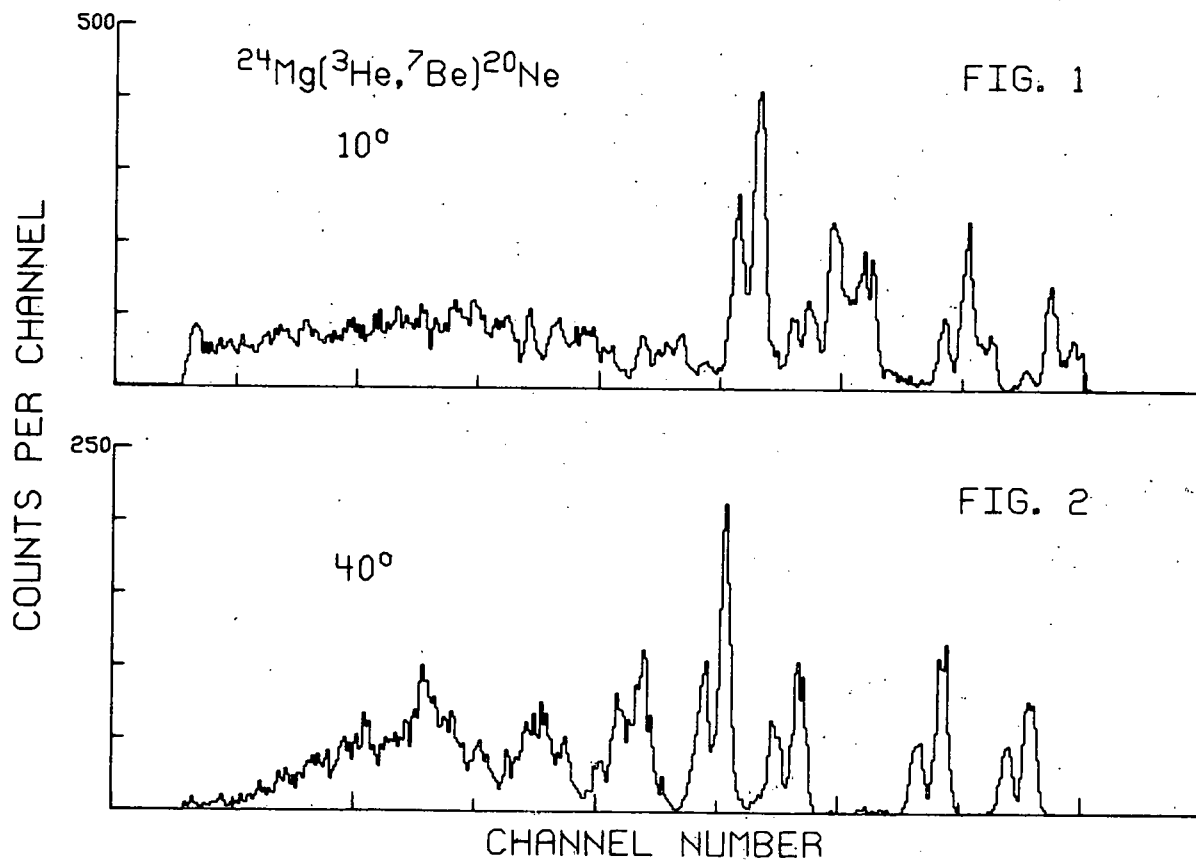
D.L. Show, J.A. Nolen, and B.H. Wildenthal

Angular distributions of direct single nucleon transfer reactions have shapes which depend in definitively characteristic ways upon the orbital angular momentum (ℓ) transferred in the reaction. Lee and Schiffer pointed out several years ago that in many cases the shapes of the angular distributions depend also, in more subtle ways, on the total spin (j) transferred.[1] Such effects were first noted for ℓ=1 transfers in (d,p) reactions, while subsequent studies[2,3] showed that j-dependence could be discerned in different types of reactions and for several ℓ-values. We concern ourselves here with ℓ=2 transfer via the (p,d) reaction in the sd-shell and the differences in shape between j=5/2 and j=3/2 angular distributions. Several investigations[3-6] have noted that for (d,p) and (p,d) reactions characterized by deuteron energies in the range 7-18 MeV, those transitions transferring j=5/2 have "fatter" angular distributions than those transferring j=3/2. That is, the differential cross-sections for j=5/2 transfer do not decrease as the detection angle is moved away from the main ℓ=2 maximum as rapidly as do those for j=3/2 transfer.

We have studied the $^{30}$Si(p,d)$^{29}$Si reaction using a 35 MeV proton beam from the MSU Cyclotron and a wire proportional counter in the focal plane of a split-pole spectrograph. The first five states of $^{29}$Si have energies and $J^{\pi}$ of 0.000 MeV-1/2$^+$, 1.273 MeV-3/2$^+$, 2.032 MeV-5/2$^+$, 2.427 MeV-3/2$^+$, and 3.069 MeV-5/2$^+$. Thus we have deuteron energies about 50% and more larger than those for which j-dependence of the present type has been previously reported. The first two excited states are strongly populated in the (p,d) reaction with ℓ=2 angular distributions. The shapes are compared in Fig. 1. The normalizations of the distributions have been adjusted to make the forward maxima coincide. The curve is calculated for the j=5/2 reaction according to the prescription of Ref. 5.

One can see from Fig. 1 that the distribution for the first 3/2$^+$ state (which must correspond to j=3/2 transfer) falls off markedly faster from the first maximum than the distribution for the first 5/2$^+$ state. This same trend is evident in the distributions for the weakly populated 2.427 MeV and 3.069 MeV states, which ensures that the effect is not merely an effect of different Q-values, but the statistical scatter keeps this higher excitation energy pair from forming an equally conclusive example.

Thus, we observe in the present study j-dependent effects for ℓ=2 transfer which are completely consistent with those outlined by Lee and Schiffer. The qualitative difference between the present shapes of different j-values are smaller than those observed at lower energies, which is also consistent with the extrapolation of the various results obtained at lower energies. The stability of this j-dependent effect and its magnitude seem to be such that reliable s-d shell spectroscopic information can be extracted from reasonably precise (p,d) or (d,p) angular distributions measured at any of a rather wide range of energies.

### References

1. L.L. Lee, Jr. and J.P. Schiffer, Phys. Rev. Letters 12, 108(1964).

2. L.L. Lee, Jr. and J.P. Schiffer, Phys. Rev. 136, B405(1964).

3. J.P. Schiffer, L.L. Lee, Jr., A. Marinov, and C. Mayer-Broicke, Phys. Rev. 147, 829(1966).

4. C.M. Glashausser, Thesis, Princeton Univ.

5. M.C. Mermaz, C.A. Whitten, Jr., J.W. Champlin, A.J. Howard, and D.A. Bromley, Phys. Rev. C4, 1778(1971).

6. B.H. Wildenthal and P.W.M. Glaudemans, Nucl. Phys. A108, 49(1968).

← Fig. 1



$^{30}$Si(p,d)$^{29}$Si

$E_p$ = 35 MeV

□ $E_x$ = 1.273 MeV 3/2$^+$
▲ $E_x$ = 2.032 MeV 5/2$^+$
— DWBA FOR 5/2$^+$

dσ/dΩ (ARBITRARY UNITS)

$\theta_{c.m.}$

W. Benenson, E. Kashy, and I.D. Proctor
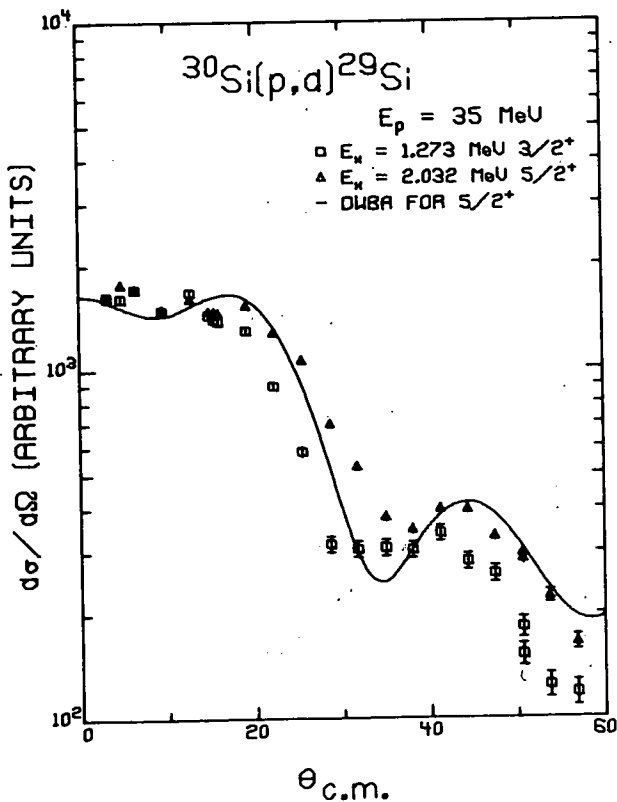
The study of mass multiplets in the sd shell has three distinct facets; a) mass measurements of $T_z=-3/2$ nuclei with the $(^3He,^6He)$ reaction, b) remeasurements with higher precision of the $T=3/2$ levels of $T_z=\pm1/2$ nuclei, c) shell model calculations of the $T_z$ dependence of the masses of the members of multiplet. The results are expressed in terms of the isobaric mass multiplet equation (IMME) which is usually written as,

$$M(T_z) = a + bT_z + cT_z^2.$$

Since there are four members of a $T=3/2$ multiplet, the IMME predicts that d, the coefficient of the cubic term required to fit the masses, will be zero. In terms of the four masses $M(T_z)$ the d-coefficient can be written

$$d = \tfrac{1}{6}[M(3/2)-M(-3/2)+3M(1/2)-3M(-1/2)].$$

The $T_z=\pm3/2$ levels are necessary for a determination of d, but the accuracy of the $T_z=\pm1/2$ masses is three times more important. That is the reason for adding remeasurements of the $T=3/2$ levels in the $T_z=\pm1/2$ nuclei. During the past year the following experiments have been completed.

i) mass of $^{25}Si$[1] and $^{37}Ca$ using $(^3He,^6He)$.

ii) the energies of the $T=3/2$ levels in $^{25}Al$, $^{25}Mg$, $^{37}Ar$, and $^{37}K$, using (p,t) (p,h), and (p,d).

iii) the mass of $^{25}Na$ using (d,$^3He$).

iv) the energy level schemes of $^{25}Si$[1] and $^{21}Mg$ using $(^3He,^6He)$.

v) mass of $^{29}S$ using $(^3He,^6He)$.

All data is taken in the spectrograph. A single-wire resistive-readout proportional counter is the most frequently used detection device. Particle identification is performed by time-of-flight and energy loss information obtained from a plastic scintillator placed behind the wire counter. A position sensitive silicon detector is used frequently also. The method for determining Q-values, mass excesses and excitation energies consists in measuring the magnetic fields required to place the reaction of interest and a calibration reaction at the same position on the focal plane counter. Whenever possible, the calibration reaction is on a nucleus already present in the target. Forward angles (4-10°) are used to minimize kinematic energy shifts.

The $T=3/2$ levels in the A=25 system are given in Table I below. There are now three complete multiplets, and there is an evident state dependence to the coefficients. The state dependence is due to mixing of the $T=3/2$ state in the $T_z=\pm1/2$ nuclei with $T=1/2$ states of the same spin and parity. The shell model calculations give effects of this type, but fail in predicting in detail the $T_z$ dependence.

The A=37 system has changed drastically because of the improvement in accuracy over the previous measurements. This is shown in Table II.

Experiments which are presently in progress include the mass of $^{33}A$ and a study of the $T=3/2$ levels in $T_z=\pm1/2$ nuclei of A=29 and 33. The shell model calculations will be extended to all of the A=4n+1 multiplets in the sd shell.

References

1. W. Benenson, J. Dreisbach, I.D. Proctor, G.F. Trentelman, and B.M. Preedom, Phys. Rev. C5, 1426(1972).

| J | $^{25}Na$ | $^{25}Mg$ | $^{25}Al$ | $^{25}Sc$ | b | c | d |
|---|---|---|---|---|---|---|---|
| $5/2^+$ | 0.0 | * | † | 0.0 | -4405(8) | 221(4) | 4.5(4.2) |
| $3/2^+$ | 90 | 80 | 71(1) | 40(5) | -4395(8) | 216(4) | 7.3(4.3) |
| $1/2^+$ | 1068 | 1009 | 940(15) | 815(15) | -4319(18) | 204(6) | 4.4(9.0) |

*$E_x$=7780(5)      †$E_x$=7904(5)

TABLE I

A=25,T=3/2 Levels

All energies in keV with errors in parenthesis.

| | $^{37}Ar(E_x)$ | $^{37}K(E_x)$ | $^{37}Ca(ME)$ | b | c | d |
|---|---|---|---|---|---|---|
| Present | 4993(6) | 5045(4) | 13144(20) | -6200(8) | 200(5) | -2.4(4.9) |
| Previous* | 5010(30) | 5048(3) | 13230(50) | -6189(30) | 182(30) | 5(17) |

*From J. Cerny, Ann. Rev. of Nuc. Sci., Vol. 18, p. 27.

TABLE II

A=37,T=3/2 Excitation Energies and Mass Excesses

All energies in keV with errors in parenthesis.

# Shell Model Calculation for $^{24}$Ne

R.G.H. Robertson and B.H. Wildenthal

A large basis shell model calculation for the A=24, T=2 system, with particular emphasis on $^{24}$Ne, has now been completed. Recent investigations of $^{24}$Ne via the $^{22}$Ne(t,p$\gamma$)$^{24}$Ne reaction[1] have provided reliable spin assignments and electromagnetic decay properties for many levels. Interestingly, the $^{24}$Ne spectrum resembles the two-particle spectrum of $^{18}$O, and is in sharp contrast to the highly rotational isobar $^{24}$Mg. One of the principal objectives of the calculation, then, was to see whether the same Hamiltonian[2] which was successful for $^{24}$Mg could account for the properties of $^{24}$Ne. The Hamiltonian used was one derived by adjustment of the Kuo matrix elements to fit various energy levels in the A=18-22 mass region. No data from A$\geq$23 was employed in the fit. In order to keep the dimensionality of the basis space manageable, at least four particles were required to occupy the $d_{5/2}$ shell, and no more than two were allowed in the $d_{3/2}$ shell.

Figure 1 shows the shell model calculation for $^{24}$Ne compared with experiment and with the projected Hartree-Fock calculation of Khadkikar et al.,[3] and the projected Hartree-Bogoliubov

calculation of Goeke et al.[4] The agreement between the shell model calculation and experiment is sufficiently good to warrant a $3^+$ assignment for the 4.89 MeV level. This is in accord with the experimental observation that the state is very weak in (t,p), as would be expected for an unnatural parity transition.

Results of electromagnetic transition rate calculations are shown in Table I. Standard effective charges of 0.5e have been added to the proton and neutron charges for calculation of E2 rates, and free-nucleon g-values have been used for the M1 rates. The agreement with experiment is excellent.

## References

1. A.J. Howard, R.G. Hirko, D.A. Bromley, K. Bethge, and J.W. Olness, Phys. Rev. C1, 1446(1970); K. Bharuth-Ram, K.P. Jackson, K.W. Jones, and E.K. Warburton, Nucl. Phys. A137, 262(1969).

2. J.B. McGrory and B.H. Wildenthal, Phys. Letters 34B, 373(1971).

3. S.B. Khadkikar, S.C.K. Nair, and S.P. Pandya, Phys. Letters 36B, 290(1971).

4. K. Goeke, A. Faessler, and H.H. Wolter, Nucl. Phys. A183, 352(1972).

## TABLE I

### Electromagnetic Decay Properties and Lifetimes of $^{24}$Ne Levels

| $J^\pi$ | $E_x$(MeV) | $\tau$(ps) Calc. | $\tau$(ps) Exp. | $J^\pi$ | $E_x$(MeV) | Branch(%) Calc. | Branch(%) Exp. |
|---|---|---|---|---|---|---|---|
| $2^+$ | 1.9808 | 0.71 | $1.0^{+0.2}_{-0.4}$ | $0^+$ | 0.00 | 100 | 100 |
| $2^+$ | 3.867 | 0.02 | <0.1 | $0^+$ | 0.00 | 4 | 10 |
| | | | | $2^+$ | 1.9808 | 96 | 90 |
| $4^+$ | 3.96 | 0.90 | | $2^+$ | 1.9808 | 100 | 100 |
| $0^+$ | 4.6757 | 3.53 | >1.5 | $2^+$ | 1.9808 | 98 | 100 |
| | | | | $2^+$ | 3.867 | 2 | 0 |
| $3^+$ | 4.89 | 0.04 | | $2^+$ | 1.9808 | 93 | 100 (weak) |
| | | | | $2^+$ | 3.867 | 6 | 0 |
| | | | | $4^+$ | 3.96 | 1 | 0 |
| $2^+$ | 5.58 | 0.03 | | $0^+$ | 0.00 | 3 | <5 |
| | | | | $2^+$ | 1.9808 | 95 | 100 |
| | | | | $2^+$ | 3.867 | 2 | <5 |
| $3^+$ | 5.64 | 0.02 | | $2^+$ | 1.9808 | 34 | |
| | | | | $2^+$ | 3.867 | 54 | |
| | | | | $4^+$ | 3.96 | 11 | |

Fig. 1

$^{24}_{10}Ne_{14}$

## Three-Neutron Transfer Reaction Mechanism
### E. Kashy, W. Benenson, and I.D. Proctor
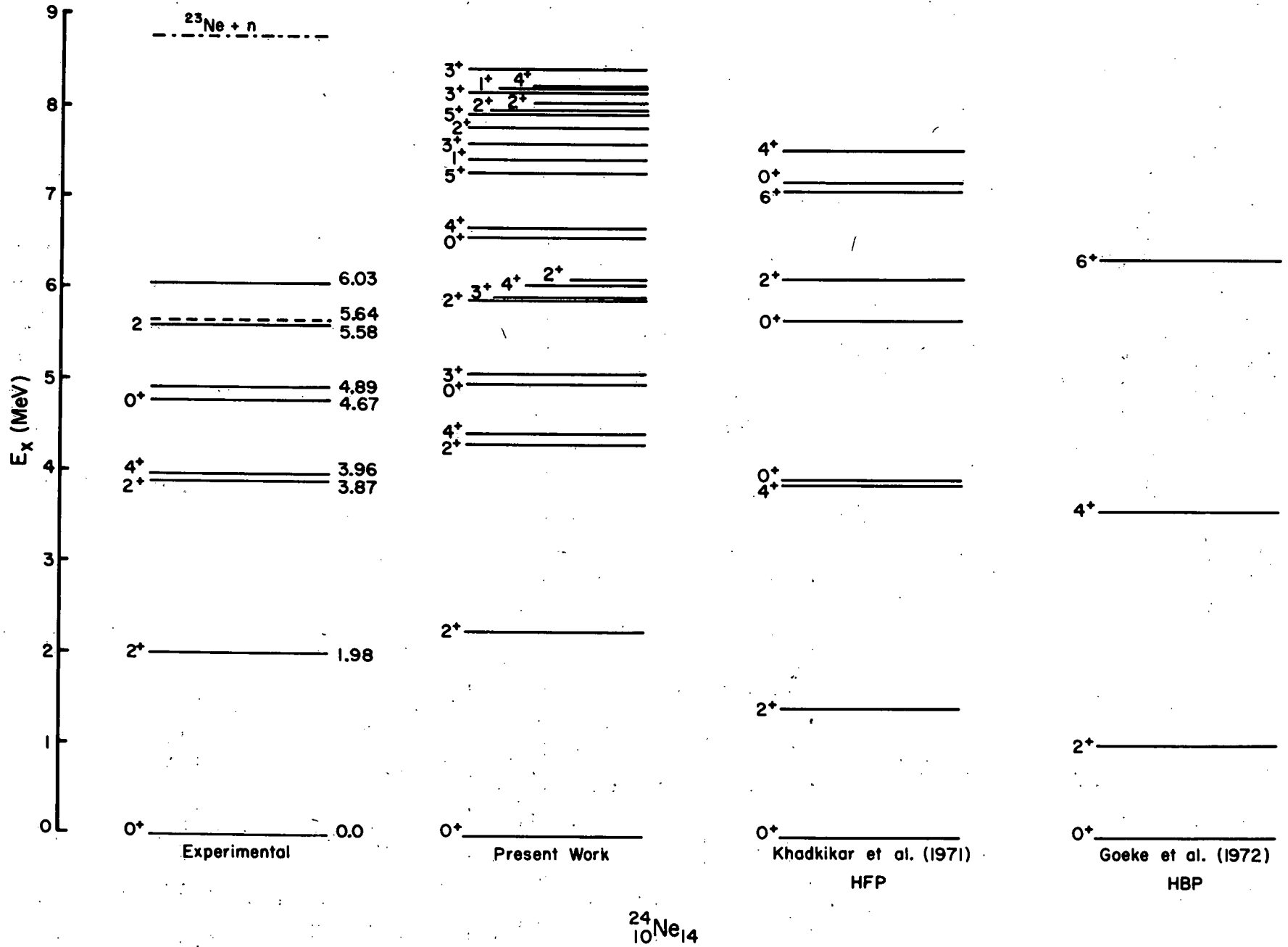
In the course of our investigation of proton
rich nuclei via the ($^3$He,$^6$He) reaction, we have
been struck by the large variation in some of
the measured cross sections, and by the fact
that the $f_{7/2}$ shell cross sections are as large
and sometimes greater than those in the 1p and
2s-1d shell. For example the (0.25 μb/ster)
cross section in the $^{40}$Ca to $^{37}$Ca ground state
transition is about 7 times smaller than for the
$^{58}$Ni to $^{55}$Ni transition. Table I is a partial
list of the measured cross sections and indicates
the typically small magnitude (∿1 μb/ster) for
this reaction.

The most striking variation is found in the
bombardment of $^{13}$C. The 2$^+$ level of the residual
nucleus $^{10}$C is excited approximately 40 times
more strongly than the 0$^+$ state of that nucleus.
The measured angular distribution for the 2$^+$
level is shown in Fig. 1 and exhibits some of the
characteristics usually associated with a direct
reaction mechanism. Part of the large enhancement
of the 2$^+$ excitation relative to the 0$^+$ can be
understood qualitatively on a very simple model,
but does not account for the factor of 40 ob-
served. This phenomenon is presently being in-
vestigated by G. Bertsch who is carrying out a
calculation of the 3n-pickup spectroscopic fac-
tors for the reactions using 1p-shell model wave
function for the states of $^{13}$C, $^{12}$C, and $^{10}$C.

### TABLE I

($^3$He,$^6$He) Laboratory Cross Section

| Target | Residual Nucleus | $E_x$ (MeV) | $J^\pi$ | $d\sigma/d\Omega$ μb/ster | $\theta$ (LAB) |
|---|---|---|---|---|---|
| $^{12}$C(0$^+$)$^a$ | $^9$C | 0.0 | 3/2$^-$ | 2.8 ±0.3 | 11° |
| $^{13}$C(1/2$^-$) | $^{10}$C | 0.0 | 0$^+$ | 0.21±0.03 | 9° |
| | | 3.35 | 2$^+$ | 7.7 ±0.2 | 9° |
| $^{24}$Mg(0$^+$) | $^{21}$Mg | 0.0 | 5/2$^+$ | 1.3 ±0.1 | 8° |
| | | 0.21 | 1/2$^+$ | 0.05±0.02 | 8° |
| | | 1.08 | – | 0.42±0.05 | 8° |
| $^{40}$Ca(0$^+$) | $^{37}$Ca | 0.0 | 3/2$^+$ | 0.24±0.03 | 8° |
| | | 1.63 | 1/2$^+$ | 0.07±0.02 | 8° |
| $^{46}$Ti(0$^+$) | $^{43}$Ti | 0.0 | 7/2$^-$ | 0.60±0.17 | 9° |
| $^{54}$Fe(0$^+$) | $^{51}$Fe | 0.27 | 7/2$^-$ | 0.70±0.20 | 9° |
| $^{58}$Ni(0$^+$) | $^{55}$Ni | 0.0 | 7/2$^-$ | 1.81±0.20 | 9° |

$^a$G.F. Trentelman, B.M. Preedom, and E. Kashy,
Phys. Rev. C3, 2205(1971).

Figure 1 →

## Search for the Lowest T=2 Level of $^{24}$Al
### E. Kashy, W. Benenson, and I.D. Proctor

We have measured $^6$He spectrum from the
$^{27}$Al($^3$He,$^6$He)$^{24}$Al reaction in order to identify
the lowest T=2 state in $^{24}$Al, i.e. the coulomb
analog to $^{24}$Ne and $^{24}$Si ground states. The level
would represent the fourth member of a T=2 isospin
multiplet and the first instance of a test of the
IMME for T>3/2. The data shows peaks in the re-
gion of th spectrum where the level is expected
from Coulomb systematics, but there is no enhance-
ment expected (or observed) which would make the
state easily identifiable. A better understanding
of the reaction mechanism would yield the spin and
we are presently investigating that aspect by mea-
suring angular distributions of the ($^3$He,$^6$He)
reaction.

The other promising avenue is a comparison of
the $^6$He spectra with spectra from reactions which
because of isospin conservation do not populate
T=2 levels of $^{24}$Al. In this respect, we note that
interestingly, the $^6$He spectra we have measured to
levels up to 5 MeV (i.e., T=1 levels) show a very
similar excitation of the levels of $^{24}$Al as the
previously measured spectra of tritons from the
$^{24}$Mg($^3$He,t)$^{24}$Al reaction.[1] If this similarity
persists in the region of 6 MeV excitation where
the T=2 state is expected, the presence of a peak
in the $^6$He spectrum and not in the triton spectrum
would be a good clue for its identification. Since
the resolution in the previous ($^3$He,t) data is of
∿85 keV,[1] we are planning to repeat that measure-
ment with special emphasis on the region of ex-
citation around 6 MeV and with improved resolution.

### References

1. N. Mangelson, M. Reed, C.C. Lu, and F.
   Ajzenberg-Selove, Phys. Letters 21, 661(1966).

$^{13}$C($^3$He, $^6$He)$^{10}$C
$E_x$ = 3.35
1/2$^-$ → 2$^+$
$E_{3He}$ = 70.6 MeV

G.S.(.107 ± .015 μb/sr)
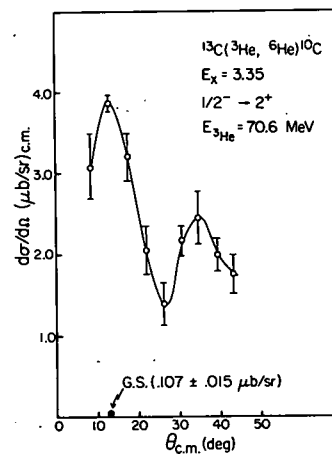
# On an ℓ-Forbidden M1 Transition in $^{38}$Cl and the Purity of States
## Whose Energies Obey the Particle-Hole Transformation Rule

S. Maripuu, B.H. Wildenthal, and A.O. Evwaraye*

The analysis of the energies of the low-lying states of $^{38}$Cl and $^{40}$K was one of the early quantitative successes of nuclear shell model theory.[1,2] If we speak in terms of an $^{16}$O core, then the first states of $^{38}$Cl should arise in lowest order from the configuration $(\nu d_{5/2})^6$, $(\pi d_{5/2})^6$, $(\nu s_{1/2})^2$, $(\pi s_{1/2})^2$, $(\nu d_{3/2})^4$; $(\pi d_{3/2})^1$, $(\nu f_{7/2})^1$, where $\nu$ denotes neutrons and $\pi$ denotes protons. Similarly, the lowest states of $^{40}$K should arise from the configuration formed by adding two more protons to the $d_{3/2}$ orbit. The $d_{5/2}$ and $s_{1/2}$ orbits are thus always filled, as is the $\nu d_{3/2}$ orbit, and we describe $^{38}$Cl in terms of $(\pi d_{3/2}^1 - \nu f_{7/2}^1)$ couplings and $^{40}$K in terms of $(\pi d_{3/2}^{-1} - \nu f_{7/2}^1)$ couplings. In the early shell model predictions of this region, these simple configurations were assumed and it was shown that the observed energies of the $2^-$, $3^-$, $4^-$, and $5^-$ states in $^{40}$K can be obtained almost exactly by applying the appropriate particle-hole transformation rule to the energies of the first $2^-$, $3^-$, $4^-$, and $5^-$ states of $^{38}$Cl.

The accuracy achieved in this transformation was then, and has been since, taken as confirming that the wave functions of the states involved did indeed conform closely to the simple initial assumptions. In addition, subsequent measurements[3,4] have disclosed a higher lying multiplet in each nucleus which can be described in similar fashion as couplings of a $d_{3/2}$ particle (hole) with a $p_{3/2}$ particle, although the transformation of energies is not as accurate as for the lower sets of states.

Recently, however, measurements have revealed some characteristics of $^{38}$Cl states which are difficult to reconcile with the simple description just outlined.[5,6] Chief among these data is a strong M1 transition from the $3^-$ state of the $(d_{3/2}-p_{3/2})$ multiplet to the $4^-$ state of the $(d_{3/2}-f_{7/2})$ multiplet. This transition is, of course, ℓ-forbidden to the extent that the wave functions of the states actually follow the description given heretofore. Other data which cast doubt on the purity of these $^{38}$Cl states are the spectroscopic factors for (d,p) stripping on $^{37}$Cl.[7] These experiments show some admixing of ℓ=1 into the supposed $(d_{3/2}-f_{7/2})$ $3^-$ state.

We have calculated energies and wave functions for $^{38}$Cl, $^{39}$K, and $^{40}$K in a model space which includes active $d_{5/2}$, $s_{1/2}$, $d_{3/2}$, $f_{7/2}$, and $p_{3/2}$ particles, using the codes of French, Halbert, McGrory, and Wong.[8] The two-body matrix elements used in our Hamiltonian were calculated from the Sussex relative oscillator matrix elements[9] with space truncation effects added,[10] and the

single-particle energies were chosen to yield calculated spectra for $^{38}$Cl, $^{39}$K, and $^{40}$K in simultaneous best agreement with the experimental spectra. These values for $d_{5/2}$, $s_{1/2}$, $d_{3/2}$, $f_{7/2}$, and $p_{3/2}$ are, respectively, -9.40, -4.90, -2.67, -2.52, and 0.00 MeV. Some of these results for $^{38}$Cl and $^{40}$K are summarized in Fig. 1 and Table III.
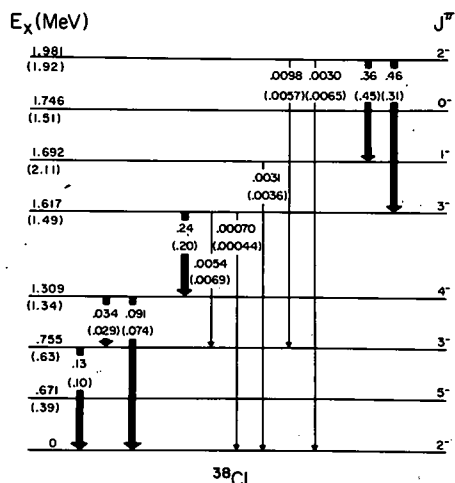


Fig. 1    Experimental and theoretical excitation energies and M1 strengths (in W.U.) of $^{38}$Cl. The theoretical values are given in brackets. The experimental numbers refer to the Brookhaven experiment.[4]

The consequences of these wave functions for M1 transitions and S-factors are shown in Tables I and II. Our predictions for these observables (our M1 calculations use operators calculated from the bare-nucleon g-factors) are in uniform good agreement with the observed values. In particular, for $^{38}$Cl, the mixing of the ℓ=1 and ℓ=3 strengths for the $3^-$ states and, most striking, the anomalously large $3_2^- \rightarrow 4_1^-$ M1 transition strength are correctly predicted.

The difficulty of accounting for this M1 transition, enhanced when it should be severely retarded according to simple ideas, has been frequently noted of late.[11,12] No previous calculation seems to have had even qualitative success in reproducing the observed strength. It is thus of interest to see how the correct strength emerges from the present wave functions. The components in the wave functions of the $3_2^-$ and $4_1^-$ states which are the important contributors to this strength are as follows, with amplitudes preceding the component specification (we now revert to isospin conventions):

$$-.37[(d_{3/2}^5)_{3/2,3/2} \ f_{7/2}] + -.87[(d_{3/2}^5)_{3/2,3/2} \ f_{7/2}]$$

TABLE I

M1 Transitions in $^{38}$Cl and $^{40}$K

| | $^{38}$Cl | | | | $^{40}$K | | |
|---|---|---|---|---|---|---|---|
| | M1 Strength (W.U.) | | | | M1 Strength (W.U.) | | |
| $J_i \rightarrow J_f$ | Argonne[5] | Brookhaven[4] | Theory | $J_i \rightarrow J_f$ | Argonne[5] | Frankfurt[6] | Theory |
| $3^-_1 \rightarrow 2^-_1$ | .23 | .13 | .10 | $3^-_1 \rightarrow 4^-$ | .150 | .170 | .087 |
| $4^- \rightarrow 3^-_1$ | .062 | .034 | .029 | $2^-_1 \rightarrow 3^-_1$ | .127 | .140 | .091 |
| $4^- \rightarrow 5^-$ | .170 | .091 | .074 | $5^- \rightarrow 4^-$ | .030 | .030 | .027 |
| $3^-_2 \rightarrow 4^-$ | .38 | .24 | .20 | $2^-_2 \rightarrow 2^-_1$ | .0130 | .0100 | .0045 |
| $3^-_2 \rightarrow 3^-_2$ | .0084 | .0054 | .0069 | $2^-_2 \rightarrow 3^-_2$ | .0026 | .0023 | .0016 |
| $3^-_2 \rightarrow 2^-_1$ | .00105 | .00070 | .00044 | $3^-_2 \rightarrow 2^-_1$ | .0033 | .0020 | .0048 |
| $1^- \rightarrow 2^-_1$ | .0050 | .0031 | .0036 | $3^-_2 \rightarrow 3^-_1$ | .0046 | .0025 | .0053 |
| $2^-_2 \rightarrow 3^-_1$ | .0174 | .0098 | .0057 | $3^-_2 \rightarrow 4^-$ | .0030 | .0016 | .0012 |
| $2^-_2 \rightarrow 2^-_1$ | .0053 | .0030 | .0065 | $1^- \rightarrow 2^-_1$ | .0076 | .0038 | .0222 |
| $2^-_2 \rightarrow 1^-$ | .62 | .36 | .45 | $0^- \rightarrow 1^-$ | .47 | .20 | .91 |
| $2^-_2 \rightarrow 3^-_2$ | .80 | .46 | .31 | | | | |

TABLE II

Spectroscopic Factors of the
$^{37}$Cl(d,p)$^{38}$Cl Reaction

| | | Exp [5] | | Theory | |
|---|---|---|---|---|---|
| $E_x$(MeV) | $J^\pi$ | S($\ell=3$) | S($\ell=1$) | S($\ell=3$) | S($\ell=1$) |
| .0 | $2^-$ | .85 | | .88 | .03 |
| .67 | $5^-$ | .78 | | .92 | |
| .76 | $3^-$ | .59 | .09 | .72 | .17 |
| 1.32 | $4^-$ | .70 | | .81 | |
| 1.62 | $3^-$ | | .40 | .15 | .46 |
| 1.69 | $1^-$ | | .81 | | .80 |
| 1.75 | $0^-$ | | 1.08 | | .94 |
| 1.98 | $2^-$ | | .70 | .007 | .76 |

$-.39[s^{-1}_{1/2}(d^6_{3/2})_{2,1}\ f_{7/2}]+-.13[s^{-1}_{1/2}(d^6_{3/2})_{2,1}\ f_{7/2}]$

and

$.33[s^{-1}_{1/2}(d^6_{3/2})_{0,1}\ f_{7/2}]+.25[s^{-1}_{1/2}(d^6_{3/2})_{0,1}\ f_{7/2}]$

Since the weightings of these three pairs of components from the M1 single-particle matrix elements are about 1 to 3 to 3, respectively, we see that the excitations from the $s_{1/2}$ to the $d_{3/2}$ orbit are of comparable importance to the mixing between $f_{7/2}$ and $p_{3/2}$ excitations in contributing allowable paths for the M1 transition. (The $s_{1/2}$ particles, as well as $f_{7/2}$ and $p_{3/2}$,

have their spins parallel to the orbital angular momentum, thus producing strong isovector contributions to the M1 strengths.[13]) And, of course, in another sense these $s^{-1}_{1/2}$ components are vital because they provide the fragmentation of the wave functions from which the coherent strength necessary to reproduce the observed enhancement can be built up. The dominating aspect of the coherence of these fragments is pointed up dramatically when we consider that the $3^-_2 \rightarrow 2^-_1$ transition has individual contributions of equivalent size to those for the $3^-_2 \rightarrow 4^-_1$ and that those for the $3^-_2 \rightarrow 3^-_1$ transition are actually considerably larger (as pointed out by Erné[14]). However, in these cases the signs of the individual components are such that the various contributions cancel each other.

The general conclusions from the present calculations are:
1) The ($d_{3/2}-f_{7/2}$) and ($d_{3/2}-p_{3/2}$) multiplets in $^{38}$Cl are about 80% pure, with considerable $f_{7/2}-p_{3/2}$ mixing only between the $3^-$ states.
2) The 5%-20% admixtures of the $s^{-1}_{1/2}$ configuration in these $^{38}$Cl states are vital to account for the observed anomalous M1 strength between the $3^-_2$ and $4^-_1$ states.
3) The purity of the analogous multiplets in $^{40}$K is considerably higher, and, in consequence, no anomalies in M1 strength are predicted, again in accordance with observation.

TABLE III

Configuration Mixing in $^{38}$Cl and $^{40}$K
(intensities in %)

| $^{38}$Cl | $E_x$(MeV) Exp | $E_x$(MeV) Calc | $J^\pi$ | $d^5_{3/2}f_{7/2}$ | $d^5_{3/2}p_{3/2}$ | $s^{-1}_{1/2}d^6_{3/2}f_{7/2}$ | $s^{-1}_{1/2}d^6_{3/2}p_{3/2}$ |
|---|---|---|---|---|---|---|---|
| | 0 | 0 | $2^-$ | 82 | 3 | 7 | 2 |
| | .67 | .39 | $5^-$ | 86 | | 5 | |
| | .76 | .63 | $3^-$ | 68 | 17 | 7 | 2 |
| | 1.31 | 1.34 | $4^-$ | 77 | | 8 | |
| | 1.62 | 1.49 | $3^-$ | 14 | 45 | 28 | 1 |
| | 1.69 | 2.11 | $1^-$ | | 81 | 12 | 3 |
| | 1.75 | 1.51 | $0^-$ | | 97 | | 1 |
| | 1.98 | 1.92 | $2^-$ | 1 | 77 | 16 | 1 |

| $^{40}$K | $E_x$(MeV) Exp | $E_x$(MeV) Calc | $J^\pi$ | $d^{-1}_{3/2}f_{7/2}$ | $d^{-1}_{3/2}p_{3/2}$ | $s^{-1}_{1/2}f_{7/2}$ | $s^{-1}_{1/2}p_{3/2}$ |
|---|---|---|---|---|---|---|---|
| | 0 | 0 | $4^-$ | 96 | | 2 | |
| | .03 | -.02 | $3^-$ | 91 | 5 | 2 | |
| | .80 | 1.06 | $2^-$ | 87 | 7 | | 2 |
| | .89 | .79 | $5^-$ | 96 | | | |
| | 2.05 | 1.99 | $2^-$ | 6 | 89 | | |
| | 2.07 | 1.93 | $3^-$ | 2 | 76 | 18 | |
| | 2.10 | 2.54 | $1^-$ | | 96 | | |
| | 2.63 | 2.19 | $0^-$ | | 98 | | |

4) The differences between $^{38}$Cl and $^{40}$K are consequences of the freedom to excite particles within the sd-shell which exists for $^{38}$Cl and which does not exist for $^{40}$K. In other words, the differences are consequences of the breakdown of the assumptions upon which the particle-hole transformation are based, e.g. that $^{32}$S is a good closed shell nucleus. Since both experiment and the present calculations definitely indicate that these differences exist, the question which remains is why does the energy transformation scheme based on the assumption of pure configurations work so well.

### References

1. S. Goldstein and I. Talmi, Phys. Rev. 102, 589(1956).

2. S.P. Pandya, Phys. Rev. 103, 956(1956).

3. R.M. Freeman and A. Gallman, Nucl. Phys. A156, 305(1970).

4. G.A.P. Engelbertink and J.W. Olness, Phys. Rev. C5, 431(1972).

5. R.E. Segel et al., Phys. Rev. Letters 25, 1352(1970).

6. R. Bass and R. Wechsung, Phys. Letters 32B, 602(1970).

7. J. Rapaport and W.W. Buechner, Nucl. Phys. 83, 80(1966).

8. J.B. French, E.C. Halbert, J.C. McGrory, and S.S.M. Wong, Advances in Nuclear Physics, Vol. 2 (Plenum Press, New York, 1970), p. 193.

9. J.P. Elliott et al., Nucl. Phys. A121, 248(1968).

10. S. Maripuu and G.I. Harris, BAPS, 16, 1166(1971) and to be published.

11. D. Kurath and R.L. Lawson, Phys. Rev. C6, 901(1972).

12. P. Goode, BAPS 17, 34(1972).

13. S. Maripuu, Nucl. Phys. A123, 357(1969).

14. F. Erné, W.A.M. Veltman, and J.A.J.M. Wintermans, Nucl. Phys. 88, 1(1966).

* Present Address: Department of Physics, Antioch College, Yellow Springs, Ohio 45387

The $^{39}$K(p,t)$^{37}$K and $^{39}$K(p,$^3$He)$^{37}$Ar Reaction

W.A. Lanford, B.H. Wildenthal and J. Johnson

Because of the unexpected outcome of the Davis et al.[1] solar neutrino experiment, there is much interest in the nuclear structure of the mass-37 isobars $^{37}$Ca, $^{37}$K, $^{37}$Ar, and $^{37}$Cl. The reaction used to detect neutrinos is $\nu+^{37}$Cl$\rightarrow^{37}$Ar$+e^-$, and the calculated cross-section for this process depends on knowing something about the nuclear structure of $^{37}$Cl and $^{37}$Ar. The wave functions of Wildenthal et al.[2] have been used to calculate the neutrino absorption cross-section on $^{37}$Cl.[3]

This study of the $^{39}$K(p,t)$^{37}$K and $^{39}$K(p,$^3$He)$^{37}$Ar reaction was undertaken partly to test these calculated wave functions for mass 37 via a type of observable which might sensitive to details which do not affect the results of other kinds of measurements. Conversely, since the calculated wave functions do manage to account for the concensus of present data in this region, another motivation for this pair of experiments was to test our knowledge of the two-nucleon transfer reaction mechanism in a case where we feel relatively confident of our knowledge of the mixed configuration shell-model wave functions.

Shown in Fig. 1 are spectra of the $^{39}$K(p,t)$^{37}$K and $^{39}$K(p,$^3$He)$^{37}$Ar reactions observed with a position-sensitive proportional counter in the focal plane of the Enge magnetic spectrograph at a bombarding energy of 40 MeV. The angular distributions of these states are presently being analyzed.

### References

1. R. Davis, BAPS 17, 527(1972).

2. B.H. Wildenthal, E.C. Halbert, J.B. McGrory, and T.T.S. Kuo, Phys. Rev. C4, 1266(1971).

3. W.A. Lanford and B.H. Wildenthal, Phys. Rev. Letters 29, 606(1972).



## Study of the Germanium Isotopes with the (p,d) Reaction

D.L. Show, J.A. Nolen, W.A. Lanford, and B.H. Wildenthal
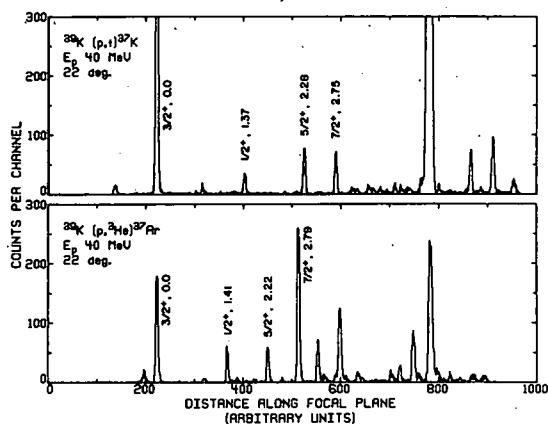
We have begun a study of the Germanium isotopes via the (p,d) reaction. While some of the level structure of these nuclei has been established by gamma ray studies,[1,2] and direct reaction work,[3,4] the direct reaction studies have been hindered by the need for a resolution of <20 keV for many of the states. We have used the 35 MeV proton beam from the MSU Cyclotron to study the (p,d) reaction on $^{70,72,74}$Ge between 6° and 60° in the lab. The deuterons were analyzed in an Enge split-pole magnetic spectrograph and detected in nuclear emulsions. The energy resolution for these spectra vary from 5-9 keV, FWHM. Spectra recorded at 6° are shown in Fig. 1. Scanning of plates exposed at the other angles is in progress.

Preliminary studies using a position-sensitive wire proportional counter in the focal plane of the magnet indicate that at a proton energy of 25 MeV and large scattering angles (90°-120°) the J dependence of $\ell=1$ transitions is sufficiently strong to allow unique spin assignments to levels populated with $\ell=1$ transfer. Also, work on the $^{60}$Ni(p,d) reaction indicates that the $\ell=3$, forward angle, J-dependence is strong at $E_p=35$ MeV.

We plan to continue the 35 MeV studies on the other stable Germanium isotopes ($^{73,76}$Ge) and use the data to extract energy levels, $\ell$-transfer, and spectroscopic factors. We can also use this data to make spin assignments to the states populated by $\ell=3$ transfer because of the J-dependence previously mentioned. We will then repeat the experiment for all the isotopes at 25 MeV and $\theta_L=90°-120°$ to get spin assignments for those states populated by the $\ell=1$ transfer.

### References

1. C. Murray, N.E. Sanderson, J.C. Willmott, Nucl. Phys. A171, 435(1971).

2. S. Muszynski and S.K. Mark, Nucl. Phys. A147, 459(1970).

3. T.H. Hsu, R. Fournier, B. Hird, J. Kroon, G.C. Ball, and F. Ingebretsen, Nuclear Phys. A179, 80(1972).

4. L.H. Goldman, Phys. Rev. 165, 1203(1968).

# The Structure of $^{38}$K via the $^{39}$K(p,d)$^{38}$K

J.A. Rice and B.H. Wildenthal

In conjunction with studies of other odd-neutron, odd-proton s-d shell nuclei presently being pursued at the Cyclotron Laboratory, the study of $^{38}$K via the $^{39}$K(p,d)$^{38}$K reaction has been undertaken at a proton bombarding energy of 35 MeV. The work was motivated by the need for a critical evaluation of recent shell-model predictions[1,2] through the extraction of accurate excitation energies and $\ell=0$ and $\ell=2$ spectroscopic factors. To this end, (p,d) angular distributions from thin natural potassium targets (93% $^{39}$K) were taken utilizing the MSU Cyclotron and split-pole spectrograph. Deuteron spectra were recorded both on nuclear emulsion plates and with a wire proportional counter. The angular distributions were taken between 3° and 55° with special concentration at angles less than 30° to facilitate the unambiguous extraction of $\ell=0$ and $\ell=2$ spectroscopic factors. The cross-section normalization was performed by comparisons of proton elastic scattering data to optical model calculations.[3] A typical plate spectrum with a resolution of approximately 8 keV FWHM is shown below. Excitation energies, obtained from the plate data only, were extracted by a least-squares fit of energy levels calculated via the spectrograph calibration to corresponding low-lying levels known to $\leq 2$ keV from gamma ray studies.[4] Energy levels observed in the present work along with the gamma ray and other single neutron pick-up work are given below in Table I.

DWBA analysis[5] of the deuteron angular distributions is near completion and preliminary results indicate the observation of essentially all of the $\ell=0$ and $\ell=2$ ($d_{3/2}$) strengths and approximately one-fourth of the $\ell=2$ ($d_{5/2}$) strength below 6 MeV of excitation. The distribution of observed spectroscopic strengths favors the 11.0h+ASPE and 12.5p+$^{17}$O calculations of Wildenthal et al.[1] and the Tabakin predictions of Dieperink and Brussaard.[2]

## References

1. B.H. Wildenthal, E.C. Halbert, J.B. McGrory, and T.T.S. Kuo, Phys. Rev. C4, 1266(1971).

2. A.E.L. Dieperink and P.J. Brussaard, Nucl. Phys. A128, 34(1969).

3. Proton parameters of F.D. Becchetti and G.W. Greenlees, Phys. Rev. 182, 1190(1969).

4. W.K. Collins, C.S.C. D.Longo, L. Alexander, E. Berners, and P. Chagnon, University of Notre Dame Progress Report, 1971.

5. Proton channel (Ref. 3) and deuteron parameters of F. Hinterberger, G. Mairle, V. Schmidt-Rohr, G.J. Wagner, and P. Turek, Nucl. Phys. A111, 265(1968) used in computer code DWUCK, P.D. Kunz, University of Colorado.
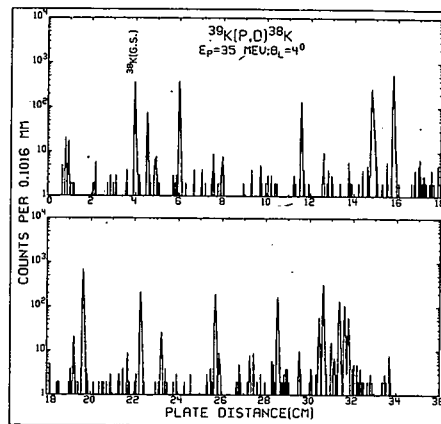
Fig. 1

## TABLE I

Energy Levels in $^{38}$K

| $E_x$ (keV)[a] | $E_x$ (keV)[b] | $E_x$ (keV)[c] |
|---|---|---|
| 0 | 0 | 0 |
| 130 | 131 | 130 |
| 459 | 460 | 450 |
| 1699 | 1699 | 1700 |
| 2404 | 2404 | 2400 |
| 2615 | 2614 | |
| 2649 | 2649 | |
| 2829 | 2832 | |
| 2872 | 2871 | |
| | 2995 | |
| 3320 | 3319 | |
| 3343 | 3347 | |
| 3433 | 3432 | 3440 |
| 3617 | | |
| | 3670 | |
| 3704 | | |
| 3820 | | |
| 3860 | | |
| 3939 | | |
| 3981 | | 4000 |
| 4177 | | |
| 4218 | | |
| 4583 | | |
| 4657 | | 4670 |
| 4698 | | |
| 4982 | | |
| 5234 | | 5250 |
| 5434 | | |
| 5611 | | |
| 5723 | | |
| 5791 | | 5780 |
| 5842 | | 5850 |
| 5877 | | |
| 5928 | | |
| 5961 | | |

[a] Present Work: errors approximately $\pm 2$ keV to 2600 keV and an additional $\pm 1$ keV/MeV above 2600 keV.

[b] Reference 3: errors $\leq 2$ keV except the 3347 keV level which is $\pm 3$ keV.

[c] G. Ronsin, M. Vergnes, G. Rotbard, J. Kalifa, and I. Lanck, to be published; no errors given.

# Study of the Proton Rich Nuclei in the $1f_{7/2}$ Shell

I.D. Proctor, W. Benenson, and E. Kashy

The proton rich nuclei $^{43}$Ti, $^{47}$Cr, $^{51}$Fe, and $^{55}$Ni are being studied by the ($^3$He,$^6$He) reaction at 70 MeV. Since the line of nuclear stability in the $1f_{7/2}$ shell is at least two neutrons from the N=Z line, these measurements will extend the three neutron transfer ($^3$He,$^6$He) reaction to its maximal value for study of proton rich $T_z$=-1/2 nuclei. Mass measurements for $^{43}$Ti, $^{47}$Cr, $^{51}$Fe, and $^{55}$Ni have been completed and recently reported.[1] The energy level structure of these Z=N+1 members of the heaviest known mirror pairs are currently under investigation with special emphasis on identification of the $1/2^+$ and $3/2^+$ neutron hole states.

These experiments are performed using the Enge split-pole magnetic spectrograph. Previous measurements[2,3,4] using the ($^3$He,$^6$He) reaction in this laboratory have used silicon position sensitive detectors and photographic emulsions in the focal plane of the spectrograph to detect the $^6$He particles. These methods were not able to satisfactorily discriminate the $^6$He particles from the very strong $\alpha$ background encountered in the measurements on the $1f_{7/2}$ shell nuclei. To overcome the particle identification problem, a wire proportional counter for position information was combined with a plastic scintillator to measure the time-of-flight (TOF) of the particles. Identification of a $^6$He particle is performed by requiring that the energy losses in the proportional counter and plastic scintillator fall within selected limits, and that the TOF of the particle is the same as that of a triton (tritons have the same TOF as $^6$He particles of the same rigidity). Using this scheme, we have measured $^6$He cross sections as low as 20 nb/sr in the presence of an $\alpha$ background of 20 mb/sr.
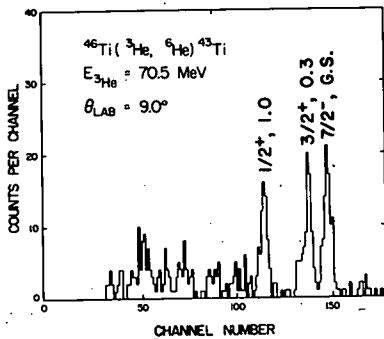
Spectra obtained for $^{43}$Ti, $^{47}$Cr, and $^{55}$Ni are shown in Figs. 1 to 3 respectively. The energy level and spin-parity assignments shown are preliminary. Spin-parity assignments are from a comparison with the known mirror levels populated in the (p,$\alpha$) reaction.[5] Further identification of the levels populated in the ($^3$He,$^6$He) reaction in the $1f_{7/2}$ shell nuclei will be obtained by comparing angular distributions with those obtained to states of known spin and parity in the $^{26}$Mg($^3$He,$^6$He) reaction.

## References

1. I.D. Proctor, W. Benenson, J. Dreisbach, E. Kashy, G.F. Trentelman, and B.M. Preedom, Phys. Rev. Letters 29, 434(1972).

2. W. Benenson, J. Dreisbach, I.D. Proctor, G.F. Trentelman, and B.M. Preedom, Phys. Rev. C5, 1426(1972).

3. G.F. Trentelman and I.D. Proctor, Phys. Letters 35B, 570(1971).

4. G.F. Trentelman, B.M. Preedom, and E. Kashy, Phys. Rev. Letters 25, 53(1970).

5. J. Nolen, W. Benenson, and E. Kashy, unpublished.

$^{50}$Cr($^3$He, $^6$He)$^{47}$Cr
$E_{^3He}$ = 70.5 MeV
$\theta_{LAB}$ = 9.0°

Figure 2



$^{46}$Ti($^3$He, $^6$He)$^{43}$Ti
$E_{^3He}$ = 70.5 MeV
$\theta_{LAB}$ = 9.0°

Figure 1



$^{58}$Ni($^3$He, $^6$He)$^{55}$Ni
$E_{^3He}$ = 66.3 MeV
$\theta_{LAB}$ = 9.0°
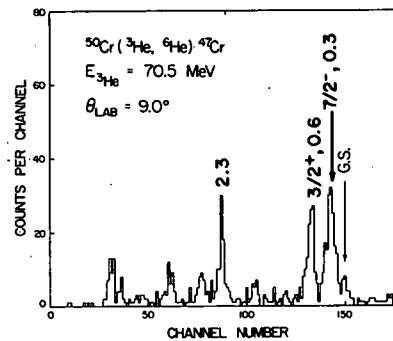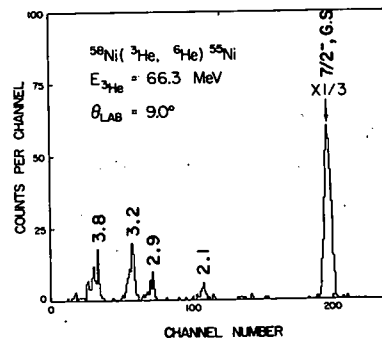
Figure 3

# Low-Lying States of $^{48}$V from the $^{48}$Ti(p,nγ) and $^{45}$Sc(α,nγ) Reactions*

L.E. Samuelson, W.H. Kelly, R.A. Warner, R.R. Todd,** F.M. Bernthal
Wm.C. McHarris, E.M. Bernstein,** and R. Shamu**

The $^{48}$Ti(p,nγ)$^{48}$V reaction was used to study the states of $^{48}$V below 3.34 MeV of excitation. Proton beams of 4.81 to 7.03 MeV in 50 keV steps were furnished for the excitation function measurements by the WMU Tandem Van de Graaff. Proton beams at four different energies for the γ-γ coincidence measurements and at six different energies for the γ-ray angular distribution measurements were furnished by the MSU Cyclotron. The excitation functions and γ-ray angular distributions were measured by detecting deexciting γ rays in a 2.5%-efficient Ge(Li) detector while the γ-γ coincidences were measured using the Ge(Li)-Ge(Li) spectrometer described in the article on $^{56}$Co in this same publication. The target was a 99.36% isotopically enriched $^{48}$Ti foil of 0.66 mg/cm$^2$ thickness (approximately 30 keV thick at the beam energies used). A typical γ-ray singles spectrum is shown in Fig. 1, while an integral coincidence spectrum and a typical gated coincidence spectrum is shown in Fig. 2. Typical excitation functions for excited states below 2 MeV in $^{48}$V are shown in Fig. 3.

Some examples of the analyses of the γ-ray angular distributions are shown in Fig. 4. A least squares fit to the experimental γ-ray angular distributions using the computer code GADFIT[1] was made to the equation.

$$W(\theta) = A_0[1+A_2^*P_2(\cos\theta)+A_4^*P_4(\cos\theta)].$$

Absolute cross sections and the γ-ray mixing-ratio dependent parameters $A_2^*=A_2/A_0$ and $A_4^*=A_4/A_0$ (i.e. δ-ellipses) were calculated using the statistical CN computer code MANDY.[2] For these calculations, nine proton channels and all known open neutron channels were included as "extra" open exit channels. Comparisons of relative cross sections for the population of each state, and of the γ-ray angular distributions with the predictions of the statistical CN theory has then led to the spin assignments shown on the $^{48}$V excited-state level scheme in Fig. 5, and to the γ-ray multiple mixing ratios listed in Table I.

The WMU Tandem Van de Graaff was used to provide alpha beams of 6.8, 7.8, 9.8, and 12.0 MeV for the $^{45}$Sc(α,nγ)$^{48}$V γ-ray singles experiments. The γ-ray spectrum taken at 12.0 MeV is shown in Fig. 1. Since alpha particles are expected to preferentially excite high spin states in the residual $^{48}$V nucleus, this experiment is expected to give qualitative confirmation of high spin assignments made in the (p,nγ) work and to allow identification of other high spin states not identified therein. Since the analyses of

these data are not yet complete, only the confirmations of high spin assignments are indicated in Fig. 1.

## References

1. GADFIT, computer code written by R. Warner, unpublished.

2. E. Sheldon and R.M. Strang, Computer Physics Communication 1, 35(1969); and references cited therein.

## TABLE I

γ-ray Energies and Mixing Ratios of $^{48}$V Measured Using the $^{48}$Ti(p,nγ)$^{48}$V Reaction

| Energies (keV) | Mixing Ratio[a] | Transition Assumed[b] |
|---|---|---|
| 308.3±0.1 | E2 | 2+→4+ |
| 112.5±0.1 | -0.14<δ<-0.02 | 1+→2+ |
| 427.9±0.1 | -0.15<δ<-0.12 | 5+→4+ |
| 98.0±0.1 | -0.08<δ<+0.37 | 1-→1+ |
| 210.4±0.1 | +0.01<δ<+0.07 | 1-→2+ |
| 185.5±0.1 | -0.02<δ<+0.07 | 4+→5+ |
| 613.4±0.1 | -0.21<δ<-0.17 | 4+→4+ |
| 199.3±0.2 | -0.23<δ<+0.03 | 6+→5+ |
| 627.3±0.2 | E2 | 6+→4+ |
| 226.3±0.1 | -0.08<δ<-0.06 | 2-→1- |
| 324.2±0.1 | -0.21<δ< 0.16 | 2-→1+ |
| 436.8±0.1 | -0.21<δ< 0.14 | 2-→2+ |
| 151.7±0.2 | -- | 3+→4+ |
| 456.7±0.1 | -0.03<δ<-0.01 | 3+→2+ |
| 746.9±0.1 | -0.05<δ<+0.00 | 3+→4+ |
| 310.8±0.1 | - | 3-→2- |
| 537.2±0.2 | E2 | 3+→2+ |
| 1099.3±0.2 | -0.21<δ<+0.22 | 4±→4+ |
| 637.3±0.2 | -- | 5+→6+ |
| 651.2±0.2 | -0.26<δ<-0.03 | 5+→4+ |
| 756.4±0.1 | -0.02<δ<+0.13 | 2+→3+ |
| 1101.0±0.2 | -0.05<δ<+0.03 | 2+→1+ |
| 1212.9±0.2 | +0.14<δ<+0.28 | 2+→2+ |
| 501.8±0.2 | -0.11<δ<-0.06 | 4-→3- |
| 812.2±0.3 | E2 | 4-→2- |
| 586.3±0.2 | - | 5±→4± |
| 1167.8±0.2 | -0.20<δ<+0.07 | 3+→4+ |
| 1472.5±0.2 | -0.12<δ<+0.07 | 3+→2+ |
| 1780.9±0.3 | -- | 3+→4+ |
| 899.4±0.2 | - | 3-→4± |
| 1253.3±0.2 | - | 3-→2- |

[a]Missing mixing ratios could not be measured because of insufficient peak statistics. An exception is the 310.8-keV γ ray where a systematic analysis error makes the results dubious.

[b]The mixing ratios shown were calculated for the indicated spin and parity sequences. It should be noted that the parities were not measured in the present experiments and therefore have been assumed.
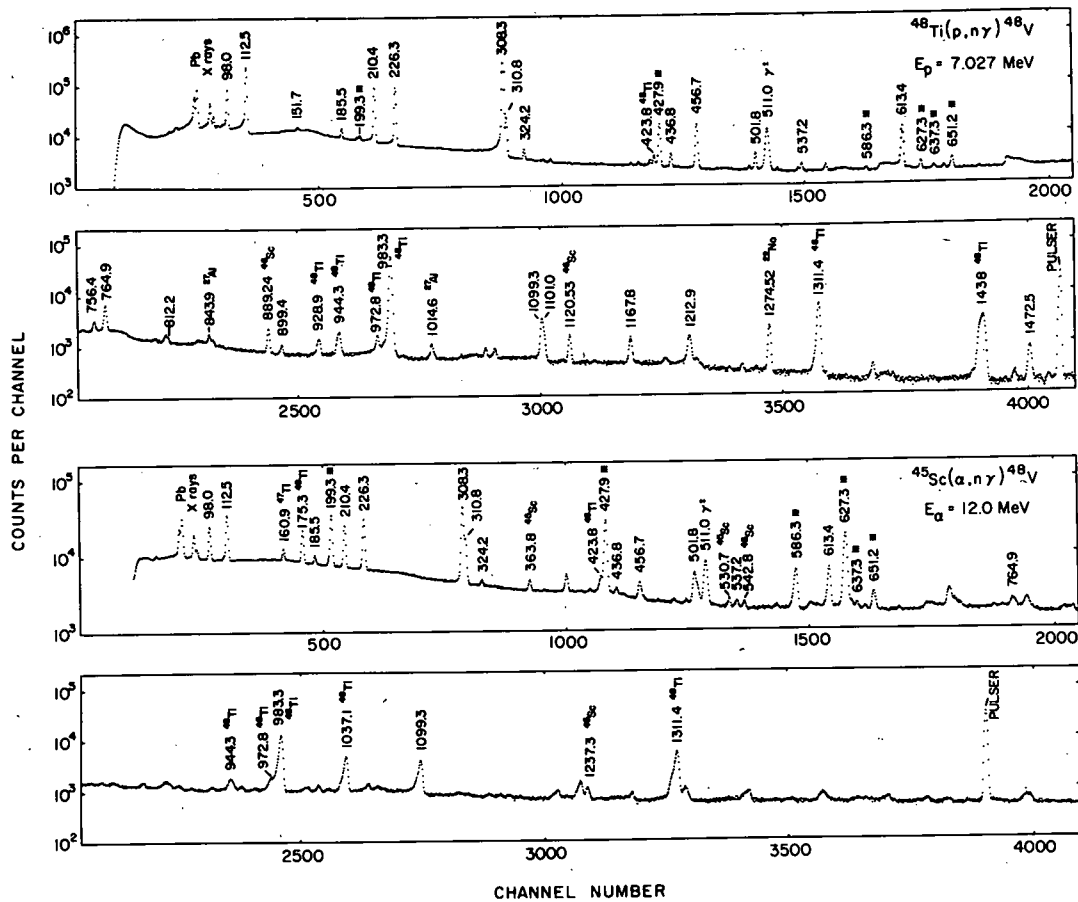
Fig. 1   Singles γ-ray spectra of the $^{48}$Ti($p,n\gamma$)$^{48}$V reaction at $E_p$=7.027 MeV and the $^{45}$Sc($\alpha,n\gamma$)$^{48}$V reaction at $E_\alpha$=12.0 MeV.  In both spectra γ-rays believed to deexcite "high" spin states are indicated with an asterisk.
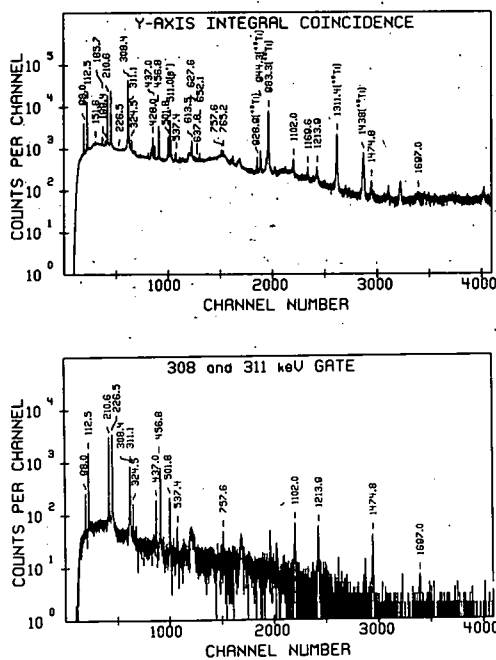


Fig. 2   Integral coincidence spectrum and the 308-311 keV doublet gated spectrum at $E_p$=7.03 MeV taken with the 7.4%-efficient Ge(Li) detector.  The gate was set on the opposite axis which was taken with the 2.5%-efficient Ge(Li) detector.  Careful background subtraction using adjacent continuum has been included.  The final energies are slightly different from those values labeling the peaks.
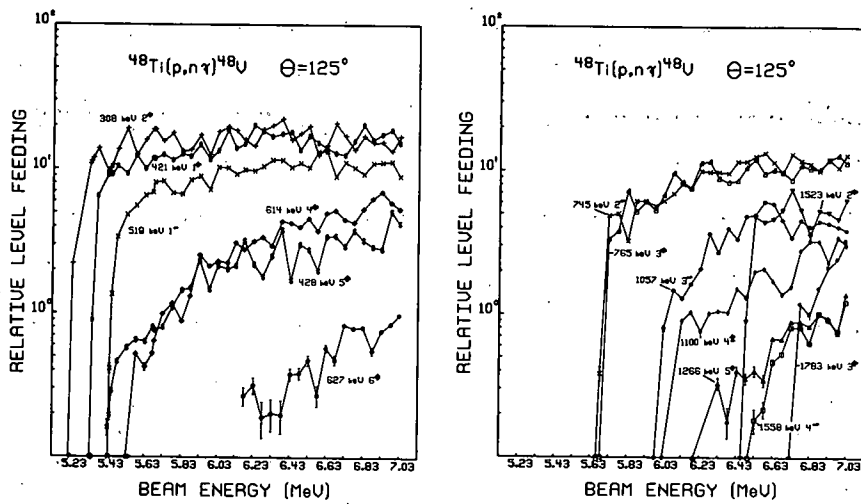
Fig. 3 Excitation functions for fourteen excited states of $^{48}$V lying below 1.8 MeV of excitation. The data were taken at $\theta=125°$, a zero of $P_2(\cos\theta)$. The appropriate intensities of de-exciting and feeding $\gamma$ rays have been added and subtracted to obtain the relative cross sections. The thresholds were calculated using Q=-4.803 MeV for the ground state.

Fig. 4 Analyses of several $\gamma$-ray angular distributions from the $^{48}$Ti(p,n$\gamma$)$^{48}$V reaction. Shown for the $\gamma$-ray transition in question are its angular distribution, the theoretical $\delta$-ellipse plots with the experimental values of $A_2^*$ and $A_4^*$ drawn in as a rectangle (initial spin values labeling their appropriate ellipses), and a plot of chi-square per degree of freedom (reduced chi-square) versus arc tangent $\delta$. The $\gamma$ ray energies shown are slightly different from their final values.



18
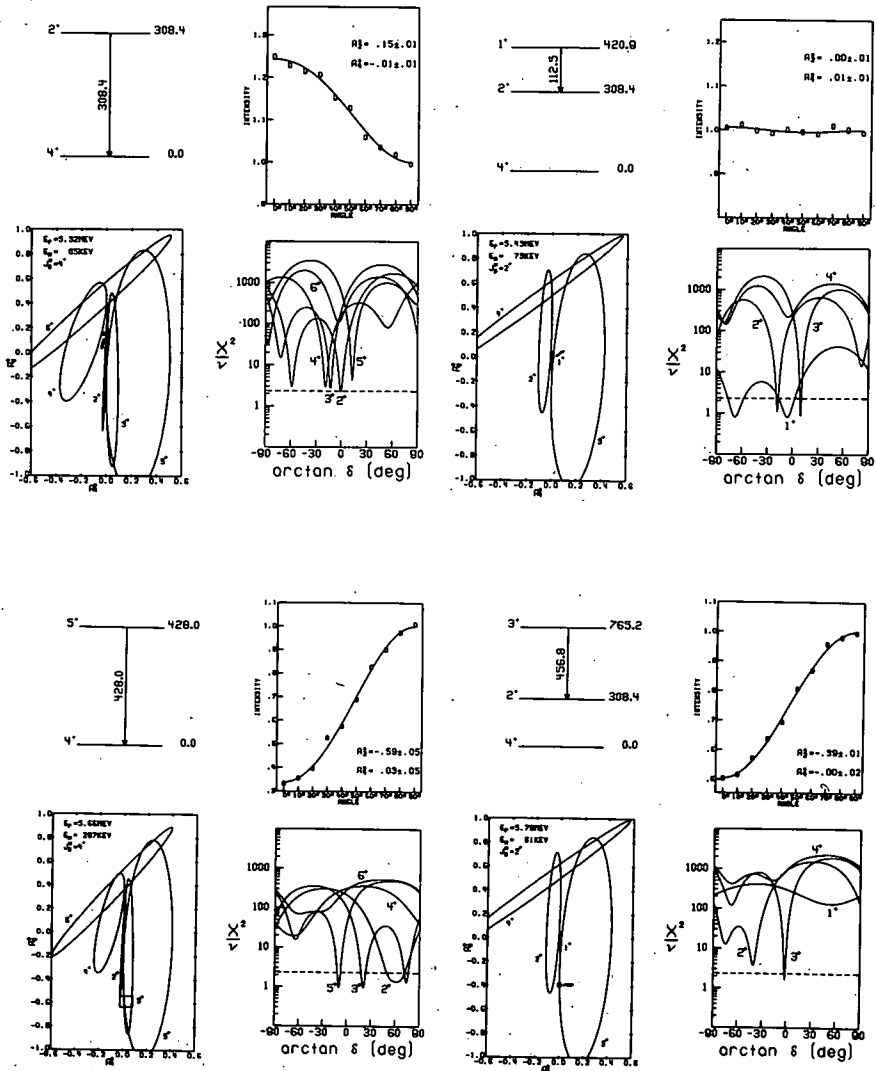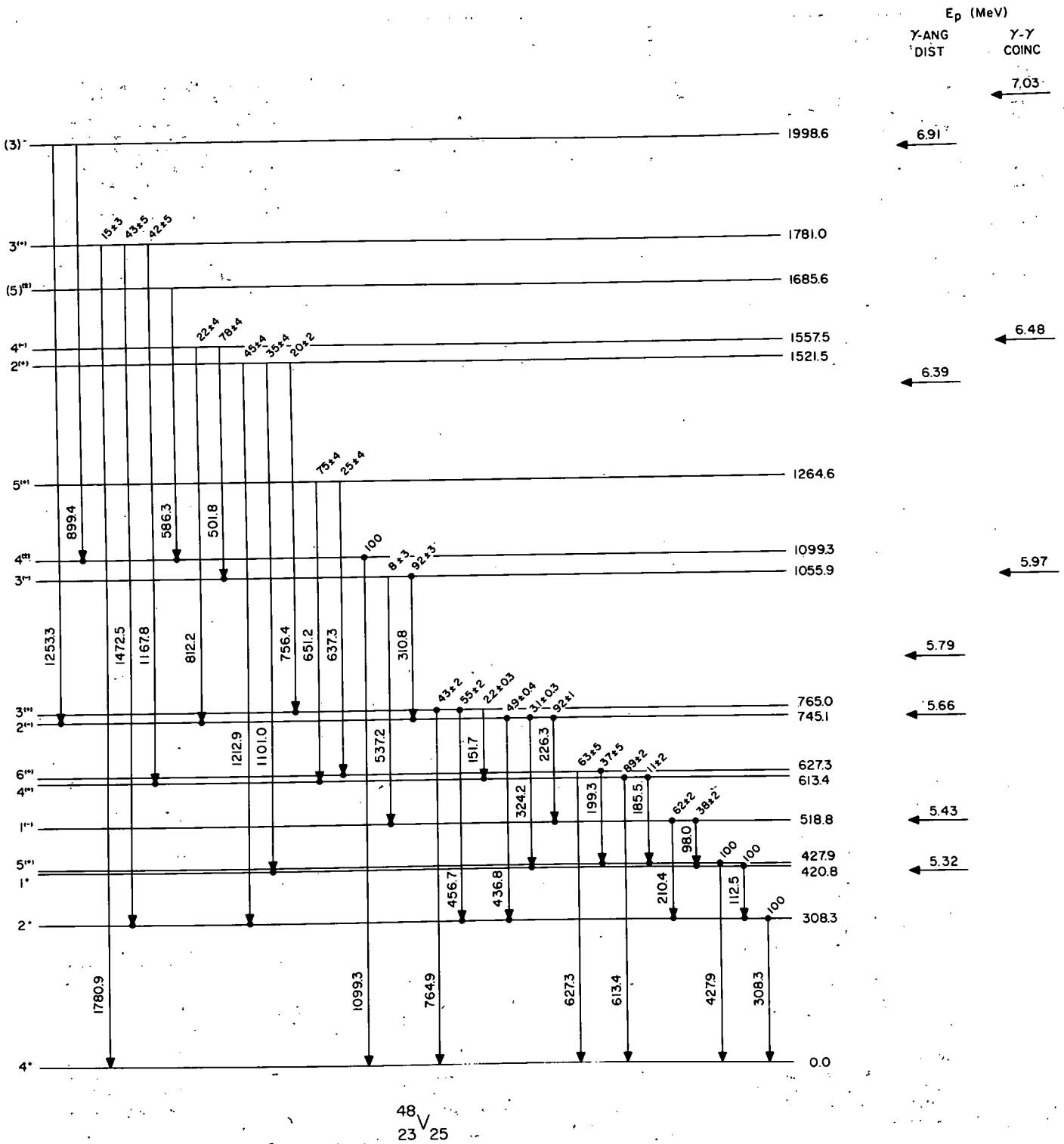
Fig. 5    The excited-state level scheme of $^{48}$V.  The arrows on
the right indicate the maximum possible excitation for
the labeled incident proton energy.  The spin assignments
on the left (except for the ground state) are all from
this work.  The γ-ray and level energies shown are the
final values.

19

R.R. Doering, A.I. Galonsky, and R.A. Hinrichs

In the preceding annual report we presented preliminary angular distributions and optical-model parameters for 70 MeV $^3$He elastic scattering from $^{50}$Ti and $^{51}$V. During the past year we have refined both the data and its theoretical analysis. In particular, we found it necessary to modify the optical-model search code GIBELUMP in order to obtain sufficient numerical accuracy for the small, back-angle cross sections observed in $^3$He elastic scattering at 70 MeV.[1] Figure 1 illustrates the inadequacy of a few commonly used codes. The solid reference curve has been computed with our modified version of GIBELUMP (SGIB) and is considered accurate to better than one percent at all angles. The discrepancies between the back-angle oscillations of the less accurate calculations result from insufficient numbers of terms and losses of significance in the partial-wave sums. SGIB allows the user to employ enough partial waves and integration steps to overcome these difficulties.

The fits to our data were generated with 60 partial waves, a 22 F matching radius, and a 0.05 F integration step size. The optical-model parameters were fairly well determined except for a continuous ambiguity related to the strength of the spin-orbit potential. The table lists best-fit parameters from grid searches on $V_{SO}$. Fits to the $^{51}$V data for the $V_{SO}$=0.0 and 3.0 MeV cases are shown in Fig. 2. The smooth drop in the angular distribution at large angles is particularly sensitive to the optical-model parameters. Our preliminary calculations with GIBELUMP required a spin-orbit potential of a few MeV to damp out the erroneous back-angle oscillations (see Fig. 1). The more accurate SGIB results indicate little preference for any particular $V_{SO}$ less than about 3 MeV. Other recent analyses of $^3$He elastic scattering tend to either agree with this result[2,3] or prefer a spin-orbit potential of about 2-4 MeV.[4,5] In all cases the parameters of the real, central potential appear correlated with the spin-orbit strength. Current polarization and spin-flip data suggest that the $^3$He spin-orbit potential is around 2-5 MeV. In an effort to further restrict this continuous ambiguity, we are currently comparing our empirical $^3$He optical-model potentials with "theoretically realistic" nucleon-nucleus folding-model predictions based on refinements of calculations by Abul-Magd and El-Nadi.[6] We are also in the process of extracting deformation parameters from macroscopic DWBA analyses of inelastic $^3$He scattering to low-lying $2^+$ and $4^+$ states in $^{50}$Ti and $3/2^-$, $5/2^-$, $9/2^-$, and $11/2^-$ states in $^{51}$V.

References –

1. R.R. Doering, BAPS 17, 590(1972).
2. P.P. Urone, et al., Nucl. Phys. A167, 383(1971).
3. P.B. Woollam, et al., Nucl. Phys. A189, 321(1972).
4. C.B. Fulmer and J.C. Hafele, Phys. Rev. C5, 1969(1972).
5. H.P. Morsch and R. Santo, Nucl. Phys. A179, 401(1972).
6. A.Y. Abul-Magd and M. El-Nadi, Prog. Theor. Phys. 35, 798(1965).
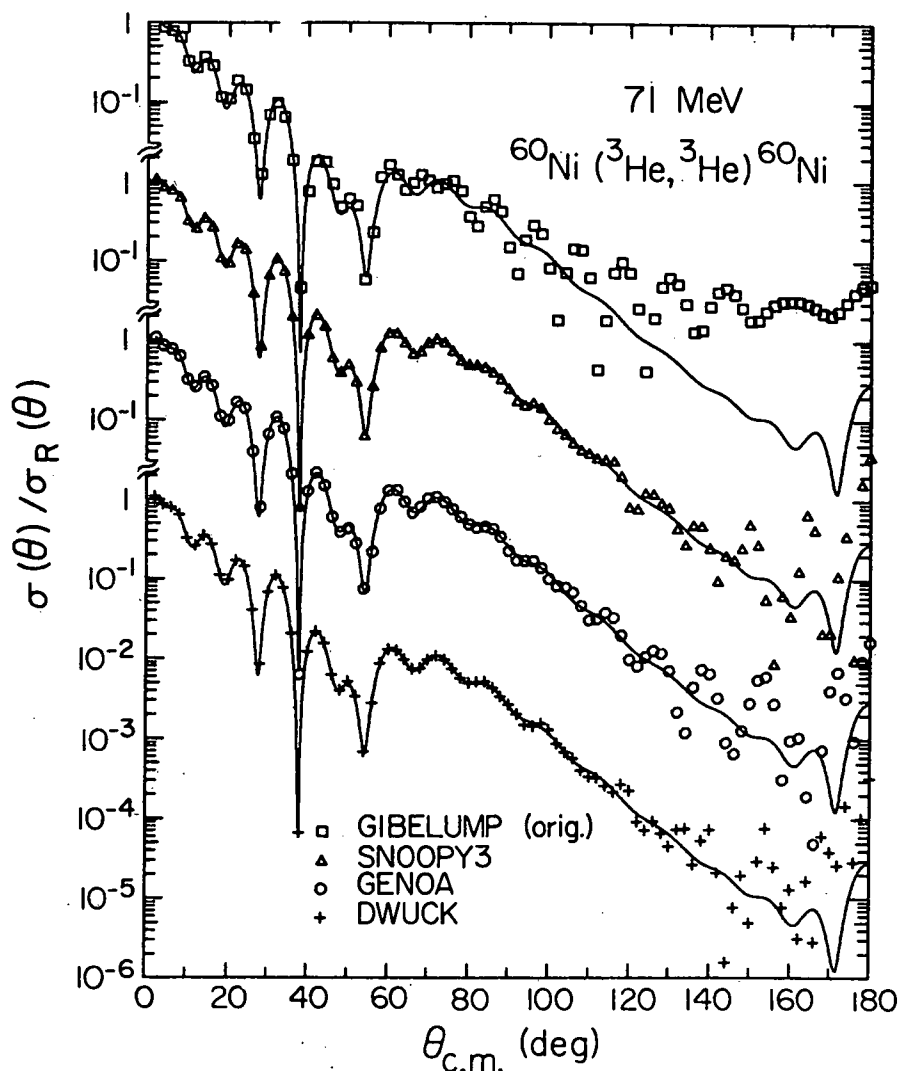
Fig. 1    Comparison of elastic scattering calculated with 4 codes from the same potential. The reference lines are from a more accurate calculation with a modified version of GIBELUMP (SGIB)

TABLE I

70 MeV $^3$He Optical-Model Parameters

| | $V_R$ | $r_R$ | $a_R$ | $W_D$ | $r_I$ | $a_I$ | $V_{SO}$ | $\chi^2/N$ |
|---|---|---|---|---|---|---|---|---|
| $^{50}$Ti | 103.6 | 1.24 | .747 | 19.9 | 1.25 | .795 | 0.0 | 6.7 |
| | 113.4 | 1.17 | .794 | 19.1 | 1.27 | .799 | 3.0 | 8.7 |
| $^{51}$V | 106.5 | 1.22 | .768 | 19.3 | 1.24 | .825 | 0.0 | 8.6 |
| | 123.2 | 1.11 | .842 | 18.4 | 1.27 | .820 | 3.0 | 17 |
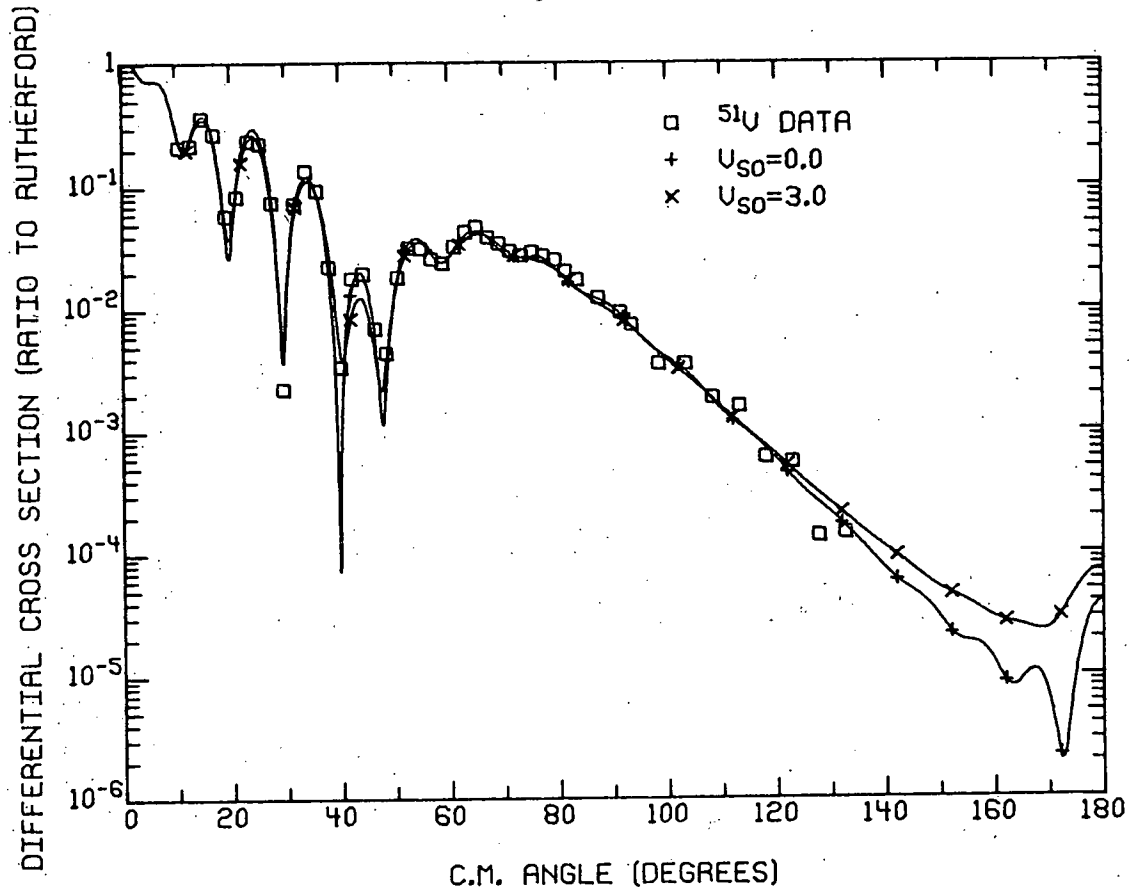


Fig. 2    Best fits to 70 MeV $^3$He elastic scattering from $^{51}$V with the spin-orbit potential fixed at 0.0 and 3.0 MeV.   Corresponding optical-model parameters are listed in the table.

Electromagnetic Transitions in $^{56}$Co Below 2.85 MeV of Excitation
from the $^{56}$Fe(p,nγ)$^{56}$Co Reaction

L.E. Samuelson, W.H. Kelly, R.A. Warner, R.R. Todd,* Wm.C. McHarris
F.M. Bernthal, E.M. Bernstein,* and R. Shamu*

As a continuation of our study of $^{56}$Co using $^{56}$Fe(p,nγ)$^{56}$Co, we have recently performed two-dimensional γ-γ coincidence experiments using proton beams with energies of 7.38 and 8.36 MeV (corresponding to excitations in $^{56}$Co of 1.89 and 2.85 MeV, respectively) supplied by the MSU cyclotron. The purposes of these experiments were to confirm the decay scheme[1,2] previously proposed from γ-ray thresholds that were obtained from excitation functions up to 1.8 MeV of excitation, and to search for those electromagnetic transitions deexciting higher lying states.

The target was an iron foil enriched to 99.4% $^{56}$Fe having a thickness of 0.90 mg/cm$^2$. A Ge(Li)-Ge(Li) spectrometer positioned in the geometry shown in Fig. 1 was used to detect the coincident γ rays. The lead block placed between the detectors served as a beam dump as well as an attenuator for coincident Compton events scattering from one detector into the other. A typical fast-slow coincidence circuit utilizing constant-fraction timing discrimination (2τ≈50 nsec) was used. The coincidence events were stored on magnetic tape and later sorted off-line using background subtraction. The 7.38-MeV spectrum accumulated 1 million coincidence events in 12 hours of counting, while the 8.36-MeV spectrum accumulated close to 7 million coincidence events in 31 hours. Typical singles counting rates for both runs were 7000 cts/sec in the 2.5%-efficient detector and 20,000 cts/sec in the 7.4%-efficient detector. Typical beam currents were about 7 nA.

The two integral spectra, as well as some representative gated spectra from the run with $E_p$=8.36 MeV, are shown in Fig. 2. (A complete set of the gated spectra are given in Ref. 3.) In all, some 35 definite and 7 possible γ rays were identified to be from $^{56}$Co. These include 21 γ rays previously reported to be in coincidence with neutrons by Del Vecchio et al.[4] using the same reaction. The excited-state decay scheme for $^{56}$Co, which is consistent with the γ-γ coincidence data, is shown in Fig. 3. The spin assignments for states below and including the 1720.3-keV state are based upon excitation function and γ-ray angular distribution work previously reported by us,[1,2] while the remaining spin assignments are those of Schneider and Daehnik.[5] The parity assignments are based upon shell-model considerations as well as experimental ℓ-transfers in particle transfer work. (See Ref. 5 and references cited therein.) The γ-ray energies (and, hence, level energies) were determined using the well-known energies[6]

of the simultaneously present $^{56}$Fe γ rays (arising from the $^{56}$Fe(p,p'γ) reaction) and by counting in the presence of γ-ray energy standards of $^{75}$Se, $^{88}$Y, $^{113}$Sn, $^{137}$Cs, and $^{22}$Na.

The γ-ray properties resulting from the work done on $^{56}$Co[1-3] have been compared with shell-model predictions calculated by McGrory.[7] In McGrory's calculations, $^{56}$Co was represented as a $^{40}$Ca core plus 14 or 15 nucleons in the $f_{7/2}$ orbit and the remainder in the $p_{3/2}$, $f_{5/2}$, or $p_{1/2}$ orbits. He used Kuo-Brown matrix elements for the effective two-body Hamiltonian and single particle energies which best reproduced the $^{57}$Ni spectrum. The resulting $^{56}$Co wave functions were used to calculate the reduced transition probabilites, B(M1) and B(E2), from which γ-ray multipole mixing ratios and γ-ray branching ratios were determined. In general, the agreement between theory and experiment was quite good. The results will be presented in the Physical Review.

### References

1. L.E. Samuelson, R.A. Warner, W.H. Kelly, R.R. Todd, and W.C. McHarris, BAPS 16, 12(1971).

2. L.E. Samuelson, Michigan State University Cyclotron Laboratory Annual Report 1970-71, p. 65.

3. L.E. Samuelson, Ph.D. Thesis, Michigan State University, (1972).

4. R. Del Vecchio, R.F. Gibson, and W.W. Daehnik, Phys. Rev. C5, 446(1972).

5. M.J. Schneider and W.W. Daehnik, Phys. Rev. C4, 1649(1971).

6. D.C. Camp and G.L. Meredith, Nucl. Phys. A166, 349(1971).

7. J.B. McGrory, private communication.

* Present Address: Department of Physics, Western Michigan University, Kalamazoo, Michigan.

γ-γ COINC
GEOMETRY
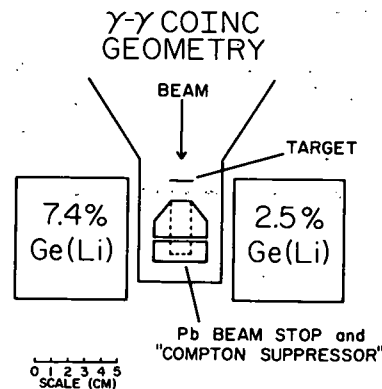
Fig. 1. Geometry for the γ-γ coincidence experiment. The squares represent the position of the Ge(Li) detectors' cryostat caps.

# High Resolution Studies of the $^{59}$Co and $^{60}$Ni(p,d) Reactions

J. Nolen, R.G.H. Robertson, and S. Ewald

The low-lying energy levels of the odd-odd nucleus $^{58}$Co are predominantly of the configuration $(\pi f_{7/2}^{-1})$ coupled to mixtures of neutrons in the $p_{3/2}$, $f_{5/2}$, and $p_{1/2}$ shells.[1,2] However, it is also known that the main $(\pi f_{7/2}^{-1})(\nu f_{7/2}^{-1})$ multiplet strength is in the excitation energy region near 2.7 MeV. The degree to which this $f_{7/2}$ neutron hole strength mixes with the low-lying levels is not known. We are studying the $^{59}$Co(p,d) reaction to shed light on this question and to determine more accurately the detailed wave functions of the low-lying levels of $^{58}$Co.

It is necessary in this work to determine accurately the relative amounts of $\ell=3$ and $\ell=1$ strength in the transition to each level. Since transitions to levels of spin $2\leq J\leq5$ are possibly of such a mixture it is very important to resolve as many energy levels as possible in this experiment. If members of unresolved doublets were individually single $\ell$-value transitions the DWBA could be used to extract the relative yields and good resolution would not be as critical.

Data have been recorded on photographic emulsions at proton bombarding energies of 30 MeV and 35 MeV. The MSU cyclotron-magnetic spectrograph combination were used in the dispersion matching mode to achieve an energy resolution of 5 keV FWHM corresponding to line widths 0.2 mm FWHM. With this resolution the 8 keV doublet at 365.6 keV and 373.7 keV was clearly resolved thereby permitting separate DWBA analysis of each level.

The scanning of the Co plates is nearly complete, but only a preliminary DWBA analysis has been done. A sample $^{58}$Co spectrum is shown in the figure. To check or verify the DWBA prediction we are also studying the transitions from the $^{60}$Ni(p,d) reaction which, for angular momentum reasons, have unique $\ell$-values. It would not be possible to use the DWBA to extract reliable spectroscopic strength from the mixed transitions in Co if good fits were not obtained for the pure transitions in the nearby even-even Ni target. Since $^{59}$Co and $^{60}$Ni both have four neutrons outside the closed N=28 subshell it will also be interesting to see the effect of the change in proton number on the neutron configurations in these targets.

The $^{60}$Ni(p,d) angular distributions were measured at 35 MeV over the angular range 3°-90° with a resistive wire proportional counter in the focal plane of the Enge split-pole spectrograph. In order to verify that certain of the transitions, in regions of unresolved states, are dominated by single levels high resolution data were also recorded on photographic emulsions at a few angles.

This 35 MeV Ni data also extends to higher bombarding energies previous studies in this mass region of (p,d) and (d,p) j-dependence.[3,4] At this bombarding energy the $3/2^-$, $1/2^-$, $\ell=1$ j-dependence seems to be almost completely washed out. At scattering angles less than 90° there is very little effect as indicated in the figure. At angles between 90° and 120° there seems to be only a weak indication of what was a characteristic dip in the $1/2^-$ curves at lower energies. The $5/2^-$, $7/2^-$, $\ell=3$ j-dependence, also shown in the figure, is more pronounced at this energy than it was at the lower energies. The effects are qualitatively the same as in the earlier work: A shift of the primary maximum of the $5/2^-$ curve 4° towards smaller scattering angles relative to the $7/2^-$ curve and the conventional DWBA prediction; and a washing-out of structure in the $7/2^-$ angular distribution relative to the $5/2^-$ curve and the DWBA prediction. Published calculations[5,6] indicate that this qualitative structure difference may be due to the D-state component of the deuteron wave function. However, quantitative calculations at this energy have not been done.

## References

1. R.G.H. Robertson and R.G. Summers-Gill, Can. J. Phys. 49, 1186(1971).

2. M.J. Schneider and W.W. Daehnick, Phys. Rev. C5, 1330(1972).

3. C. Glashausser and M.E. Rickey, Phys. Rev. 154, 1033(1967).

4. J.L. Yntema and H. Ohnuma, Phys. Rev. Letters 19, 1341(1967).

5. R.C. Johnson and F.D. Santos, Particles and Nuclei, 2, 285(1971).

6. G. Delic and B.A. Robson, Nucl. Phys. A193, 510(1972).
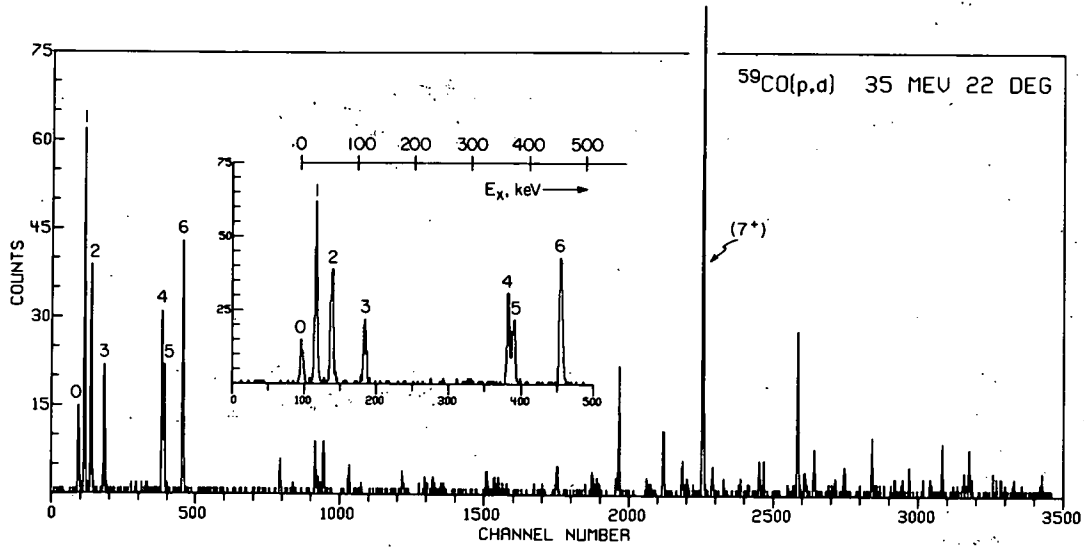
Fig. 1

# $^{60}NI(P,D)$     35 MEV



Fig. 2

24
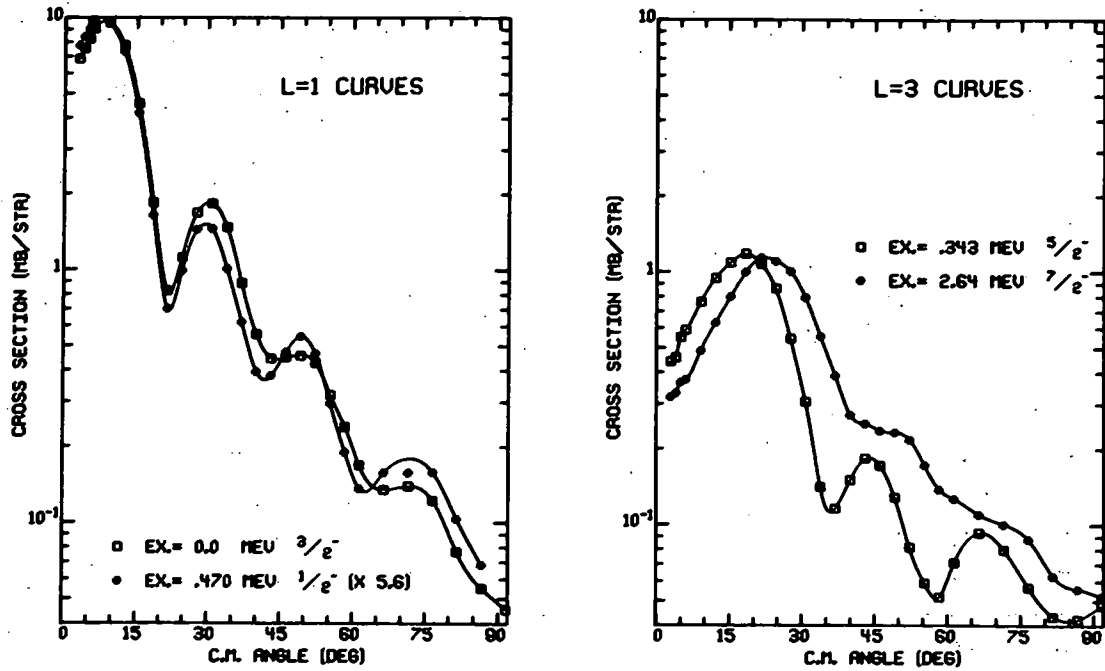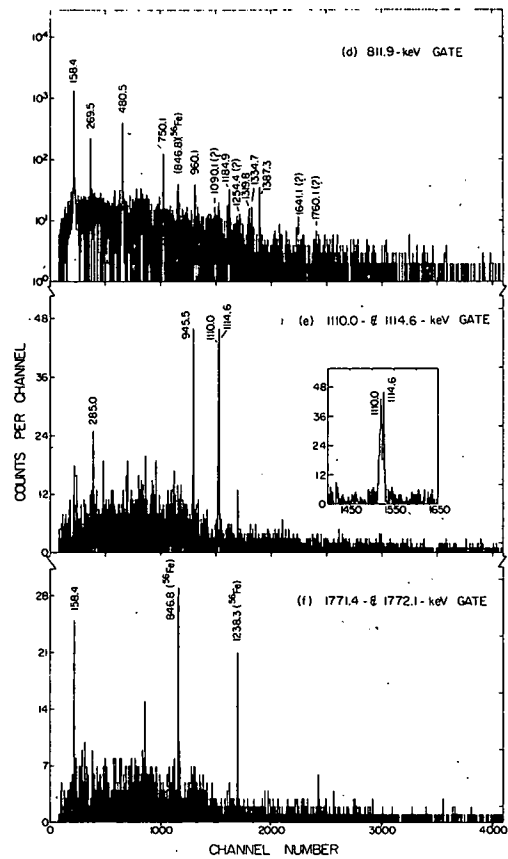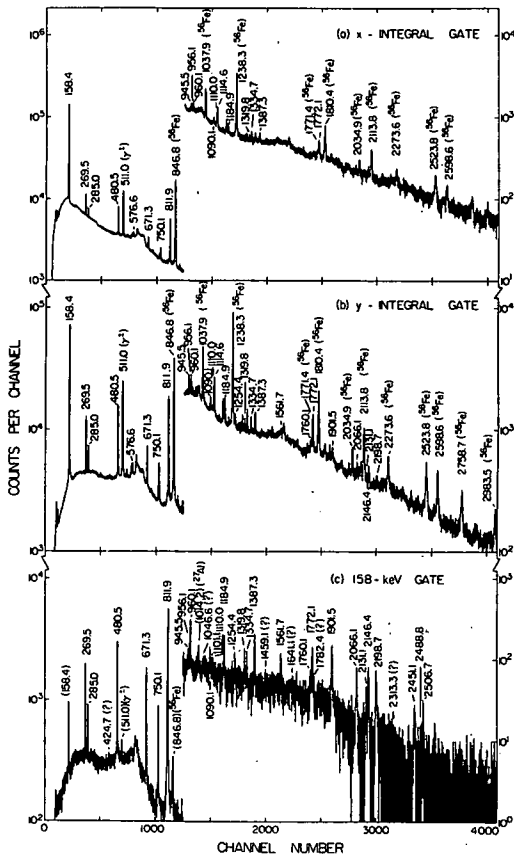
Fig. 2     Integral and representative gated spectra from the $^{56}$Fe(p,n γ-γ)$^{56}$Co γ-γ coincidence experiment with $E_p$=8.36 MeV.



Fig. 3     Excited state decay scheme of $^{56}$Co from the $^{56}$Fe(p,nγ)$^{56}$Co reaction. Dots denote definite coincidence relationships between γ-ray transitions entering and γ-ray transitions leaving a given state. The beam energies (and the corresponding maximum possible $^{56}$Co excitations) at which the γ-γ coincidences and previous γ-ray angular distributions were taken are shown on the right side. Spin and parity assignments are briefly described in the text. Asterisked values are not from the present experiment but are from Ref. 4.
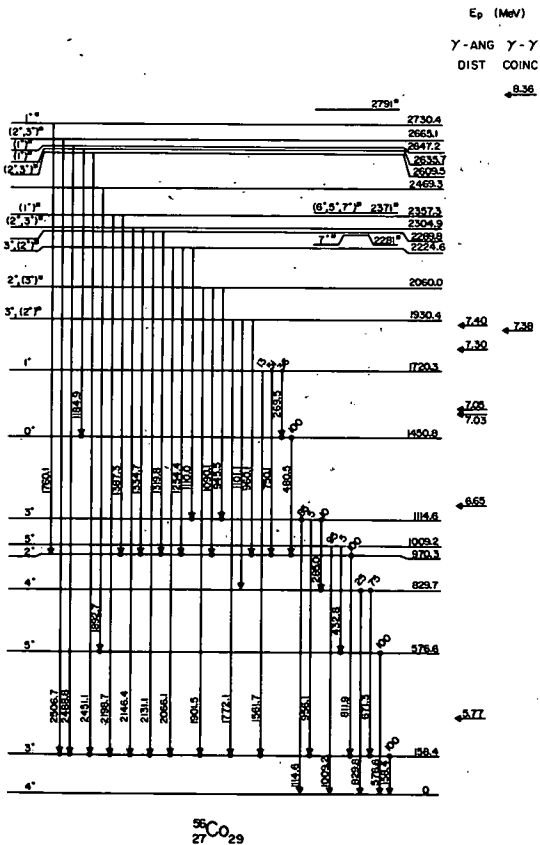
# The Isospin Interaction-(p,n) to Analog States

A. Galonsky, R. Hinrichs, T. Amos, J. Branson,
R. Doering and D. Patterson

In (p,n) transitions between isobaric analog states (IAS) the isospin interaction may be the main, in many cases the total, interaction causing the transition. Consequently, the most direct manner of studying the isospin interaction is through these transitions.

Excitation of the IAS by (p,n) was studied with targets of $^{27}$Al, $^{51}$V, and $^{90}$Zr at proton energies of 22, 30, and 40 MeV. A typical time-of-flight spectrum is shown in Fig. 1 for the Zr target with $E_p$=30 MeV. The ground state (unresolved) of $^{90}$Nb is near channel 860 (and 360) and the IAS, the only prominent single state, is near channel 820 (and 320). Angular distributions of the IAS at the three bombarding energies are shown in Fig. 2 for $^{27}$Al(p,n)$^{27}$Si, in Fig. 3 for $^{51}$V(p,n)$^{51}$Cr, and in Fig. 4 for $^{90}$Zr(p,n)$^{90}$Nb. In each of these figures there are three sets of data plotted twice each for comparison with various DWBA calculations. On the right side comparison is made with a pure volume interaction and on the left side with a pure surface interaction for the $\vec{t} \cdot \vec{T}$ term of the generalized optical model. The volume interaction has the same geometry as the real well in the optical-model potential, and the surface interaction has the geometry of the derivative of that well. As noted on the figures, three different sets of optical-model parameters were used.

Figure 2 demonstrates that a surface interaction is to be favored over a volume interaction for $^{27}$Al. A look at the $^{51}$V and $^{90}$Zr results in Figs. 3 and 4, however, shows that the isospin form factor is more complicated. For these two targets the surface interaction fits better at 22 and 30 MeV but not at 40 MeV. A mixture of surface and volume is indicated.

We used a complex mixture, $-Vf(X_R)+i4W\frac{d}{dx}f(X_I)$. The Becchetti and Greenlees best-fit parameters were used for generating the distorted waves and for the geometries of the interaction. The results of the calculation, the dotted curves in Fig. 5, lack the structure contained in some of the data. Variations of the interaction were made in which V/W and $r_I$ were separately changed; the distorted waves were unchanged. The results for V/W=2/3 are given by the solid curves in Fig. 5. To obtain the dashed curves we let V/W=2, as in the Becchetti-Greenlees potential, but we increased $r_I$ to 1.35 F. It is seen that a reasonable fit is obtained in most cases.

The isospin strengths obtained from both the real and the complex analyses diminished with increasing proton energy for all three targets. Most of the decrease occurs between 22 and 30 MeV, perhaps indicating a surprising persistence of compound-nucleus effects.

It is clear that there are enough parameters in the analysis to allow a variety of solutions that fit some of the data very well and all of the data reasonably well. If the ambiguities are to be removed, and underlying simplicities or systematics in the interaction discovered, there will have to be more and better data. We hope to provide some of this.
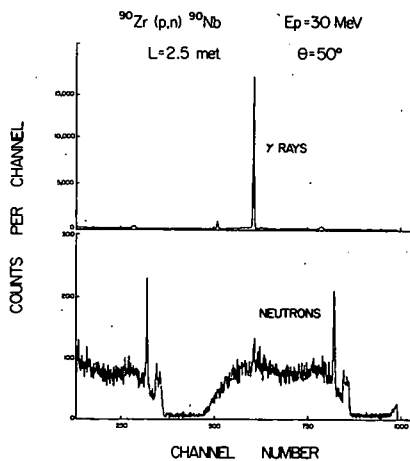


Fig. 1
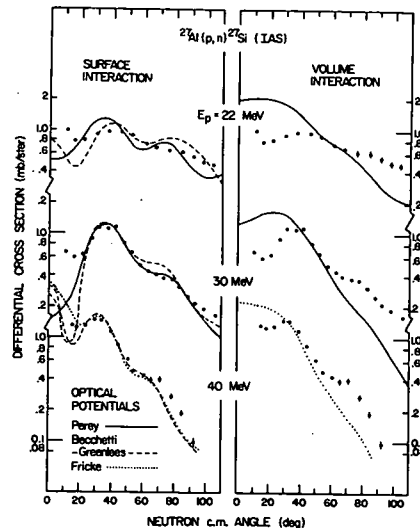


Fig. 2
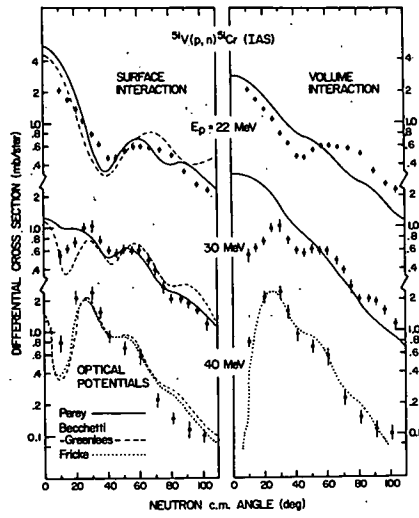
Fig. 3
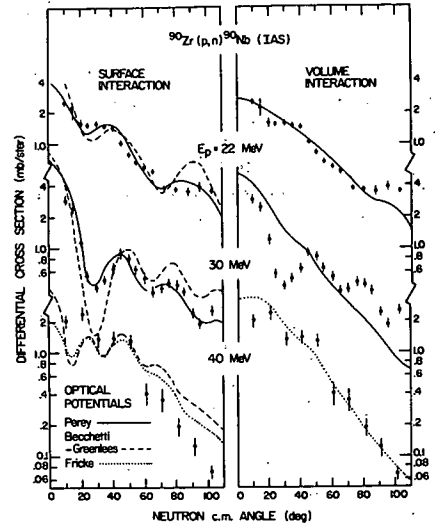


Fig. 4
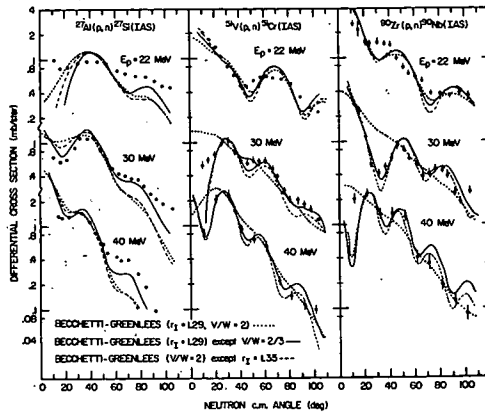


Fig. 5

# Measurement of $\beta^+$ Endpoint of $^{63}$Ga*

R.B. Firestone, K. Kosanke, Wm.C. McHarris, and W.H. Kelly

The decay of 32.4-sec $^{63}$Ga has been studied in great detail by Giesler, McHarris, et al. at this laboratory.[1] An important missing piece of data at this point is the $\beta^+$ endpoint energy for decay to the ground state of $^{63}$Zn. From the systematics of this region, the $\beta^+$ endpoint has been predicted to be 4.6 MeV.

In order to measure this endpoint, a pilot B plastic scintillator was constructed 4.5 cm in diameter and 9 cm deep. This scintillator was mounted on an EMI 95308 photomultiplier tube. The tube was operated at 1000 V and the resolution for 662-keV conversion electrons was 20% (FWHM). This was acceptable because the detector was designed primarily for high energy particles and even then only to measure endpoints. All sources were measured both with and without absorbers in front of the detector such that correction could be made for the contribution of γ-ray Compton electrons to the spectra.

Sources of $^{63}$Ga were produced using 30-MeV protons from the Michigan State University sector focussed cyclotron on a natural Zn target. Because of the short half-life (32.4-sec) of $^{63}$Ga, recoils

from the target were collected by a He-thermalizer jet transport system and deposited in front of the detector on a moving tape transport so as not to allow a build up of longer lived activities. The energy calibration of the system was performed using $^{64}$Ga and $^{144}$Pr standards.

A modified Fermi-Kurie plot (2) for $^{63}$Ga decay is shown in Fig. 1. A tentative endpoint of 4.5$\pm$0.1 MeV is measured, although it was necessary to strip out higher energy betas from the $^{64}$Ga decay which are also produced. This is in good agreement with the prediction. Transitions to excited states were not resolvable, and in future experiments β-γ coincidence data will be taken to determine these.

## References

1. G.C. Gielser, Ph.D. Thesis, Michigan State University, COO-1779-55 (1971); G.C. Gielser, MSU Cyclotron Laboratory Annual Report for 1970-71, p. 67.

2. J.G. Kramer, B.J. Farmer, and C.M. Class, Nucl. Instr. and Methods 16, 289(1962).
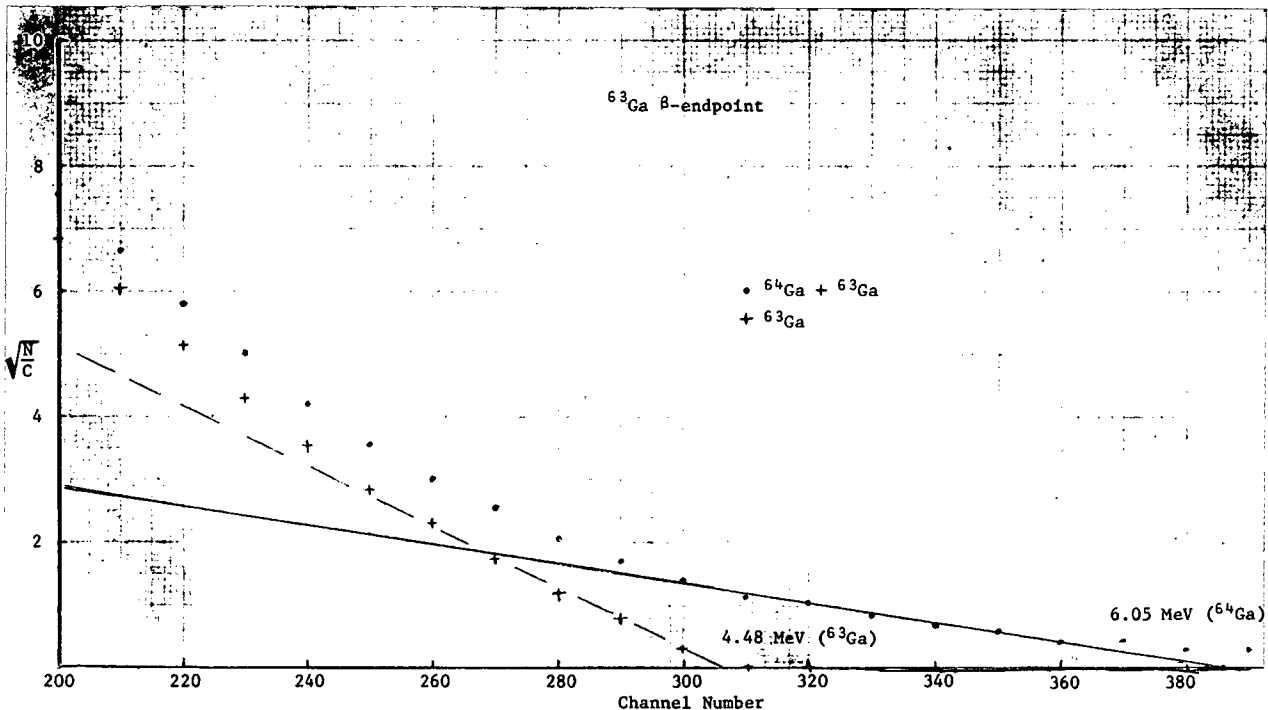
Fig. 1  Adjusted Kurie plot of betas from $^{63}$Ga and $^{64}$Ga decay measured with a large Pilot B plastic scintillator detector. Non-linearity at lower energies is due to lower energy beta branches which were not resolvable in a Kurie plot.

# The Odd-Odd Nucleus $^{116}_{51}Sb_{65}$*

C.B. Morgan,  Jean Guile, R.A. Warner, W.B. Chaffee, W.C. McHarris,
W.H. Kelly, E.M. Bernstein,** and R. Shamu**

Experimental investigations are underway of the states of both odd- and even-mass antimony isotopes. Radioactive decay, particle transfer and (p,nγ) reactions are being used in a co-ordinated way to determine the low-lying states and their properties. These studies are motivated by an interest in the systematic behavior of the excited states and in the residual p-n interaction in this region of the periodic table. We have already studied extensively the radioactive decays of the odd-mass telluriums to the antimonies. Most recently we have begun experiments on $^{116}$Sb.

Previous experiments[1] with a Ge(Li)-NaI(Tl) coincidence spectrometer on the decay of the 2.5-hour $^{116}$Te have suggested excited states at 93.5 and 723.5 keV with another state tenatively placed at 196.5 keV. Internal conversion experiments[2] have shown the 93.5-keV transition to be an E2 and a 103.2-keV transition an E1.

To date, we have performed only a few in-beam gamma-ray experiments using the $^{116}Sn(p,n\gamma)^{116}Sb$ reaction: namely, excitation functions and γ-γ [Ge(Li)-Ge(Li)] coincidence measurements.

Figure 1 is the Ge(Li) gamma-ray spectrum obtained at approximately 1.0 MeV of excitation. Figure 2 contains integral and typical gated coincidence spectra. Table 1 summarizes the coincidence relationships that have been observed. Figure 3 is a <u>preliminary</u> decay scheme suggested by these data.

Since the 93.5 keV transition is an E2,[2] one expects this transition to be delayed. No prompt coincidences have been seen with this gamma ray. Conflicting coincidence data indicate that some of the transitions maybe doublets.

Additional gamma-ray experiments will be performed at higher resolution as well as timing ans coincidence experiments at a low excitation energy. Gamma-ray angular distributions combined with particle transfer experiments will be performed as well.

## References

1. O. Rahmouni, Le Journal de Physique 29, 550(1968).

2. R.W. Fink, G. Anderson and J. Katele, Arkiv Fysik 19, 323(1961).

TABLE I

Summary of Prompt γ-γ Coincidence Results and the Excitation Energies at Which Each Transition was First Observed

| Gated γ-Ray (keV) | Excitation (keV) | Coincident γ-Ray (keV) |
|---|---|---|
| 103 | 155 | 108,158,308,353,364, 551, 712 |
| 108 | 380 | 103,364 |
| 158 | | 103,353,481 |
| 308 | 680 | 103 |
| 353 | 580 | 103,158 |
| 364 | 580 | 103,108 |
| 367 | 1180 | 103,551 |
| 395 | 1280 | 629 |
| 404 | 980 | 411 |
| 411 | 480 | 404,471 |
| 424 | 580 | 481,706 |
| 455 | 680 | 158 |
| 471 | 780 | 103,411 |
| 481 | 680 | 158,364,424,518 |
| 518 | 680 | 481,706 |
| 551 | 680 | 103,367 |
| 629 | 880 | 103,364,395 |
| 706 | 1480 | 424,518 |
| 712 | 980 | 103 |

Fig. 1 Typical $^{116}$Sb singles spectrum taken at approximately 1.0 MeV of excitation via the (p,nγ) reaction.
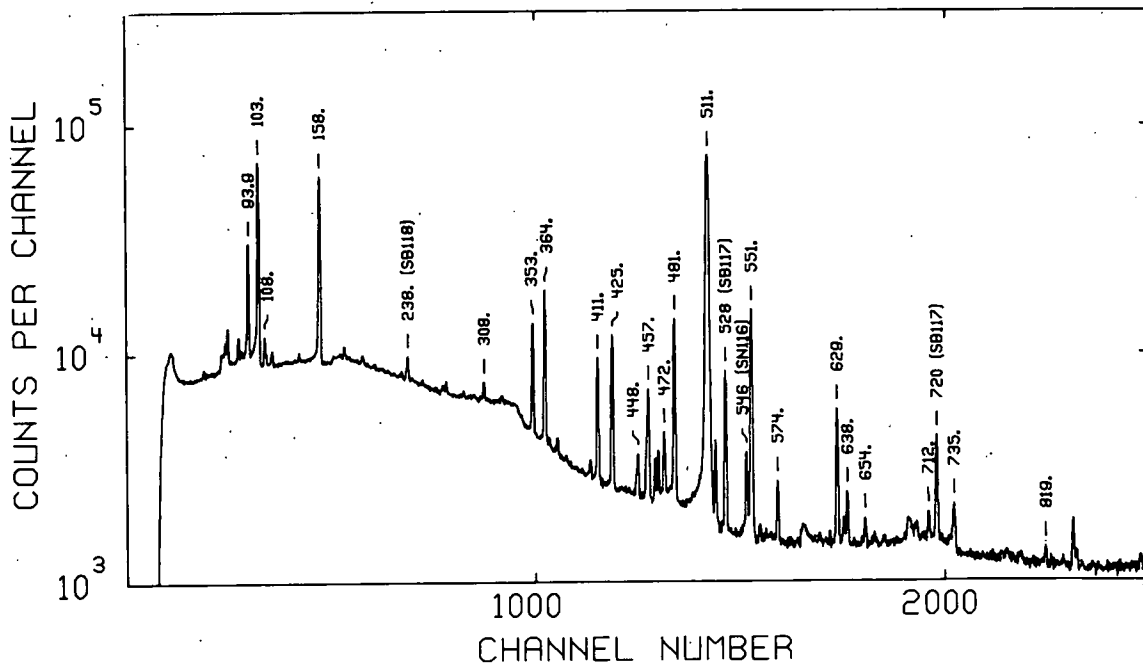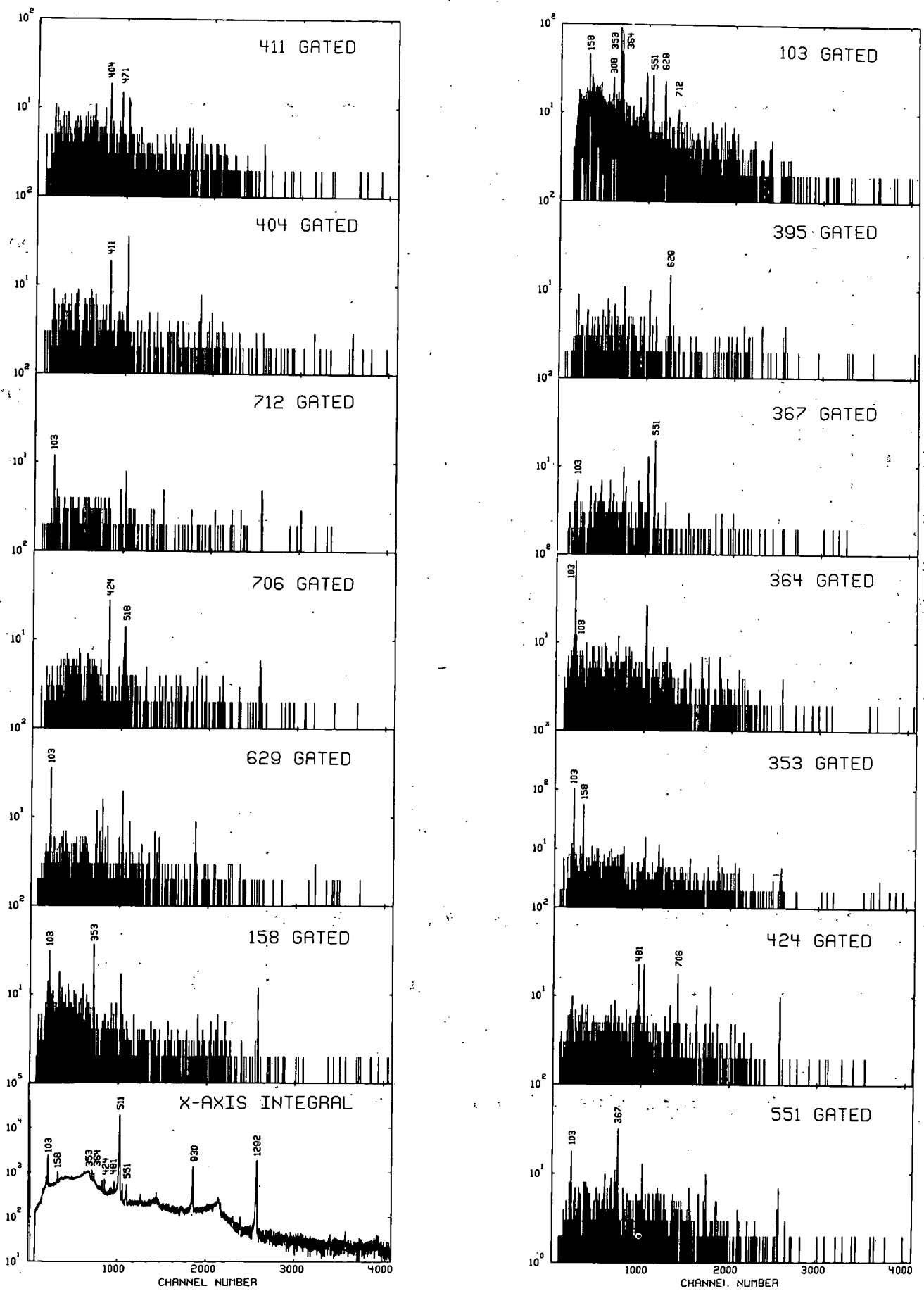
Fig. 2   Integral and gated spectra of $^{116}$Sb γ-γ coincidence.
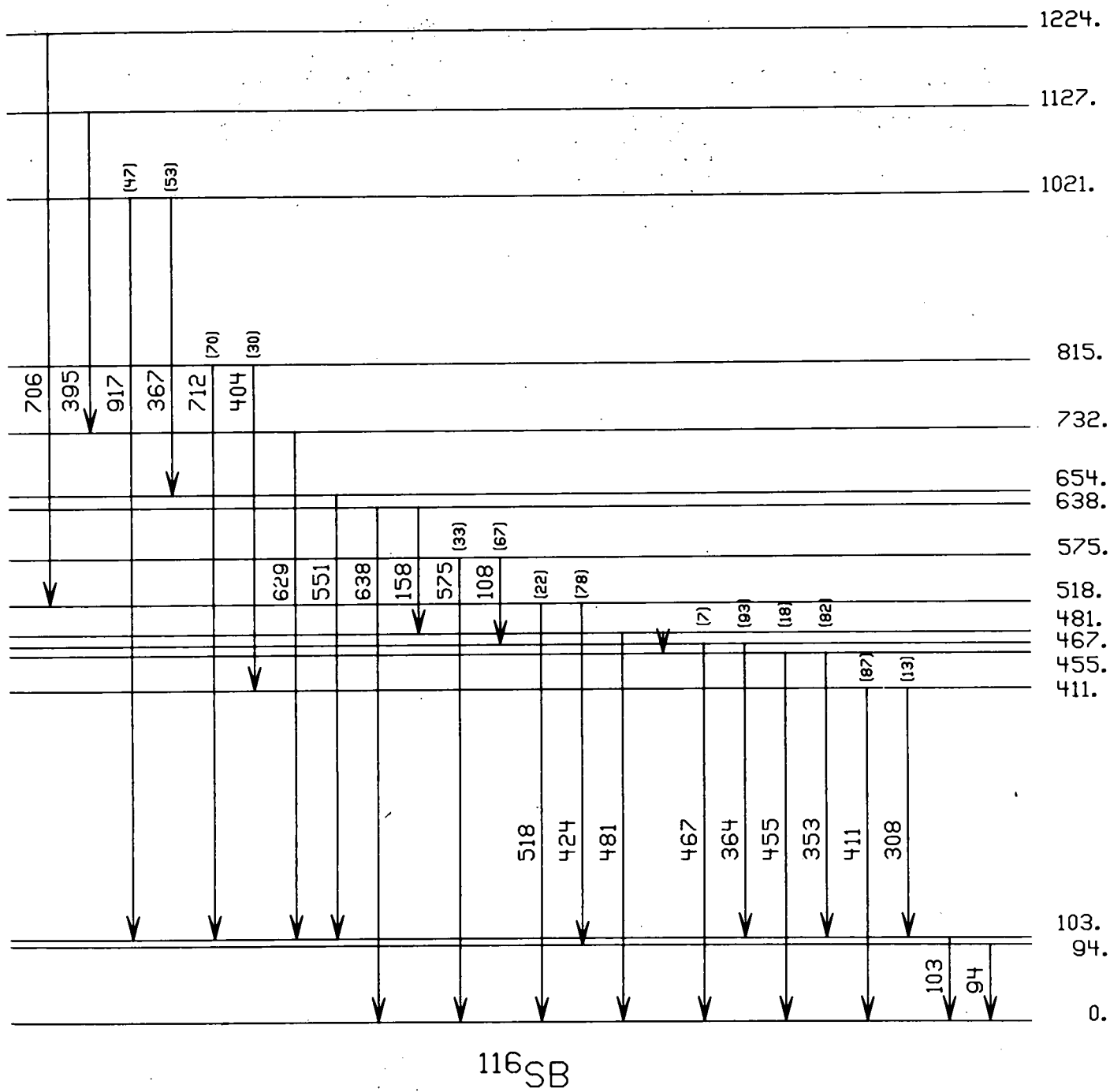
Fig. 3  A preliminary level scheme for $^{116}$Sb.

W.B. Chaffee, C.B. Morgan, R.A. Warner, Wm.C. McHarris,
W.H. Kelly, E.M. Berntein,** and R. Shamu**

A systematic investigation of the energy levels of the odd-odd nucleus $^{118}_{51}$Sb has been undertaken using gamma-ray spectroscopy with the reaction $^{118}_{50}$Sb(p,nγ)$^{118}_{51}$Sb, and also by using charged particle spectroscopy with the reactions $^{118}$Sn($^{3}$He,t)$^{118}$Sb, $^{117}$Sn($^{3}$He,d)$^{118}$Sb, and $^{117}$Sn($^{4}$He,t)$^{118}$Sb.

Very little has been known about the excited states of this nuclide. The ground state ($J^{\pi}=1^{+}$) with half-life of 3.5 minutes, an isomeric state ($8^{-}$) with half-life of 5.1 hour and an isomeric state with half-life of 0.87 seconds are all that have been reported.[1] The two spin assignments are well documented,[2,3] although the energy of the $8^{-}$ level at 190 keV is ambiguous.

For the (p,nγ) experiments, enriched metallic $^{118}$Sn targets were bombarded with protons from the MSU sector-focused cyclotron and from the Western Michigan University tandem-Van de Graaff accelerator. A series of excitation functions were obtained – using beam energies from 4.45 MeV to 6.30 MeV. These energies provided excitation from 70 keV below threshold to 1800 keV above. Gamma rays resulting from the reaction were detected by one of several Ge(Li) detectors, processed by standard state-of-the art electronics and Northern Scientific ADC's. Data were stored for later analysis on the Cyclotron Laboratory's Sigma 7 computer.

By raising the energy of the proton beams in slow stages and counting the emitted gamma radiation it was possible to identify, by the rapid increase in intensity, those gamma's which were due to the de-excitation of states in $^{118}$Sb and the threshold energies for these states. The accompanying $^{118}$Sn(p,γ)$^{119}$Sb* whose Q-value is +5.12 MeV, contains intense gamma transitions at 270.3 and 644.1 keV. Since the change of excitation for these gammas over the bombardment energy range was small, the intensity of these transitions provided a convenient normalization, with the relative intensity of these two providing a check on the data reduction techniques. Subsequent analyses of the spectral data were made using the peak fitting program SAMPO.[4] Two such spectra are shown in Fig. 1. The upper spectrum was taken with a proton beam energy of 5.40 MeV, corresponding to an excitation of 880 keV. The lower spectrum, taken with a proton beam of 4.45 MeV, was below threshold for the $^{118}$Sn(p,nγ)$^{118}$Sb Reaction.

A series of gamma-gamma prompt coincidence experiments were also performed. A pair of Ge(Li) detectors in 180° geometry bracketed the beam line. A wedge shaped block of lead with an axial hole drilled partially through it was placed directly behind the target and between the two detectors. This acted as a beam stop, and reduced Compton scattering between the two detectors. The coincidence output from each detector, timed to <40 n seconds with a TPHC, was stored as two halves of a word on magnetic tape for processing later. Setting gates on selected peaks and recovering the data from the tape using background subtraction made the observation of the gamma cascades possible. An "any-coincidence" spectrum and two selected gated coincidence spectra are illustrated in Fig. 2. This run was at a bombardment energy of 5.54 MeV which corresponds to an excitation of 1000 keV.

A study of the levels of $^{118}$Sb by charged particle transfer reactions was also carried out in order to aid in the placement of the excited states. These used beams of $^{4}$He and $^{3}$He particles at energies from 32 MeV to 40 MeV. Evaporated enriched (96.6%, for $^{118}$Sn, 78.8%, for $^{117}$Sn) targets were mounted in the scattering chamber of the Enge split-pole spectrometer and the reaction particles were focussed on NTB 25μ plates. All of these data have not yet been analyzed so only preliminary findings are included in the decay scheme. The lowest energy levels of $^{118}$Sb, as seen on four of the plates, is illustrated in Fig. 3.

A total of 86 gamma rays have been identified as probably belonging to the de-excitation of the levels of $^{118}$Sb below 1300 keV. Of these, 52 have been identified as being in coincidence with one or more other transitions. With these coincident gammas, the threshold values from the excitation curves and the levels obtained from the plate data, a preliminary decay scheme has been obtained and is shown in Fig. 4.

Experiments attempting to find the threshold of any gammas which might be feeding the $8^{-}$ state were of limited success. These experiments indicate that the $8^{-}$ state lies at an excitation <200 keV. No gamma-rays feeding this state have been identified. No evidence of the reported isomeric state with lifetime of 0.875 sec. has been found.

## References

1. C.M. Lederer, J.M. Hollander, and I. Perlman, Table of Isotopes, 6th Ed., 1967, p. 261 and references cited therein.

2. H.H. Bolotin, A.C. Li, and A. Schwarzschild, Phys. Rev. 124, 213(1961).

3. A.D. Jackson, Jr., E.H. Rogers, Jr., and G.J. Garrett, Phys. Rev. 175, 65(1968).

4. J.T. Routti, S.G. Prussin, Nucl. Instr. and Methods 72, 125(1969).

FIGURE 1



FIGURE 2



FIGURE 3



FIGURE 4

Recently there has become available a large amount of experimental information on the N=82 nuclei. Proton and neutron transfer reactions, inelastic proton, neutron and alpha scattering, and electromagnetic transitions have all been studied in an attempt to understand the structure of these nuclei. Experimental evidence indicates that Z=50, N=82 forms a good doubly closed core, and the N=82 nuclei are then formed by adding from 1-14 protons in the next major proton shell.

Two different theoretical approaches have been applied to these nuclei. The approach used by Waroquier and Heyde,[1] Freed and Miles,[2] and Rho[3] is based on BCS quasiparticle theory which works quite well for single closed shell nuclei such as the N=82 nuclei. This theory is quite easy to calculate with—for example the energy matrices are generally less than 40x40.

The calculation we report here was done in the standard shell model formalism using the Oak Ridge-Rochester shell model codes.[4] The basis space for the calculation included the $1g_{7/2}$, $2d_{5/2}$, $2d_{3/2}$, and $3s_{1/2}$ single particle orbitals—the $h_{11/2}$ orbital was not included and hence no negative parity states were calculated. However, this basis space must be truncated in order to keep the dimensionality of the energy matrices to such a size that they can be diagonalized.

The shell model calculations of Wildenthal were actually done by distributing active protons over the $1g_{7/2}-2d_{5/2}$ orbitals in all Pauli allowed ways, and in addition including those configurations which allowed one particle in either the $3s_{1/2}$ or $2d_{3/2}$ orbitals and distributed the remaining (n-1) protons over the $1g_{7/2}-2d_{5/2}$ space. This led to energy matrices which were 290x290 for the $7/2^+$ states in $^{139}$La.

The two-body interaction was parameterized in terms of the modified surface delta interaction. The 2 parameters of the interaction, as well as the 4 single particle energies—a total of 6 parameters—were obtained by a fitting technique which required an rms minimum between calculated and experimental level energies.

Two sets of calculations were done. The parameters for the first Hamiltonian were obtained by fitting to nuclei from $^{136}$Xe to $^{145}$Eu. (A=136-145 Hamiltonian) The second set of calculations was done using parameters obtained from fitting to nuclei from $^{136}$Xe to $^{140}$Ce. (A=136-140 Hamiltonian) The basis space was the same for both sets of calculations, only the parameters of the Hamiltonian differed. The basic difference between the two Hamiltonians is the $g_{7/2}-d_{5/2}$

single particle splitting, which increases from 500 keV for A=136-145 Hamiltonian to 900 keV for the A=136-140 interaction. Good agreement is obtained between the calculated energies and their experimental counterparts with both Hamiltonians for nuclei around A=138-140.[5,6]

We present here the results for the B(E2) transition rates for $^{138}$Ba and the B(M1) and B(E2) rates for $^{139}$La. An effective proton charge of 1.5 was used, consistent with that found for the s-d shell and the lead region. We also increased $g_{\ell}^{p}$ from the free particle value of 1.0 to 1.1, based on recent results by Nagamiya and Yamazaki.[7]

Table I shows a comparison between experiment and theory for $^{138}$Ba. We also show the results of the quasi-particle calculations of Waroquier and Heyde. For the $2_1^+ \rightarrow 0_{g.s.}^+$ transition, the A=136-145 interaction predicts a B(E2) 10% too low, A=136-140 predicts a B(E2) 30% low, while if a value of $e_p$=1.5 is used in the WH calculation, their B(E2) is 50% low. The $6^+ \rightarrow 4^+$ transition in the N=82 nuclei is an isomeric transition, and thus has a small B(E2). The quadrupole moment of the first excited $2^+$ state in $^{138}$Ba is predicted oblate, but too large by the shell model.

Tables 2-5 shows the results for $^{139}$La. Freed and Miles used the free particle values for $g_p^{\ell}$ and $g_p^{s}$, while WH fit to the known magnetic dipole moments to get $g_s^{p}$. The B(M1) from $7/2^+ \rightarrow 5/2^+$ is forbidden in the single quasiparticle picture since the initial and final states differ in the orbital angular momentum quantum number, so the B(M1) is due solely to admixtures in the wave functions. The two shell model calculations are consistent with experiment.

References

1. M. Waroquier and K. Heyde, Nucl. Phys. A164, 113(1971).

2. N. Freed and W. Miles, Nucl. Phys. A158, 230(1970).

3. M. Rho, Nucl. Phys. 65, 497(1965).

4. J.B. French, E.C. Halbert, J.B. McGrory, and S.S.M. Wong, Advances in Nuclear Physics, Vol. III, eds. M. Baranger and E. Vogt, (Plenum Press, New York, 1969).

5. B.H. Wildenthal, Phys. Rev. Letters 22, 1118(1969).

6. B.H. Wildenthal and D. Larson, Phys. Letters 37B, 266(1971).

7. S. Nagamiya and T. Yamazaki, Phys. Rev. C4, 1961(1971).

| Observables | Interaction A=136-145 | Interaction A=136-140 | Waroquier & Heyde | Experiment |
|---|---|---|---|---|
| B(E2) $2^+_1 \to 0^+$ g.s. | 392 $e^2f^4$ $e_p$=1.5 | 308 $e^2f^4$ $e_p$=1.5 | 426 $e^2f^4$ $e_p$=2 | 442 $e^2f^4$ |
| B(E2) $4^+_1 \to 2^+_1$ | 5.2 $e^2f^4$ $e_p$=1.5 | 27.4 $e^2f^4$ $e_p$=1.5 | 2.19 $e^2f^4$ | 12 $e^2f^4$ |
| B(E2) $6^+_1 \to 4^+_1$ | 17.1 $e^2f^4$ $e_p$=1.5 | 0.47 $e^2f^4$ $e_p$=1.5 | 1.48 $e^2f^4$ | 2.3 $e^2f^4$ |
| Quadrupole Moment of $2^+_1$ | -27.3 $ef^2$ $e_p$=1.5 | -30.4 $ef^2$ $e_p$=1.5 | -8 $ef^2$ | -11$\pm$15 $ef^2$ |

Table 1

$^{139}$La Electromagnetic Properties

| Observables | Interaction A=136-145 | Interaction A=136-140 | Freed & Miles | Heyde & Waroquier | Experiment |
|---|---|---|---|---|---|
| Magnetic Moment Of Ground State | 2.21 n.m. $g_\ell$=1.1 | 2.15 n.m. $g_\ell$=1.1 | 1.70 n.m. | 2.80 n.m. $g_\ell$=1 $g_s$=2.66 | 2.78 n.m. |
| Quadrupole Moment of Ground State | 19.4 $ef^2$ $e_p$=1.5 | 27.3 $ef^2$ $e_p$=1.5 | -0.6 $ef^2$ $e_p$=1.0 | +24.8 $ef^2$ $e_p$=2.0 | +23 $ef^2$ |
| $5/2^+ \to 7/2^+$ g.s. B(E2) | 1.26 $e^2f^4$ $e_p$=1.5 | 0.22 $e^2f^4$ $e_p$=1.5 | 0.10 $e^2f^4$ | 0.27 $e^2f^4$ | 4.8 $e^2f^4$ |
| $5/2^+ \to 7/2^+$ g.s. B(M1) | .00384 n.m.$^2$ | .00136 n.m.$^2$ | .00042 n.m.$^2$ | .0000057 n.m.$^2$ | .0046 n.m.$^2$ |
| Magnetic Moment of $5/2^+$ 1st Excited State | 4.80 n.m. $g_\ell$=1.1 | 4.86 n.m. $g_\ell$=1.1 | | | |
| Quadrupole Moment of $5/2^+$ 1st Excited State | -9.94 $ef^2$ $e_p$=1.5 | -21.0 $ef^2$ $e_p$=1.5 | | | |

Single particle values
$g_\ell$=1.0   $g_s$=5.585

Table 2

B(M1)'s in $^{139}$La ($g_\ell$=1.1)

| 2*Initial State | 2*Final State | Interaction A=136-140 | Interaction A=136-145 | 2*Initial State | 2*Final State | Interaction A=136-140 | Interaction A=136-145 |
|---|---|---|---|---|---|---|---|
| $5_1$ | $7_1$ | .00136 n.m.$^2$ | .00384 n.m.$^2$ | $3_1$ | $5_1$ | .887 n.m.$^2$ | .117 n.m.$^2$ |
| $5_2$ | $7_1$ | .00127 | .000839 | $3_2$ | $5_1$ | .455 | .222 |
| $5_3$ | $7_1$ | .00127 | .00385 | $3_3$ | $5_1$ | .179 | .258 |
| $5_4$ | $7_1$ | .000756 | .00225 | $3_4$ | $5_1$ | .500 | 1.19 |
| $7_2$ | $7_1$ | .00642 | .00961 | $5_2$ | $5_1$ | .0115 | .00486 |
| $7_3$ | $7_1$ | .0000167 | .000169 | $5_3$ | $5_1$ | .00375 | .00971 |
| $7_4$ | $7_1$ | .00253 | .00791 | $5_4$ | $5_1$ | .000316 | .00818 |
| $9_1$ | $7_1$ | .0571 | .0490 | $7_1$ | $5_1$ | .00102 | .00288 |
| $9_2$ | $7_1$ | .00350 | .00293 | $7_2$ | $5_1$ | .00149 | .00453 |
| $9_3$ | $7_1$ | .0000522 | .00219 | $7_3$ | $5_1$ | .000106 | .000118 |
| $9_4$ | $7_1$ | .0104 | .00147 | $7_4$ | $5_1$ | .000384 | .00389 |

Table 3

B(E2)'s in $^{139}$La ($e_p=1.5$)

| 2*Initial State | 2*Final State | Interaction A=136-140 | A=136-145 | 2*Initial State | 2*Final State | Interaction A=136-140 | A=136-145 |
|---|---|---|---|---|---|---|---|
| $3_1$ | $7_1$ | $3.7\ e^2f^4$ | $47.5\ e^2f^4$ | $5_2$ | $5_1$ | $50.4\ e^2f^4$ | $54.2\ e^2f^4$ |
| $3_2$ | $7_1$ | <0.01 | 104 | $5_3$ | $5_1$ | 167 | 252 |
| $5_1$ | $7_1$ | 0.2 | 1.3 | $7_2$ | $5_1$ | 116 | 218 |
| $5_2$ | $7_1$ | 322 | 491 | $7_3$ | $5_1$ | 65.2 | 0.3 |
| $7_2$ | $7_1$ | 6.0 | 0.1 | $3_1$ | $5_1$ | 338 | 500 |
| $7_3$ | $7_1$ | 48.4 | 182 | $3_2$ | $5_1$ | 72.2 | 50 |
| $9_1$ | $7_1$ | 5.7 | 61.0 | $1_1$ | $5_1$ | 682 | - |
| $9_2$ | $7_1$ | 222 | 224 | $1_2$ | $5_1$ | 115 | 207 |
| $11_1$ | $7_1$ | 197 | 311 | $9_1$ | $5_1$ | 232 | 196 |
| $11_2$ | $7_1$ | 2.9 | 0.01 | $9_2$ | $5_1$ | 21.6 | 109 |

Table 4

Characteristics of Low-Lying Levels in $^{139}$La

| $J_\nu^\pi$ | $E_{calc}$ | $E_{expt}$ | Interaction | Model Wave Function (Largest Components)[c] | | |
|---|---|---|---|---|---|---|
| $7/2^+$g.s. | 0.0 | 0.0 | I [a] | $.74(g_7)^5_{J=7}(d_5)^{2,0}_{J=0}$ | $+.46(g_7)^3_{J=7}(d_5)^{4,0}_{J=0}$ | $+.43(g_7)^7_{J=7}$ |
| $7/2^+$g.s. | 0.0 | 0.0 | II [b] | $.66(g_7)^5_{J=7}(d_5)^{2,0}_{J=0}$ | $+.65(g_7)^7_{J=7}$ | $+.28(g_7)^3_{J=7}(d_5)^{4,0}_{J=0}$ |
| $5/2^+_1$ | 0.064 | 0.166 | I | $.70(g_7)^{4,0}_{J=0}(d_5)^3_{J=5}$ | $+.65(g_7)^{6,0}_{J=0}(d_5)^1_{J=5}$ | $-.26(g_7)^{2,0}_{J=0}(d_5)^5_{J=5}$ |
| $5/2^+_1$ | 0.193 | 0.166 | II | $.79(g_7)^{6,0}_{J=0}(d_5)^1_{J=5}$ | $+.56(g_7)^{4,0}_{J=0}(d_5)^3_{J=5}$ | $-.15(g_7)^{2,0}_{J=0}(d_5)^5_{J=5}$ |

Table 5

[a] A=136-145 interaction.
[b] A=136-140 interaction.
[c] Half-integral spins are given as two times their value, i.e. 7/2=7. The additional quantum numbers labeling a few components are the seniorities, e.g. $(g_7)[4,2]$ refers to the seniority 2, coupling of four 7/2 particles coupled to total angular momentum J.

# Low-Lying States of $^{140}$Pr from a Study of the $^{140}$Ce(p,nγ)$^{140}$Pr and $^{141}$Pr(p,d)$^{140}$Pr Reactions*

Jean Guile, R.W. Goles, C.B. Morgan, R.A. Warner, Wm.C. McHarris,
W.H. Kelly, E.M. Bernstein,** and R. Shamu**

In the past year we have undertaken an investigation of the energy levels in yet another odd-odd nucleus, $^{140}_{59}$Pr$_{81}$. Three other studies of this nuclide have been conducted. The first was that done by Fulmer and co-workers[1] in 1962. From a study using the (d,t) reaction on $^{141}$Pr with 60-keV resolution, this group proposed a level scheme. Two years later Krehbiel[2] irradiated $^{141}$Pr with 22 MeV bremsstrahlung and observed two coincident γ-rays of 644±15 keV and 98±5 keV. He also noted that the 98 keV transition was delayed with respect to the 644 keV transition. Taking this information as our starting point, we are examining the excited states of $^{140}$Pr using both the $^{140}$Ce(p,nγ)$^{140}$Pr and $^{141}$Pr(p,d)$^{140}$Pr reactions. Just recently it has come to our attention that a related $^{141}$Pr(p,d)$^{140}$Pr study has been conducted with 30 MeV protons at Texas A&M by Helton and Hiebert.[3] With an achieved resolution of 14 keV on an Enge split-pole spectrograph, they obtained excitation energies up to 430 keV via the (d,t) reaction using 20 MeV deuterons. Their angular distribution measurements were performed with a thin window Ge(Li) detector. Unfortunately, we have not had the opportunity to compare their data with ours.

In our $^{140}$Ce(p,nγ)$^{140}$Pr work both oxide (enriched) and evaporated metal (natural) targets have been used. By incrementing the bombarding energy in small steps from just below that energy required to produce the $^{140}$Pr ground state to approximately 2 MeV of excitation, we have been able to single out those γ-rays of interest. This technique also enables us to place upper limits on the energy of the level deexcited by a particular γ-ray. The energies and relative intensities of the observed γ-rays at 2 MeV of excitation are given in Table I. A γ-γ coincidence experiment has also been performed to help us place these γ-rays in a consistent decay scheme. Although the data resulting from this experiment need a great deal more study, our preliminary results indicate a decay scheme similar to the skeleton shown in Fig. 1. One should note the absence of the previously reported 640 keV transition. Coincidence measurements indicate a strong 140.4 keV-241.2 keV-640.6 keV cascade. This is not displayed in the present decay scheme due to some apparently conflicting evidence concerning its placement. Some of the data indicate that the first excited state may actually be a doublet with a 1.4 keV spacing. The evidence is not yet conclusive and thus the first excited state in our preliminary decay scheme is displayed without any doublet character.

In our $^{141}$Pr(p,d)$^{140}$Pr study we bombarded evaporated metal targets with 35 MeV protons. One of the resulting spectra is displayed beside our decay scheme for easy comparison of the populated levels. The 9 keV resolution attained in this experiment with the Michigan State University magnetic spectrograph has allowed us to resolve several doublets and to place more precise energy values on the deuteron groups. An angular distribution experiment has been performed and the data are now being analyzed.

Although all our results are preliminary at this stage, thus far we are much encouraged by the agreement of this two-sided attack on $^{140}$Pr.

## References

1. R.H. Fulmer, A.L. McCarthy, and B.L. Cohen, Phys. Rev. 128, 1302(1962).

2. H. Krehbiel, Phys. Letters 13, 65(1964).

3. V.D. Helton and J.C. Hiebert, Final Report on Research at the Texas A&M University Cyclotron for the period June 1, 1970-December 31, 1971. ORO-3398-45 (March, 1972).

## TABLE I

Energies and Relative Intensities of γ-rays Observed in $^{140}$Pr at 2 MeV of Excitation

| Energy (keV.) | Relative γ-ray Intensity |
|---|---|
| 98.0±0.3 | 12.0±0.9 |
| 126.9±0.4 | 5.5±0.7 |
| 132.9±0.3 | 41.4±1.9 |
| 140.4±0.3 | 17.4±0.9 |
| 162.0±0.3 | 43.0±3.1 |
| 164.1±0.3 | 41.2±2.0 |
| 212.9±0.5 | 1.5±0.3 |
| 227.3±0.5 | 1.1±0.9 |
| 241.2±0.5 | 49.2±2.1 |
| 243.0±0.5 | 38.7±2.5 |
| 257.2±0.2 | 78.4±4.3 |
| 263.3±0.2 | 10.3±1.2 |
| 270.9±0.2 | 17.3±1.4 |
| 286.7±0.4 | 3.1±0.4 |
| 361.1±0.4 | 2.3±0.2 |
| 368.5±0.4 | 2.8±0.2 |
| 384.6±0.4 | 5.1±0.3 |
| 390.9±0.4 | 3.1±0.3 |
| 393.0±0.4 | 5.5±0.3 |
| 412.4±0.4 | 5.9±0.2 |
| 419.6±0.4 | 8.5±0.3 |
| 546.7±0.4 | 6.5±0.3 |
| 574.4±0.4 | 7.6±0.4 |
| 612.6±0.4 | 4.6±0.3 |
| 633.0±0.4 | 6.1±0.8 |
| 640.6±0.2 | ≡100 |
| 669.5±0.4 | 14.7±0.8 |
| 762.5±0.4 | 8.6±0.4 |
| 876.5±0.3 | 13.8±0.5 |
| 888.0±0.5 | 5.5±0.3 |
| 903.9±0.3 | 16.4±0.5 |
| 939.1±0.4 | 8.2±0.4 |
| 966.9±0.4 | 2.5±0.3 |
| 1035.6±0.4 | 3.8±0.5 |
| 1053.5±0.4 | 5.8±0.4 |
| 1182.9±0.4 | 4.9±0.4 |
| 1201.3±0.4 | 7.3±0.5 |
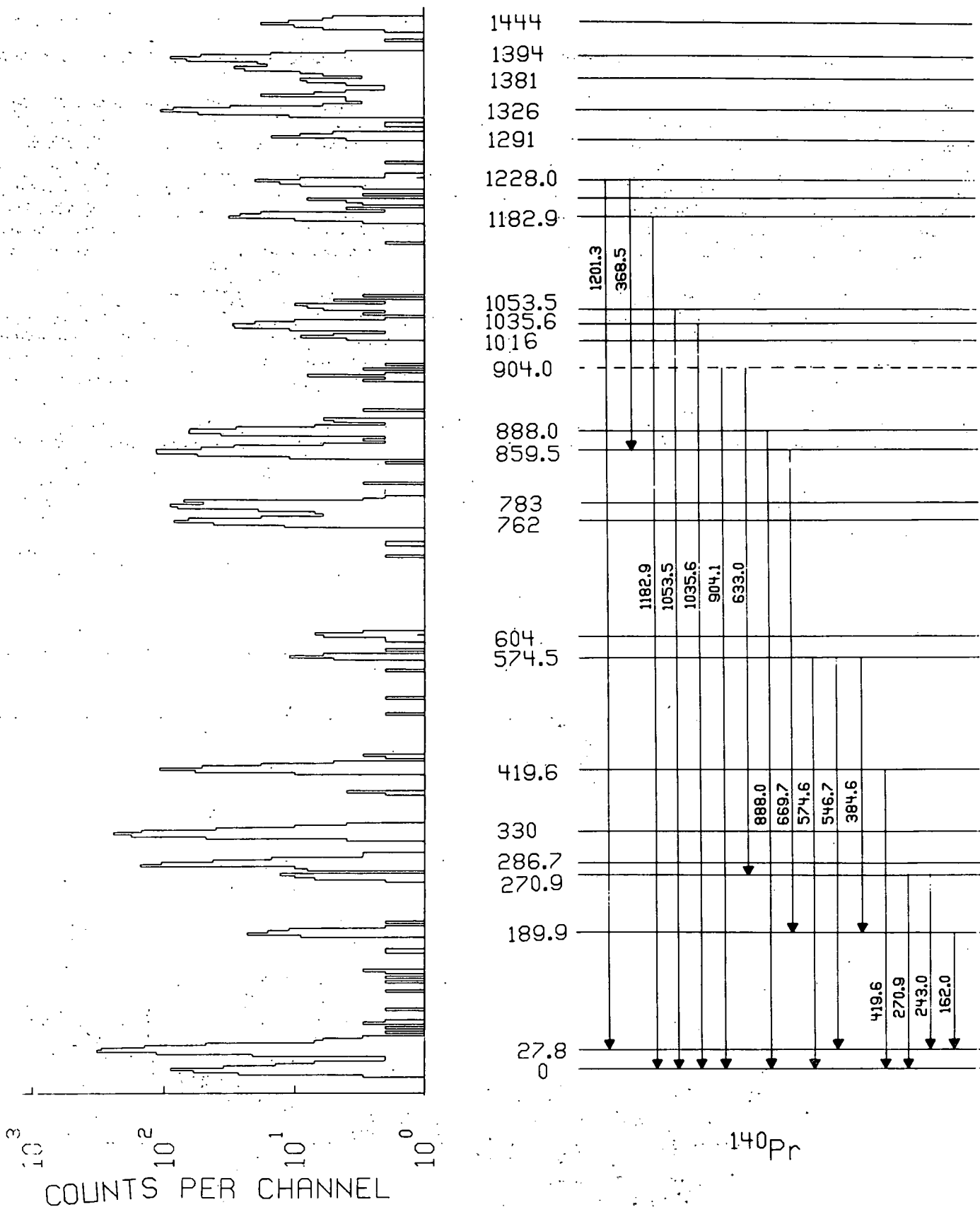
Fig. 1    A preliminary level scheme for $^{140}$Pr incorporating the current (p,d) and (p,nγ) results.   The (p,d) spectrum shown was taken at 45° using 35-MeV protons.

# Lifetime of the 629-keV 11/2⁻ State in $^{141}$Pm*

R.A. Warner, R.R. Todd, R.E. Eppley,** W.H. Kelly, and Wm.C. McHarris

In a recently published study[1] of the decay of $^{141m}$Sm, the level at 628.7 keV excitation in $^{141}$Pm was determined to have $J^{\pi}$=11/2⁻. Transitions to and from this state had been identified in simple one-parameter delayed coincidence experiments. The half-life of this level is now measured to be 0.70±0.02 μsec.

The parent activity was produced by the ($^{3}$He,4n) reaction at 40 MeV on separated $^{142}$Nd. This reaction strongly populates 22.1-min $^{141m}$Sm. The source was not counted until about 10 min after the activation, in order to reduce interference from the 11.3-min $^{141g}$Sm activity. The detectors used in the experiment were a Ge(Li) coaxial crystal with 10.4% efficiency (at 1332 keV and 25 cm, relative to the efficiency of a 7.6x7.6 cm NaI(Tl) crystal), and one-half of a 20x20 cm NaI(Tl) annulus. The signals from these detectors were processed essentially as indicated in Fig. 1. The timing signals from the annulus were derived from that portion of the γ-ray spectrum above the annihilation peak, as 97% of the γ-ray intensity feeding the 629-keV state lies in transitions with energy greater than 538 keV. These transitions depopulate a 3 quasiparticle multiplet centered at about 2 MeV and fed strongly in the $^{141m}$Sm decay.

The 2 ADC's scaled addresses corresponding to the energy deposited in the Ge(Li) counter and the time interval between the pulses from the 2 detectors. These addresses were then recorded in pairs on magnetic tape by EVENT,[2] a task of the JANUS II timesharing system. A isometric view of the spectrum is displayed
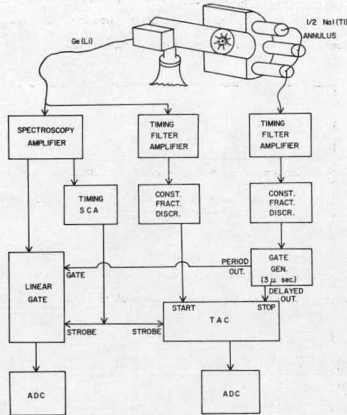


Fig. 1 Diagram of the experimental electronics.
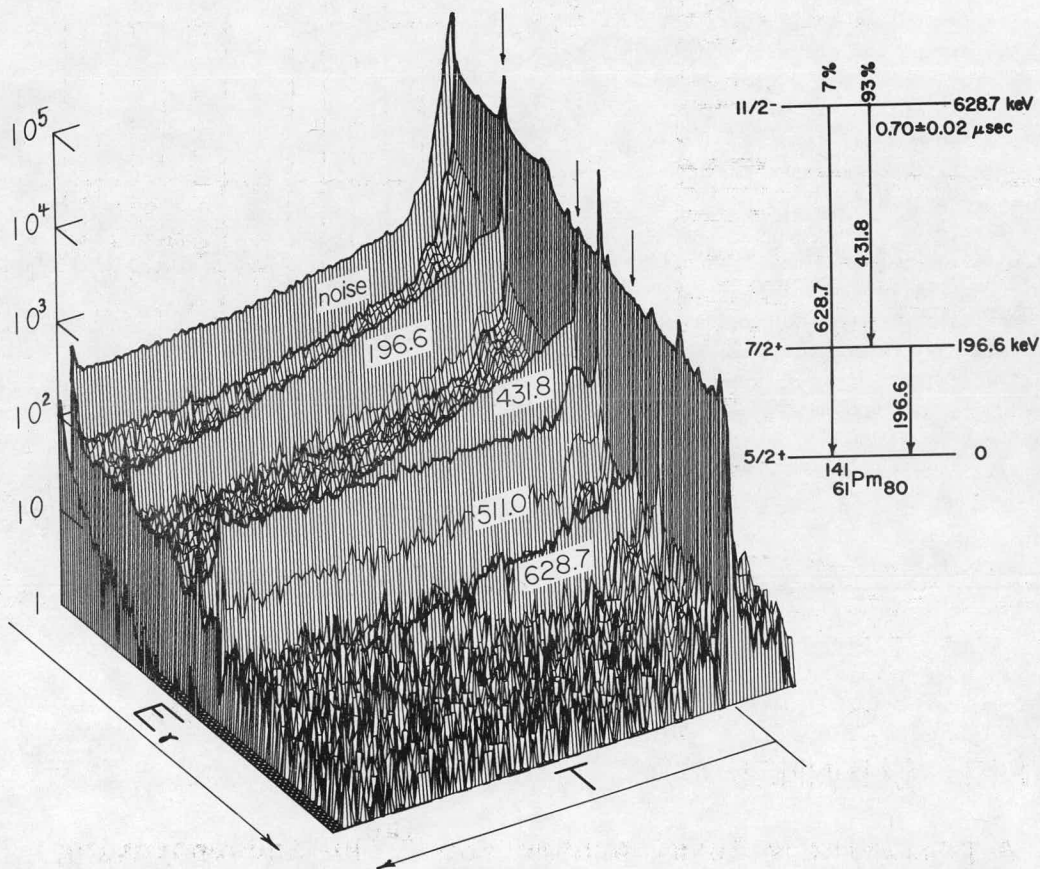


Fig. 2  Isometric view of the 2-parameter data compressed into a 128x128 channel array. The levels and transition relevant to the measurement are shown in the inset.
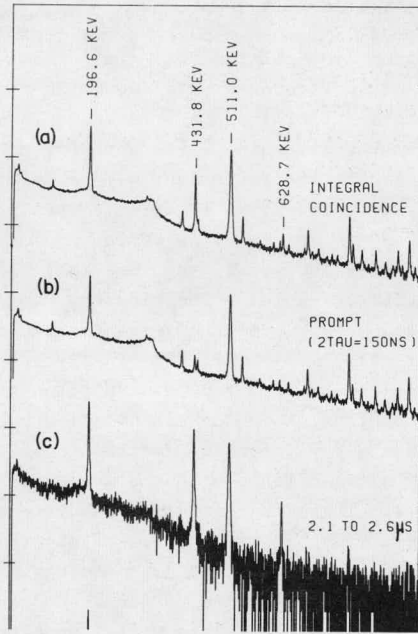
Fig. 3  The Ge(Li) energy spectrum, showing (a) all events, (b) pulses in prompt coincidence with the NaI pulses, and (c) pulses following the NaI pulses by from 2.1 to 2.6 µsec.

in Fig. 2 along with a diagram including only those levels and transitions of interest here.

Figure 3 contains the Ge(Li) energy spectrum separated into prompt and delayed components, while Fig. 4 shows the distribution in time for different peaks in the energy spectrum. Background subtraction was used in the sorting program[3] to remove from the spectra those events in the continuum under the gated peak. The bump just to the left of the prompt peak in the time distribution is the result of an instrumental problem which has little effect on most of the data. The 196.6-, 431.8-, and 628.7-keV transitions all have components decaying with the same half-life, which, when computed from the combined data, is $0.70 \pm 0.02$ µsec. From the known[1] 628.7-keV to 431.8-keV branching ratio, the E3 transition is found to be enhanced by

40% and the M2 transition to be retarded by a factor of 6 when compared with the Moszkowski single-particle estimates.

References

1. R.E. Eppley, R.R. Todd, R.A. Warner, Wm.C. McHarris, and W.H. Kelly, Phys. Rev. C5, 1084(1972).

2. D.L. Bayer, Programs 8 and 13 in MSU Sigma-7 Users Manual.

3. G. Giesler, Program 35 in MSU Sigma-7 Users Manual.
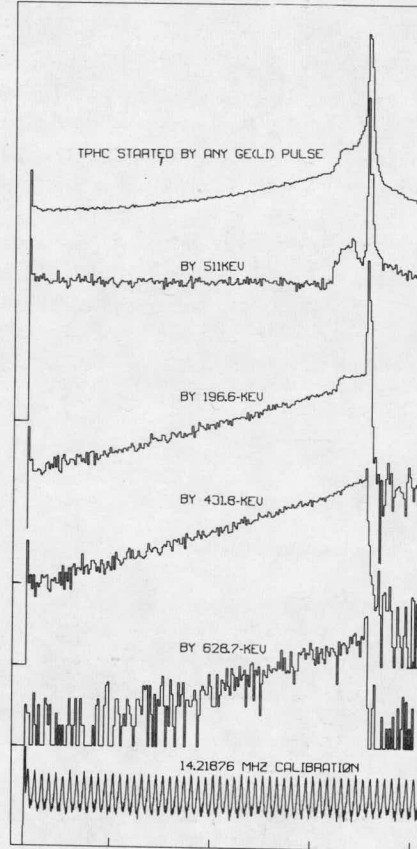
Fig. 4  Distributions in time with respect to the NaI pulses for events in various parts of the Ge(Li) spectrum.

R.R. Todd,** R.E. Eppley,*** R.A. Warner,
Wm.C. McHarris, and W.H. Kelly

As a part of a series of gamma-ray spectro-scopic studies of nuclei near the N=82 closed shell we have recently reported on the decay of $^{141m}$Sm[1] and its subsequent population of a three-quasiparticle multiplet in the daughter $^{141}$Pm. Here, we briefly report on an investigation of the $^{141g}$Sm decay scheme which completes our studies on this isotope.

The $^{141g}$Sm activity has been produced by two methods: the $^{142}$Nd($^3$He,4n)$^{141m+g}$Sm (Q=-27.3 MeV) reaction, and indirectly by the $^{144}$Sm(p,4n)$^{141}$Eu $\overset{EC}{\to}$ $^{141}$Sm reaction (Q=-36.8 MeV). The second method was used to check the results of the first and was an attempt to enhance the re-lative production of $^{141g}$Sm in order to distinguish it better from $^{141m}$Sm which is abundantly pro-duced in the first reaction. The results using this second reaction were only partially successful be-cause of other strong competing reactions.

We have measured the half-life to be 11.3±0.3 min and the γ-rays associated with the $^{141g}$Sm decay have been identified by following the decay through several half-lives. The decay scheme has been constructed using various experimental configurations which include two-dimensional γ-γ coincidence,

anticoincidence and γ-511-511-keV triple coin-cidence experiments.

The study of $^{141g}$Sm is complicated by the pre-sence of the longer-lived and more intense $^{141m}$Sm activity in the same spectra, and by the additional difficulty that almost 90% of the $^{141g}$Sm decay is directly to the ground state of $^{141}$Pm. The strong interference masks many weaker transitions that might be expected.

The energies and relative intensities of the γ-rays observed are presented in Table I. The γ-γ two-dimensional coincidence results [Ge(Li)-Ge(Li)] are presented in Table II. In Fig. 1 we present the decay scheme we have deduced from the current data. The transition and excited state energies are given in keV and the disintegration energy $Q_\epsilon$ is a calculated value.[2] The log(ft) values shown on the decay scheme have been cal-culated by assuming the total EC plus β$^+$ feeding to the $^{141}$Pm ground state by $^{141g}$Sm to be 86.2%.[3]

On the basis of log(ft) values and relative gamma-ray intensities, the spins and parities of the excited states shown in Fig. 1 (excepting the questionable state of 728.0 keV) are expect-ed to be 1/2$^+$, 3/2$^+$, or 5/2$^+$. Since the beta
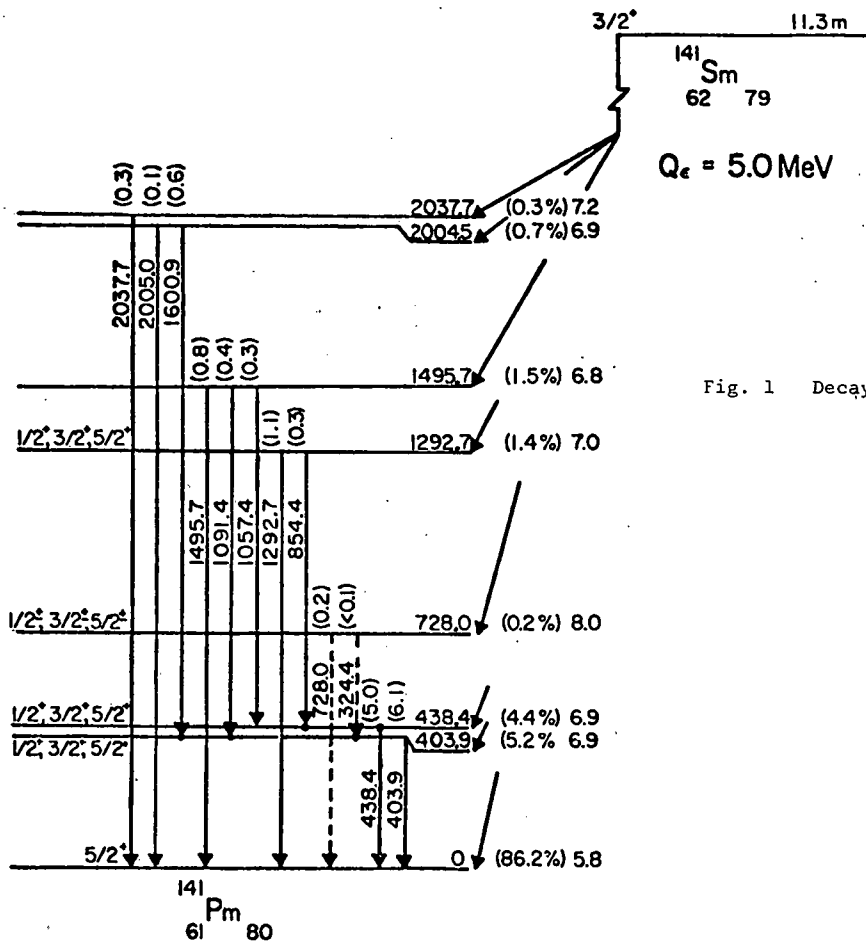


Fig. 1    Decay Scheme of $^{141g}$Sm.

transition to the 728.0-keV state has a log(ft)=8.0, this transition may be either allowed or first-forbidden. Thus the spin of this state is also expected to be 1/2, 3/2, or 5/2.

### References

1. R.E. Eppley, R.R. Todd, R.A. Warner, Wm.C. McHarris, and W.H. Kelly, Phys. Rev. C5, 1084(1972).

2. William D. Myers, and Wladyslaw J. Susatchki, UCRL 11980(1965).

3. R.R. Todd, Ph.D. Thesis (1972) unpublished.

TABLE I

$^{141g}$Sm Summary of γ-Ray Energies and Relative Intensities

| Energy (keV) | Singles Intensities |
|---|---|
| 324.4±0.2 | ≤1 |
| 403.9±0.1 | ≡100 |
| 438.4±0.1 | 82.6±3 |
| 728.0±0.2 | 7.9±0.5 |
| 854.4±0.2 | 3.7±0.3 |
| 1057.4±0.1 | 5.5±0.4 |
| 1091.9±0.2 | 6.1±0.4 |
| 1292.7±0.1 | 16.9±0.5 |
| 1495.7±0.2 | 12.3±0.4 |
| 1600.9±0.3 | 10.3±0.5 |
| 2000.5±0.5 | 1.2±0.2 |
| 2037.9±0.5 | 5.4±0.4 |

TABLE II

Summary of γ-γ Coincidence Results for $^{141g}$Sm

| Gate Energy (keV) | γ-Rays Seen in Coincidence (keV) |
|---|---|
| 324.4 | 196.6, 403.8, 511.0, 777.4 |
| 403.9 | 324.4, 511.0, 1091.9, 1600.9 |
| 438.4 | 854.4, 1057.7 (very weak) |
| 854.4 | 511.0 |
| 1091.9 | 403.9, 511.0 |
| 1292.7 | 511.0 |
| 1600.9 | 403.9 |

# Some New Transitions in the Decay of $^{142}$Eu*

M.F. Slaughter,** R.R. Todd, R.A. Warner and W.H. Kelly

Four previously unreported γ-ray transitions belonging to the decay of 1.2-min $^{142}$Eu have been discovered in the course of a search for the decay of $^{141}$Eu. In this study, $^{144}$Sm oxide was bombarded with 40-MeV and 45-MeV protons, and γ-ray activities were counted with a Ge(Li) detector during several consecutive intervals; the first intervals started 1 min. after each few second activation.

Figures 1a and 1b contain the spectra from activation at 40 MeV and 45 MeV respectively, accumulated during the 5-min periods following each bombardment by 3.5 min. An energy of 40 MeV should be about optimum for the $^{144}$Sm(p,3n)$^{142}$Eu reaction.

Six γ-ray peaks, two of which were previously reported,[1] were assigned to the decay of $^{142}$Eu because of their observed common half-life and their relative strengths from the activations at the two beam energies. These transitions and their relative intensities are listed in Table I. There is not yet sufficient data to place these transitions in a decay scheme.

## TABLE I

Gamma Rays from the Decay of $^{142}$Eu

| Energy | Relative Intensity |
|--------|--------------------|
| 556.8 | 70 |
| 565.0 | 5 |
| 754.5 | 13 |
| 768.2[a] | ≡100 |
| 1015.9 | 13 |
| 1023.5[a] | 68 |

[a]Previously reported in Ref. 1.

## References

1. H.P. Malan, H. Munzel, and G. Pfenning, Radiochemica Acta 5, 24(1966).

Fig. 1    Spectra of γ-rays counted during the 5-min periods following by 3.5 min the bombardment of $Sm_2O_3$ enriched to 95.1% in $^{144}$Sm by (a) 40-MeV and (b) 45-MeV protons.

(b)
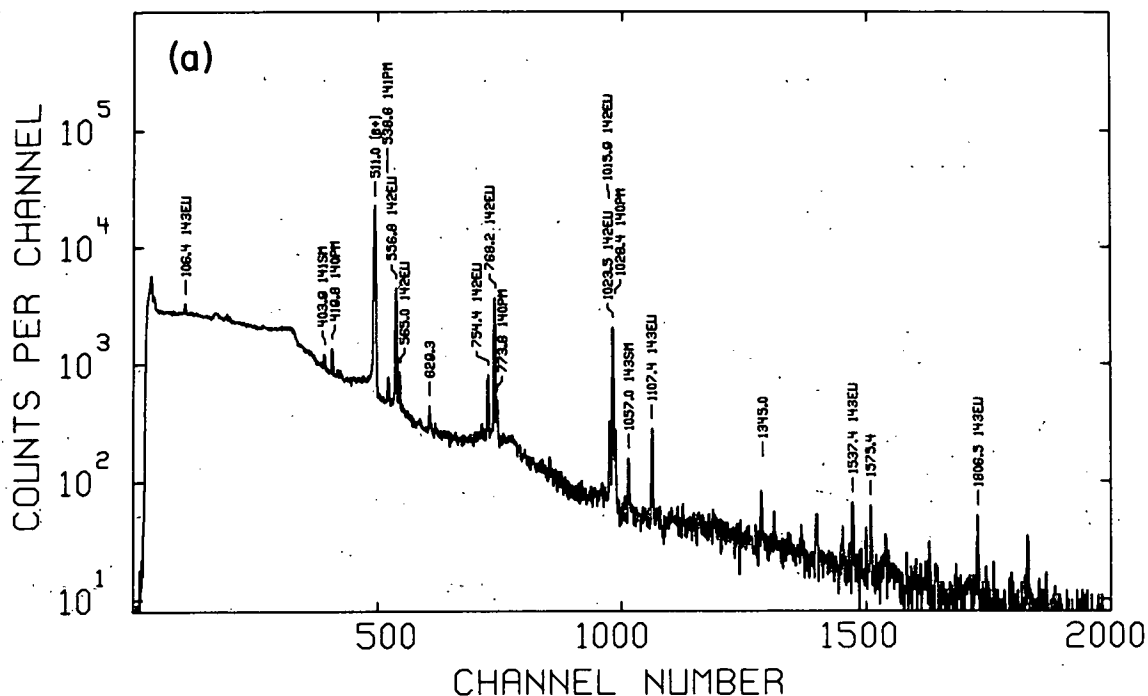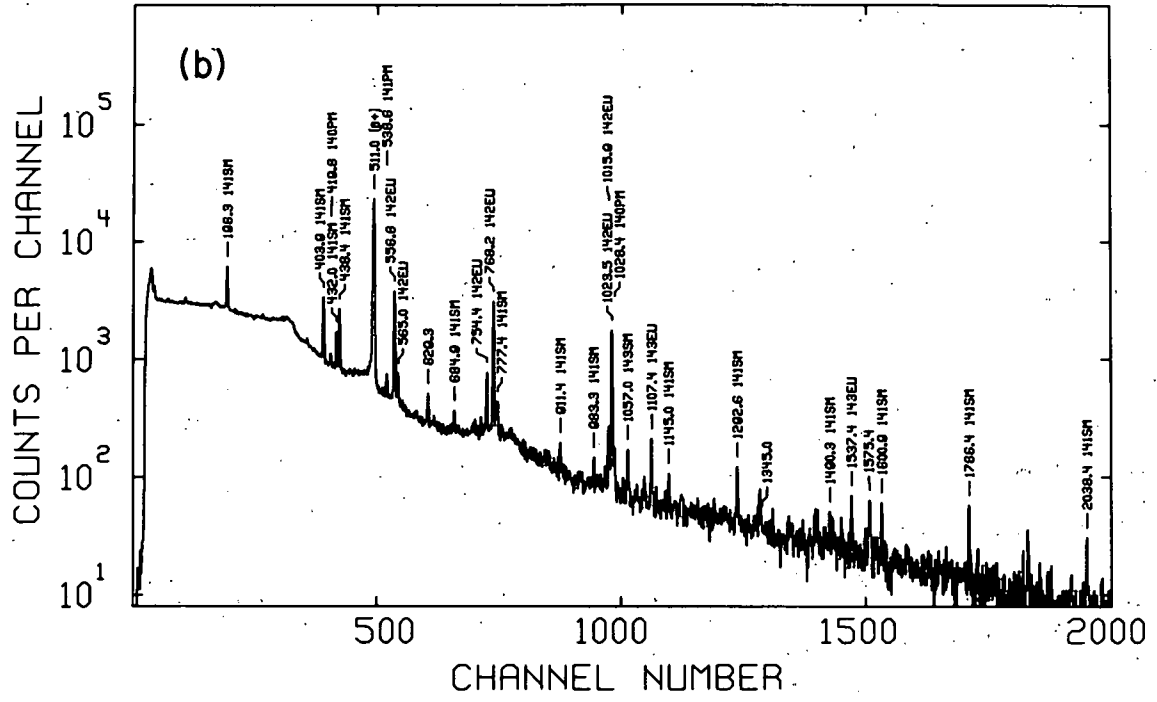
$$^{142}Nd(p,p')$$

Duane Larson, S.M. Austin, and B.H. Wildenthal

As part of our study of inelastic proton scattering on the N=82 isotones, we have studied the $^{142}Nd(p,p')$ reaction at a proton energy of 30 MeV. The targets were fabricated by vacuum evaporation of isotopically enriched (97.5%) $Nd_2O_3$ onto a 20 $\mu g/cm^2$ carbon foil. Target thickness was estimated to be approximately 100 $\mu g/cm^2$.

Use of the high resolution system developed by Blosser et al.[1] enabled us to obtain an energy resolution of 7-9 keV FWHM for the inelastically scattered peaks.

A spectrum taken at 40° in the lab is shown in Fig. 1, along with the excitation energies of the labeled peaks. The calibration energies were taken from Raman et al.[2] and are noted in Table 1.

From systematics in the N=82 nuclei, the 3⁻ collective state is expected to be the strongest state in the (p,p') spectra, and this should correspond to the state we observe at 2084 keV in $^{142}Nd$. Table 1 shows a comparison of the states we observe with the previously known states in $^{142}Nd$. These results are preliminary, as the emulsions exposed at other angles are still in the process of being scanned.

### References

1. H.G. Blosser et al., Nucl. Instr. and Methods 91, 61(1971).

2. S. Raman, et al., submitted to Nucl. Phys., 1972.

TABLE I

Energies of States in $^{142}Nd$

| $E_x$ (present) | $E_x$ (Raman et al.) | $J^\pi$ (previous) |
|---|---|---|
| 0.000 | 0.000 | $0^+$ |
| 1.576 | 1.576 | $2^+$ |
| 2.084 | 2.084 | $(3^-)$ |
| 2.101 | 2.101 | $(4^+)$ |
| 2.210 | 2.209 | $(6^+)$ |
| | 2.217 | $0^+$ |
| 2.384 | 2.385 | $(1,2)^+$ |
| 2.438 | | |
| 2.582 | 2.583 | $(1,2)^+$ |
| 2.738 | | |
| 2.847 | 2.846 | $(2^+)$ |
| 2.937 | ... * | |
| 2.977 | | |
| 3.081 | 3.080 | |
| 3.244 | | |
| 3.319 | | |
| 3.366 | | |
| 3.414 | | |
| 3.578 | | |
| 3.708 | | |
| 3.782 | | |
| 3.833 | | |
| 3.976 | | |
| 4.007 | | |
| 4.034 | | |

*Many levels observed above this excitation.
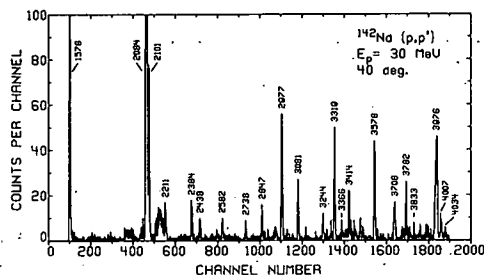


Fig. 1    Spectrum of (p,p') on $^{142}Nd$.

# The $\beta^+/\epsilon$ Decay of $^{143}$Sm*

R.B. Firestone, Wm.C. McHarris, and W.H. Kelly

The decay of $^{143}$Sm has been studied most thoroughly by Frenne and Heyde, et al.[1,2] They produced $^{143}$Sm by the ($\alpha$,n) reaction on natural $Sm_2O_3$ (3.09% $^{144}$Sm). A decay scheme was presented along with several log(ft) values.

The study of $^{143}$Sm decay is of considerable interest in the light of previous work[3,4] on the neighboring odd-Z, N=81 isotones, $^{141}$Nd and $^{145}$Gd. All three isotones have 11/2$^-$ metastable states at 720-756 keV with 60- to 85-sec half-lives. The $^{143}$Sm and $^{145}$Gd metastable states were found to have small β-branches in their decays.[5,6]

Of further interest are the 7/2$^+$ first excited states in the daughters of all three isobars. These appear to be the $1g_{7/2}$ quasiparticle states predicted for N=82 nuclei by Kisslinger and Sorenson.[7] These states occur at 145.4, 271.9, and 329.5 keV in $^{141}$Pr, $^{143}$Pm, and $^{145}$Eu respectively. The log(ft) values given for the decay to the 7/2$^+$ states in $^{141}$Pr and $^{145}$Eu were 8.8 and 7.5. Prior to this study, no value was reported for the log(ft) to the corresponding state in $^{143}$Pm, but since the transition to this state is from the 3/2$^+$ ground state of $^{143}$Sm, the second-forbidden transition might be expected to be in the range 10<log(ft)<14. The transition in $^{141}$Nd is also second-forbidden, suggesting that the $^{143}$Sm decay to the 7/2$^+$ state may also show an abnormally low log(ft) value.

In an attempt to measure this log(ft) and to determine more precisely other properties of the decay scheme for $^{143}$Sm, the reaction $^{142}$Nd($\tau$,2n)$^{143}$Sm was first tried. This reaction proved unsatisfactory, as the rather loosely bound α-particles in this region make the ($\tau$,$\alpha$n) reaction more probable. The problem is compounded by the fact that $^{143}$Sm decay goes overwhelmingly to the ground state of $^{143}$Pm.

The reaction $^{144}$Sm(p,2n)$^{143}$Eu, in which the 2.6-min $^{143}$Eu, quickly decays to its $^{143}$Sm daughter, has been used with more success. [The $^{143}$Eu decay is discussed in another section.] Singles γ-ray spectra have been taken using a 10.4% Ge(Li) detector with 2.1-keV (FWHM) resolution and a peak-to-Compton ratio of 38:1 at 1332 keV. A series of singles spectra were taken at 9-min intervals to identify transitions corresponding to the 8.8-min $^{143}$Sm, and weak transitions were verified through several experiments. A singles spectrum is shown in Fig. 1.

Additional coincidence experiments were performed to determine the $^{143}$Sm decay scheme. Coincidences between 10.4% Ge(Li) and 7.0% Ge(Li) detectors were recorded on magnetic tape. Coincidence gates on the 271.9-keV and 458.8-keV transitions are shown in Fig. 2. Direct ground-state transitions were indicated by their absence in coincidence data and their intensity in β-γ coincidence experiments. A decay scheme for $^{143}$Sm is given in Fig. 3, based on the above
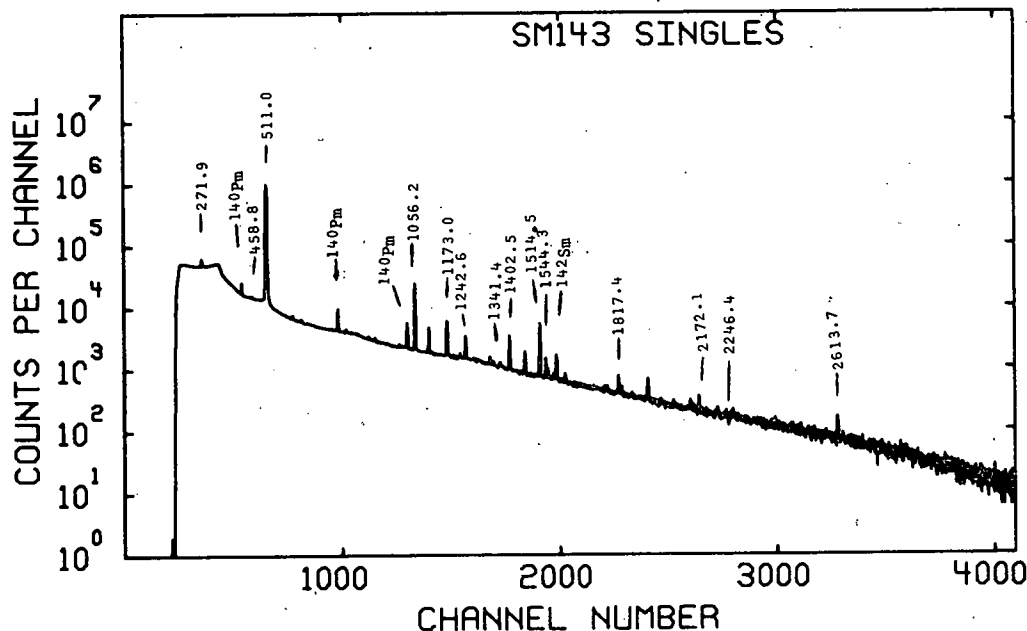


Fig. 1 $^{143}$Sm singles spectrum taken with 10.4% Ge(Li) detector.

results and $^{142}$Nd($\tau$,d) reaction studies of Wildenthal et al.[8]

The log(ft) for the second forbidden decay to the 271.9 keV level is seen to be 8.1, much lower than usual, but similar to those for the corresponding decays of $^{145}$Gd and $^{141}$Nd.

## References

1. D. deFrenne, K. Heyde, L. Dorikens-Vanpraet, M. Dorikens, and J. Demuynk, Nucl. Phys. A110, 273(1968).

2. D. deFrenne, E. Jacobs, and J. Demuynk, Z. Phys. 237, 327(1970).

3. D.B. Beery, W.H. Kelly, and Wm.C. McHarris, Phys. Rev. 171, 1283(1968).

4. R.E. Eppley, Wm.C. McHarris, and W.H. Kelly, Phys. Rev. C3, 282(1971).

5. J. Felsteiner and B. Rosner, Phys. Letters 31B, 12(1972).

6. R.E. Eppley, Wm.C. McHarris, and W.H. Kelly, Phys. Rev. C2, 1929(1970).

7. K.S. Kisslinger and R.A. Sorenson, Rev. Mod. Phys. 35, 853(1963).

8. B.H. Wildenthal, E. Newman, and R.L. Auble, Phys. Rev. C3, 1199(1971).
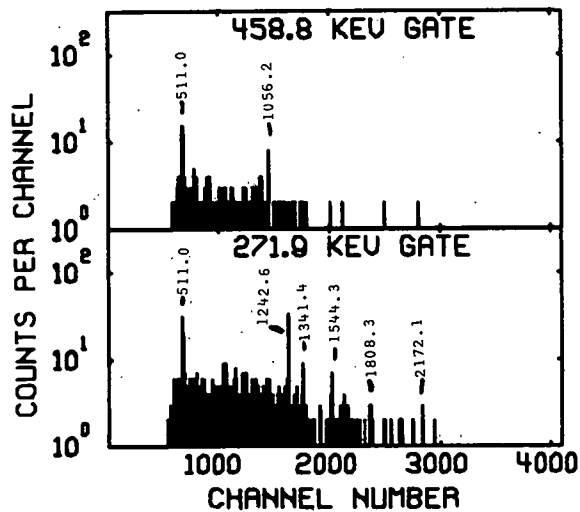
Fig. 2   $^{143}$Sm 10.4% Ge(Li)-7.0% Ge(Li) coincidence spectra (2$\tau$=80 nsec).
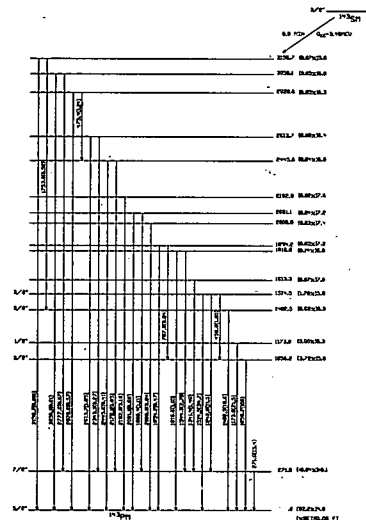


Fig. 3   $^{143}$Sm decay scheme. Levels below 2 MeV placed from coincidence data. Spins determined from $^{142}$Nd($\tau$,d) studies.[8]

# The $\beta^+/\varepsilon$ Decay of $^{143}$Eu*

R.B. Firestone, Wm.C. McHarris, and W.H. Kelly

The decay of $^{143}$Eu was first studied by Kotajima and Malan,[1,2] who measured its half-life (2.6 min) and β-endpoint energy (4.0 MeV). No γ-ray decay schemes were reported, presumably because of the weak transitions and the interference of the short lived $^{143}$Sm daughter decay. $^{143}$Sm decay has been part of a continuing study of N=81 isotones by the Nuclear Spectroscopy Group at Michigan State University, and the $^{143}$Eu decay scheme is a welcome by-product of this study.

$^{143}$Eu was prepared by the reaction $^{144}$Sm(p,2n)$^{143}$Eu on a separated isotope target (95.10% $^{144}$Sm), using 28-MeV protons from the Michigan State University Sector-Focussed Cyclotron. As the $^{143}$Sm daughter has an 8.8-min half-life, a series of 9-min spectra were taken to so that transitions arising from varying decays could be separated by half-life. Additional singles spectra have been taken to confirm the weaker $^{143}$Eu transitions. One such spectrum is shown in Fig. 1. This spectrum was taken with a 10.4% Ge(Li) detector of 2.1 keV (FWHM) resolution at 1332 keV.

In addition to the singles spectra, coincidence information was collected. Figure 2 shows coincidence spectra for gates set on the 107.6-keV and 1106.6-keV γ's. In this experiment coincidences between 10.4% Ge(Li) and 7.0% Ge(Li) detectors within a resolving time of 80 nsec were recorded in pairs on magnetic tape. Direct ground state transitions were determined by their intensities in γ-γ coincidence experiments as well as their failure to appear in coincidence work.

From the $^{144}$Sm(p,d)$^{143}$Sm reaction data of Jolly and Kashy,[3] levels in $^{143}$Sm were found at 0.110 MeV (1/2$^+$), 0.76 MeV (11/2$^-$), 1.11 MeV (5/2$^+$), 1.36 MeV (7/2$^+$), 1.53 MeV (5/2$^+$), 1.72 MeV (5/2$^+$), 1.95 MeV (1/2$^+$), 2.06 MeV (5/2$^+$), 2.16 MeV (7/2$^+$), and 2.29 MeV (7/2$^+$).

Combining the above information, a decay scheme for $^{143}$Eu has been prepared, and is shown in Fig. 3. Some of the higher lying levels were strongly suggested by the data but are only tentatively placed at this time. Approximately 98% of the observed γ-ray intensity is placed in this level scheme and log(ft) values have been calculated from the measured intensities.

## References

1. K. Kotajima, K.W. Brockman, Jr., and G. Wolzak, Nucl. Phys. 65, 109(1965).

2. H.P. Molon, H. Munzel, and G. Pfenning, Radiochem Acte 5, 24(1966).

3. R.K. Jolly and E. Kashy, MSUCL-28, 1970.
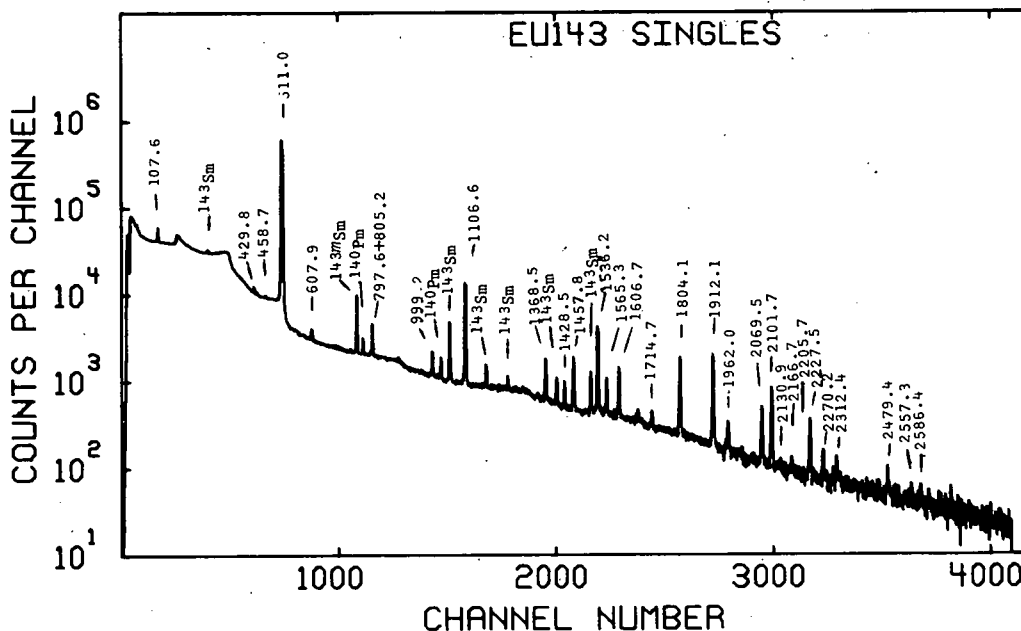
Fig. 1 $^{143}$Eu singles taken with a 10.4% Ge(Li) detector.
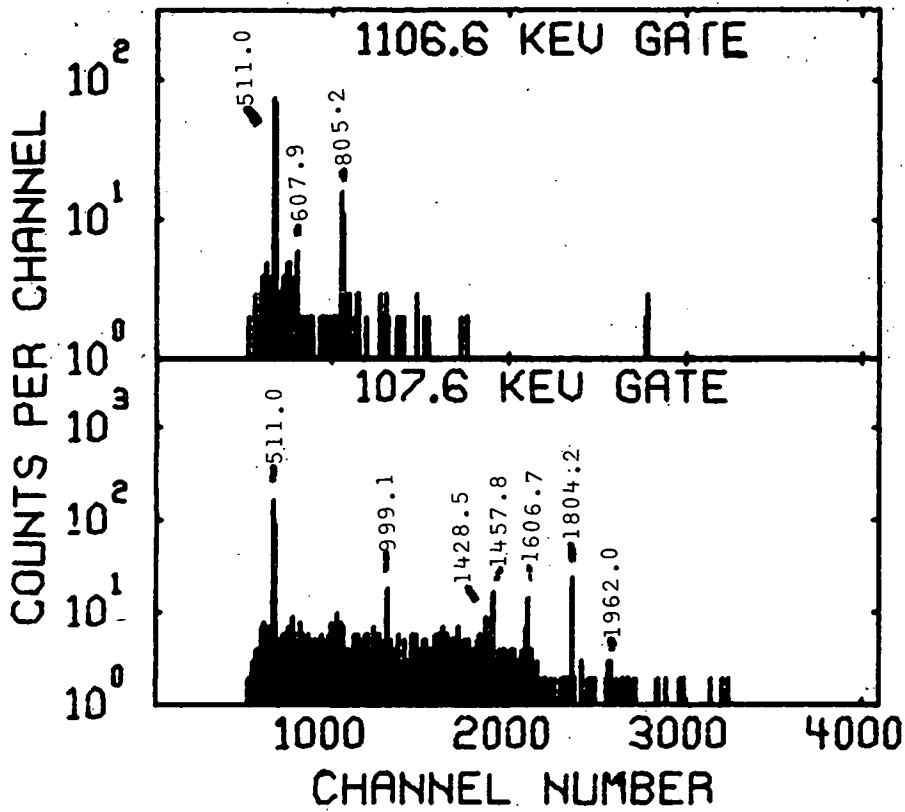
Fig. 2  $^{143}$Eu 10.4%
$\overline{Ge(Li)}$=7.0% Ge(Li)
coincidence spectra
(2τ–80 nsec).

Fig. 3  $^{143}$Eu decay scheme.
Levels below 2 MeV placed from
coincidence data.  Spins deter-
minded from $^{144}$Sm(p,d) studies.[3]
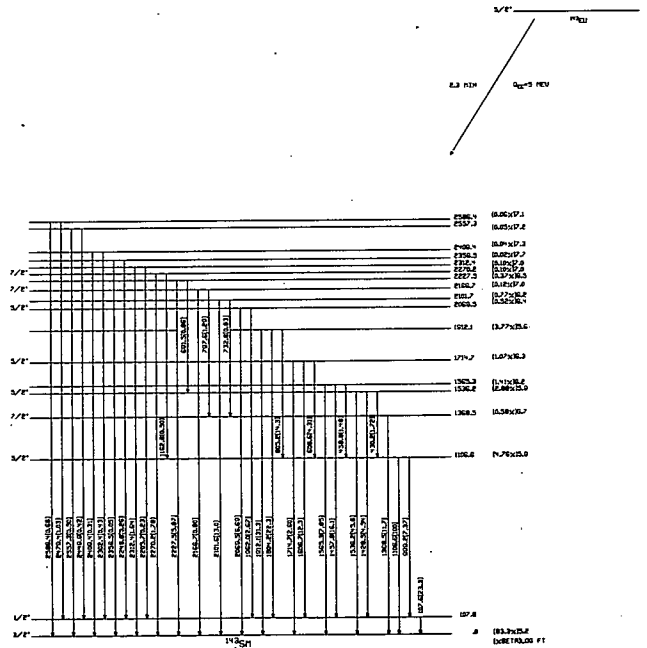
# Anomolous $\varepsilon/\beta^+$ Decay Branching Ratios

R.B. Firestone and Wm.C. McHarris

The β decay of proton-rich nuclei can involve two competing processes, electron capture and positron decay, if sufficient decay energy ($W_o$=1022 keV) is available. These processes may be abbreviated as,

Electron capture ($\varepsilon$):    $p^+ + e^- \to n + \nu$

Positron decay ($\beta^+$):    $p^+ \to n + e^+ + \nu$
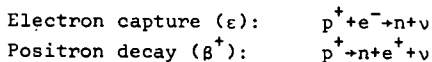
where the protons and neutrons are assumed to be bound particles.

Theoretical predictions of these $\varepsilon/\beta^+$ branching ratios have been made,[1-2] and several experimental verifications of these predictions have been shown.[3-10] Nevertheless, such measurements have been difficult, and a few[7-8] have indicated significant disagreement with theory. Inherent to the theoretical predictions lies the assumption of the vector-axial vector form of the beta-interaction. This, in turn, forms the basis of the two-component neutrino theory. Thus, it is clear that measurements of $\varepsilon/\beta^+$ branching ratios are important to an understanding of the beta-decay process.

Such measurements have been done at the Michigan State University Cyclotron Laboratory using a highly accurate method. Nuclei near the N=81 closed shell were chosen such that several beta decays to various excited daughter states could be studied simultaneously. β-γ coincidence measurements were done to yield relative $\beta^+$ feedings to daughter states, and these values were normalized to a "good" transition to determine $\varepsilon/\beta^+$ branching ratios. Theoretically it should not be significant which transition was chosen, but here a "good" transition was taken as a fast transition in which good statistics were obtainable. Instead of measuring the positrons directly, sufficient absorber material was placed around the radioactive material to annihilate all of the positrons, and the annihilation quanta $\gamma^\pm$ were measured in an 8x8-in. NaI split annulus. Coincidence between 511-keV γ's in each half of the annulus was considered a positron event, and a third γ-ray coincidence in a large Ge(Li) detector (10.4% relative to 3x3-in NaI) labeled the daughter state coincident to the positron. A resolving time for all three events of $2\tau$≈50 nsec. and the use of only direct ground state γ-ray transitions to identify the daughter state made the results quite unambiguous, and the chance rate was virtually negligible. A spectrum for $^{145}$Gd is shown in Fig. 1. The measurements made so far for $^{145}$Gd, $^{143}$Eu, and $^{143}$Sm decays are given in Table I. Although most of the experimental data fit the predictions quite well, there is considerable deviation in the transitions to the 808.5- and 1041.9-keV levels of $^{145}$Eu, the 1173.8-keV level in $^{143}$Pm, and the 1566.3-keV level in $^{143}$Sm. The last case

indicates strong hindrance of the electron capture decay, while it is the positron decay that is hindered for the others.

## TABLE I

Comparison of Experimental and Theoretical $\varepsilon/\beta^+$ Ratios

| Decay | Daughter Level | $\varepsilon/\beta^+$ (Experimental) | $\varepsilon/\beta^+$ (Theory) | log(ft) |
|---|---|---|---|---|
| $^{145}$Gd→$^{145}$Eu | 808.5 | >10 | 0.44 | 6.9 |
| | 953.4 | 2.2 ∓0.7 | 0.53 | 8.2 |
| | 1041.9 | 0.94±0.1 | 0.55 | 6.5 |
| | 1757.8 | ≡1.2 ±0.1 | 1.2 | 5.6 |
| | 1880.6 | 1.4 ±0.1 | 1.4 | 5.6 |
| | 2494.8 | 3.7 ±0.4 | 4.0 | 6.7 |
| | 2642.2 | 4.9 ±0.5 | 4.3 | 6.4 |
| $^{143}$Sm→$^{143}$Pm | 1056.7 | ≡6.4 ±0.5 | 6.4 | 6.2 |
| | 1173.8 | 30±6.3 | 7.9 | 6.6 |
| | 1403.9 | 24±5.2 | 15. | 6.6 |
| | 1515.5 | 34±7 | 19. | 6.0 |
| $^{143}$Eu→$^{143}$Sm | 1107.4 | ≡0.73±0.11 | 0.73 | 5.4 |
| | 1537.1 | 1.2 ±0.2 | 1.1 | 5.5 |
| | 1566.3 | 0.51±0.12 | 1.3 | 6.1 |
| | 1715.7 | 3.6 ±3.0 | 1.5 | 5.8 |
| | 1912.9 | 1.7 ±0.3 | 1.8 | 5.2 |
| | 2070.5 | 1.4 ±0.5 | 2.5 | 6.0 |
| | 2102.8 | 3.1 ±1.7 | 2.6 | 6.9 |

It is notable that the deviant transitions involve hindered decays with large log(ft) values. This suggests that allowed beta-decay theory may breakdown for hindered decay. The inhibition of positron decay could be evidence of Fierz interference terms in the beta-decay matrix element or, more precisely, scalar and tensor forces participating in the interaction. If this is indeed the case, an overhauling of beta-decay theory is needed to accommodate these new facts. Additional work is now in progress to measure x-ray—γ-ray coincidences to obtain electron capture feedings directly. Such data will be used to obtain even less ambiguous $\varepsilon/\beta^+$ ratios.

## References

1. A.H. Wapstra, G.J. Nijgh, R. van Lieshout, Nuclear Spectroscopy Tables, North-Holland Publishing Co., Amsterdam (1959).

2. P.F. Zweifel, Phys. Rev. 96, 1572(1954); 107, 329(1957).

3. M.L. Perlman, J.P. Welker, and M. Wolfsburg, Phys. Rev. 110, 381(1958).

4. B.L. Robinson, R.W. Fink, Rev. Mod. Phys. 32, 117(1960).

5. D. Berenyi, Nucl. Phys. 48, 121(1963).

6. E.J. Ronopinski, The Theory of Beta Radioactivity, Oxford University Press, New York (1965).

7. I. Adam, K.S. Toth, and M.F. Roche, Nucl. Phys. A121, 289(1968).

8. R.E. Eppley, Wm.C. McHarris, and W.H. Kelly,
   Phys. Rev. C3, 282(1971).

9. J.B. Gerhoit, Phys. Rev. 109, 897(1958).

10. R. Sherr and R.H. Miller, Phys. Rev. 93,
    1076(1954).
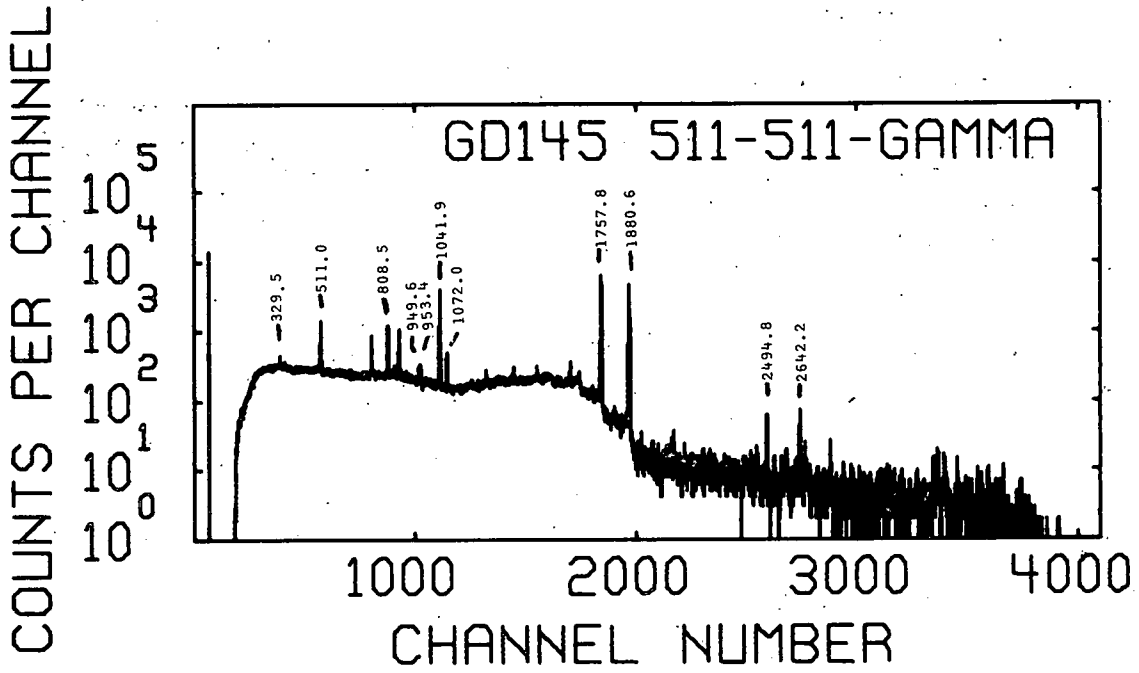
Fig. 1   Pair coincidence spectrum showing $\beta^+$ feedings from $^{145g}$Gd decay.

# The (p,t) Reaction on $^{165}$Ho, $^{163}$Dy, and $^{161}$Dy*

R.W. Goles, R.A. Warner, and Wm.C. McHarris

The (p,t) reaction on $^{165}$Ho, $^{163}$Dy, and $^{161}$Dy has been conducted as part of a continuing investigation of this reaction on rare earth nuclei. Previous work involving the (p,t) reaction on the spherical $^{141}$Pr nucleus[1] and the strongly deformed $^{159}$Tb nucleus[2] has show this reaction to be a very powerful tool for probing the collective characteristics of these nuclei. In particular, the study of the deformed $^{159}$Tb(p,t) reaction[2] revealed large cross sections associated with the population of β- and γ-vibrational and ground state rotational band members.

In the present study ≃300 μg/cm$^2$ metallic targets of the rare earth elements, of 95% or greater isotopic purity, were bombarded with 30 MeV protons accelerated by the Michigan State University sector focussed cyclotron. The scattered tritons were analyzed with an Enge split-pole magnetic spectrometer and collected on nuclear emulsions. Overall experimental resolution determined in these studies was ≃12 keV.

## $^{165}$Ho Results

The characteristics of the triton spectrum obtained from $^{165}$Ho are very much like those exhibited by the previously discussed $^{159}$Tb(p,t) spectra[2] and are illustrated in Fig. 1. In this spectrum, one finds a strong population of the $K^{\pi}=7/2^-$[523] ground state rotational band with level spacings similar to those occurring in the same band in the $^{165}$Ho nucleus.

From Coulomb excitation experiments conducted on $^{165}$Ho by Seaman et al.,[3] one would expect from systematics to observe the $K^{\pi}=3/2^-$ and $11/2^-$ γ-vibrational bands at ≃500 keV and ≃700 keV, respectively, and indeed one does observe a set of states originating at 562 keV of excitation which appear to have some intensity interrelationships. Furthermore, the lowest three energy states of this set exhibit spacing which are characteristic of a $K=3/2$ rotational band if the simple first order rotational energy expression is assumed. If one parameterizes this simple rotational energy expression, one finds convincing evidence for the presence of additional band members up to a spin of 15/2. However, no evidence for the presence of a $K=11/2$ γ-vibrational band could be found in our spectrum. The results of the $^{165}$Ho(p,t) spectrum are summarized in Table 1.

As in the case of $^{159}$Tb, the (p,t) reaction on $^{165}$Ho is found to strongly populate rotational as well as vibrational states in the residual nucleus. The present study has identified six members of the $K=7/2$ ground state rotational band and seven members of the $K=3/2$ γ-vibrational band. Moreover, with the single exception of the 755 keV peak, these states completely exhaust all significant (p,t) reaction strength occurring below the pairing gap.

Experimental angular distributions of the previously discussed states appear in Fig. 2 along with appropriate distorted wave predictions. The finite-range, two-neutron pickup predictions for various ℓ-transfers were calculated using the distorted wave code DWUCK.

As in the two previous (p,t) angular distribution studies involving $^{141}$Pr,[1] and $^{159}$Tb,[2] the $^{165}$Ho(p,t) ground state transition proceeds through a strong dominant ℓ=0 transfer as is evidenced by the very good agreement between the experimental points and theory. The first two excited ground state band members, the 9/2$^-$ and 11/2$^-$ states, exhibit very similar angular distributions. The position of the relative maxima occurring in these curves are reiniscent of ℓ=2 angular shapes which are referenced with the data for comparison; however, the deep minimum occurring at 30°, along with the unusual strength of the observed diffraction proton makes simple ℓ=2 assignments for these states extremely uncertain. This phenomenon has its analog in the $^{159}$Tb(p,t) angular distribution study where a completely similar situation exists for the first two excited member of the $^{157}$Tb ground state band. The remaining members of the $^{163}$Ho ground state band exhibit angular distributions which cannot be explained in terms of any single dominant angular momentum transfer.

The angular distribution exhibited by the first two members of the γ-vibrational band are very much like those exhibited by the 7/2$^-$ and 11/2$^-$ members of the ground state rotational band. Again, the positions of the maxima and minima occurring in these curves can be and are compared with ℓ=2 predicted shapes. The remaining states in this band exhibit complex angular shapes which do not appear to have any single dominating angular momentum components.

Angular distributions of five additional states of unknown origin were also determined in this study and appear in Fig. 2 under the heading "Other States". The 755 keV state appearing in this group is a relatively strong state which exhibits no apparent relationship to any other peaks appearing in the $^{165}$Ho(p,t) spectra. Its angular distribution is flat and unstructured and is in no way related to any single dominant angular momentum transfer. Being below the pairing gap, this state must certainly be a collective excitation, but of what particular type is not clear from our data alone.

The 1.19 MeV, 1.30 MeV, and 1.45 MeV states exhibit distributions which are similar to each other as well as to all previously discussed states exhibiting some $\ell=2$ characteristics. Again the $\ell=2$ character is suggested solely on the basis of the positions of the relative maxima in these distributions.

The 1.38 MeV state appears to be populated by a pure $\ell=0$ wave; however, the positions of the experimental maxima and minima appear to be systematically shifted form values they assumed in the experimental ground state distribution—an effect that has been previously observed and discussed in Ref. 2. Nevertheless, the overall shape and underlying strength of this experimental curve undoubtedly expresses its dominant $\ell=0$ character and further suggests a $\beta$ or pairing vibrational origin for this state.

The remaining states in this category exhibit complex angular shapes which at present cannot be understood.

## $^{161}$Dy and $^{163}$Dy Results

Unlike all previous odd-mass, rare earth isotopes studied in this program, these isotopes are odd neutron nuclei. Thus one would expect to observe a very high density of low energy states in the (p,t) spectra of these nuclei. This expectation was born out as is illustrated in Figs. 3 and 4 which contain (p,t) spectra of $^{161}$Dy and $^{163}$Dy, respectively. As one can see from these figures, most triton peaks have a multiple composite nature making interpretation of these spectra extremely difficult.

Compounding this problem is the fact that one would not expect a strong population of the ground state in either (dysprosium) isotope. And, indeed, one is hard pressed to find a consistent set of states which would establish a position for the ground state or would otherwise tie down the relative energy peak of either spectra. Only in the $^{161}$Dy(p,t) results does one find those states which are sufficiently resolved from their surroundings to suggest a common origin. Located at the low excitation end of the $^{161}$Dy(p,t) spectra, the three prominent peaks exhibit a spacing similar to the first three members of the previously determined[4] $K^\pi=5/2^+$[642] rotational band. The presence of additional members of this proposed band cannot be determined because of the composite nature of most of the higher lying peaks. Furthermore, a ground state cannot be found whose position is consistent with the known excitation energy of the band. This by no means eliminates the possibility of the suggested band origin of these states but adds no credit to it. On the other hand, one would expect a strong population of this band to occur since it can be populated

directly by a one step pickup of a pair of coupled neutrons from the highest filled orbital below the $K^\pi=5/2^+$[642] orbit which characterizes the ground state of $^{161}$Dy and contains the lone "optical" neutron in this nucleus. However in order to make a conclusive statement as to the nature of these and other states occurring in the $^{161}$Dy and $^{163}$Dy(p,t) spectra much higher resolution experiments (FWHM <5 keV) must be conducted.

## References

1. R.W. Goles, R.A. Warner, Wm.C. McHarris, and W.H. Kelly, Phys. Rev. C6, 587(1972).

2. R.W. Goles, R.A. Warner, Wm.C. McHarris, and W.H. Kelly, Phys. Rev. Letters 24, 802(1972).

3. G.G. Seaman, E.M. Bernstein, and J.M. Palms, Phys. Rev. 161, 1223(1967).

4. K.G. Rensflet, S.A. Hjorth, and W. Klemra, Stockholm Annual Report (1971).

TABLE 1

States Populated Through the $^{165}$Ho(p,t)$^{163}$Ho Reaction

| Energy[a] (keV) | Theory (keV) | Assignment[b] $J^\pi$ |
|---|---|---|
| 0 | --- | $7/2^-$ |
| 100 | --- | $9/2^-$ |
| 224 | 222 | $11/2^-$ |
| 369 | 367 | $13/2^-$ |
| 533 | 533 | $15/2^-$ |
| 560 | --- | $3/2^{-\prime}$ |
| 618 | --- | $5/2^{-\prime}$ |
| 695 | 699 | $7/2^{-\prime}$ |
| 720 | 722 | $17/2^-$ |
| 755 | --- | --- |
| 791 | --- | --- |
| 807 | 804 | $9/2^{-\prime}$ |
| 826 | --- | --- |
| 898 | --- | --- |
| 912 | --- | --- |
| 926 | 931 | $11/2^{-\prime}$ |
| 1060 | --- | --- |
| 1075 | 1082 | $13/2^{-\prime}$ |
| 1117 | --- | --- |
| 1156 | --- | --- |
| 1175 | --- | --- |
| 1194 | --- | --- |
| 1232±5 | --- | --- |
| 1245±5 | --- | --- |
| 1259±5 | 1256 | $15/2^{-\prime}$ |
| 1286±5 | --- | --- |
| 1308±5 | --- | --- |
| 1345±5 | --- | --- |
| 1373±5 | --- | --- |
| 1419±5 | --- | --- |
| 1441±5 | --- | --- |
| 1457±5 | --- | --- |
| 1513±5 | --- | --- |

[a] All energy uncertainties are ±3 keV unless otherwise specified.

[b] $I$ = member of ground state rotational band; $I'$ = member of $K=K_o-2$ $\gamma$-vibrational band.
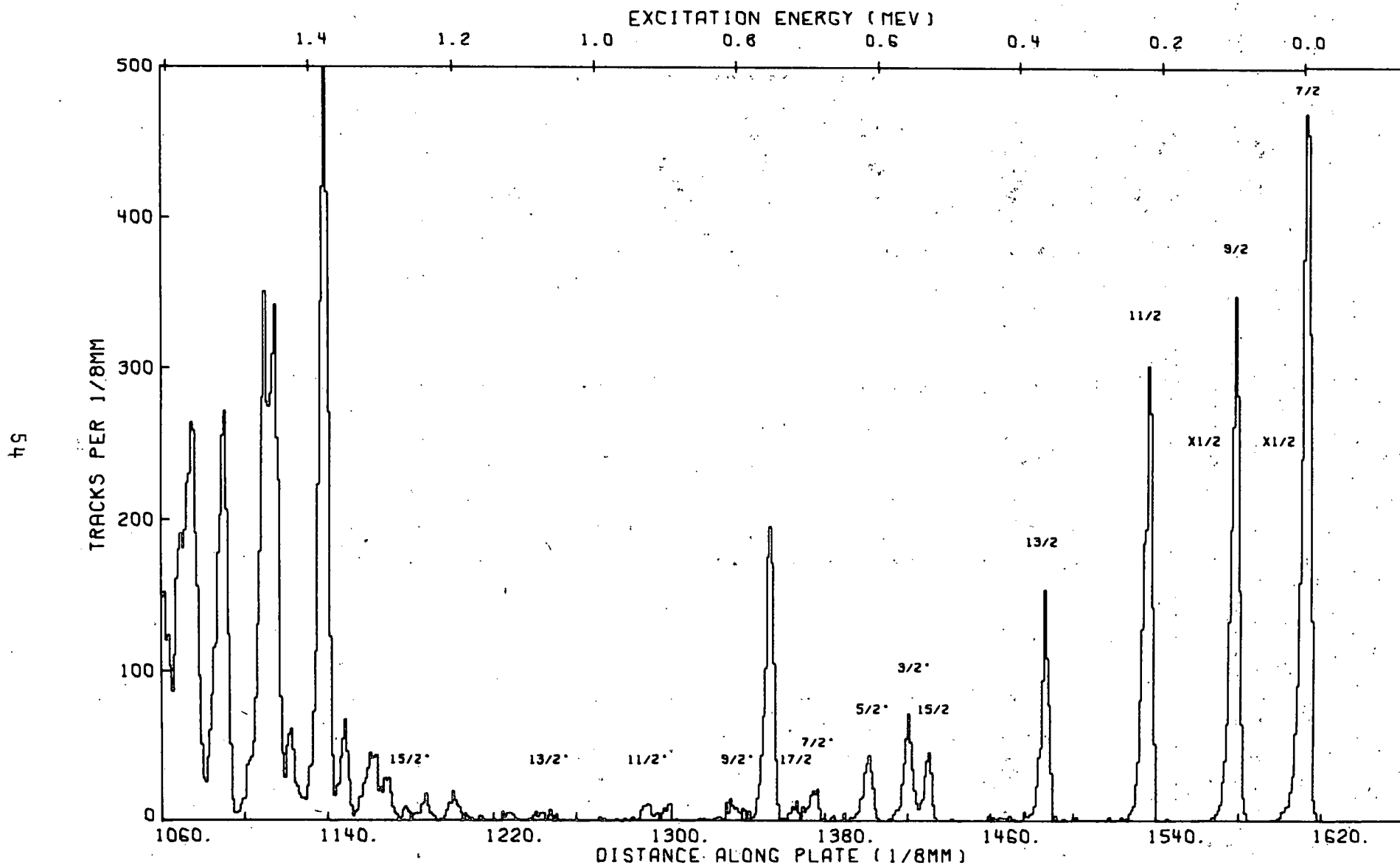
Fig. 1    $^{165}$Ho(p,t) spectrum taken at the laboratory angle of 20°.
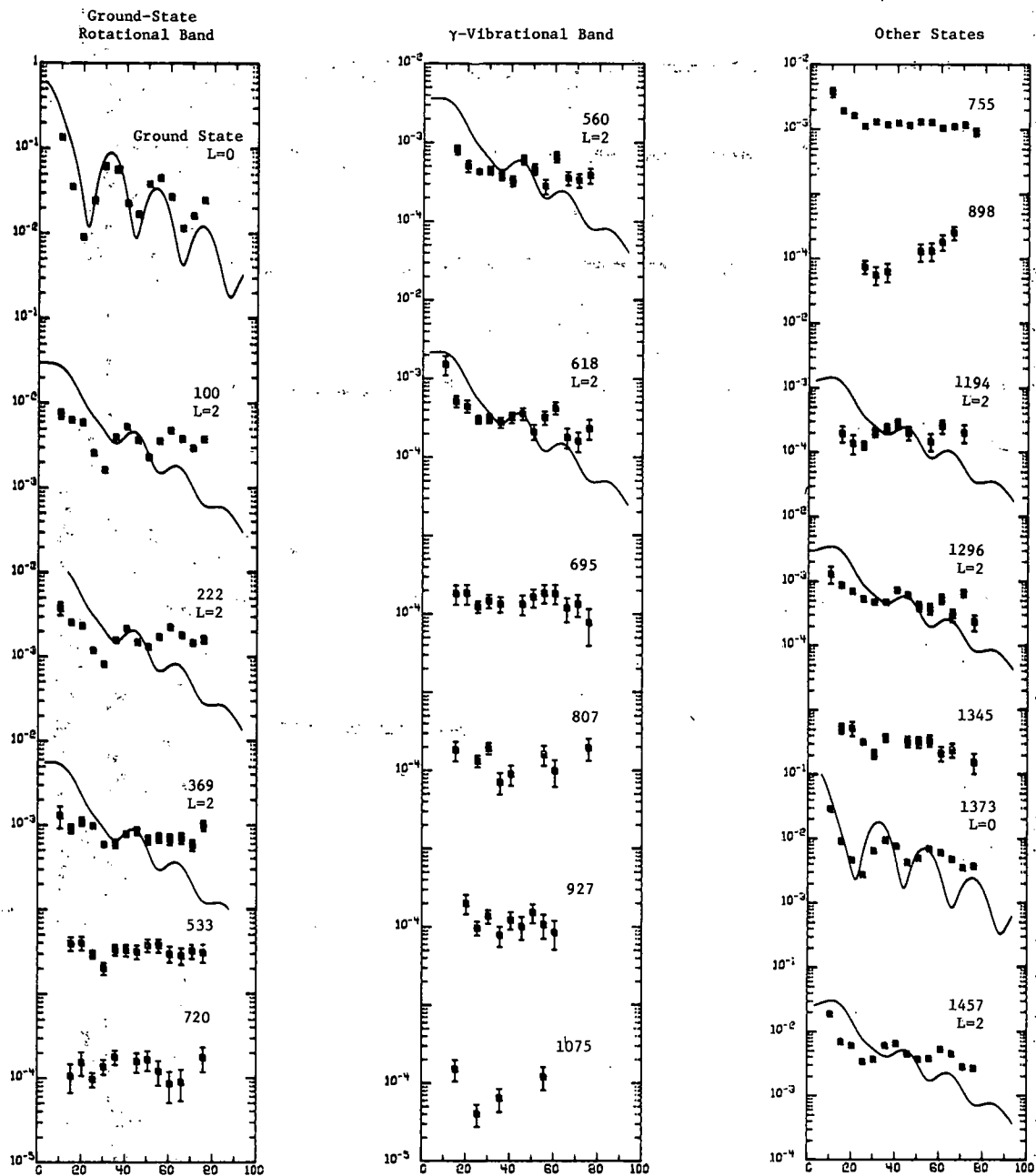
Fig. 2  Relative angular distributions of states populated through the $^{165}$Ho$(p,t)$ reaction. Relative cross sections have been normalized to reflect measured absolute values.
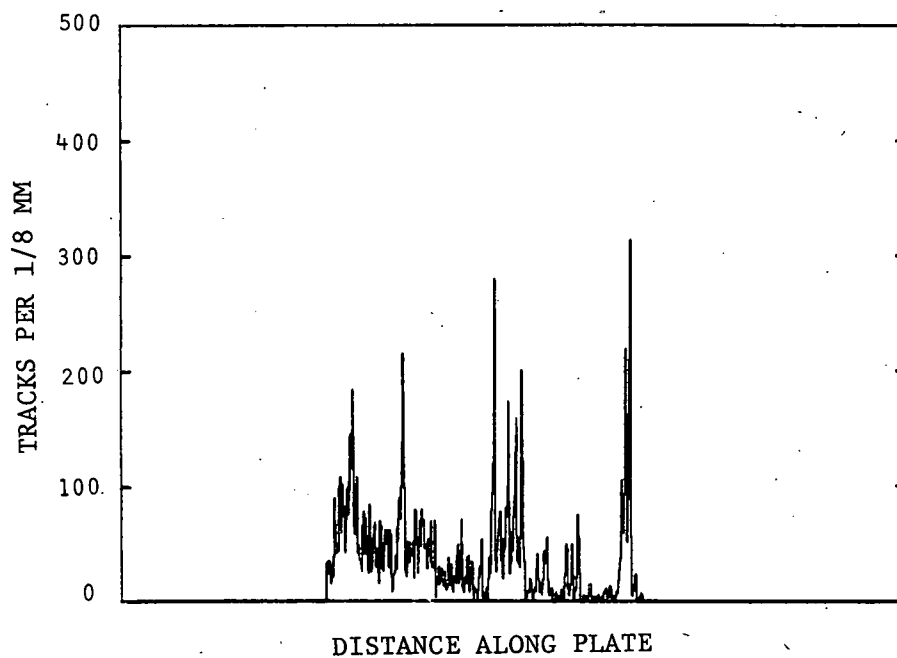
Fig. 3    $^{161}$Dy(p,t) spectrum taken at the
laboratory angle of 20°.
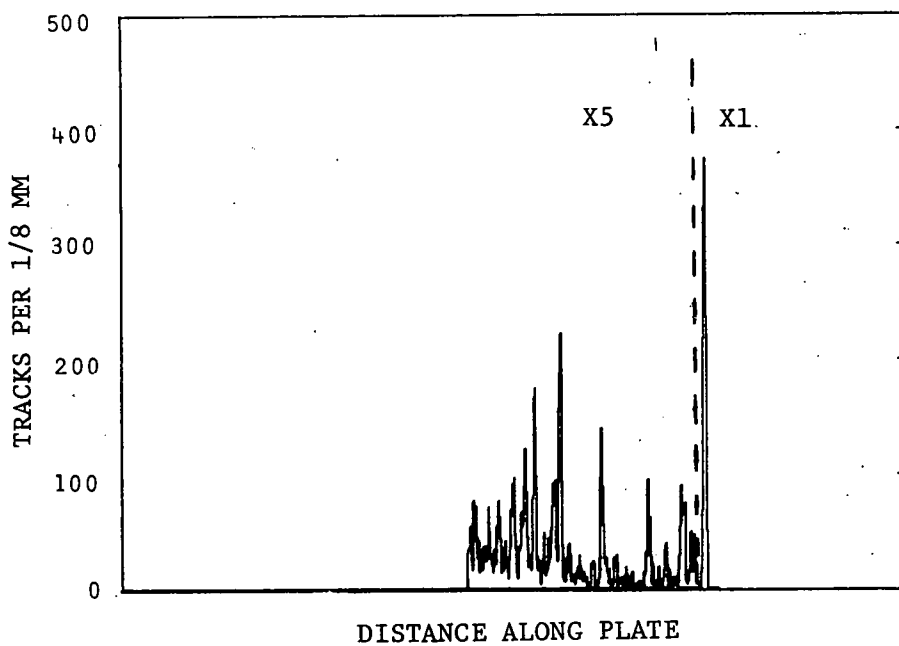


Fig. 4    $^{163}$Dy(p,t) spectrum taken at the
laboratory angle of 30°.

# Study of $^{173}$Hf Levels Populated in the Decay of $^{173}$Ta*

I. Rezanka,** I.M. Ladenbauer-Bellis,** F.M. Bernthal,
T. Tamura,** and W.B. Jones**

In collaboration with the group at the Yale
Heavy Ion Accelerator Laboratory, we have com-
pleted a study of the decay of 3.6-hour $^{173}$Ta to
levels in $^{173}$Hf. The low-lying high-spin states
in $^{173}$Hf were recently studied in the $^{171}$Yb($\alpha$,2n$\gamma$)
reaction,[1] and although the perturbed rotational
band built on the 7/2+[633] Nilsson state was
clearly indicated there remained several ambiguities
concerning the lowest-lying states and band-head
transitions between the several Nilsson states in-
volved. It was therefore appropriate to carry out
a detailed study of the $^{173}$Ta decay in an effort
to resolve those ambiguities.

To produce the $^{173}$Ta, the $^{12}$C beam from the
Yale Heavy Ion Accelerator was used to bombard
natural metallic holmium foil rolled to a thick-
ness ~10 mg/cm$^2$. Excitation function measurements
determined the maximum yield for the desired
$^{165}$Ho($^{12}$C,4n)$^{173}$Ta reaction to be at 83 MeV.
The carrier-free Ta activity was chemically
isolated from other elements by the solvent ex-
traction technique described on page 60 of this
report.
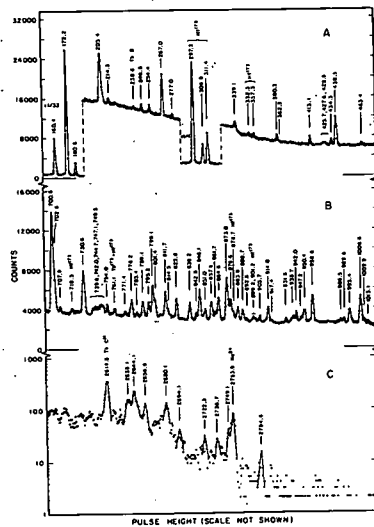


Fig. 1    Selected portions of the γ-ray spectrum
from $^{173}$Ta decay.

The γ-ray singles spectrum of $^{173}$Ta (Fig. 1)
was taken in the region 60-4000 keV with a
35 cm$^3$ coaxial detector (resolution 2.0 keV
FWHM at 660 keV). The lower-energy portion
of the spectrum was studied with a 3-mm deep
Si(Li) detector (resolution 200 eV FWHM at
6 keV). In addition, γ-γ coincidence data have
been acquired with a second detector, 15 cm$^3$
in volume. Three-parameter ($E_{\gamma 1}$-$E_{\gamma 2}$-t) coin-
cidence events were digitized and recorded
serially on magnetic tape for later sorting.

In order to obtain reliable information on
the Q-value of $^{173}$Ta, a β+-γ coincidence experi-
ment was performed in which a 3x3" NaI(Tl)
crystal served as the γ-ray detector and a 1x1"
anthracene crystal was used for registering the
positrons. The end-point energy of the positron
group coincident with the most prominent group
of γ-rays near 170 keV was found to be 2480±150 keV.

To establish the coincidence relations among
the low energy transitions in $^{173}$Hf, an e$^-$-γ
coincidence experiment has also been carried out
with a surface barrier silicon detector (500μ
depletion depth, resolution 5 keV FWHM at 624 keV)
and the 35 cm$^3$ Ge(Li) device. As isomeric
states were expected for these low-energy tran-
sitions, the time spectrum was sorted according
to selected e$^-$-γ coincidence gates. The half-
lives of the 107.2-keV (5/2$^-$[512]) and 197.5-keV
(7/2+[633]) levels were determined to be 182±20
and 160±40 ns, respectively. Details of the
lower-lying levels in $^{173}$Hf are shown in Fig. 2.
It will be noted in Fig. 2 that the 197.5-keV
level is in fact a closely-spaced doublet, pre-
sumably composed of the 7/2+[633] bandhead and
the 7/2$^-$ member of the 5/2$^-$[512] rotational band.
The lifetime measured for the 90.3-keV transitions
from this state would therefore arise from the
7/2+[633]→5/2$^-$[512] E1 component, since the intra-
band 7/2$^-$→5/2$^-$ M1 is not expected to have such a
long half-life.

$^{173}$Ta → $^{173}$Hf
LOW-LYING LEVELS IN $^{173}$Hf
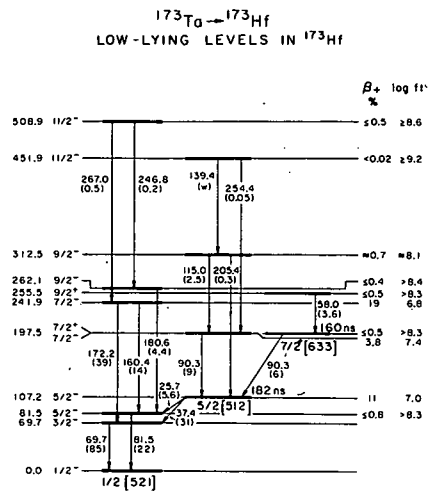


Fig. 2    The level structure of $^{173}$Hf below 600 keV
as determined from $^{173}$Ta decay data.

Multipolarities have been assigned to the
more prominent transitions on the basis of the
photon intensities measured in this work and
the conversion electron intensities of Ref. 2.
Rotational states built on the ground 1/2$^-$[512]

Nilsson orbital and the 5/2⁻[512] and 7/2⁺[633] bands were observed. Spin and parity assignments have been made for several higher-lying levels on the basis of log(ft)'s, γ-ray intensities, and conversion coefficients. The complete decay scheme for $^{173}$Ta is shown in Fig. 3.

The lifetime of the 7/2⁺[633] state in $^{173}$Hf provides the second measurement of an absolute E1 transition rate betweeen the 7/2⁺[633] and 5/2⁻[512] intrinsic states, $^{173}$Yb being the other case for which experimental data are available. Such ΔK=1 E1 transitions are well-known to exhibit unusual branching intensity patterns that result from numerous small components contributing to the total E1 transition amplitude. As a consequence, their Nilsson-model hinderance factors $[F_n = B(E1)_N/B(E1)_{exp}]$ can vary over many orders of magnitude.

It is now commonly recognized that the Coriolis interaction is a principal contributor to such large fluctuations in ΔK=1 E1 strengths between the same intrinsic states. In the case of $^{173}$Hf the strongly admixed 5/2⁺[642] component in the 7/2⁺[633] band presumably gives rise to a large 5/2⁺[642] → 5/2⁻[512] amplitude that adds coherently to the principal 7/2⁺[633] → 5/2⁻[512] component. But inclusion of such Coriolis-admixed components

in a more detailed Nilsson calculation is still often incapable of explaining observed E1 transition rates in such cases. We have considered the simple first-order correction to the E1 transition moment:

$$B(E1) = \frac{3}{4\pi} e_{eff}^2 \left(\frac{\hbar}{m\omega_0}\right) [a_{7/2^+} \langle \tfrac{7}{2} 1 \tfrac{7}{2} -1 | \tfrac{5}{2} \tfrac{5}{2} \rangle$$

$$(U_{7/2^+} U_{5/2^-} - V_{7/2^+} V_{5/2^-}) G(E1; 7/2^+ \to 5/2^-)$$

$$+ a_{5/2^+} \langle \tfrac{7}{2} 1 \tfrac{5}{2} 0 | \tfrac{5}{2} \tfrac{5}{2} \rangle (U_{5/2^+} U_{5/2^-} - V_{5/2^+} V_{5/2^-})$$

$$G(E1; 5/2^+ \to 5/2^-)]^2$$

where the even parity subscripts refer to the wave amplitudes for the strongly Coriolis-mixed Ω=5/2 and 7/2 members of the $i_{13/2}$ family of neutron orbitals, the $(U_iU_f - V_iV_f)$ are the usual E1 pairing reduction factors for the orbitals involved, and G(E1) is calculated in the Nilsson scheme as before.

For estimates of the $a_{\Omega^+}$ we refer to the results obtained by Hultberg et al.[1] in their fit for the perturbed energies of the 7/2⁺[633] rotational band excited in the $^{171}$Yb(α,2n)$^{173}$Hf reaction.
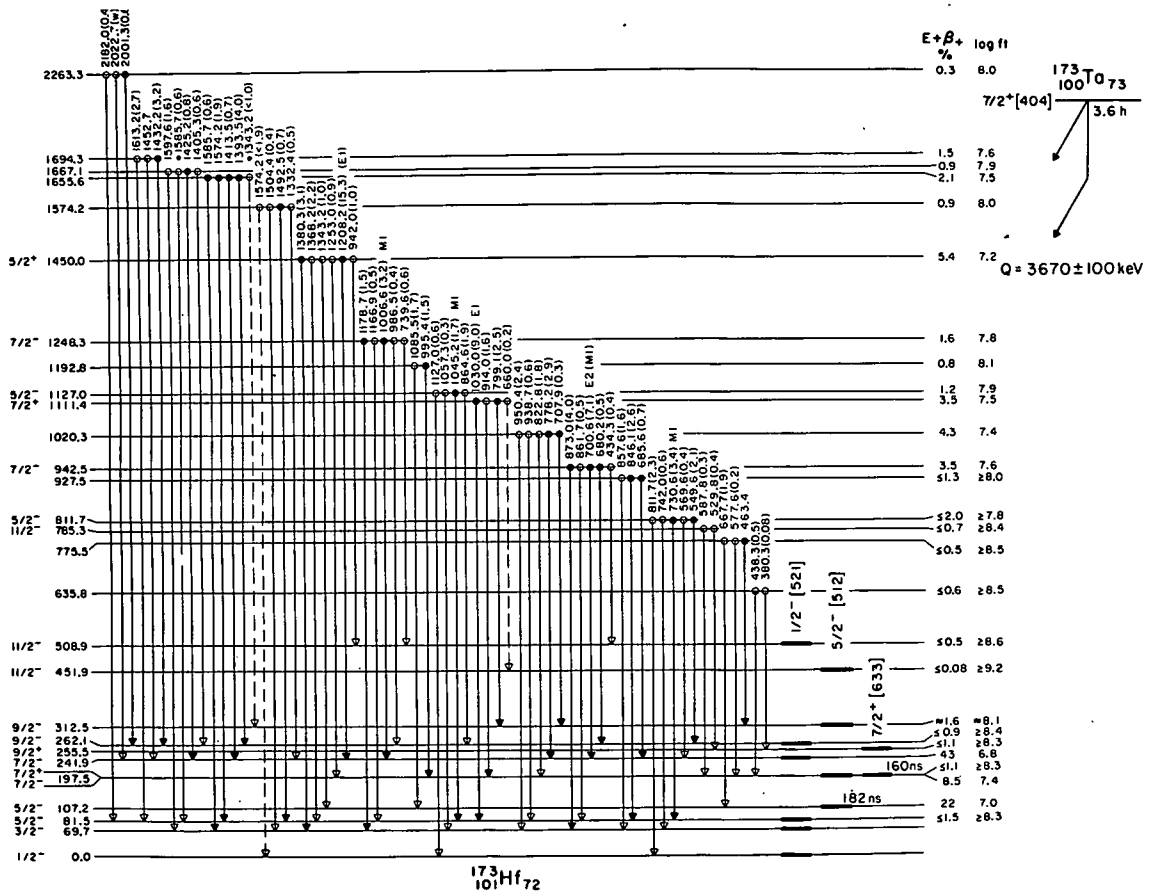


Fig. 3 Decay of $^{173}$Ta to levels in $^{173}$Hf.

The amplitudes of the $7/2^+[633]$ and $5/2^+[642]$ components contributing to the $7/2^+$ band head are found by these authors to be 0.98 and 0.21, respectively. The results of our calculation are summarized below:

Calculated E1 Transition Probability for the 90.3-keV $7/2^+[633] \rightarrow 5/2^-[512]$ Transition in $^{173}$Hf

| Method | $T_{1/2}(E1)$ (nsec) | $F_N$ |
|---|---|---|
| Nilsson Model* | 8.3 | 24 |
| Nilsson Model with pairing | 2300 | 0.12 |
| Nilsson Model with Coriolis mixing and pairing | 410 | 0.49 |

*The deformation parameters assumed were $\epsilon_2 = 0.26$, $\epsilon_4 = 0.02$.

A close examination of the pairing reduction factors in Eq. (1) reveals the extreme sensitivity of the above results to the presumed location of the Fermi surface. Most notably, the factor $(U_{7/2^+}U_{5/2^-} - V_{7/2^+}V_{5/2^-})$ is estimated to be only $-0.06$. Obviously a small inaccuracy in this quantity could significantly alter our results. The conclusion to be drawn is that we still know relatively little about the many factors which influence $\Delta K=1$ E1 transitions in such cases.

Further details of the $^{173}$Hf levels and transitions may be found in a forthcoming publication.[3]

### References

1. S. Hultberg, I. Rezanka, and H. Ryde, to be published.

2. B. Harmatz and T.H. Handly, Nucl. Phys. A121, 481(1968).

3. Submitted to Physical Review C.

# The Decay of $^{177}$Ta to Levels in $^{177}$Hf*

B.D. Jeltema** and F.M. Bernthal

Recent years have seen intense study of the odd-neutron Hf and W isotopes. Interest in this region has been generated by the presence of low-lying positive parity states associated with the strongly perturbed $i_{13/2}$ family of Nilsson single particle orbitals in these nuclei. Much of the work has employed in-beam γ-ray spectroscopy, primarily using (α,xnγ) reactions on appropriate Yb or Hf targets. For example, work at the MSU Cyclotron Laboratory has detailed the rotational band structure of $^{179}$W and $^{181}$W,[1] the former of which is an isotone of $^{177}$Hf and is characterized by a neutron structure similar to that of $^{177}$Hf.

Theoretical analysis of the perturbed rotational-band structure of such nuclei requires as much information as possible about the higher-lying perturbing Nilsson states and their associated rotational bands that mix into the lower-lying bands observed in the (α,xnγ) experiments. This information on higher states can often be obtained from decay scheme studies. Therefore, it was decided to study levels of $^{177}$Hf populated in the EC-β$^+$ decay of $^{177}$Ta. The most recent $^{177}$Ta decay scheme is that proposed by West, Mann, and Nagle[2] from their work using NaI(Tℓ) scintillation detectors. It seemed reasonable to expect that Ge(Li) detectors might produce significant new data.

The $^{177}$Ta sources were prepared by bombarding natural lutetium foil (97.4% $^{175}$Lu) with 29 MeV alpha particles produced by the MSU Cyclotron, the predominant reaction being $^{175}$Lu(α,2n)$^{177}$Ta. Typical bombardments were at 1 μa beam current for 15 hours. The source was then allowed to decay for three to four days to allow eight-hour $^{176}$Ta to decay from the sample. The tantalum activity was separated from other activities by dissolving the target in 6M HCl, precipitating the lutetium as LuF$_3$, and then extracting TaF$_6^-$ from the supernate with a small amount of diisopropyl ketone (DIPK). The carrier-free Ta was back-extracted into distilled water to yield a solution which could be evaporated to produce clean "point" sources of high specific activity.

Energies and intensities of γ-rays emitted by the decay of $^{177}$Ta were studied using a Ge(Li) detector with a photopeak efficiency of 10.4% at 1333 keV (relative to a 3x3 in NaI(Tℓ) detector). Optimum resolution of this system is 2.1 keV FWHM at the same energy. The $^{177}$Ta singles spectra were analyzed using the computer program SAMPO which does a least squares fit of the γ-ray peaks to a Gaussian function with exponential tails. Table I lists the preliminary results of this work.

To determine the cascade relationships of $^{177}$Ta decay, γ-γ coincidence experiments have also been performed. Two detectors, each with photopeak efficiencies of approximately 7%, were placed at 180° geometry with the source sandwiched between graded lead absorbers to reduce coincidences due to x-ray and Compton backscatter events. Using the real time computer tasks TOOTSIE and IIEVENT, the addresses of coincidence events were serially recorded on magnetic tape to be recovered later, off-line. In the recovery process, the operator is free to set gates on any part of the spectrum he desires.

Preliminary results of the $^{177}$Ta decay experiments are shown in the level scheme (Fig. 1). Previously unknown γ-rays which have been seen in singles and placed in the decay scheme have energies of 494.9, 805.7, and 1002.9 keV. New γ-rays tentatively placed in the decay scheme on the basis of coincidence data include 311.8, 398.3, 257.1, 105.7, 315.7, and 421.1 keV. Transitions of 71.6 and 313.3 keV (seen in singles but not in coincidence) were included in the decay scheme since they are well known from $^{177m}$Lu decay.[3] The levels at 1002.9 and 742.0 keV had not been placed before this work. Spin assignments are consistent with those of West et al.[2] and with the (d,p)-(d,t) reaction work of Rickey and Sheline.[4]

The proposed level at 741.7 keV is of special interest, since it lies so close to the level at 746.0 keV earlier[2] associated with the 7/2$^+$[633] Nilsson orbital. Our coincidence data clearly show the 420.7- and 424.6-keV transitions to be in coincidence with the 208.3-keV γ-ray, but not with each other. The Ge(Li) singles spectrum of Fig. 2 shows the γ-ray doublet of interest at 421-425 keV. The 420.7-keV transition had early been identified[5] and was tentatively associated with a 3/2$^-$ isomer proposed to lie at 420.9 keV.[2] That assignment seems now to have been incorrect, but the apparent large K-conversion coefficient of the 420.7-keV transition is still unexplained. Work on the $^{177}$Ta decay is continuing.

## References

1. F.M. Bernthal and R.A. Warner, this report p. 65.

2. H.I. West, Jr., L.G. Mann, and R.J. Nagle, Phys. Rev. 124, 527(1961).

3. A.J. Haverfield, F.M. Bernthal, and J.M. Hollander, Nuclear Physics A94, 337(1967).

4. R.A. Rickey, Jr., and R.K. Sheline, Phys. Rev. 170, 1157(1968).

5. B. Harmatz, T.H. Handley, and J.W. Mihelich, Phys. Rev. 119, 1345(1960).

Energies and Relative Intensities of γ-rays Seen
in $^{177}$Ta Decay

| Energies ($\pm$.2 keV) | Intensity ($\pm$10%) |
|---|---|
| 96.7 | 0.49 |
| 113.0 | 563. |
| 136.7 | 0.64 |
| 177.0 | 0.19 |
| 197.1 | 0.27 |
| 208.3 | 100. |
| 249.7 | 3.3 |
| 313.3 | 0.22 |
| 321.3 | 2.3 |
| 354.9 | 0.36 |
| 391.6 | 0.10 |
| 420.7 | 3.8 |
| 424.6 | 12.6 |
| 452.9 | 0.28 |
| 491.6 | 3.5 |
| 494.9 | 0.54 |
| 508.0 | 8.4 |
| 526.1 | 2.0 |
| 549.6 | 0.71 |
| 597.8 | 1.1 |
| 604.6 | 2.6 |
| 632.8 | 3.3 |
| 734.4 | 4.6 |
| 736.4 | 1.8 |
| 745.9 | 25. |
| 805.7 | 0.27 |
| 847.4 | 2.9 |
| 944.5 | 6.3 |
| 1002.9 | 0.11 |
| 1057.7 | 33. |
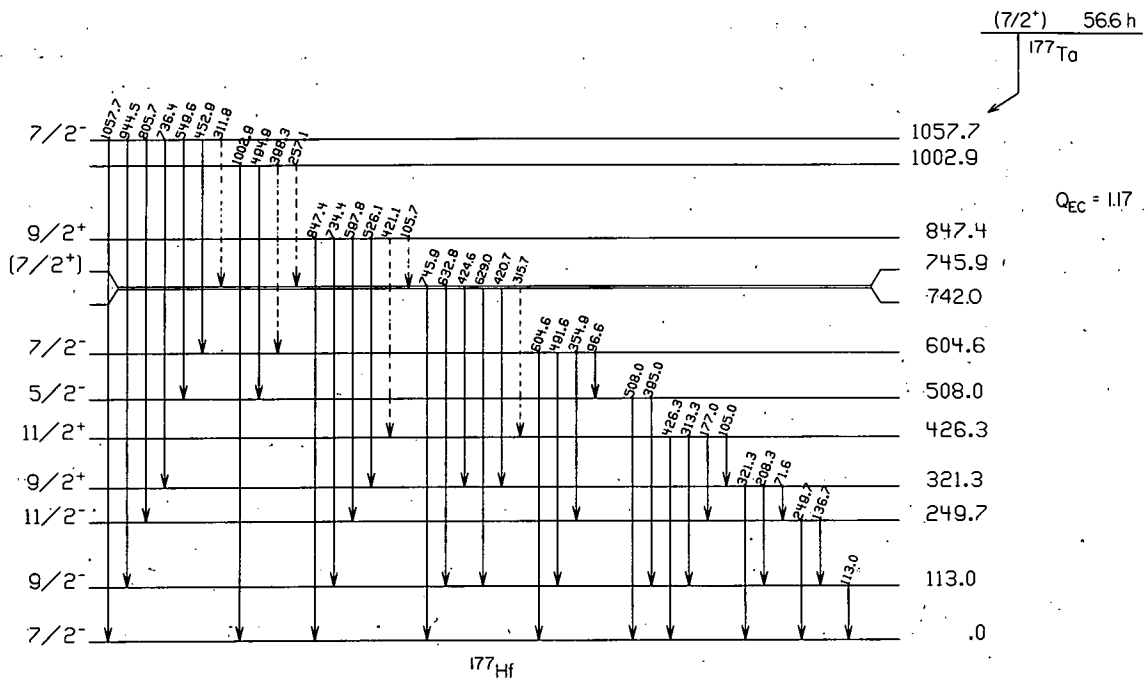


Fig. 1    Decay of $^{177}$Ta to levels in $^{177}$Hf.
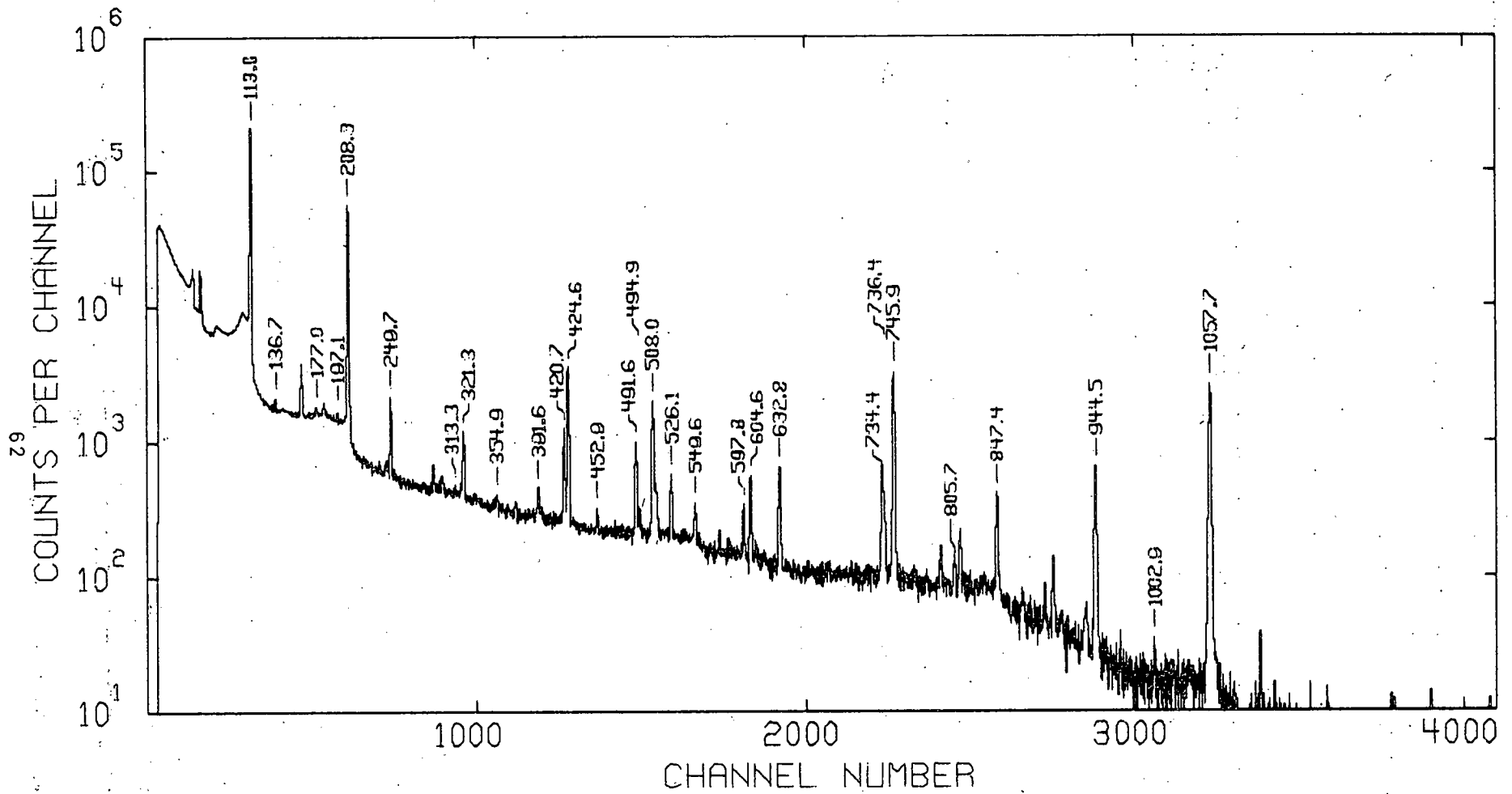
Fig. 2   The γ-ray singles spectrum from decay of $^{177}$Ta to $^{177}$Hf.   Some of the unlabeled peaks also belong to $^{177}$Ta decay.

# Levels in $^{179}$W Populated in the $^{177}$Hf($\alpha$,2n$\gamma$) Reaction[*]

F.M. Bernthal and R.A. Warner

A study of the rotational band structure of $^{179}$W has been completed as the first in the series of ($\alpha$,xn$\gamma$) investigations of the odd-neutron species in the upper reaches of the "rare-earth" region of deformation. The $^{179}$W nucleus is particularly interesting because of its apparent similarity to the $^{177}$Hf isotone that has been so thoroughly studied as the product of $^{177m}$Lu decay. The Coriolis interaction found to exercise so profound an influence on the $i_{13/2}$ family of Nilsson orbitals in other nuclei is no less important in the 9/2$^+$[624] band in $^{179}$W. Analysis of the perturbations associated with these orbitals and the effects of those perturbations on the $\gamma$-ray decay probabilities, energy-level ordering, and neutron-transfer cross-sections is a principle objective of this program of study.

In the $^{179}$W experiments, 26-MeV beams of $\alpha$-particles from the MSU sector-focused cyclotron were allowed to impinge on a thick, metallic target of $^{177}$Hf metal (92% enriched) and the prompt $\gamma$-ray spectrum was accumulated in both singles and coincidence modes. Figure 1 shows the prompt singles $\gamma$-ray spectrum of $^{179}$W obtained with a 43 mm dia. by 26 mm deep Ge(Li) detector with resolution 2.3 keV FWHM and efficiency 6.5% at 1333 keV. Because the target used in this experiment was about 0.5 mm thick, the ($\alpha$,n$\gamma$)$^{180}$W lines

also appear prominently in the spectrum. The problems of $\gamma$-ray intensity normalization attendant to such a thick target precluded detailed $\gamma$-ray angular distribution measurements, but some useful qualitative data were obtained from complementary $^{181}$Ta(p,3n$\gamma$) cross-bombardments carried out with thin tantalum targets.

In addition to the $\gamma$-ray singles measurements, detailed $\gamma$-$\gamma$ coincidence spectra were obtained with a 2.5% efficient Ge(Li) detector placed at 180° geometry to the 6.5% device already described. Resolving time for the coincidence system was typically $\sim$20 nsec FWHM, though the cyclotron RF period ($\sim$60 nsec) determines the effective resolving time.

The band structure of $^{179}$W deduced from the $\gamma$-ray data is shown in Fig. 2. The most notable feature of the level scheme is the large perturbation associated with the 9/2$^+$[624] band.

The structure reported here is in essential agreement with that deduced from independent $^{178}$Hf($\alpha$,3n$\gamma$) and $^{181}$Ta(p,3n$\gamma$) experiments at Stockholm[1] and Milan.[2] Of special importance to the correct interpretation of the $^{179}$W level structure is the placement of the 11/2$^+$ level at 372.9 keV. The $\gamma$-$\gamma$ coincidence data clearly indicate the 253-keV transition to be in coincidence with the 120-, 95.9-, and 137.7-keV lines, thus supporting the level sequence shown in Fig. 2 for the low-lying
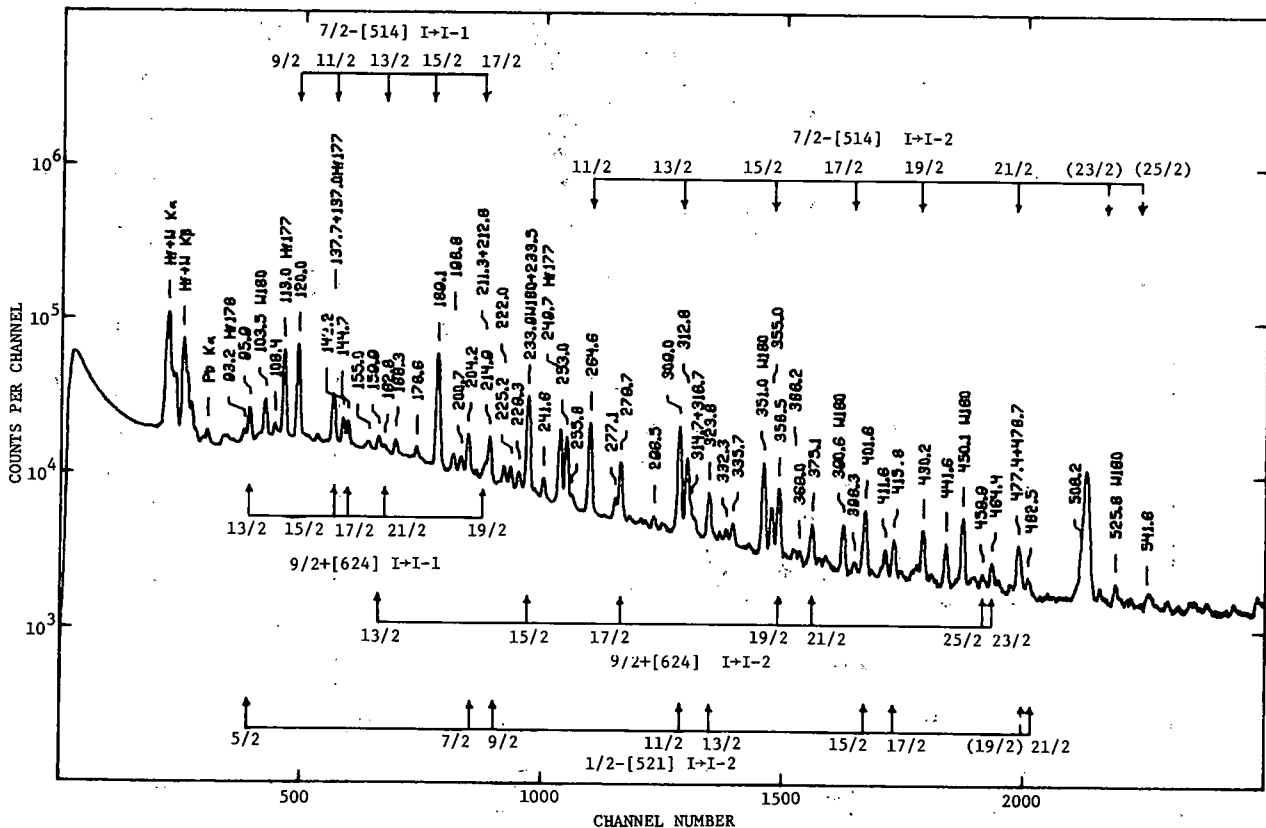


Fig. 1    The $^{177}$Hf($\alpha$,2n$\gamma$)$^{179}$W in-beam $\gamma$-ray singles spectrum.

Fig. 2 The level structure of $^{179}$W deduced from the $^{177}$Hf($\alpha$,2n$\gamma$) reaction.
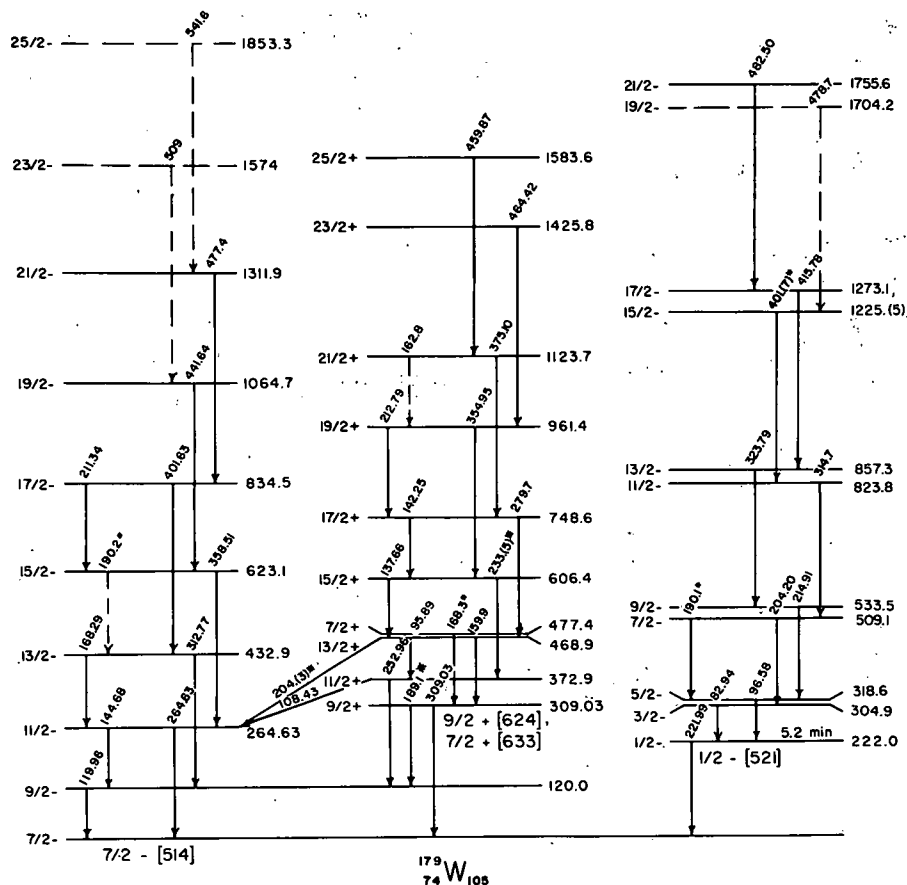
$9/2^{+}$[624] band members. In addition, the angular distribution of the 253-keV $\gamma$-ray is found in the $^{181}$Ta(p,3n$\gamma$) data to be consistent with that expected for a dipole transition.

We also note in Fig. 2 that the even-parity band has substantial K=$7/2^{+}$ character because of the very close-lying $7/2^{+}$[633] state at 477.4 keV. Identification of other members of this $7/2^{+}$ band would be of considerable importance to the Coriolis band-mixing calculations for $^{179}$W. The strong influence of the near-lying $7/2^{+}$[633] band on the $9/2^{+}$[624] band is seen in Fig. 3 where the magnitude of the perturbations in $^{179}$W contrasts sharply with the relatively mild perturbations of the $9/2^{+}$ band in $^{177,179}$Hf and $^{181}$W.

The perturbed band structure characteristic of this and other Nilsson states emanating from high-j shell-model states can often be described by diagonalizing the complete Coriolis interaction matrix for the rank j+1/2 basis set of Nilsson orbitals. The results of such a calculation should yield eigenvectors that are consistent with those required to explain the neutron-transfer "finger-print" patterns. We have carried out such a calculation for the $^{179}$W $9/2^{+}$[624] band and are able to reproduce the experimental levels of Fig. 2 to $\pm$3 keV. provided the Coriolis matrix elements near the Fermi surface are somewhat reduced. Details of the calculation and a comparison of the eigenvectors

required to reproduce the observed energy levels with the $C_{j\ell}$ values implied by the transfer reaction work of Casten et al.[3] will be described in a forthcoming publication.

References

1. Th. Lindblad, private communication (1972).

2. C.B. Birattari, et al., preprint, University of Milan (1972).

3. R. Casten, P. Kleinheinz, P.J. Daly, and B. Elbek, preprint (1971).
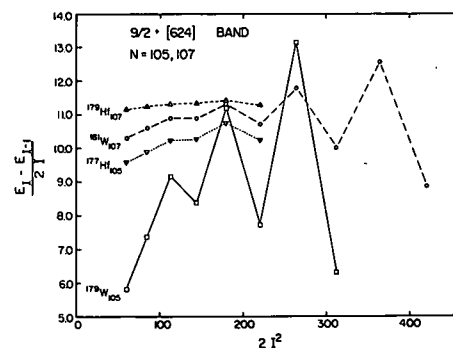
Fig. 3 Plot of $E_{I}-E_{I-1}$/2I vs. $2I^{2}$ for the $9/2^{+}$[624] rotational band in N=105 and 107 isotones.

# Levels in $^{181}$W Populated in the $^{180}$Hf($\alpha$,3n$\gamma$) Reaction *

F.M. Bernthal and R.A. Warner

The in-beam $\gamma$-ray spectroscopy work on N=105 $^{179}$W has been extended to $^{181}$W in order to study further the behavior of the 9/2$^+$[624] band in this and other neutron-deficient nuclei as one moves toward the heavier limits of the "rare-earth" region of deformation. The experimental arrangement for these experiments was quite similar to that already described for the $^{179}$W study, except that in this case a $^{180}$Hf self-supporting metal foil ($\sim$1.3 mg/cm$^2$) prepared by the argon heavy-ion sputtering technique of Sletten[1] was used as the target material. The thin foil target allowed angular distribution data to be obtained in the $^{181}$W experiments to aid in assigning the $\gamma$-ray lines to their corresponding bands.

The $^{180}$Hf($\alpha$,3n$\gamma$) reaction was carried out with 35-MeV $\alpha$-particles from the MSU Cyclotron. A typical singles $\gamma$-ray spectrum taken with a 43 mm dia. by 26 mm deep Ge(Li) detector is shown in Fig. 1. Most of the prominent $\gamma$-ray transitions have been placed in the $^{181}$W level scheme of Fig. 2. Of particular interest is the 92-keV transition which is in coincidence with the $\gamma$-ray transitions up to spin 19/2$^+$ in the ground 9/2$^+$[624] band. We therefore have tentatively associated the 92-keV transition with an isomeric state thought to exist at 906 keV. Such a state would presumably be composed of the 9/2$^+$[624] neutron and two of the four proton orbitals 9/2$^-$[514], 1/2$^-$[541], 5/2$^+$[402], and 7/2$^+$[404] known to lie near the Fermi surface in the Z=74 isotopes. If the proposed state is indeed three-particle in character, it should have a relatively long half-life, and experiments to measure the lifetime of the 92-keV line have been

undertaken. Preliminary results are consistent with a 906-keV isomer de-exciting to the spin 19/2 member of the 9/2$^+$[624] band. Several other transitions in the $^{181}$W spectrum remain unassigned and are presumably associated with the weakly populated 5/2$^-$[512] band or, as some evidence suggests, with a band built on the tentative 906-keV three-particle state.

The assigned locations of the 7/2$^-$[514] and 5/2$^-$[512] band-heads are consistent with the $^{181}$Re decay data of Daly et al.[2] In Fig. 3 a plot of the 7/2$^-$[514] and 9/2$^+$[624] band energy spacing as a function of $I^2$ is shown. The perturbation of the 9/2$^+$[624] band is comparable to that seen in $^{177}$Hf, but much less than the sharp perturbations characterizing that band in $^{179}$W and $^{183}$Os (cf. Pg. 63 and Pg. 70 of this report). On the other hand, the normally serene 7/2$^-$[514] band also experiences some minor perturbation near its band-head and at higher spins in $^{181}$W. The influence of the very close-lying members of the 5/2$^-$[512] band may be important for the lower-spin perturbations here.

A detailed analysis of the 9/2$^+$[624] band in terms of Coriolis coupling to the other i$_{13/2}$ orbitals is in progress. Our preliminary results reproduce the energies of the 9/2$^+$[624] band members through spin 25/2 to $\pm$1 keV of experiment if one accepts an ad hoc attenuation of Coriolis matrix elements near the Fermi surface. Work on the $^{181}$W level scheme is continuing.

## References

1. G. Sletten and P. Knudson, preprint (1971).

2. P.J. Daly, K. Ahlgren, K.J. Hofstetter, and R. Hochel, Nucl. Phys. A161, 177(1971).
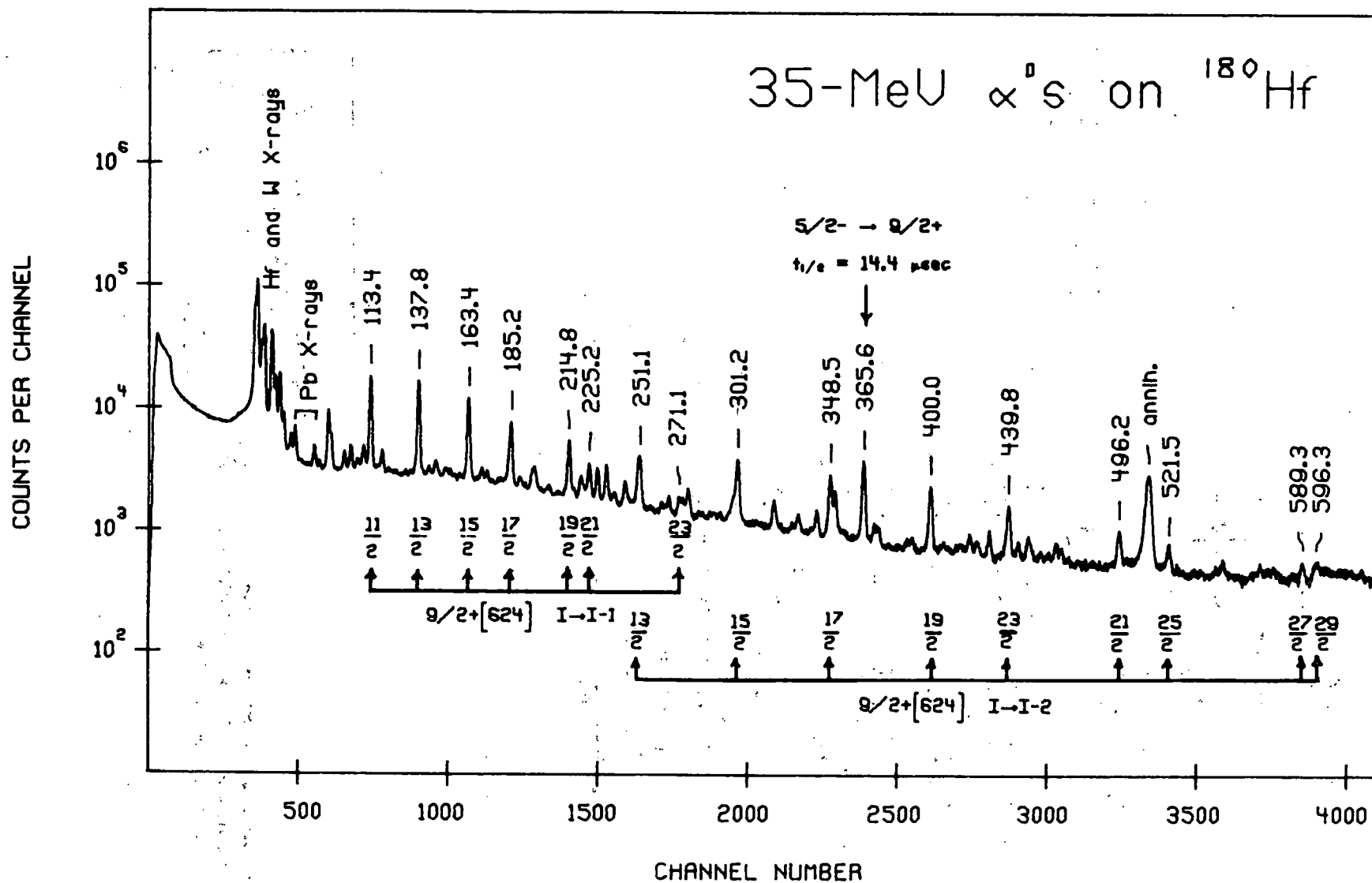
Fig. 1    The prompt singles γ-ray spectrum from the $^{180}$Hf($\alpha$, 3nγ)$^{181}$W reaction (35 MeV).
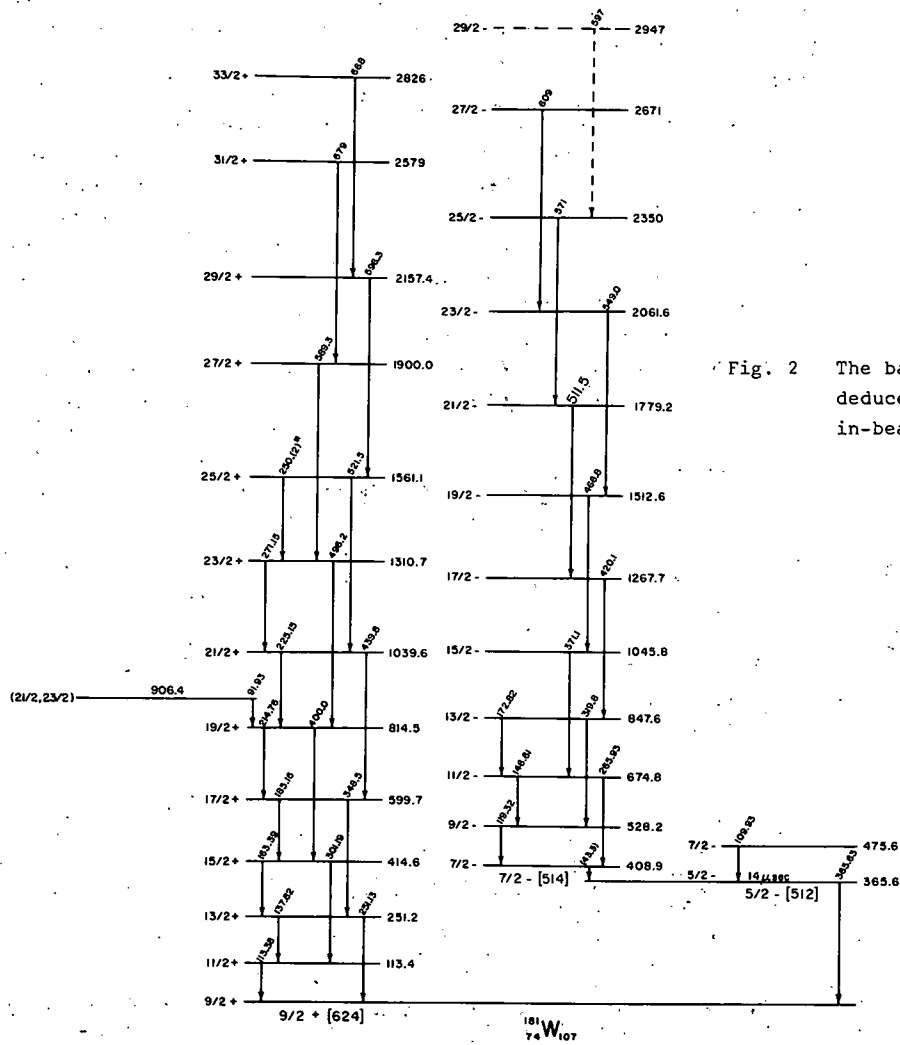
Fig. 2    The band structure of $^{181}$W as deduced from the $^{180}$Hf($\alpha$,3n$\gamma$) in-beam $\gamma$-ray spectrum.



Fig. 3    The rotational energy spacing $E_I-E_{I-1}/2I$ as a function of $2I^2$ for the $7/2^-$[514] and $9/2^+$[624] bands in $^{181}$W.
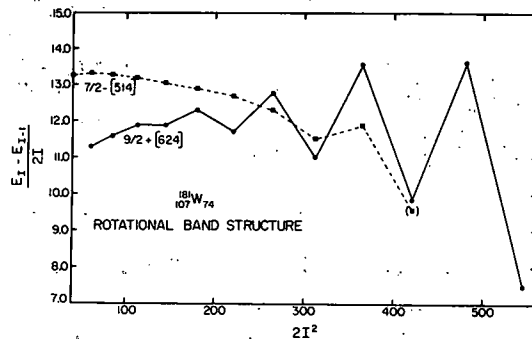
# Search for the "Phase Transition" Effect at High Spins in Even-Even Nuclei Near the Edge of the Rare-Earth Deformed Region*

R.A. Warner and F.M. Bernthal

Since the early prediction[1] of a phase transition in deformed nuclei and the subsequent discovery[2] of marked increases in nuclear moments of intertia near 14 units of angular moentum for some rare-earth nuclei, there has been considerable speculation regarding the relationship of the prediction to the discovery. A more detailed explanation for the observed phenomenon has recently been offered,[3] and suggests that the behavior seen occurs specfically because of the presence of low-$\Omega$ states from the $i_{13/2}$ neutron orbital near the Fermi level in the nuclei studied. Meanwhile more experimental data have become available,[4] demonstrating the effect in a number of nuclei with $88 < N \leq 104$.

As it might be argued that all known cases fall within the region allowed by the description of Stephens and Simon,[3] it seemed essential to investgate moments of inertia in which the irregularity would not be predicted (by this model) to occur at such low angular momenta.

The states of interest are produced in ($\alpha$,xn) reactions on self-supporting metallic foils. Gamma-gamma coincidence data are used to establish the yrast cascades, and $\gamma$-ray anisotropies are measured to verify that the transitions observed have angular distributions consistent with the stretched-E2 assignments.

Data have already been obtained on states in $^{180}W$ and $^{182,184,186,188}Os$. In addition to these nuclei with $N \geq 106$, data have been collected on the $N=90$ and 92 nuclei $^{154,156}Gd$ in a further attempt to define limits for the region of "backbending" moments of inertia. Some sample coincidence spectra are displayed in Fig. 1, and in Fig. 2 the moments of inertia are plotted versus rotational frequency (according to the convention adopted by Johnson et al.[2]) for those data which have been analyzed.

## References

1. B.R. Mottelson and J.G. Valatin, Phys. Rev. Letters 5, 511(1960).
2. A. Johnson, H. Ryde, and J. Sztarkier, Phys. Letters 34B, 605(1971).
3. F.S. Stephens and R.S. Simon, Nucl. Phys. A183, 257(1972).
4. P. Thieberger, A.W. Sunyar, P.C. Rogers, N. Lark, O.C. Kistner, E. der Mateosian, S. Cochavi, and E.H. Auerbach, Phys. Rev. Letters 28, 972(1972). R.M. Lieder, H. Beuscher, W.F. Davidson, P. Jahn, H.-J. Probst, and C. Mayer-Böricke, Phys. Lett. 39B, 196(1972). A. Johnson, H. Ryde and S.A. Hjorth, Nucl. Phys. A179 753(1972). H. Beuscher, W.F. Davidson, R.M. Lieder, and C. Mayer-Böricke, Phys. Lett. 40B, 449(1972).
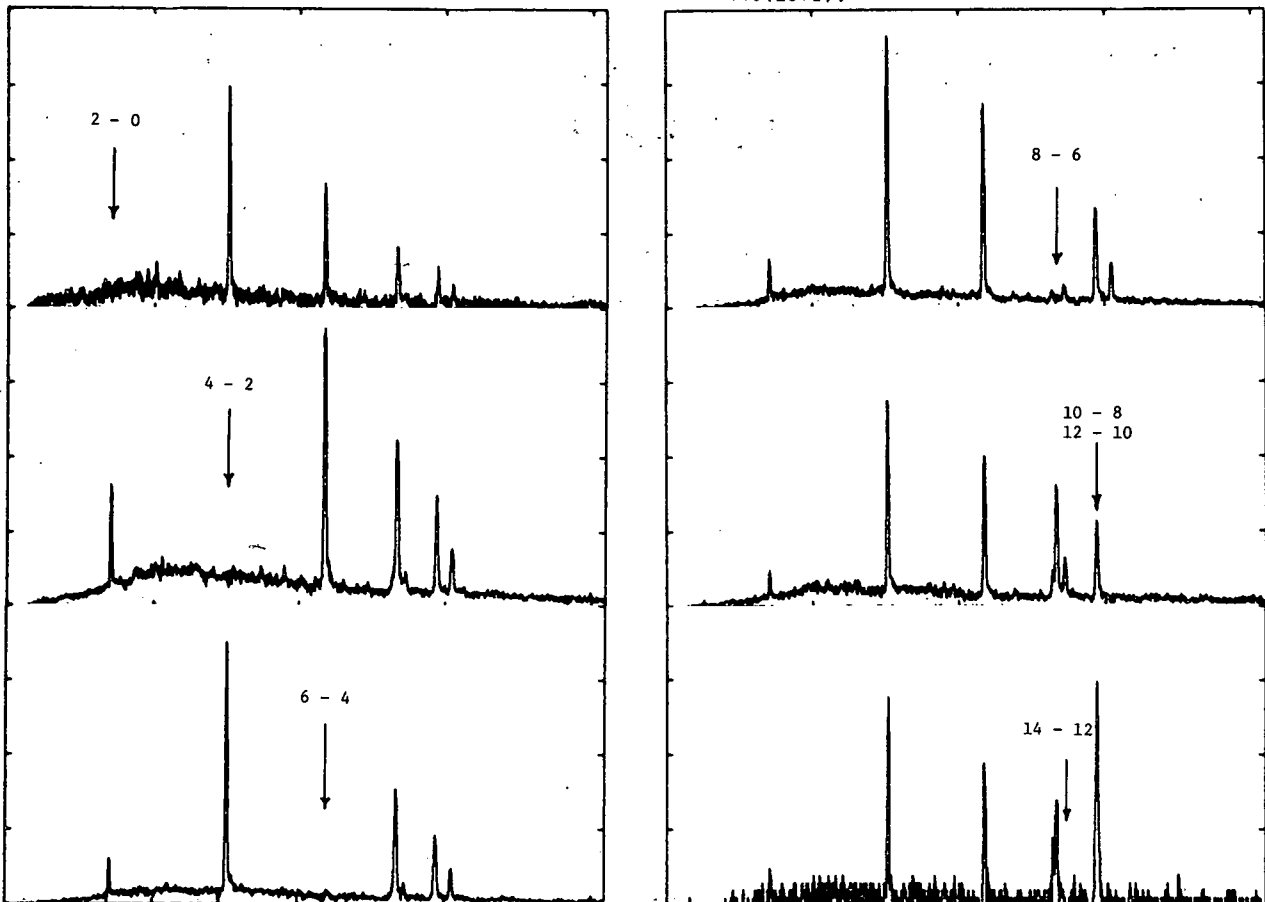
Fig. 1 Gamma-rays in coincidence with selected transitions in $^{182}Os$, prepared by the reaction $^{182}W(\alpha,4n)$. The location of the gate for each spectrum is marked. Notice that the 10-to-8-12-to-10 doublet is the only peak appearing in its own gate.
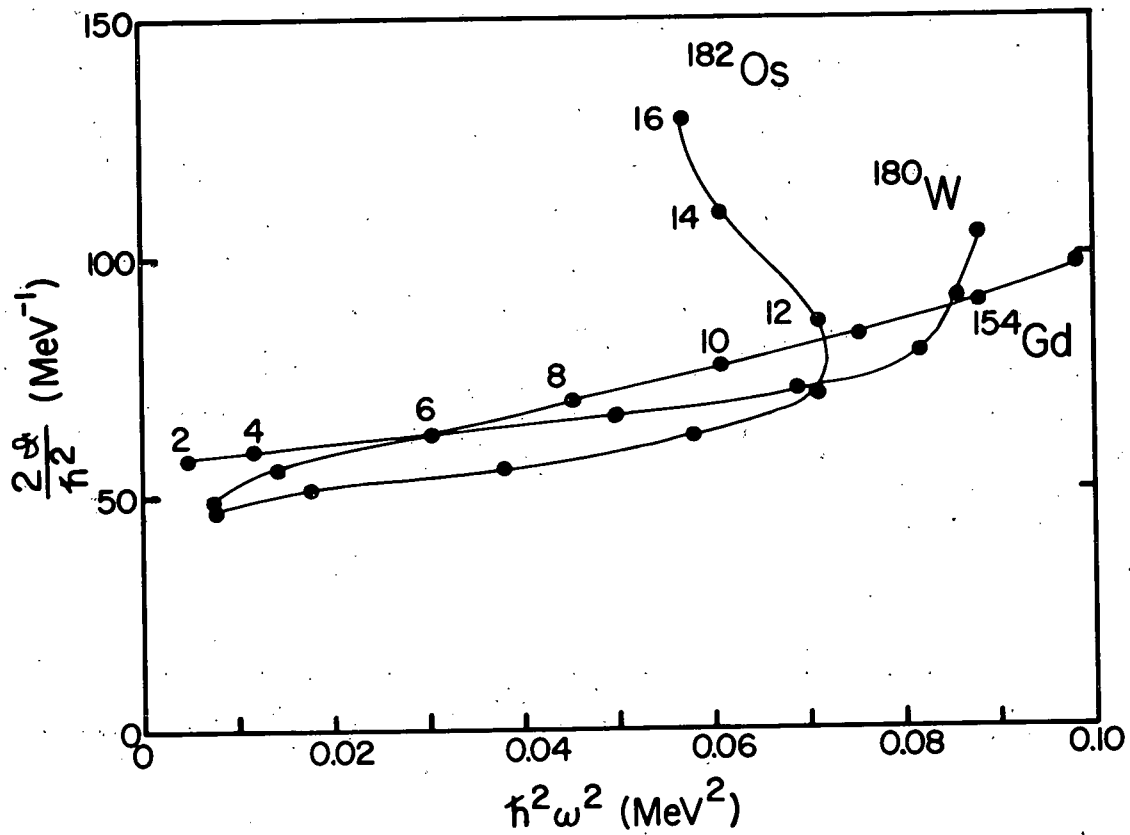
Fig. 2  Moment of inertia plotted against rotational frequency for three of the nuclei being studied.

F.M. Bernthal, R.A. Warner, C.L. Dors, and G. Sletten**

In-beam $(\alpha, xn\gamma)$ study of the odd-neutron species in the heavier "rare-earth" deformed region has been extended to the osmium isotopes. The first data obtained have been those for $^{183}$Os, produced by the $^{182}$W$(\alpha,3n\gamma)$ reaction (Fig. 1). In this experiment, a self-supporting foil of $^{182}$W (94% enriched) prepared at Niels Bohr Institute by the argon-ion sputtering method,[1] was bombarded with 35-MeV α-particles from the MSU Cyclotron. Preliminary analysis of the γ-ray singles and γ-γ coincidence data has identified members of the ground $9/2^+[624]$ rotational band up to spin 29/2 and again we find this band, based on the $i_{13/2}$ family of Nilsson orbitals, to be strongly perturbed—even more strongly than is the corresponding band in $^{179}$W. In Fig. 2 we show a plot of the $9/2^+[624]$ band level spacing in $^{183}$Os as a function of $I^2$. Analysis of this highly distorted band structure by the Coriolis matrix diagonalization technique is underway, and data on other low-lying bands in this isotope of Os are being analyzed.

Preliminary data have also been obtained on $^{187}$Os from the $^{186}$W$(\alpha,3n\gamma)$ reaction. This isotope should be of particular interest because of the presence at 257 keV of the $11/2^+[615]$ Nilsson orbital. The rotational band associated with this orbital is expected to be strongly populated in the in-beam studies, and should yield valuable further information on the effects of rotation-particle coupling on the band structure associated with the $i_{13/2}$ neutron orbitals in nuclei near the edge of the deformed region. It is worth noting that the increasing complexity and difficulty in interpreting the level structure of nuclei in this and similar regions often requires that decay data be used to supplement the in-beam data. In those cases where the decays of iridium isotopes to the odd-A osmium isotopes are not well understood, we have undertaken complimentary decay-scheme experiments.

References

1. G. Sletten and P. Knudson, preprint (1971).
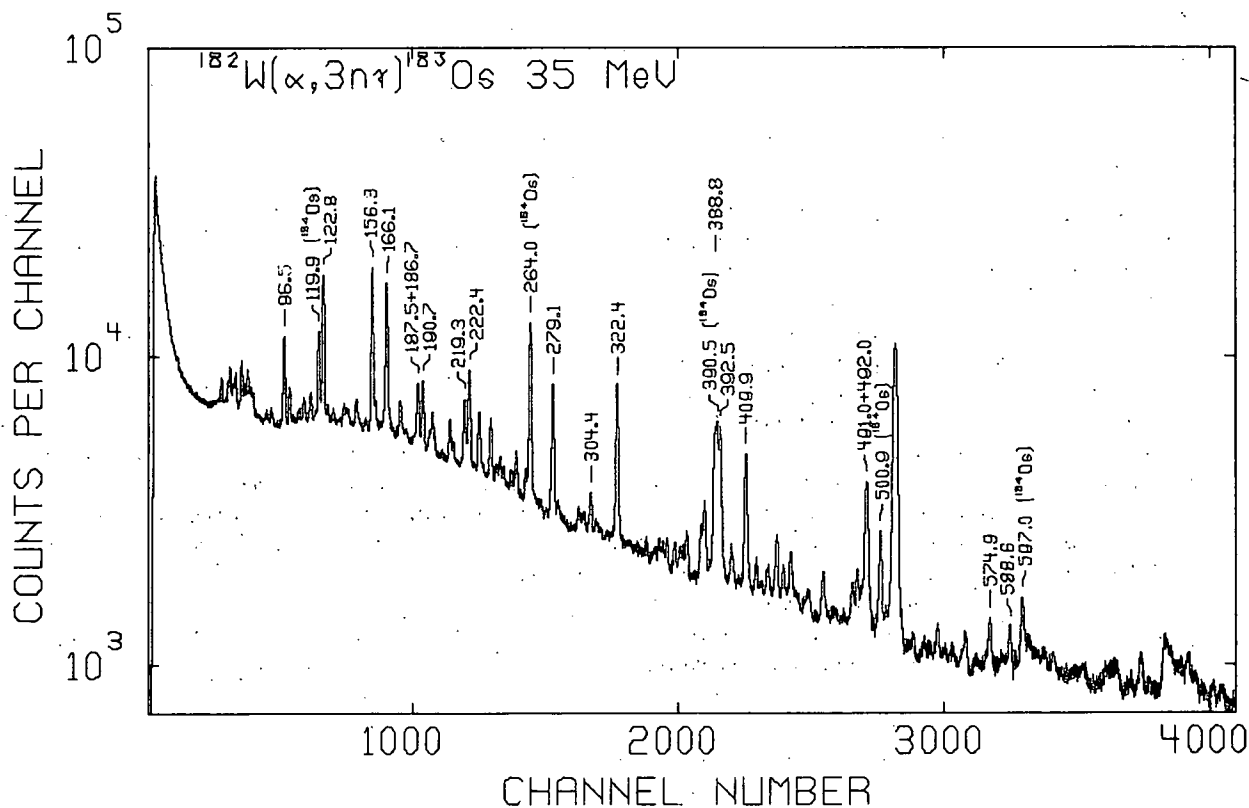
Fig. 1 The γ-ray singles spectrum from the $^{182}$W$(\alpha,3n\gamma)^{183}$Os Reaction.
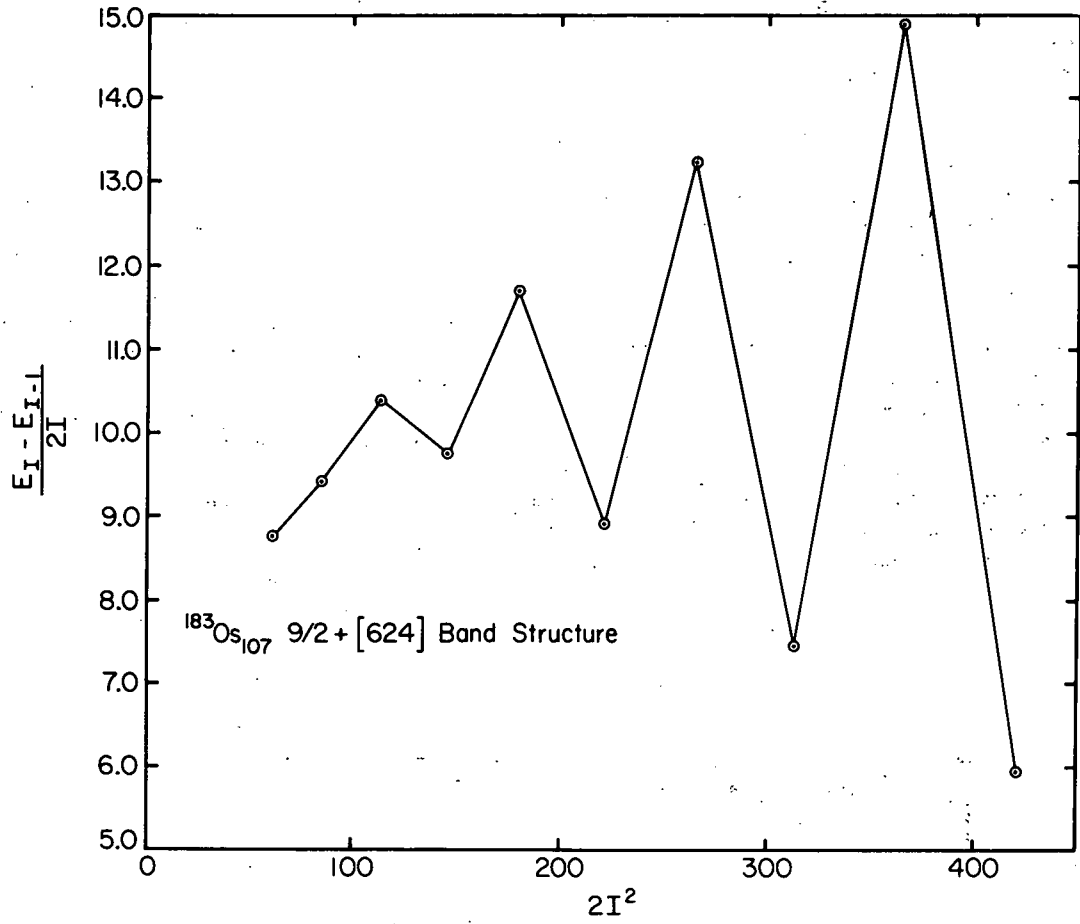
Fig. 2    Plot of $E_I-E_{I-1}/2I$ vs. $2I^2$ for the $9/2^+[624]$ ground band of $^{183}$Os.

The figure is labeled: $^{183}$Os$_{107}$ $9/2+[624]$ Band Structure

# Levels in $^{199}$Hg Populated in the Decay of $^{199}$Tl*

G. Mathews** and F.M. Bernthal

In supplement to the early NaI(Tl) work of Bauer, et al.[1] the γ-ray spectrum associated with EC decay of $^{199}$Tl (7.4 hour) has been re-investigated with Ge(Li) detectors. Levels in $^{199}$Hg have been previously investigated by Coulomb excitation, transfer reactions, and $^{199}$Au decay studies. This previous work has recently been summarized in Ref. 2.

We here report the observation of 17 new γ-rays arising from the $^{199}$Tl decay. All of these newly observed transitions have been placed in the preliminary revised $^{199}$Tl decay scheme shown in Fig. 1.
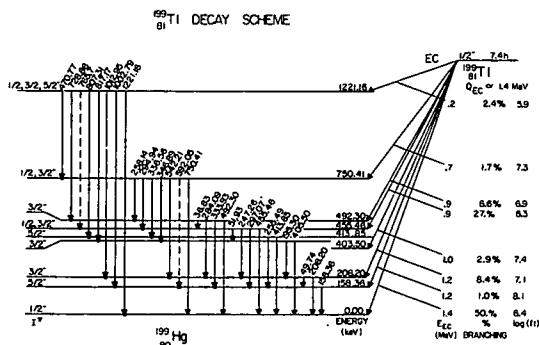


Fig. 1 Proposed scheme for the EC decay of $^{199}$Tl to levels in $^{199}$Hg.

The $^{199}$Tl sources were prepared by the $^{197}$Au(α,2n) reaction on gold foils ≃100 mg/cm$^2$ thick. Typical α-particle beam energy was ≃29 MeV.

Singles γ-ray spectra were taken with a 10.4% efficient Ge(Li) detector having resolution

2.4 keV FWHM and peak-to-Compton ratio ∿35:1 at 1333 keV. A typical singles spectrum is shown in Fig. 2.

The $^{199}$Tl peaks were assigned by following their decay rates relative to that of the known 455.5-keV $^{199}$Tl γ-ray. Assignments to $^{198}$Tl and $^{200}$Tl were made in a similar way on the basis of normalization to the 636.8 and 368.0-keV transitions in those decays, respectively. The γ-ray energies and intensities associated with $^{199}$Tl decay are summarized in Table 1. A 592.0-keV transition is assigned to $^{199}$Tl decay on the basis of coincidence and half-life data, although the strong 591.8-keV $^{200}$Tl transition obscures the line in singles. The analysis of all singles data was effected with use of the photopeak fitting code, SAMPO. On the basis of this analysis, the 25 γ-rays listed in Table I have been assigned to $^{199}$Tl decay. Also included in the $^{199}$Tl decay scheme are low-energy transitions at 36.83, 49.74, and 51.93 keV identified in previous work.[3] The data of Ref. 1 are shown for comparison.

The level scheme of Fig. 1 was constructed with the aid of γ-γ coincidence data acquired with two Ge(Li) detectors positioned at 180° geometry. Data for the complete 4096×4096 coincidence matrix were stored serially on magnetic tape for later analysis. In Fig. 3 we show representative coincidence spectra obtained in this way. The spectra for the 403.5, 492.3, 817.7, and 1062.8-keV transitions show, in part, the basis on which we have assigned new levels at 750.4 and 1221.2 keV in $^{199}$Hg populated in the decay of $^{199}$Tl. The log(ft) values for EC-β$^+$
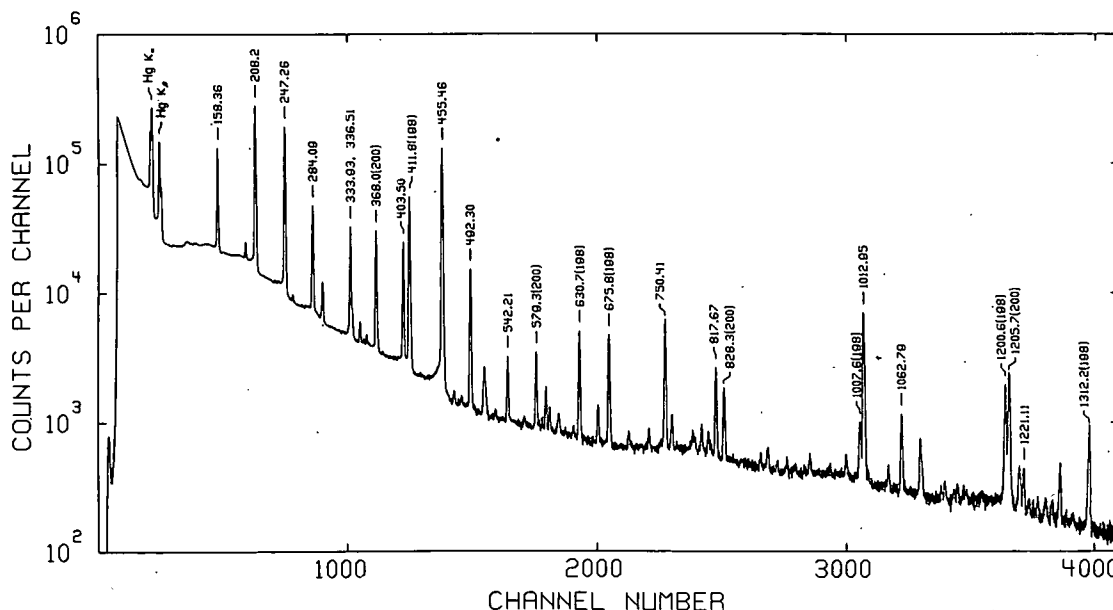


Fig. 2 Gamma-ray singles spectrum from $^{199}$Tl decay. Prominent contaminant lines from $^{198}$Tl and $^{200}$Tl are identified also.
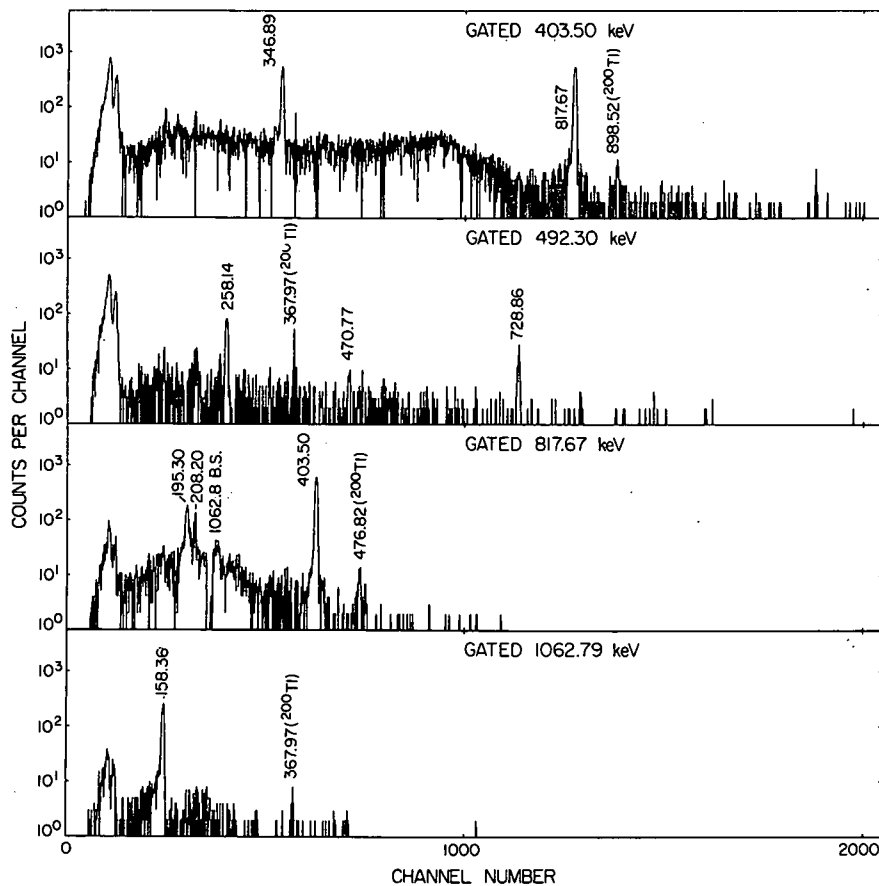
Fig. 3   The 403.5, 492.3, 817.7, and 1062.8-keV γ-γ coincidence spectra from $^{199}$Tl decay.

decay of $^{199}$Tl have been calculated on the basis of an assumed Q-value of 1.4 MeV derived from β-decay systematics, and a previously measured[4] 50% EC-β$^+$ feeding to the $^{199}$Hg ground state. The tentative spin and parity assignments are consistent with the data compilation of Lewis.[2] It is worth noting that the relatively low log(ft) for EC-decay to the 1221.16-keV level seems to point to an allowed β-decay. If this were the case, then an even parity would be indicated for that state. Such an assignment would be difficult to account for on the basis of elementary shell-model considerations. However, the uncertainty in the 0.2-MeV decay energy makes this log(ft) value somewhat questionable without the aid of precise data on the $^{199}$Tl Q-value.

References

1. R.W. Bauer, L. Grodzins, and H.H. Wilson, Phys. Rev. 128, 694(1962).

2. M.B. Lewis, Nuclear Data Sheets for A=199, B6, 355(1971).

3. B. Jung and J. Svedburg, Nucl. Phys. 20, 630(1960).

TABLE I

Energies and Relative Intensities of γ-rays from $^{199}$Tl Decay

| Present Work | | Bauer et al. | |
|---|---|---|---|
| Energies (keV) | Intensities (rel) | Energies (keV) | Intensities (rel) |
| 158.36±.05 | 40    ±.2 | 158.4 | 40    ±4 |
| 195.30±.05 | 2.1 ±.2 | 195.2 | 7.0±1.4 |
| 208.20±.05 | 9.    ±5 | 208.2 | 88    ±9 |
| 247.26±.05 | 75.    ±4 | 247.2 | 68    ±7 |
| 255.49±.11 | .10±.03 | 254 | |
| 258.14±.10 | .58±.06 | | |
| 284.09±.05 | 17.8 ±.9 | 284.0 | 10    ±2 |
| 294.94±.09 | .42±.04 | | |
| 297.07±.06 | 2.8 ±.3 | | |
| 333.93±.05 | 14.2 ±.7 | 333.9 | 12.0±2.4 |
| 336.56±.08 | 1.14±.11 | | |
| 346.89±.08 | 1.07±.11 | | |
| 403.50±.05 | 13.9 ±.7 | 403.4 | 3.0±0.6 |
| 413.85±.08 | 1.59±.16 | | |
| 455.46±.05 | 100±5 | 455.1 | 100    ±10 |
| 470.77±.10 | .31±.06 | | |
| 492.30±.05 | 12.3 ±.6 | 492.8 | 8.0±1.6 |
| 542.21±.05 | 2.13±.21 | | |
| *592.0 ±.11 | <0.8 | | |
| 728.86±.11 | .36±.04 | | |
| 750.41±.05 | 8.4 ±.4 | | |
| *765.7 ±.15 | <.05 | | |
| 807.31±.11 | .40±.04 | | |
| 817.67±.07 | 3.26±.20 | | |
| 1012.95±.05 | 14.2 ±.7 | | |
| 1062.79±.07 | 2.05±.21 | | |
| 1221.16±.12 | .24±.03 | | |

*Observed in coincidence spectrum only.

W.T. Wagner and G.M. Crawley

A high resolution study of inelastic proton scattering on these nuclei is a powerful technique for testing nuclear structure models and the direct reaction mechanism in this region of A. Utilizing dispersion-matching methods with extensive use of the on-line tuning technique of Blosser et al.,[1] exposures have been taken at 35 MeV bombarding energy on nuclear emulsions in the Enge split-pole spectrograph. Results have been obtained for the three isotopes $^{207}$Pb, $^{208}$Pb, and $^{209}$Bi at angles between 10° and 100° with a typical resolution of less than 10 keV (FWHM). A spectrum of $^{208}$Pb is displayed below.

This spectrum reveals the collective states of $^{208}$Pb as well as the weakly excited levels. Even with the small exposure length a number of unnatural parity states are evident; the 4$^-$ state at 3.475 MeV of excitation is discernible as well as the 6$^-$ and the 4$^-$ states at 3.920 and 3.961 MeV, respectively. The background is small and discrete structure is apparent up to about 7.4 MeV excitation energy where $^{208}$Pb becomes unstable to neutron decay.

For the doubly-magic nucleus, $^{208}$Pb, extensive shell model theories have been constructed giving nuclear wave functions for both the natural and unnatural parity states. Some work has also been done on $^{207}$Pb and $^{209}$Bi. With the direct reaction scattering codes available and the reasonably well understood two nucleon effective interaction, the natural parity state wave functions given by microscopic theory can be tested. Including the effects of knock-on exchange, core polarization, and the tensor and spin-orbit two

nucleon force will permit a thorough investigation of the theory. Further, observation of the unnatural parity states should allow determination of the tensor and $\underline{L} \cdot \underline{S}$ components of the force since scattering into such states is apparently sensitive to these two components especially at higher energies. The low background of typical spectrograph data encourages a search for the giant dipole and quadrupole states. The strengths of these resonances spread over a considerable region of excitation energy (about 2 MeV), both having weak but strongly forward peaked angular distributions on the order of 500 μb/sr maximum at this energy.

Although the odd mass nuclei are essentially single particle in behavior, inelastic scattering gives information on their collective characteristics. Indeed, the low-lying multiplets in $^{207}$Pb and $^{209}$Bi have been successfully described by the weak coupling model so that analysis of higher lying states would be interesting.

Elastic scattering from these nuclei will also be studied so that optical model parameters needed for inelastic scattering calculations can be obtained. The feasibility of using a position sensitive wire proportional counter in the spectrometer focal plane for this less resolution-dependent study of elastic and collective states is currently being determined.

References

1. H.G. Blosser, G.M. Crawley, R. deForest, E. Kashy, and B.H. Wildenthal, Nucl. Instr. and Methods 91, 61(1971).



$^{208}$PB(P,P) AT 40 DEG -- Q = 176 UC -- PLATE 853B
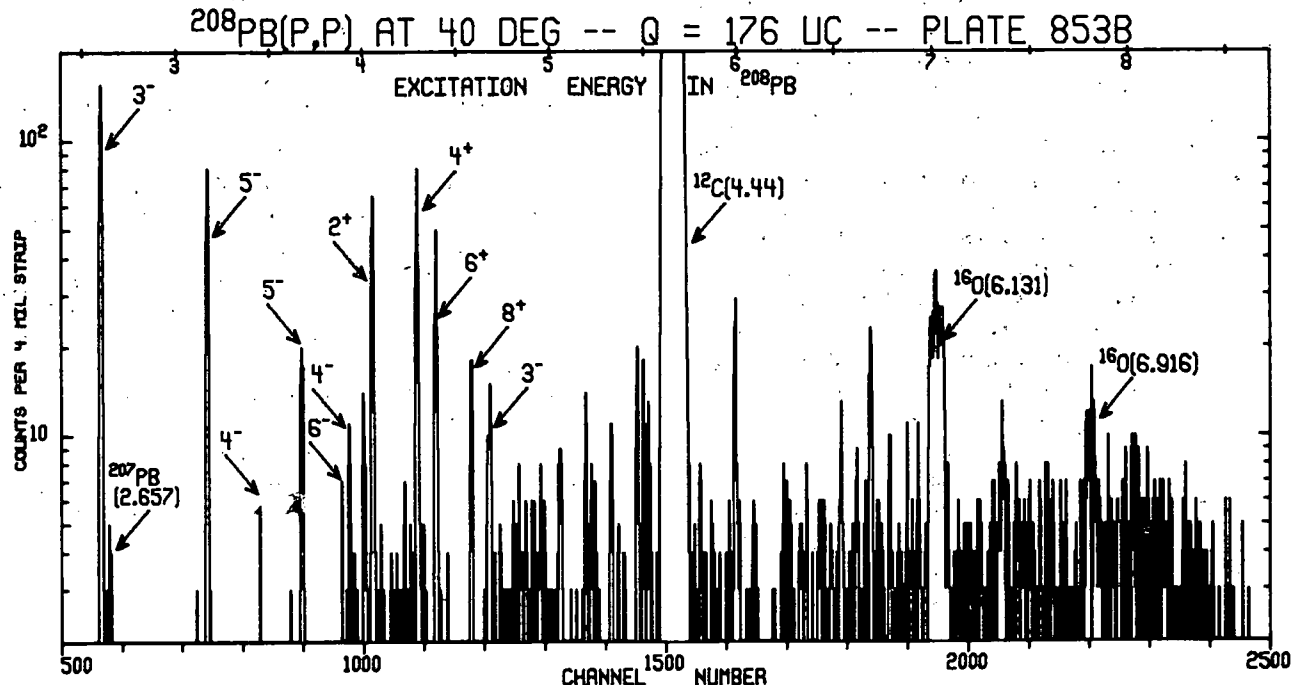
The Pb isotopes are a region of the nuclear chart which is especially well suited to test the shell model in detail for several reasons: (1) $^{208}$Pb is believed to be a relatively good closed core. (2) The neutron single particle states are known from the $^{208}$Pb(p,d)$^{207}$Pb reaction. (3) Assuming the shell model and using a reasonable basis, all the Pb isotopes should be calculable using these known single particle energies and only the T=1 part of the two-body interaction. Except for renormalization effects, and assuming charge symmetry, this T=1 interaction depends only on proton-proton scattering, not on the less well determined proton-neutron scattering.

In order to make such a test, the (p,d) and (p,t) reactions are being studied on all the stable Pb isotopes using both nuclear emulsions and the position sensitive proportional counter in the focal plane of a magnetic spectrometer. By using the identical experimental set-up for studying both reactions on all four targets, we are able to measure relative cross sections on the various isotopes to a few percent. Hence, we can accurately deduce spectroscopic factors for the (p,d) reaction on the lighter Pb isotopes relative to those for single hole states seen in the $^{208}$Pb(p,d)$^{207}$Pb reaction. Such a procedure eliminates many of the usual ambiguities in conventional DWBA analysis.

## The $^{208}$Pb(p,d)$^{207}$Pb and $^{207}$Pb(p,d)$^{206}$Pb Reaction

### W.A. Lanford and G.M. Crawley

The study of $^{208}$Pb(p,d)$^{207}$Pb reaction provides the basis for understanding the (p,d) reactions on the lighter isotopes of Pb. The strong states seen in this reaction correspond to the $3p_{1/2}$, $2f_{5/2}$, $3p_{3/2}$, $1i_{13/2}$, $2f_{7/2}$, and $1h_{9/2}$ single neutron hole states. The study of the transitions to these single hole states provides a calibration of the DWBA analysis (both in strength and angle dependence) which makes the analysis of the (p,d) reaction on the lighter isotopes of Pb less ambiguous. In addition, many states are seen excited in this reaction; the strength to these non-single neutron hole states indicates some of the limitations of shell model calculations based on a $^{208}$Pb closed core. It is also possible that these weak transitions result from multi-step processes in the reaction mechanism.

Since the $^{207}$Pb ground state corresponds to a $p_{1/2}$ neutron hole outside $^{208}$Pb, the $^{207}$Pb(p,d)$^{206}$Pb reaction excites states in $^{206}$Pb with configurations of the form $(p_{1/2})^{-1}x(L_j)$ where $L_j$ stands for the available single neutron hole states (the same ones which are strongly ex-

cited in $^{208}$Pb(p,d)$^{207}$Pb). Shown in Fig. 1 are spectra of the $^{208}$Pb(p,d)$^{207}$Pb and $^{207}$Pb(p,d)$^{206}$Pb reactions observed with the position sensitive proportional counter. These spectra are plotted with a common Q-value scale (approximately), and are labeled with the dominant L-value as determined by the angular distributions.
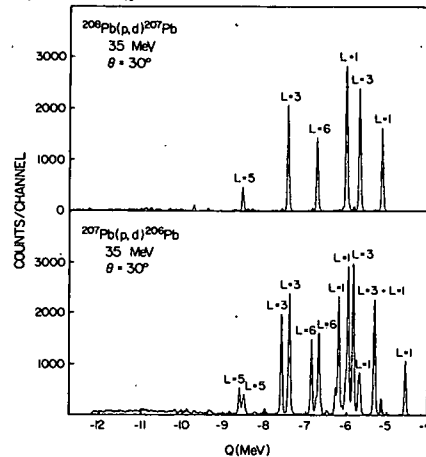


Fig. 1   Spectra of the $^{208}$Pb(p,d)$^{207}$Pb and $^{207}$Pb(p,d)$^{206}$Pb reactions observed with the position sensitive proportional counter in the focal plane of the magnetic spectrometer. The spectra have a common Q-value scale (approximate).

It turns out that the strong states observed above 2.0 MeV have very simple shell model configurations of $(p_{1/2})^{-1}$ weakly coupled to the $i_{13/2}$, $f_{7/2}$, and $h_{9/2}$ single neutron hole states. This can be seen by looking at highest L=6, 3, and 5 transitions shown in Fig. 1. Note that the strength in the $^{208}$Pb(p,d)$^{207}$Pb reaction to these states is split to close doublets in the $^{207}$Pb(p,d)$^{206}$Pb reaction. The low-lying states have more mixed configurations.

## The $^{206}$Pb(p,d)$^{205}$Pb and $^{204}$Pb(p,d)$^{203}$Pb Reactions

### W.A. Lanford

These experiments conducted with the identical experimental setup and the $^{208}$Pb(p,d)$^{207}$Pb reaction provide spectroscopic data on the lighter isotopes of Pb with which to test the shell model. Shown in Fig. 2 are spectra of the $^{206}$Pb(p,d)$^{205}$Pb and $^{204}$Pb(p,d)$^{203}$Pb reaction observed with the position sensitive proportional counter. These spectra are plotted on a common Q-value scale (approximately). Previous measurements[1] of the $^{206}$Pb(d,t)$^{205}$Pb reaction led to spectroscopic factors which were in serious disagreement with shell model predictions. Preliminary analysis of our results indicates very good agreement between theory and experiment.
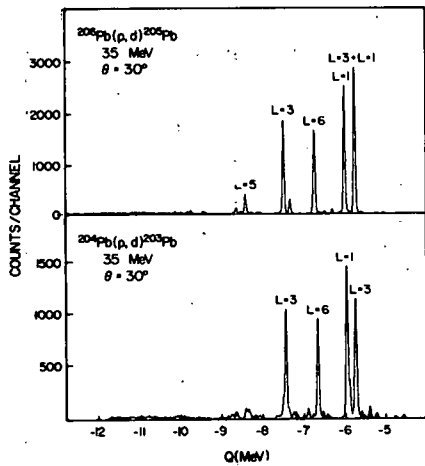
Fig. 2   Spectra of the $^{206}$Pb(p,d)$^{205}$Pb and $^{204}$Pb(p,d)$^{203}$Pb reactions observed with the position sensitive proportional counter in the focal plane of the magnetic spectrometer.   The spectra have a Common Q-value scale (approximate).

It is interesting to note that, except for the lowest L=1 and L=3 transitions, the spectra look very much like the $^{208}$Pb(p,d)$^{207}$Pb spectra shown in Fig.  1.   Notice that the L=1, 6, 3, and 5 transitions occur at about the same Q-value in all reactions.   This is a further indication of how good simple shell model calculations should be for these isotopes.   In the simplest model of a spherical shell model with a very weak residual interaction, except for the strength to the lowest L=1 and L=3 transitions, the (p,d) reaction on all the even isotopes of Pb should be the same.   Preliminary evaluation of the strengths to the $p_{3/2}$, $i_{13/2}$, $f_{7/2}$, and $h_{9/2}$ orbits indicates that this is not too far from the case.

Reference

1. Robert Tickle and John Bardwick, Phys. Rev. 178, 2006(1969).

The (p,t) Reaction on the Stable Isotopes of Lead

W.A. Lanford

The (p,t) reaction is being studied on all the stable Pb isotopes using a 35 MeV proton beam.   The triton spectra are recorded using either nuclear emulsions or the position sensitive proportional counter in the focal plane of our split-pole magnetic spectrometer.   Figure 3 shows spectra of the (p,t) reaction on $^{208}$Pb, $^{207}$Pb, $^{206}$Pb, and $^{204}$Pb.   The spectra are aligned so as to have a common energy (Q-value) scale.

The results are being analyzed using the two-nucleon DWBA code DWUCK and the shell model wave functions of McGrory[1] for $^{208}$Pb, $^{206}$Pb, and $^{204}$Pb. Figure 4 shows DWBA fits to the data for the $^{208}$Pb(p,t)$^{206}$Pb reaction to the lowest $0^+$, $2^+$, and $4^+$ states of $^{206}$Pb.   Each calculated cross-section has an independent normalization.   Also shown is the transition to the $3^+$ unnatural parity state at 1.339 MeV.

McGrory's shell model wave functions were used to predict the relative intensities of states of a given $J^\pi$ in the $^{208}$Pb(p,t)$^{206}$Pb and $^{206}$Pb(p,t)$^{204}$Pb reactions.   Figure 5 shows the comparison
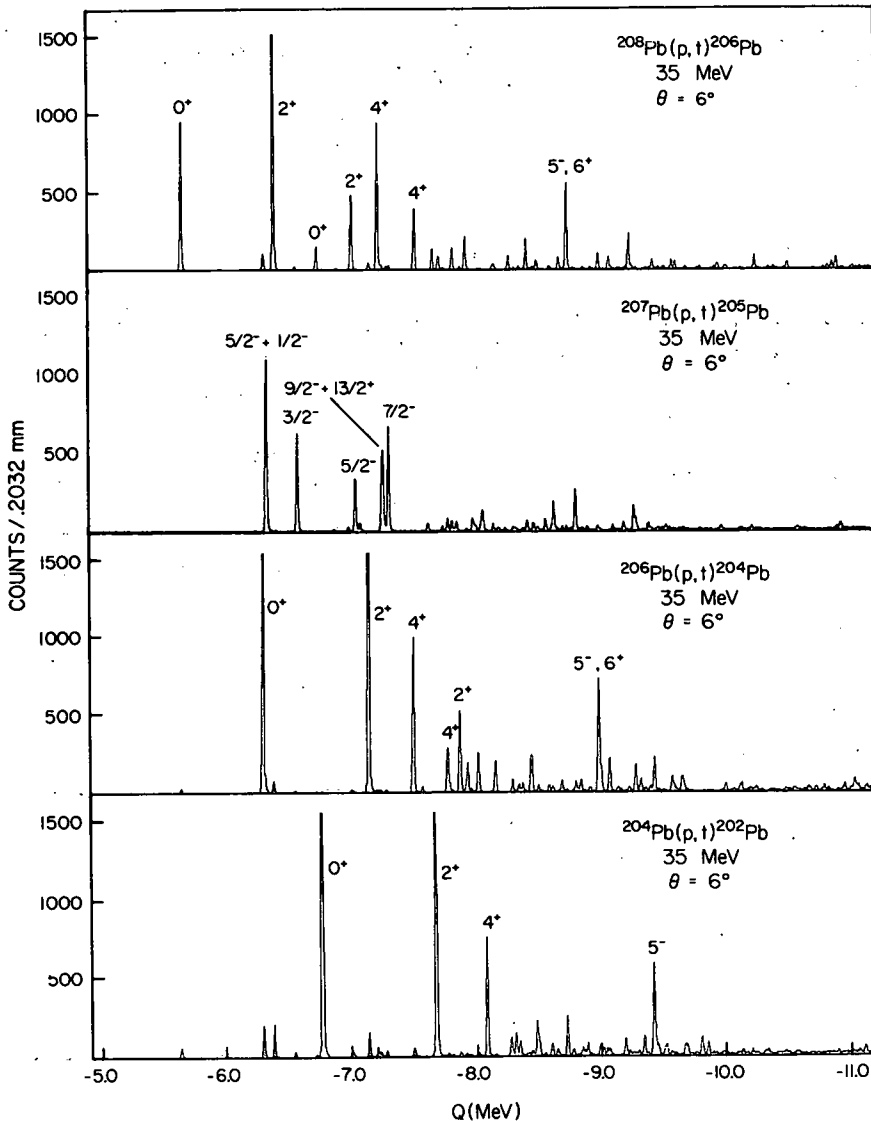


Fig. 3   Spectra of the (p,t) reaction on the stable isotopes of lead. All spectra have a common Q-value scale.
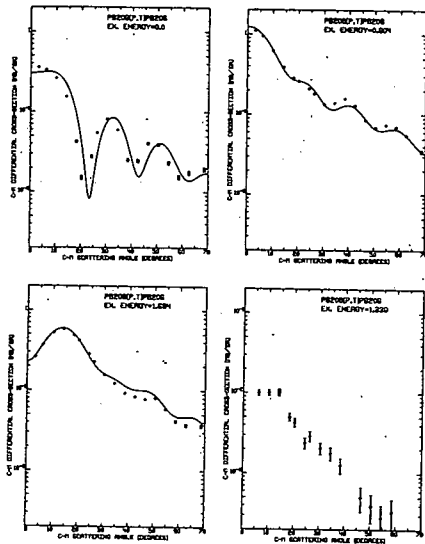
Fig. 4    Experimental and DWBA calculations for
the angular distributions of the
$^{208}$Pb(p,t) reaction to the lowest
$0^+$(0.0 MeV), $2^+$(0.804), $4^+$(1.684),
and $3^+$(1.339) states in $^{206}$Pb.

between these predictions and the experiment for
$0^+$, $2^+$, and $4^+$ states.  Note there is generally
good agreement for the relative cross-sections
of different L-transfers.

### References

1. J.B. McGrory, ORNL, private communication,
   August 1972.
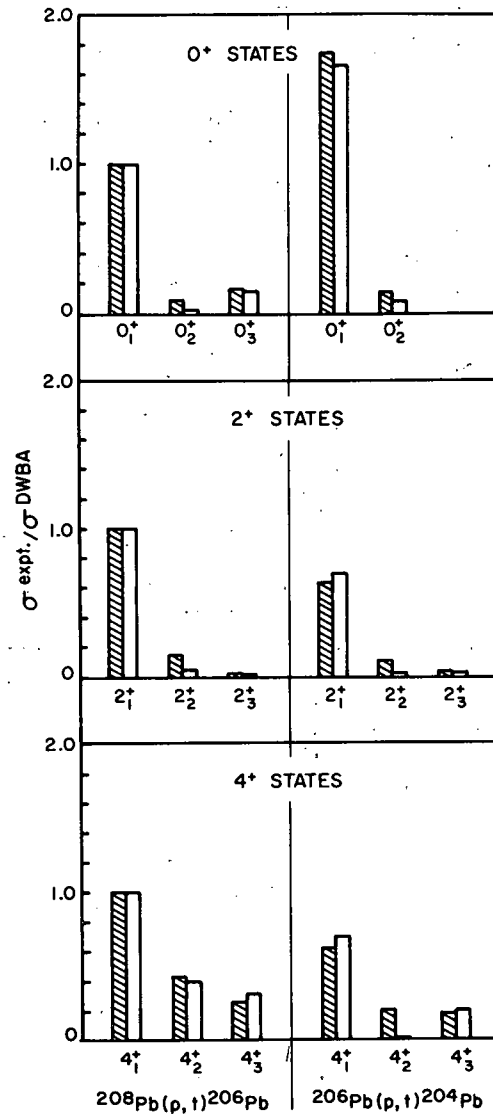
Fig. 5    The comparison of theory and experiment
for the cross-sections to the $0^+$, $2^+$,
and $4^+$ states in $^{206}$Pb and $^{204}$Pb.  Theory
and experiment are normalized for the
lowest states in $^{208}$Pb(p,t)$^{206}$Pb reaction.

# High Resolution Study of the Particle-Hole Multiplets
## in $^{208}$Bi from the $^{209}$Bi(p,d) Reaction at 35 MeV

G.M. Crawley, W. Lanford, E. Kashy, and H.G. Blosser

Recent discussions of the effective two nucleon force obtained from the two particle spectra of nuclei near closed shells[1] has again focussed attention on such nuclei. One important example near the doubly magic nucleus $^{208}$Pb, is the nucleus $^{208}$Bi with a proton outside the $^{208}$Pb core and a neutron hole in the core. In the present experiment, we have studied $^{208}$Bi by the reaction $^{209}$Bi(p,d) using the high resolution capability of the Michigan State Cyclotron. In the simplest picture of this reaction, we expect to reach states which consist primarily of a proton in the $h_{9/2}$ orbit coupled to neutron holes in the $2p_{1/2}$, $1f_{5/2}$, $2p_{3/2}$, $0i_{13/2}$, $1f_{7/2}$, and $0h_{9/2}$ orbits.

The present experiment extends the previous work[2,3] to the important $[\pi h_{9/2}, \nu^{-1} h_{9/2}]$ multi- and also with the better resolution available with the MSU Cyclotron facility checks the spin parity assignments from the (d,t) reaction. A further motivation for the experiment was the clear differentiation of angular momentum transfers provided by the angular distributions of deuterons in the (p,d) reaction with 35 MeV protons. This allows easy identification of the members of a multiplet and serves as an indication of any mixture of different $\ell$ values in a particular transition. Finally a careful comparison was made of the present $^{209}$Bi(p,d)$^{208}$Bi reaction with a $^{208}$Pb(p,d)$^{207}$Pb experiment carried out at the same energy, with the same apparatus to check the strength in the $^{208}$Bi multiplets compared to the transition strength for the single hole states in $^{207}$Pb.

The experiment was carried out using the 35 MeV proton beam from the Michigan State University isochronous cyclotron. The reaction products were analyzed in an Enge split-pole spectrograph and the deuterons were detected in NTA and NTB, 25 microns nuclear emulsions. Thin mylar absorbers were placed in front of the plates to eliminate tritons. The bismuth target used was 100 $\mu$gm/cm$^2$ thick evaporated onto a 20 $\mu$gm/cm$^2$ carbon backing.

Before making exposures the total resolution was optimized by passing first the elastically scattered protons and then the deuterons from the ground state of the $^{208}$Pb(p,d) reaction, into the speculator system[4] in the focal plane of the magnet. A total resolution of less than 5 keV FWHM for scattering angles from 6° to 50° was obtained [Fig. 1]. Two exposures were taken at each angle, one for the p and f multiplets and the other longer exposure to obtain adequate statistics on the $h_{9/2}$ and $i_{13/2}$ multiplets. In order to fully exploit the high re-

solution it was necessary to scan the nuclear emulsion in 100 micron steps and in some regions of close doublets to reduce the step size of the scan to only 50 microns.

The results in general agree quite well with the previous measurements especially for the f and p multiplets. Some differences were observed in the $[\pi h_{9/2}, \nu^{-1} i_{13/2}]$ multiplet where the states at 1.708 MeV and 1.844 MeV are assigned spin parities of 5 and 4 respectively opposite to the previous values. No evidence of a state with the correct $\ell$ transfer was found near 2.72 MeV where the 2$^-$ member of this multiplet was reported.[3] This state may appear instead at 3.057 MeV or perhaps as a close doublet with the 1$^+$ state at 2.892 MeV.

The $[\pi h_{9/2}, \nu^{-1} h_{9/2}]$ multiplet appears to be comparitively pure and a number of spin parities can be assigned especially for the strong states. A publication is currently being prepared on this work.

## References

1. J.P. Schiffer in the Two-Body Force in Nuclei, Ed. Sam M. Austin and G.M. Crawley, Plenum Press, 1972, p. 205.

2. J.R. Erskine, Phys. Rev. 135, B110(1964).

3. W.P. Alford, J.P. Schiffer, and J.J. Schwartz, Phys. Rev. Letters 21, 156(1968), and Phys. Rev. C3, 860(1971).

4. H.G. Blosser, et al., Nucl. Instr. and Methods 91, 61(1971).
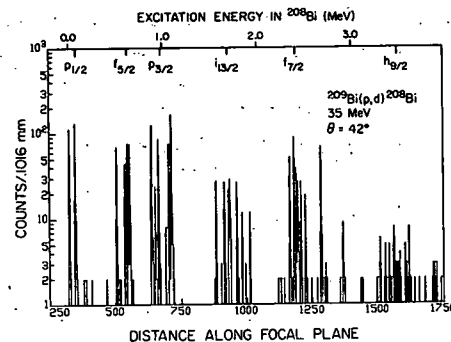
Fig. 1    Spectrum of the $^{209}$Bi(p,d)$^{208}$Bi reaction recorded at 42° with $E_p$=35 MeV. The energy scale at the top of the figure shows the location of the Q-values of the $^{208}$Pb(p,d)$^{207}$Pb reaction to the indicated single particle states.

# Nuclear Theory

## H. McManus, G. Bertsch, J. Borysowicz

### I. Reactions (Bertsch)

The ($^3$He,t) reactions was found in some cases to be dominated by an intermediate α state, in calculations done with Schaeffer (visitor, 1971). This explains unusual features found in ($^3$He,t) reactions to antianalog states, discovered at this lab. More thorough calculations have been done here by de Takacsy (visitor, 1972). At present the main effort is with a graduate student, Poon, to ulitize simple semiclassical methods to treat multistep reactions. With another visitor, Auerbach, theoretical corrections were made to the decay of analog states. The techniques and wave functions might be useful in the analysis of the (p,np̄) reaction, which also has unusual features. This is under study.

### II. Collective States (Bertsch)

We are investigating the properties of giant collective modes from a qualitative point of view. It has been shown that these states should be narrower than non-collective states.

### III. Effective Operators and Effective Forces (McManus)

As collective states in closed-shell nuclei are one of the simplest types of nuclear excitation perturbative calculations of both effective force and effective charge for particle-hole states were tried: also calculation of effective charges assuming MSDI is effective force. (With M. Dworzecka, Research Associate 71-72). This formalism was used to compare e-e' and p-p' for collective states of $^{40}$Ca using for p-p' experiments done here (G.R. Hammerstein, Research Assistant 71-72 with M. Dworzecka). Various other studies of effective operators were: effects of core polarization in (p,p') on Ca, Sr, Y, and Pb (with G.R. Hammerstein, F. Petrovich, and J. Borysowicz); extraction of effective charge from e-e' in s-d shell. (G.R. Hammerstein with Larson and Wildenthal); and comparison of e-e' with p-p' in Tin and Lead region (G.R. Hammerstein with R. Howell) using p-p' experiments done here and elsewhere. Most of this has spilled over in one form or another into analysis done by experimentalists here. Also attempted were tests of semiclassical methods in e-e' (with G.R. Hammerstein) and in π-nucleon scattering (with H.K. Lee, visitor 1972).

### IV. Mesonic Effects in Nuclei (McKellar, visitor, 71)

A stimulating visit by Bruce H.J. McKellar (71) increased our knowledge of mesic exchange currents in nuclei. While here McKellar found a generalization of Siegert's theorem limiting the role of exchange currents in parity non-conserving electromagnetic transitions, and completed other problems on the nucleon-nucleon force, including the parity violating part. Bertsch has applied the theory of the pp reaction and found an effect of possible significance to the solar neutrino problem.

### V. Cluster Model and Few Bodies (Borysowicz)

Structure of $^{16}$O and $^{12}$C has been investigated using the α-cluster model of Brink. No agreement with the elastic electron scattering is found when harmonic-oscillator clusters are used. Cluster with primitive correlations lead to a better agreement. This leads to the study of $^3$He, where N-N correlations can be taken into account more precisely. We found that N-N correlations stronger than usually assumed give a better fit to the elastic-electron scattering. The 3-body scattering problem is investigated in the framework of Faddeev eqs. Different methods are tried for the resulting integral eqs. (with J. Hetherington, N. Larson, and K. Gilbert).

# Compound and Direct Neutrons Produced by Proton Bombardment

T. Amos and A. Galonsky

Because of Coulomb-barrier effects, evaporation of neutrons comprises almost 100% of the probability for decay of a heavy compound nucleus. More than 50% of direct emissions initiated by proton bombardment can be expected to be neutrons. Therefore, a study of neutron emission should reveal the major features of the reaction mechanisms induced by proton bombardment.

Using thick targets of C, Al, Cu, Ag, Ta, and Pb, bombarded by protons of energy 22, 30, and 40 MeV, we have measured absolute neutron spectra at 0°, 30°, 60°, 90°, 120°, and 150°. The measurements were made by the time-of-flight method with a liquid scintillator. Gamma rays were suppressed by pulse-shape discrimination. The neutron energy range covered was 0.5-40 MeV. The lower limit, 0.5 MeV, took us well below the Maxwelliah peak in the evaporation part of each spectrum. This is an important improvement over our earlier data because the peak is a distinguishing feature of an evaporation spectrum and it is reassuring to actually see it in the data. Also, without the peak it would not be possible to integrate the spectra to obtain the total neutron production. Because of the non-linear pulse-height response of the scintillator with respect to neutron energy, we had to detect pulses with a range of 600 in size in order to cover the factor of 80(0.5-40 MeV) in neutron energy.

As a sample of the experimental results we present all of the Ta data in Fig. 1. Although
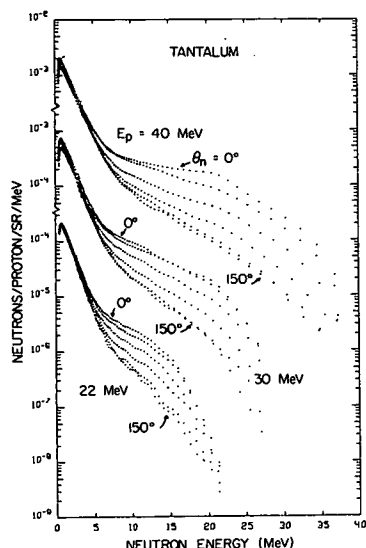
work. At low neutron energies we have the same absolute spectrum at all neutron angles. This is the isotropy expected of a compound-nucleus reaction. Furthermore, the spectrum has a peak around 1 MeV followed by an exponential fall off. A simple thermodynamic calculation of evaporation leads to such a spectrum (even when integrated through the thick target). Above about 5 MeV the data break sharply from the evaporation exponentials giving two differences: many more high-energy neutrons than could result from evaporation and a sharply forward peaked angular distribution. These are the characteristics one expects of direct reactions.

A final aspect to be noted from Fig. 1 is the strong increase in neutron yield at all energies with increasing proton bombarding energy. The total yields, that is, integrations over neutron energy and angle, are shown in Fig. 2 for all of our targets and energies. Also shown are data obtained at $E_p$=18 and 32 MeV[1] by a completely different and completely integral experimental technique, the so-called manganese-bath technique.
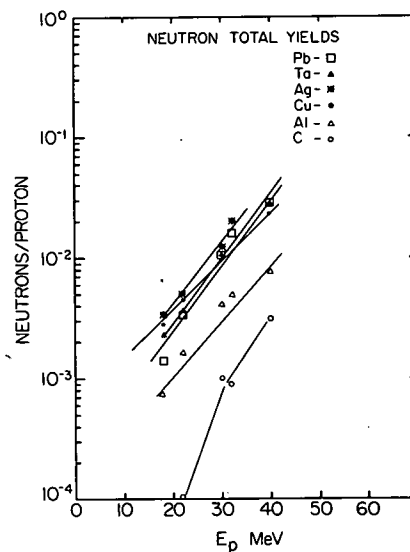


Fig. 2

In making a more quantitative analysis of the data we have had to allow for a sequence of neutron emissions from an excited compound nucleus. For each 10 MeV of proton bombarding energy about one neutron is boiled off. We followed this sequence of emissions and excitations of the residual nuclei on the computer and integrated the proton energy through the target in order to fit the compound-nucleus data. There were only two parameters, the radius, which controlled the normalization, and the level-density parameter, a, which controlled the shape of a spectrum. We used a simple degenerate-gas model



Fig. 1

manipulations of the data for comparisons with theoretical models have been made, the qualitative essence of the physics (for Ta) is all in Fig. 1. At each proton bombarding energy the data tell us there are two distinct reaction mechanisms at

in which $U=aT^2$, where U is the excitation energy of the residual nucleus and T is the temperature. For Ta, $T \sim 1-1/2$ MeV. By trial and error we were able to get good fits to the evaporation data from Cu, Ag, Ta, and Pb. The values of a so obtained are plotted against mass number, A, in Fig. 3.
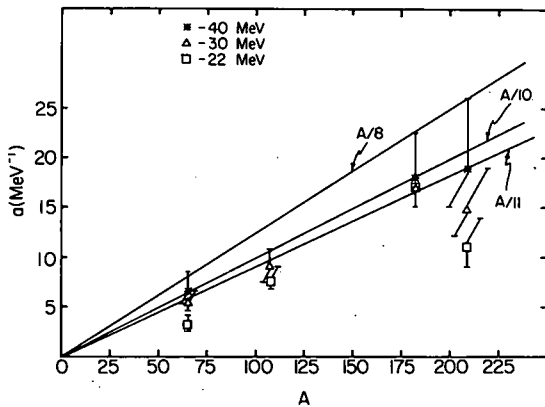


Fig. 3

The degenerate gas model predicts the value a=A/10 if $r_o=1.4$ F. A summary of low-energy data[2] shows that A/8 is a good average fit. A comparison between Ta and Pb indicates a lower level density in doubly-magic Pb in the 22- and 30-MeV data. Apparently the shell closures have an effect, but it diminishes with increasing excitation energy. We could not perform a sensible fit to the Al data because there was no clean separation of an evaporation from a direct spectrum. The carbon data did not appear to be part of any systematics.

By extrapolating the evaporation exponentials and subtracting from the observed spectra we extracted a direct or non-compound spectrum for each proton energy and neutron angle for Cu, Ag, Ta, and Pb. It is easy to imagine the results by looking at Fig. 1. Models of these neutrons, pre-equilibrium models, have been developed recently.[3] As presently constituted, these models are incapable of predicting an angular distribution for the emitted neutrons (our data, Fig. 1 for example, show a strong angular dependence). In order to make some comparison between theory and experiment we have integrated our spectra over neutron angle. We have also subtracted spectra so that we have data at $E_p$=35 MeV (subtracting 30-MeV spectra from 40-MeV spectra) and $E_p$=26 MeV (subtracting 22-MeV spectra from 30-MeV spectra). Because the neutron yields rise rapidly with energy, these subtractions are small. Most of the neutron production in the 22-MeV data occurs in the first few MeV below 22 MeV. The average proton energies for these spectra were taken to be the energy at which one half of the production had occurred, namely, 18.0, 20.1, 18.2, and 18.8 MeV for Cu, Ag, Ta, and Pb, respectively. The 26-MeV spectra

(including the evaporation parts) are shown in Fig. 4. Except for carbon they are remarkably
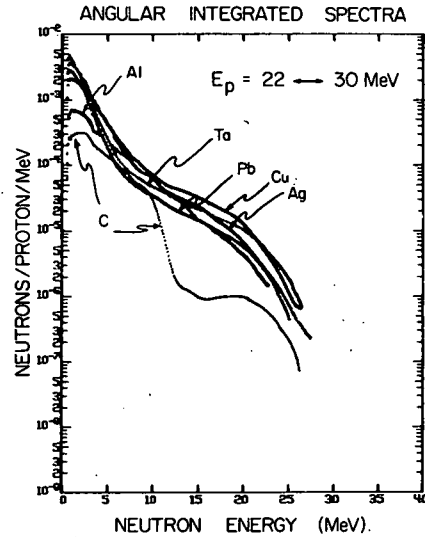


Fig. 4

similar to each other. In Fig. 5 the Ta data are compared with results of a pre-equilibrium calculation obtained through the courtesy of M. Blann, University of Rochester. Beyond the peak due to equilibrium evaporation, which is not included in Blann's calculation, there is excellent agreement in absolute values and fair agreement in the shapes.
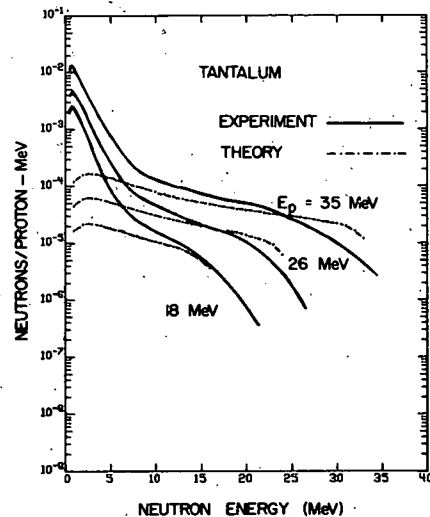


Fig. 5

Finally, we give in Fig. 6 the total probability, integrated over both angle and energy, for a direct, or pre-equilibrium, reaction resulting in the emission of a neutron. We see a dramatic increase with proton energy, but even at 35 MeV direct emission is only $\sim$20% probable. Compound nucleus reactions dominate. Even when there is a direct emission there will generally be enough excitation energy for equilibrium evaporation of one or more neutrons to follow.
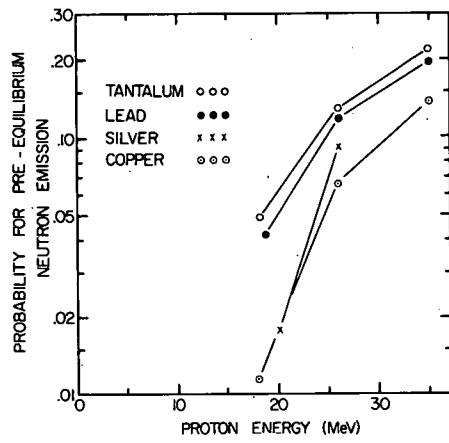
Fig. 6

The energy dependence could be studied more precisely with thin-target data, which we hope to obtain.

References

1. Y.K. Tai, G.P. Millburn, S.N. Kaplan, and B.J. Moyer, Phys. Rev. 109, 2086(1958).

2. David Bodansky, Ann. Rev. Nuclear Sci. 12, 79(1962).

3. M. Blann and A. Mignerey, Nuclear Physics A186, 245(1972) and reference given there.

# Fine Structure in Pulse Shape Discrimination

A. Galonsky and T. Amos

In the area of pulse-shape discrimination (PSD) we have discovered the existence of a fine structure in the neutron PSD signature. We observed in our NE213 scintillator 38-MeV neutrons produced by 40-MeV protons in the $^7Li(p,n)^7Be$ reaction. A contour plot of the two-dimensional PSD display is shown in the figure. The peaks labelled A and C are the ones usually observed. They correspond to gamma rays and neutrons, respectively. Our computer data-taking system, TOOTSIE, allows us to examine the time-of-flight spectrum of any portion of the data shown in the figure.

When this was done for each of the groups A through E, it was found that each of the new groups, B, D, and E, had the neutron (C) time-of-flight spectrum. Our analysis gives the following identifications of the neutron groups: B consists of protons escaping from the end of the scintillator. Its relative importance increases with neutron energy. For a given neutron energy its relative importance decreases with increasing scintillator thickness. C consists of protons recoiling from n-p scattering and stopping within the scintillator. D consists of protons from the $^{12}C(n,p)^{12}B$ reaction, and E consists of α particles from break-up by neutrons of $^{12}C$ into three α particles. C predominates at low neutron energies, but above 70 MeV the cross section for n-p scattering is less than the cross section for either $^{12}C(n,p)^{12}B$ or $^{12}C(n,n3\alpha)$. In order to determine absolute values of neutron cross sections from a calculation of scintillator efficiency it is necessary to take account of the origin of each of the above groups.

In addition to it's use in neutron time-of-flight work, the fine structure in PSD may find application in neutron spectroscopy not involving time-of-flight. Neutron spectroscopy in the upper atmosphere and in the Van Allen belts is one example that comes to mind.
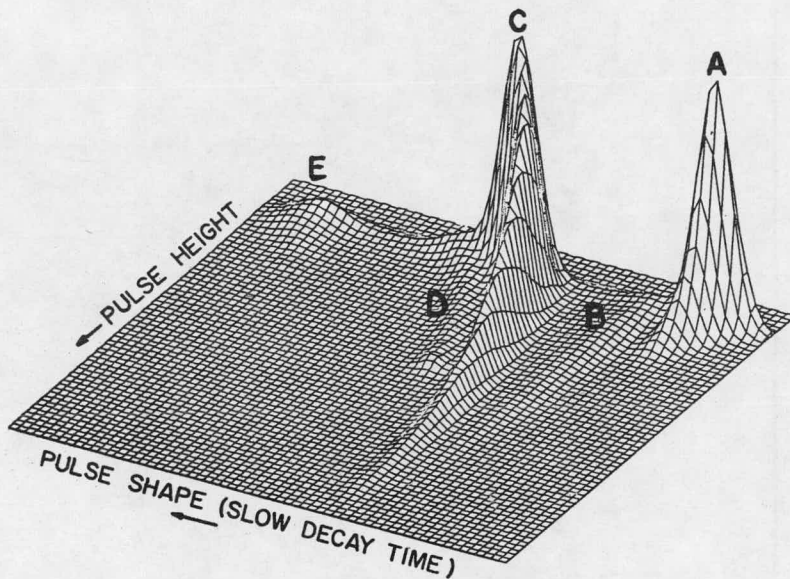


Fig. 1   Contour diagram of 2-dimensional pulse-shape-discrimination data obtained with 38-MeV neutrons incident on NE213 liquid scintillator. The labelled groups are discussed in the text.

# Nitrogen Fixation

C.P. Wolk,* S.M. Austin, J. Bortins, and A. Galonsky

In the last two years we have made a number of technical improvements in our program to use $^{13}N$ in a study of fixation of nitrogen in algae. This has resulted in the first autoradiograph of $^{13}N$ fixation of which we are aware.

One major improvement was a switch in the reactions producing $^{13}N$ from $^{16}O(p,\alpha)$ to $^{13}C(p,n)$. This improved the yield by a factor of five and, because of the lower proton energy required, eliminated the problem of the activiation of the sample holder. Most importantly production of $^{13}NO$, which was a significant problem with the O target, did not occur with the $^{13}C$ target. In the earlier work we had to eliminate the $^{13}NO$ chemically because algae fix this compound more rapidly than they fix $N_2$.

We also improved our autoradiography technique by using emulsion sensitization.[1] This reduced the average grain spacing by a factor of two. A photomicrograph of an algae with two tracks from $^{13}N$ positron decay is shown in the figure. The average grain spacing in this photo is 2 microns.

The objective of the program was to find out if $N_2$ fixation is accomplished by the heterocysts. There is one heterocyst for about 20 vegetative cells, and there are three heterocysts in the algal filament shown (all three larger, two darker, than the other cells). Based on $10^3$ tracks we can now say that the heterocysts are not the sole sites of nitrogen fixation but do perform about 25% of the fixation. We will now go on to try to discover the biochemical products made by the heterocysts and vegetative cells with their assimilated $N_2$.

## References

1. W.H. Barkas, Nuclear Research Emulsions, Academic Press, p. 131(1963).

* AEC Plant Research Laboratory.
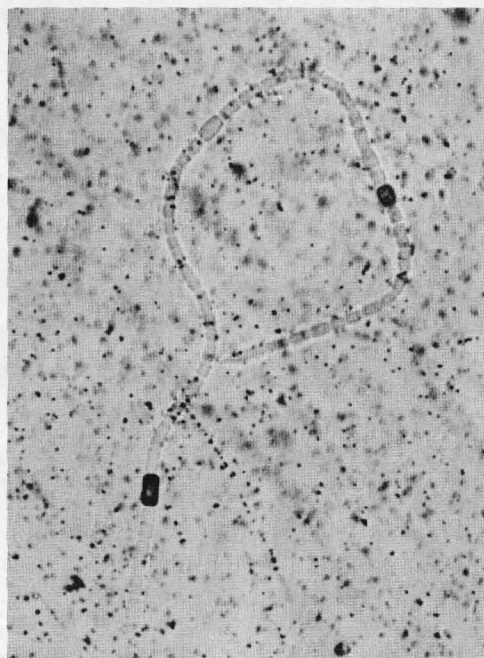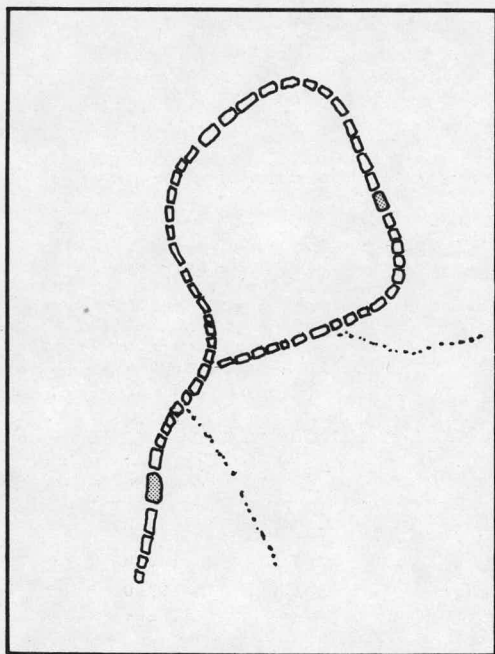
Fig. 1 Photomicrograph of a filament of $^{13}N$-fed, blue-green algae. There are two tracks from $^{13}N$ position decay. Each track originates in a vegetative cell.

# Strontium Isotopic Ratios and Trace Element Abundances,
## Aves Ridge Granities, Caribbean Basin

Charles M. Spooner[*]

An unusual recovery of about 3500 kgs. of granitic rocks from a dredge haul (12° 20' N Lat., 63° 30' W. Long.) from the Aves ridge has prompted an investigation into the strontium isotopic ratios and trace element geochemistry to determine whether these rocks have a direct origin in the upper mantle or an origin involving anatectic melting of crystal material.

The Aves ridge forms a prominent submarine feature parallel to and about 270 km to the west of the Lesser Antilles. On the basis of seismic refraction studies (Fox et al.[1]), the ridge is composed of a 5 km thick capping series of volcanic and sedimentary rocks overlying a crustal layer with $V_p = 6.0$ to 6.3 km/sec.

Three rock types: a granite, a granodiorite inclusion within the granodiorite and a granophyre were analyzed. Strontium isotopic analyses were performed on a 6-inch, 60° sector, solid source, Nier-type mass spectrometer at the MIT Geochronology Laboratory. The measured $^{87}Sr/^{86}Sr$ for the three rock types are: $0.7038 \pm 0.0007$, $0.7046 \pm 0.0023$, and $0.7080 \pm 0.0005$ respectively, expressed relative to $0.7083 \pm 0.0004$ for the Eimer and Amend $SrCO_3$ standard. Since all have low Rb/Sr ratios (less than 0.3) and since K-Ar ages range from 89 to 18.5 m.y., the strontium sitopic ratios reported are essentially the initial ratios. Since all the isotopic ratios are lower than that of present-day sea water (about 0.709), equilibration with common strontium in sea water has not taken place. It is reasonable to infer that other trace elements have similarly been unaffected by alteration or contamination.

Trace elements, including many of the rare-earth elements (REE) were analyzed by instrumental neutron activation analysis using facilities kindly provided by the MSU Cyclotron Laboratory. The samples were irradiated in powdered form without prior chemical treatment for up to 3 hours at a thermal neutron flux of $2 \times 10^{12}$ n/cm$^2$/sec in the MSU Triga reactor. Counting data were collected using a 10% Ge(Li) detector and a 4096 channel ADC using PHOLYPHEMUS. Identification of photopeaks, their integration and comparison with rock standards to yield concentrations was done using a computer procedure outlined by Baedecker.[2] Errors based on counting statistics alone range from 4% to 20% of the amount present. These data are shown in Table I.

When normalized with respect to carbonaceous chondrite abundances, the REE trend shows pronounced light rare-earth enrichment typically found in continental granitic rocks. K/Rb and Zr/Hf ratios show an expected decrease for an internally differentiated series of granties. Strongly lithophile elements, especially Th, show an unexpected decrease in terminal, granophyric stage, probably through removal by a vapor phase. This conclusion is consistent with the petrographic observations (i.e. abundant miarolytic cavities indicative of a gas phase).

The occurrence of granities in the oceanic environment is unusual; however, the great areal extent of the 6.0 to 6.3 km/sec layer throughout the Caribbean basin suggests that granitic rocks may form a substantial fraction of this layer.

The strontium isotopic and trace element results suggest an upper mantle origin from a low Rb/Sr source followed by extensive differentiation (REE results) and near surface emplacement. Perhaps these rocks and the processes forming them are common to primitive continental crusts in which case the Caribbean crust is a proto-continent.

## References

1. P.J. Fox, E. Schireiber, B.C. Heezen, The geology of the Caribbean crust: Tertiary sediments, granitic and basic rocks from the Aves ridge. Tectonophysics 12, 89(1971).

2. P.A. Baedecker, Digital methods of photopeak integration in activation analysis, Anal. Chem. 43, 405(1971).

* Department of Geology, MSU. (Supported by the USAEC and the NSF.)

## TABLE I

INAA Element Abundances, Aves Ridge Granities, in ppm

|  | R-1 (inclusion) | R-2 (granite) | R-3 (granophyre) |
|---|---|---|---|
| Na | 29600 | 23700 | 22200 |
| K | 7900 | 11200 | 10300 |
| Fe | 29600 | 26100 | 25700 |
| Mn | 249 | 329 | 955 |
| Sc | 10 | 14 | 43 |
| Ba | 669 | 1061 | 1113 |
| Th | 8 | 8 | 24 |
| Hf | 7 | 6 | 25 |
| Zr | 215 | 212 | 294 |
| Co | 138 | 153 | 180 |
| La | 16 | 14 | 32 |
| Ce | 33 | 51 | 84 |
| Sm | 3 | 17 | 8 |
| Eu | 1 | 1 | 3 |
| Lu | 0.35 | 1.2 | 0.20 |
| K/Rb | 767 | 485 | 97 |
| K/Th | 987 | 1400 | 429 |
| Zr/Hf | 31 | 35 | 12 |

Nuclear Information Research Associate Program:
Data Compilations in the Mass Region A=101-106*

R.R. Todd,** L.E. Samuelson,*** F.M. Bernthal, W.H. Kelly,
Wm.C. McHarris, and R.A. Warner

For the past year we have been participating
in the Nuclear Information Research Associate
Program (NIRA) sponsored by the National Academy
of Sciences—National Research Council and funded
by the National Science Foundation. Dr. Todd was
one of the first group of NIRA's that was selected
and he has been working on the compilations of
nuclear data of the A-chains A=101-106. At the
end of his first year he accepted a permanent
faculty position at Western Michigan University.
Upon Todd's resignation from the program,
Dr. L.E. Samuelson was selected to be the re-
placement NIRA and is working on the A=104-106
chains.

The compilations for the A=101 and 102 chains
are now complete and the results are in the final
stages of editing before being submitted for
publication. The A=103 compilation will be
completed by Dr. Todd later this year.

# Magnetic Spectrograph

H.G. Blosser, E. Kashy, and J.A. Nolen

The 90-cm Enge split-pole spectrograph has been in operation for about three years. During this period its use has steadily risen; about 60% of total beam time goes to the spectrograph including virtually all of the time devoted to both transfer reactions and inelastic scattering. A continuing series of improvements have added greatly to both the convenience with which the facility can be used and its accuracy.

An absolute calibration system[1] uses a momentum matching procedure to calibrate the spectrograph in terms of known nuclear mass differences. Recent calibration work has been directed to accurate determinations of effective radius of curvature vs. focal plane position. The large contributions of field edges to the total bending make a careful magnet recycling and setting procedure especially important. In addition we have found that the field shape depends on the rate at which the field is changed; for highest accuracy this rate is limited to 1,500 gauss per minute. Careful calibrations at 10 kilogauss have been completed and work at higher fields is in progress.

Many experiments in the spectrograph now utilize one form or another of live focal plane detector so as to minimize the effort and expense required for scanning very high resolution plates ($\sim$0.1 mm lines). The present rather standard live detector configuration uses a resistive wire proportional counter in the focal plane backed by a plastic scintillator for time-of-flight and energy information.[3] The resistive wires typically give 1 mm spatial resolution using charge division and cover 300 mm of focal plane with excellent linearity and stability. The scintillation counter timing window (triggered by the cyclotron rf) makes it possible to study rare particles in the midst of high intensity background. Using this arrangement, clean $^6$He spectra have been obtained in circumstances where the number of $^6$He particles entering the proportional counter was a factor of 10,000 less than the alpha particle background. Commercial position sensitive silicon detectors are also sometimes used for live position readout. Such detectors can give spatial resolutions of 0.25 mm over a narrow range and have been used extensively in mass measurements and other narrow range work.

An important contribution to the speed and ease with which the spectrograph can be used has come from the installation of motors and remote readouts on all important spectrograph parameters. These include the focal plane position (up-down and in-out), the target position (angle and height), the entrance aperature (choice of 7) and the scattering angle ($\sim$0.1° accuracy). The beam preparation system also allows independent variation of the energy dispersion on target and the magnification. Two sextupole lenses are also provided for optimum cancellation of aberrations. These remote controls, in conjunction with the previously described resolution meter,[2] allow the user to quickly make fine adjustments in all control elements as required for optimum resolution. At present the best resolution obtained in a reaction experiment is 3.7 keV for $^{12}$C(p,t) at 40 MeV and 3.0 keV at 30 MeV for $^{12}$C(p,p').

## References

1. G.F. Trentelman and E. Kashy, Nucl. Instr. and Methods 82, 304(1970).

2. H.G. Blosser, G.M. Crawley, R. deForest, E. Kashy, and B.H. Wildenthal, Nucl. Instr. and Methods 91, 61(1971).

3. W.A. Lanford, W. Benenson, G.M. Crawley, E. Kashy, I.D. Proctor, and W.F. Steele, BAPS 17, 895(1972).

# Accurate Q-Values and Excitation Energies Using
## Momentum Matching and Photographic Emulsions

G. Hamilton, E. Kashy, J. Nolen, and I. Proctor

Using previously developed momentum matching techniques in conjunction with photographic emulsions in the magnetic spectrograph we are able to determine excitation energies of nuclear levels and ground state Q-values with an accuracy $\sim 2$ keV. Previous measurements at MSU, including calibration of the beam energy analysis system and determination of many new nuclear masses, had utilized solid state or resistive wire proportional counters in the focal plane of the magnetic spectrograph.

The emulsion method eliminates some of the uncertainties of the detector methods. The basic difference is that with the plates all known and unknown states are recorded simultaneously on one plate during a given run. A disadvantage of this method is that more calibration lines are needed in any given measurement because the focal plane calibration must also be treated as an unknown when measurements are not being made at constant $\rho$ in the magnet. This is in practice not a limitation, however, as indicated in the example given below.

All the measurements quoted below were from spectra recorded on 21" long photographic plates with proton and deuteron line widths $\sim 0.3$ mm. The centroids were read directly from the plates using a microscopic with a stepping motor stage drive. The accuracy of the ball screw and reproducibility of the readings combined to give typical centroid uncertainties of $\sim 0.03$ mm except for very weak peaks.

One run consisted of bombarding with 35 MeV protons a thin $^{27}$Al target on a C backing. Both protons and deuterons were recorded in the emulsion. The calibration lines are indicated in Table I. In one simultaneous least squares fit to these 6 lines it is possible to determine a) the beam energy to a standard deviation of 2 keV, b) the scattering angle to a standard of 0.03°, c) the absolute radius of curvature of the calibration lines, and d) the two coefficients of a parabolic $\rho$ vs. D calibration curve for this region of the focal plane. We are using a flat plate holder instead of the slightly curve surface specified for the Enge split-pole magnet. Over this 20" section of the focal surface we find a small, but necessary, quadratic term in the $\rho$ vs. D curve but higher order terms have not been justified by the accuracy of the present calibration lines. The correlation matrix resulting from the least squares fit does indicate that the five parameters mentioned above are in fact independently determined.

Tentative new assignments and probable errors resulting from this run are given in Table I. There may be small changes in these numbers before the analysis is finalized.

The current measurement of the $^{15}$O mass excess is $2857 \pm 1$ keV, which agrees with several other recent determinations of this number. The $3/2^-$ hole state in $^{15}$O is a very strong and useful line for use as a calibration in future work involving neutron pickup reactions. The well known particle states in the 6 MeV excitation energy region in $^{15}$O are extremely weak in pickup reactions, and vice versa.

TABLE I

Preliminary Excitation Energies and Q-Values Extracted via
Momentum Matching Technique

| Peak | Previous Q (keV) | Fit Q (keV) | Previous $E_x$ (keV) | Fit $E_x$** (keV) |
|---|---|---|---|---|
| $^{27}$Al(p,d) | -10833.3±0.9* | 10833±1 | 0.0 | 0 |
| " | | | 228.2±1.0 | 228 |
| " | | | 417.0±0.4 | 418 |
| " | | | 1057.7±0.5 | 1059 |
| " | | | 1759.2±0.6 | 1760 |
| " | | | 1850 | - |
| " | | | 2068.7±0.3 | |
| " | | | 2069.5±0.3 | 2070 |
| " | | | 2071.7±0.8 | |
| " | | | 2365.0±0.5 | 2366 |
| " | -13378.5±1.2* | -13378±1 | 2545.2±0.5 | 2545 |
| " | | | 2660.8±0.4 | |
| $^{16}$O(p,d$_0$) | -13439.3±0.6 | -13441±1 | 0.0 | 0 |
| $^{27}$Al(p,d) | | | 2913.2±0.6 | 2915 |
| " | | | 3159.4±1.0 | 3161 |
| " | | | 3405 ±5 | 3403 |
| " | | | 3677 ±8 | 3680 |
| " | | | 3751 ±8 | 3753 |
| " | | | 3962 ±10 | 3962 |
| " | | | 4425 ±8 | 4430 |
| " | | | 4546 ±8 | 4547 |
| " | | | 4704 ±8 | 4705 |
| " | | | 4939 ±8 | 4941 |
| " | | | 5473,5485,5506 | 5491 |
| " | | | 5593 ±8 | 5597 |
| " | | | 5715,5741 | 5724 |
| $^{12}$C(p,d$_0$) | -16497.3±1.0 | -16497±1 | 0.0 | 0 |
| $^{27}$Al(p,p$_0$) | 0.0* | | 0.0 | -1 |
| $^{16}$O(p,p$_0$) | 0.0 | | 0.0 | 0 |
| $^{14}$N(p,p$_0$) | 0.0 | | 0.0 | 2 |
| $^{13}$C(p,p$_0$) | 0.0 | | 0.0 | 1 |
| $^{27}$Al(p,p') | | | 842.9±0.3 | 844 |
| " | | | 1013.0±0.3 | 1014 |
| " | | | 2208.9±0.6 | 2210 |
| " | | | 2732.0±0.8 | 2734 |
| $^{12}$C(p,d$_1$) | | | 1995 ±3 | 2000 |
| $^{27}$Al(p,p') | | | 3003.5±1.0 | 3003 |
| " | | | 4410 ±2 | 4404 |
| " | | | 4510.6±0.6 | 4509 |
| $^{12}$C(p,p') | -4439.2±0.3* | - 4439±1 | 4439.2±0.3 | 4439 |
| $^{27}$Al(p,p') | | | 4812 ±2 | 4810 |
| $^{16}$O(p,d$_1$) | | | 5177 ±3 | 6172 |

*Used as calibration lines.
**Estimated errors are ~2 keV.

# A Charge Division Position Sensitive Proportional Counter System

W.A. Lanford, W. Benenson, G.M. Crawley,
E. Kashy, I.D. Proctor, and W.F. Steele

We have developed, and are extensively using, a position sensitive proportional counter system for use in the focal plane of our split-pole magnetic spectrometer. The system consists of a charge-division position-sensitive proportional counter backed with a plastic scintillation counter. The scintillation counter provides an energy signal and a time signal both of which are used for particle identification. A gas handling and flow system is used to stabilize gas pressure and preserve the purity of the gas. In addition, we have a permanent electronics setup which allows particle identification with (1) the E signal from the scintillation counter, (2) the $\Delta E$ signal from the proportional counter, and (3) the time-of-flight (TOF) of the particle in the spectrograph (relative to the rf of the cyclotron). These may be used in any combination by simply changing switches.

The system has the following characteristics: for 45° incident particles. (1) Position resolution of about 1 mm (FWHM along the focal plane), (2) an active length of about 12 inches, (3) a counting rate capability greater than $5 \times 10^3$ cps, (4) extremely good particle identification.

While this system does not allow one to use the full high resolution capability of the dispersion matched cyclotron-magnetic-spectrometer combination, it has been heavily used since it first became operational. Most particle transfer reactions which are presently being studied in the lab (such as (p,d), (p,t), (p,$^3$He), ($^3$He,$^6$He), and ($^3$He,$^7$Be)) use this proportional counter system to take at least some of the data. Often the combination of plate data at a few angles and proportional counter data at the remaining angles is sufficient. Shown in Fig. 2 is a comparison of $^{208}$Pb(p,t)$^{206}$Pb reaction observed with nuclear emulsions and with the proportional counter. While the plate data has higher resolution, in this case almost all the states are resolved by the counter. There are several other spectra taken with this system in other sections of this report. There are some experiments reported, such as (p,$^3$He) and the ($^3$He,$^6$He) reactions which would have been very difficult to study with more conventional techniques but which time-of-flight particle identification puts on an equal basis with other reactions.

## References

1. H.W. Fulbright, W.A. Lanford, and R. Markham, to be published.

2. N. Williams, T.H. Kruse, M.E. Williams, J.A. Fenton, G.L. Miller, Nucl. Inst. and Methods 93, 13(1971).

Fig. 1 A schematic representation of a change division, position sensitive proportional counter. The symbol X represents the distance along the counter, and Q is the total charge pulse in the counter which divides into $q_1$ and $q_2$ depending on were the event occured.

The proportional counter is a normal transmission mounted proportional counter except (1) the center wire has a relative resistance ($\sim$4K$\Omega$) and (2) the signal from the proportional chamber is measured at both ends of the center wire with charge sensitive pre-amps. Figure 1 shows schematically how the counter works. The charge Q deposited at position X along the center wire divides according to the resistance to the preamps (which look like ground to the high frequency components of the pulse). The signal $V_1$ and $V_2$ are shaped (RC$\sim$.5 $\mu$s) and fed into computer ADC's. The computer performs the division XE/E to generate X. This counter is similar to those developed at Rochester[1] and Rutgers.[2]

Fig. 2   Spectra of the $^{208}Pb(p,t)^{206}Pb$ reaction with $E_p=35$ MeV
obtained with a nuclear emulsion (top) and with the
position sensitive proportional counter (bottom). The
resolution of the data taken with nuclear emulsions is
about 15 keV (FWHM) while that taken with the proportional
counter is about 30 keV.

91

# Cyclotron Modifications and Improvements

H.G. Blosser, H.P. Hilbert, L.L. Learn, P.S. Miller, P. Sigg, and G. Stork

## I. Alumina rf Tuning Bearings

In the spring of 1972 a major cyclotron shut-down was scheduled for the first time in seven years. The primary purpose of this shut-down was replacement of the graphite bearings supporting the main rf tuning panels in the cyclotron cavity, which had gradually deteriorated in the years of operation, as seen in Fig. 1. The basic problem appeared to be a failure of contact fingers designed to shield the bearings from rf, which led to rf heating of the bearing and the melting of the bearing housing. The tuning panels were then free to shift by as much as 2 mm, introducing sudden jumps and instabilities in the rf. The newly installed Alumina bearings do not require protective contacts and the basic wear characteristics of the Alumina are such that we expect an essentially infinite life from the new arrangement.
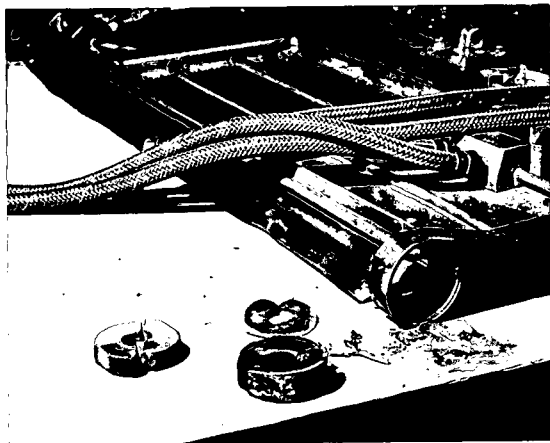


Fig. 1   Old tuning panel bearing components as removed from the Cyclotron in April 1972. One graphite disc (2 are shown) was removed from the bearing mount seen on the panel in the background. The deterioration of the bronze bushing around the graphite insert shown in the foreground is evident.

## II. New Centering Coils

During the major disassembly required to change the rf bearings a new set of beam centering coils was installed in the cyclotron. The previous centering coils had been installed in 1967 as an afterthought for the purpose of making control easier. In order to avoid a 6 week shut-down the coils were placed in the dee insulation space thereby adding capacity to the rf system and reducing the useable upper energy of the cyclotron from 56 to 45 MeV. The new coils return the rf system to its original state and we therefore expect the usable energy of the cyclotron to again extend above 50 MeV.

## III. New Central Region Design

Acceleration of heavy ions uses the third harmonic mode in our cyclotron, i.e. the orbital frequency of the ions is one-third of the rf frequency. Unfortunately the cyclotron has never given usable third harmonic beams due to the effect of the so-called gap-crossing resonance (a coupling phenonmenon between the longitudinal and transverse motions[1]). The third harmonic gap crossing difficulty was overlooked in the original design studies for the cyclotron, which concentrated on precise, high-energy proton beams as the primary operational objective. Approximately 18 months ago we decided to rectify this design deficiency: detailed study was initiated with the objective of working out an optimized central region for both second and third harmonic acceleration. As this study proceeded, it became clear that the dee angle was an extremely important factor in the gap-crossing resonance difficulties. Figure 2, repeated from last year's annual report, shows the intrinsic orbit centering error plotted vs. dee angle for first, second, and third harmonic acceleration. As the figure clearly indicates, the best dee angle is highly dependent on the harmonic number. After careful consideration of these results and of electrical and mechanical
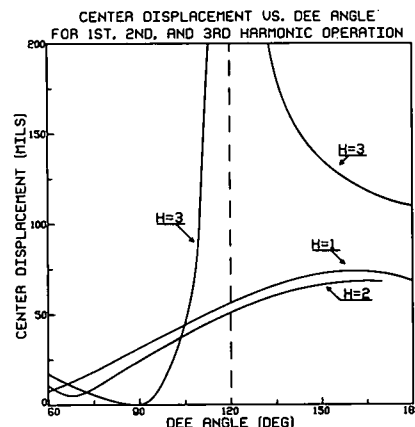


Fig. 2   Effect of gap-crossing resonance on particle orbits in the MSU Cyclotron.

factors, we decided to shift to an interchangeable dee concept in our new design, so that the dee angle could be individually selected for each harmonic and therefore set at the best value. The computing phase of this study has now been completed.[2] New dee configurations for both second and third harmonic acceleration (90° and 60° dees respectively) have been worked out. In brief the results indicate that performance of the third harmonic configuration should match present first harmonic results and second harmonic beams

(deuterons, etc.) should become the most precise of all (assuming equivalent ion source performance in each case).

## IV. New Central Plug and Source Mount

In a separated orbit cyclotron the final beam is extremely sensitive to the relative position of the ion source, the source extraction electrode (the puller), and the 180° selection slit. In a standard cyclotron configuration the puller is mounted on the dee; such mounting systems are generally rather flimsy and imprecise, and subject to thermal motion as the dee warms or cools. Central region design constraints, however, make it very difficult to devise better puller mounts unless insulators are used, and in the past insulators have generally been viewed as unreliable. Recent insulator development studies at Columbia[3] in connection with the conversion of the Nevis synchrocyclotron, however, imply that Freon-cooled Alumina insulators can now be successfully used for puller mounting. With such an arrangement it would be possible to set the source-puller geometry with great accuracy and thus eliminate the most important contribution to beam instability in our cyclotron. Unfortunately, considering the extremely severe environment in the cyclotron central region, the only way to be really sure of the feasibility of such an arrangement is via a working test.

A first such test was performed about six months ago using an assembly which could be inserted through the cyclotron ion source hole in place of the ion source. In a 72-hour run this test insulator survived without detectable damage. Its voltage holding capability gradually improved throughout the period up to a final value of 48 kilovolts (equivalent to 40 MeV proton operation in our standard turn pattern). Encouraged by this result we have proceeded with the design of a new center plug system for the cyclotron which will carry the ion source, the puller, and the 180° slit on a common 6" diameter plug inserted through a vacuum lock in the lower pole. Construction of this new plug is approximately 50% completed. When it is finished we will be able to subject the Alumina insulators to the ultimate test, namely long-term survival in the presence of an ion source. If the test is successful, insulator-mounted pullers will be introduced in all operating modes of the cyclotron. If the test is unsuccessful, we will revert to the present arrangement of mounting the puller on the dee. Even in this eventuality the new center plug will be a valuable addition since the ion source and the 180° selection slit can be mounted on the plug regardless of the result of the insulator test; the ability to change both of these components through the new lower pole vacuum lock will substantially shorten changeover time from one mode of operation to another.

As a part of the central region work, a new beam probe assembly is being constructed which will make it possible to shift from a radially sensitive probe to an axially sensitive probe in a few minutes. Such a probe change is required in dealing with coherent vertical oscillations, a beam dynamics difficulty which historically seems to recur every few months in the cyclotron.

## V. Interchangeable Dee System

A mechanical design for the interchangeable dee system has been completed; various quick release devices are included which should make it possible to change dees and be back in operation in approximately four hours including pumping time. The radio frequency properties of the various new dees have also been studied in our origional rf mock-up which was returned from Princeton for this purpose. Dee configurations which cover the required frequency range have been worked out for each mode. Results are summarized in Table I. We expect the complete new system to be operational in six to twelve months.

### References

1. M.M. Gordon, Nucl. Instr. and Methods NS-18-19, 268(1962).

2. L.L. Learn, H.G. Blosser, and M.M. Gordon, Proc. of the Sixth Interntl. Cyclotron Conference, 1972.

3. J. Rainwater, IEEE Trans. on Nucl. Sci. NS-18, 262(1971).

### TABLE I

Frequency Range Results for Various Dees Using
Existing Items and Tuning Panels—Results from
rf Model

| Dee Angle Degrees | Dee Thickness In. | Dee to Linear Spacing In. | Max. Freq. Mhz | Min. Freq. Mhz |
|---|---|---|---|---|
| 60° | 2.5 | 1.375 | 23.6 | 17.0 |
| 60° | 3.5 | .875 | 22.2 | 14.6 |
| 60° | 4.0 | .625 | 19.6 | 12.3 |
| 90° | 2.5 | 1.375 | 21.2 | 15.5 |
|  | 4.25 | .500 | 17.5 | 10.6 |
| 120° | 2.5 | 1.375 | 21.0 | 13.8 |
| 140° | 2.5 | 1.375 | 19.5 | 12.7 |
| 140° | 2.5* | 1.375 | 21.5 | 14.3 |
| 140° | 2.5 | 1.375** | 23.6 | 12.7 |

\* Existing Cyclotron Dees. Model shows coherent shift to lower frequencies due to different tuning panel structure.

\*\* Model study with special Princeton type linear configuration.

# Design Study for a Compact 200 MeV Cyclotron

M.M. Gordon, H.G. Blosser, and D.A. Johnson

A preliminary design study has been carried out for a compact cyclotron which would acclerate protons to final energies ranging up to 200 MeV, and other ions to corresponding final energies. This machine would possess the basic structural and operational features of our present 50 MeV cyclotron including the central region geometry, the phase selection slits, and the single turn (100%) extraction system. This cyclotron would provide an excellent tool for nuclear and medical research at a relatively low cost (about two million dollars).

The 200 MeV magnet would have the same gap and the same maximum field strength as our present 50 MeV magnet, and would therefore have about twice the pole diameter (125"). However, this magnet would have four (instead of three) sectors with sufficient spiral to compensate the additional relativistic defocusing.

Realistic field trimming calculations were carried out using a new computer program (Fielder) which showed that excellent results could be obtained with the use of only 17 trim coils. Thus, for 200 MeV protons, the calculated rms phase deviation is less than 3°. Moreover, the total power consumed by the 17 coils would be less than 90 kW in all cases.

The suggested design for the rf system of the 200 MeV cyclotron is closely modelled on the present Maryland and MSU machines. This rf system would operate in the 10-20 MHz range with two dees, about 90° in angular width, allowing for both even and odd harmonic operation. Since these dees would be positioned within the magnet gap, the maximum dee voltage would be restricted to about 70 kV.

As in our present machine, the 200 MeV cyclotron would be equipped with a set of radial slits

which reduce the phase width of the transmitted beam down to about 2°. The energy spread within each turn would therefore continue to have the same proportionate value: $(\Delta E)/E = 1.5 \times 10^{-4}$. This implies a final energy spread of 30 keV for 200 MeV protons. and proportionate values for lower energy protons and for other ions. This energy spread is sufficiently small so that single turn extraction would be quite feasible.

Extrapolating the results obtained for our present cyclotron, the 200 MeV proton beam would have exceptionally small emittances, namely: 0.3 mm-mrad radially and 2.5 mm-mrad axially. Because of the increased longitudinal space charge effect, however, the 200 MeV proton beam should be restricted to about 2 micro-amps in order to secure 30 keV energy resolution.

In addition to 200 MeV protons, this cyclotron would produce, for example, 280 MeV helions, 210 MeV alphas, and 290 MeV $^{12}C^{4+}$ ions. The proton (and deuteron) ion source has exceptionally high luminosity so that the high quality beam characteristics given above can be achieved with reasonable beam currents. Since helium and heavy ion sources generally have much lower outputs, some sacrifice could be made in energy resolution and emittance in order to improve the final beam current for these ions.

A more complete discussion of this design study will be found in the proceedings of the Sixth International Cyclotron Conference (Vancouver, 1972), which will soon be published.
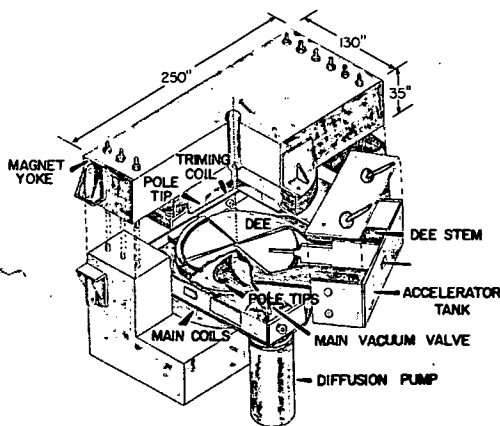


Fig. 1    Compact 200 MeV cyclotron design shown in a cut-away view.
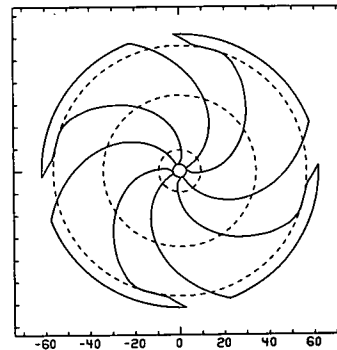


Fig. 2    Schematic diagram of four sector magnet pole tip geometry with scale in inches. Broken circles indicate locations of trim coil nos. 1, 9, and 17.

# Progress with the On-Line Isotope Separator*

K.L. Kosanke, Wm.C. McHarris, and H.P. Hilbert

To date our work toward an on-line isotope separation has been directed at two areas of the overall system. First has been the development of our He thermalizer-jet transport (see next section of this report) with a tape transport that will later be used in our complete system. Second has been with our electric quadrupole mass filter. We have directed the initial work on our overall system to these areas because we felt they would each prove to be useful research tools in themselves and could be used before the complete system is operational. The remaining work to be done will be the linking of these two pieces of hardware together.

The on-line mass separation system under construction and its operation are shown schematically in Fig. 1. A collimated cyclotron beam enters the apparatus, striking a thin target (or a series of thin targets) in an atmosphere of helium (1 to 3 atmo. of pressure). Those nuclei near the back of the targets interacting with the beam will be recoiled out of the target into the helium. The recoils are then slowed to thermal energies through collisions in the helium. Recent work by R.D. MacFarlane[1] as well as studies conducted in this lab suggests that the next step is the attachment of the recoils to large molecule clusters (with masses up to $10^8$ amu)[2] formed in the plasma generated by the cyclotron beam as it leaves the target passing through the helium atmosphere from impurities in the helium. The recoils then leave the thermalizer attached to these large molecular clusters through a pholyethylene or teflon capillary (0.02 to 0.06 in ID) accelerating to near the sonic

velocity of He (∿3 ft/msec). The capillary is run through concrete shielding to a low background area about 40 feet away. At the end of the capillary the helium will be skimmed off using a one or two stage skimmer. Quite efficiency skimming of the helium should be possible just by directing the flow from the capillary at a coinical orifice. The molecular clusters with their horendus masses are extremely well collimate (90% diverage with an angle of less than 3°) and should be passed quite efficiently through the orifice whereas the helium will diverage more rapidly and be largely pumped off. If our pumping capacity is not sufficient to reduce the pressure to $10^{-5}$ tor after the first skimming stage, a second stage will be added. The molecular clusters will be broken up and the recoils ionized in an RF or DC induced discharge setup in one of the skimming stages with the recoils directed into the ion optics associated with the electrostatic quadrupole.[3] With the quadrupole setup properly only selected masses are transmitted through it.[4] At the exit of the quadrupole the recoils will either be directed into an electron multiplier such that it is possible to obtain a mass scan or onto paper or aluminized mylar tape for conventional nuclear counting.

## References

1. R.D. MacFarlane and Wm.C. McHarris, Chap. II.C., "Techniques for the SCudy of Short Lived Nuclei" to be published in Nuclear Reactions and Spectroscopy, ed. by J. Cerny, Academic Press, New York 1973.

2. H.J. Jundas, R.D. MacFarlane, and Y. Fares, Phys. Rev. Letters 27, 556(1971).

3. Electric quadrupole supplied by Extranuclear Labs. P.O. Box 11512, Pittsburgh, Pennsylvania.

4. For a theoretical description of the Electric Quadrupole sec: W. Paul, H.P. Reinhard, and U. von Zahn, Z. Phys. 152, 143(1958).

COLLIMATED CYCLOTRON BEAM

TARGETS

NUCLEAR RECOILS

HELIUM THERMALIZER

THERMAL RECOILS
(as large Molecular clusters)
plus Helium

HELIUM JET
TRANSPORT

THERMAL RECOILS
(as large Molecular clusters)
plus Helium

HELIUM
SKIMMER

THERMAL RECOILS
(as large Molecular clusters)

IONIZER

IONIZED RECOILS

ION OPTICS

ELECTROSTATIC
QUADRUPULE

e/m SEPERATED RECOILS

NUCLEAR
COUNTING
EQUIPMENT

COLLIMATED CYCLOTRON
THIN TARGET HOLDER
HELIUM ( ~ 2 atm. pressure)
FARADAY CUP
CAPILLARY TUBE

CONCRETE SHIELDING

PUMPED WITH ROOTS BLOWER
PUMPED WITH D.P
PUMPED WITH D.P
IONIZER

ION OPTICS PACKAGE

QUADRUPOLE ASSEMBLY

TAKE-UP REEL FOR
MYLAR TAPE
LEAD SHIELDING
NUCLEAR COUNTING
EQUIPMENT

PARTICLE MULTIPLIER

Fig. 1   Block and schematic drawing of on-line mass separator under construction.

# Helium Jet System*

K.L. Kosanke, H.P. Hilbert, and Wm.C. McHarris

Our initial motivation for the construction of the helium thermalizer jet transport system was its proposed use as the first stage in an on-line mass filter (preceding section). While this remains the case, the helium thermalizer jet transport system has become a popular research tool in itself. It is being used with increasing frequency for the rapid transport of cyclotron produced activities to a low background area for conventional nuclear counting experiments. We anticipate that the helium jet system will remain an important research tool in and of itself even after we have developed an on-line mass separation capability.

The jet systems we have constructed were paterned after that developed by R.D. Macfarlane,[1] and we are grateful to him for his continued help in developing our system. While we are continuing to use polyethylene capillary ($\sim$45 feet long) we have changed to a larger diameter (0.055" ID) capillary and are using higher pressures ($\sim$3 atm.) of helium doped with small amounts ($\sim$10 ppm) of benzene vapor. This has been done to improve the efficiency of the system and to reduce its transport time. The change to larger capillary was primarily to reduce transit times by reducing the time necessary to sweep the activity recoiling from the back side of the target into the capillary through increasing the flow rate in the capillary. However, this also had the positive effect of increasing transmission efficiency. In the case of $^{26}$Si run at 3 atm efficiency increased 32% and the case of $^{23}$Mg the efficiency increased 18%.

Before we were using small amounts of benzene vapor added to the helium, the efficiency did not vary much with helium pressure (from 0.3 to 4 atm) but remained at about 5%. Since we started using small admixtures of benzene, the transport efficiency has become sensitive to helium pressure, with the efficiency increasing by about 50% upon increasing the helium pressure from 1 to 3 atmospheres. This also had the positive effect of reducing transport times by increasing the flow rate in the capillary. The
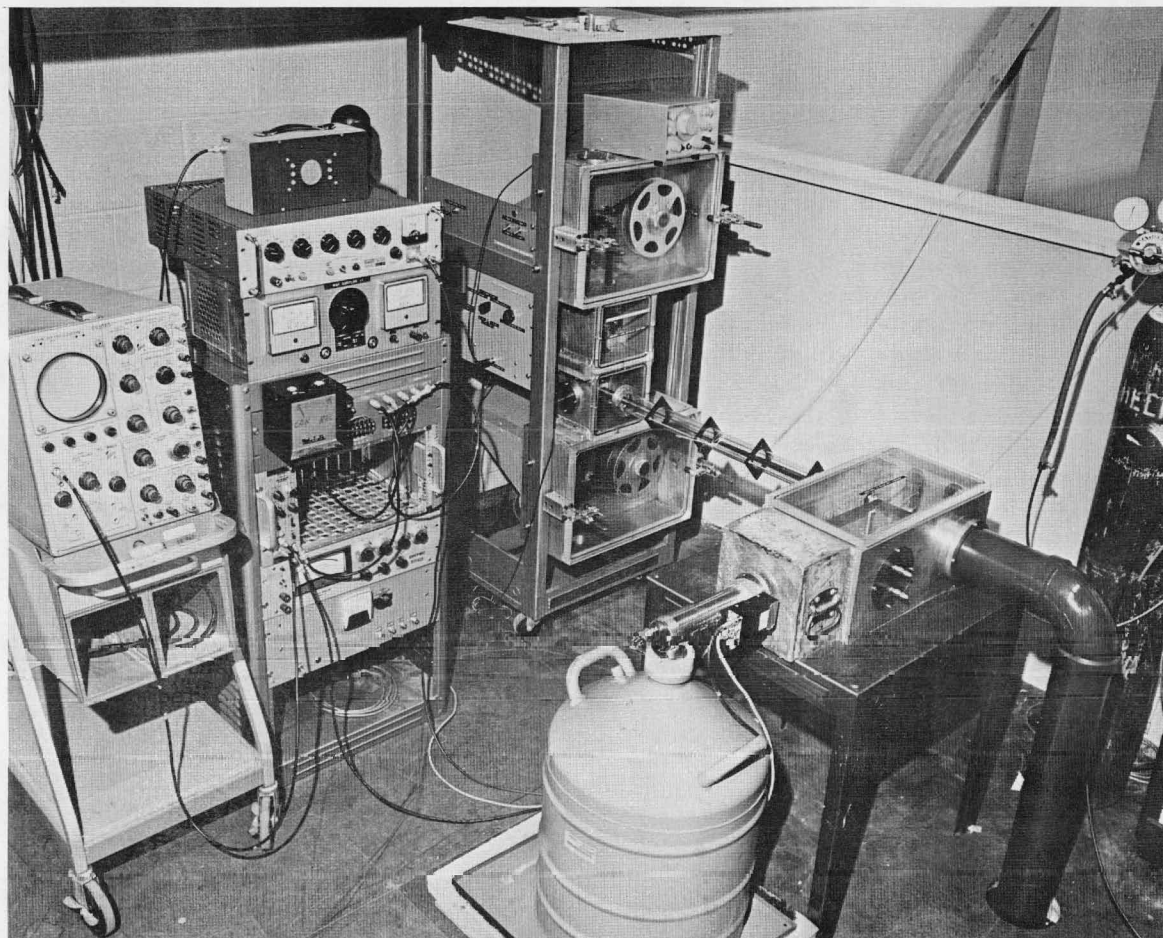


Fig. 1    Typical gamma ray singles experimental set-up using helium thermalizer jet transport system.

largest overall improvement in the helium jet system resulted from the addition of small amounts of impurities to the helium. We are using 10 ppm of benzene vapor added to the helium and obtain efficiencies improved by a factor between 5 and 10. Accordingly the present efficiency of the jet system is 90% for Co recoils. We know that we do not get 100% of the recoils coming out of the capillary to stick on the collecting surface (paper tape in this case). Judging from the radiation background build-up in the detector chamber at the end of the capillary, we believe much of the remaining 10% of the activity lost in the transport process is lost in the process of depositing it on the collecting surface.

All our observations are consistent with Macfarlane's thoughts as to the role of large molecular clusters in the transport of activities with the jet system.[2] He contends that large molecular clusters are formed from impurity molecules in the plasma of the cyclotron beam. (He has determined that the masses of these clusters to extend to $\sim 10^8$ AMU.) Further, the transverse diffusion rates of these clusters, because of their enormous molecular weights, will be very low (i.e., they diffuse only very slowly to the capillary walls and are therefore lost only at a relatively low rate). Accordingly, high transport efficiency is the result of attachment of thermalized recoils to these molecular clusters.

In an attempt to determine the effect of the pressure in the detector chamber on the transport efficiency of the jet system, we observed that we could run with only a small drop in efficiency even at atmospheric pressure. In a run where a one atmosphere gradient was maintained across the capillary there was only a 30% decreas in the transport efficiency of the jet system upon changing the pressure in the detector chamber from 0.5 mm Hg to 1 atmosphere. Further, it is thought this may be improved by modifying the collecting technique when running at atmospheric pressure. This observation has since lead us to the possibility of preforming relatively fast and sophisticated chemistry with the jet system by catching the activities in aqueous solution. However, it was felt there could be a problem in doing chemistry at this point if the recoil atoms remained attached to the molecular clusters, because the recoils are present only as very small impurities (present only in ppm) in the cluster molecules. In our first attempt at chemistry, the activities resulting from 30-MeV protons on a Zn target were trapped in 2N HCl. Activity was collected for about 30 minutes, then the solution was passed through a column of Dowex-1. A good separation of Zn and Cn was achieved. A second run at-

tempted to set an upper limit on the lifetimes for the recoil-cluster bond. Again we ran using 30-MeV protons on a Zn target. This time the activities were trapped in 8N HCL containing Zn and Cu carriers and fed into a column of Dowex-1 in an attempt at achieving a separation of 32.4-sec. $^{63}$Ga from and Zn and Cu activities. We observed an enhancement of better than a factor of 6 over a previous run in which a series of separate Zn targets were irradiated and transported using our pneumatic target transport apparatus (rabbit).[3] In this helium jet transport run there was no attmept made to improve separations by altering any of the experimental parameters from our original guesses. In this run only about 1 second elapsed between entrapment of the activities leaving the capillary in the column eluant and the eluant's leaving the column. Accordingly, it is felt that the major time consuming activity in performing chemistry following the jet system will be involved in pHysically doing the chemistry and not in freeing recoils from the clusters.

We have observed the nature of the impurity molecules used to generate the molecular clusters can have an effect on the transport efficiency of different recoils. This was observed in a run using 30-MeV protons on an Al target to produce $^{23}$Mg through a (p,$\alpha$n) reaction and $^{26}$Si through (p,2n) reaction. Clusters were formed using either benzene vapor or compressed air and water vapor. In each case the activities were transported with improved efficiency. However, the absolute transport efficiency for the $^{23}$Mg and $^{26}$Si depended on the nature of the cluster impurities. The $^{26}$Si transport efficiency increased when changing the benzene vapor to compressed air and water vapor as the major source of impurities, while the $^{23}$Mg transport efficiency decreased. Accordingly, the relative yield of $^{26}$Si could be made to increase by 36% upon switching to the compressed air and water vapor as the source of impurities.

If it is true in general that transport efficiencies of chemically different recoils in a mixture of recoils are dependent on the nature of the impurities forming the molecular clusters, then not only will it be necessary to consider different sources of impurity molecules to get peak efficiency for the particular recoils to be studied, but also by choosing different impurity molecules it may be possible to make a Z determination of the different recoils by watching their relative transport efficiencies.

In that it was the absolute transport efficiencies that changed inversely in the $^{23}$Mg-$^{26}$Si case and not merely relative transport efficiencies, this suggests that the attachment of recoils to molecular clusters may be occuring at active sites in the clusters that are chemically specific. If this is the case, then it is not

impossible to consider generating cluster molecules using carefully selected impurities such that it would be possible to achieve relatively clean chemical separations ocurring in the short times of the transport process. That is, chemistry performed on a time scale of ~50 msec and performed in such a manner that is fully compatible with placing the helium jet system on-line with an isotope separator. Note, it might be that the cluster molecules required for this would have to be generated off-line, using UV-light[4] or an electric discharge instead of the plasma generated by the cyclotron beam, because their generation required an environment that was incompatible with the efficient transport of activities with the jet system.

References

1. R.D. Macfarlane, R.A. Gouch, N.S. Oakley, and D.R. Torgeson, ORO-3820-2 (1969); Nucl. Instr. and Methods $\underline{73}$, 285(1969).

2. R.D. Macfarlane and Wm.C. McHarris, Chapter II.C., "Techniques for the Study of Short-Lived Nuclei", to be published in Nuclear Reactions and Spectroscopy, ed. by J. Cerny, Academic Press, New York, 1973.

3. G.C. Giesler, Ph.D. Thesis, Michigan State University, COO-1779-55, 1971.

4. K. Wien, Y. Fares, and R.D. MacFarlane, ORO-3820-19, to be published.

Section II

ABSTRACTS OF TALKS AT MEETINGS

July 1971–June 1972

American Phys. Soc. Tucson Meeting, Nov. 1971

The $^{14}$N(p,p')$^{14}$N Reaction at 29.8, 36.6, and 40.0 MeV and the Tensor Part of the Two-Body Force.* S.H. FOX, S.M. AUSTIN, and D. LARSON, Mich. State Univ.—Protons from the MSU Sector-Focussed Cyclotron were scattered from gas and evaporated melamine $^{14}$N targets and detected with position sensitive detectors in an Enge split-pole spectrograph. Angular distributions for elastic scattering, and the excitation of the 2.31($0^+$,T=1) and 3.95($1^+$,T=0) states were obtained at all energies. Data at 29.8 MeV were taken with a silicon detector telescope and states up to 8 MeV in excitation were observed. Optical model fits to the available elastic scattering data were made. Microscopic model DWBA calculations with exchange were made for the 2.31 reaction including central, L·S, and (most importantly) tensor forces in the two-body force. A T=1 tensor force with $r^2$ weighted integral equal to that for the OPEP tensor force is consistent with the data.

American Phys. Soc. Tucson Meeting, Nov. 1971

(p,n) Quasi-Elastic Scattering.* R.K. JOLLY, T.M. AMOS, A. GALONSKY, and R. St.ONGE,** Mich. State Univ.—Angular distributions for analogue-state excitation by the (p,n) reaction have been measured from 10° to 103° with protons of 22, 30, and 40 MeV and for targets of $^{27}$Al, $^{51}$V, and $^{90}$Zr. Neutrons were detected with a time-of-flight spectrometer using liquid scintillator. Differential cross sections vary from as much as 3 mb/ster at backward angles. For all 3 targets at 22 MeV and at 30 MeV a derivative surface interaction fits the angular distribution better than a volume interaction, but at 40 MeV the volume interaction is better for $^{51}$V and for $^{90}$Zr while the surface interaction is better for $^{27}$Al. Interaction strengths will be presented.

American Phys. Soc. Tucson Meeting, Nov. 1971

Inelastic Proton Scattering from $^{16}$O and the L·S Part of the Two-Body Force.* Sam M. AUSTIN, W. BENENSON, D. LARSON, and R. SCHAEFFER, Mich. State Univ.—At energies below 30 MeV inelastic proton scattering from $^{16}$O leaving this nucleus in its 8.88 MeV, $J^\pi=2^-$,T=0 state is fairly well described by microscopic DWBA calculations using scalar two-body forces. As the energy increases the experimental angular distributions assume an L=3 character while the central force DWBA calculations continue to predict an L=1 shape. We have made DWBA calculations for scalar, tensor, and L·S forces including the contributions of exchange. Tensor forces of T=1 type such as those from the one-pion-exchange potential have little effect on the shape of the cross-section. However, an LS force slightly larger than that recently used by Love[1] yields an L=3 shape which reproduces the cross-section and asymmetry data forward of 90°.

[1] W.G. Love, Phys. Letters 35B, 37(1971).

American Phys. Soc. Tucson Meeting, Nov. 1971

The Two-Pion Exchange Contribution to the Nucleon-Nucleon Potential.* Bruce H.J. MCKELLAR** and Geoffery N. EPSTEIN, Univ. of Sydney—We present a calculation of the $2\pi$ exchange contribution to the nucleon-nucleon potential using the method of Cottingham and Vinh Mau, but using as $\pi$N amplitude consistent with recent data and the soft pion theorems and making the continuation to the $N\bar{N}\to\pi\pi$ amplitude taking into account the S wave $\pi\pi$ phase shifts as well as the $\rho$ meson pole in the P wave. The potential obtained, which contains no arbitrary parameters, is in reasonable agreement with the phenomological potentials of the Yale Group and Hamada and Johnston.

American Phys. Soc. Tucson Meeting, Nov. 1971

Isospin Mixing of the Lowest T=2 State in $^{56}$Ni.* R. SHERR, Princeton University, W. BENENSON, E. KASHY, D. BAYER, and I. PROCTOR, Mich. State Univ. Dzubay et al.[1] found that in $^{56}$Co the T=2 $0^+$ analog of $^{56}$Fe is strongly mixed with a nearby T=1 state. To obtain further information on this doublet we have looked for the analogs of this doublet in $^{56}$Ni via the $^{58}$Ni(p,t) reaction. With a 34 MeV proton beam from the MSU Cyclotron on an 80 μg/cm$^2$ target, we obtained triton spectra with 11 keV resolution using the split-pole spectrograph and a position-sensitive detector. In the expected region of excitation for the T=2 state (9.7–10.1 MeV), we found a triplet of $0^+$ states at 9.915, 9.991, and 10.021 MeV, with relative strengths 1, 0.2, and 0.3 respectively. It appears that a T=0 state is excited as well as the sought-for T=1, T=2 doublet. From this experiment alone one cannot identify which of the levels comprise the doublet nor can one tell whether the third state is mixing with the doublet. Other experiments will be required to resolve these questions.

[1] T.G. Dzubay, R. Sherr, F.D. Becchetti, Jr., and D. Dehnhard, Nucl. Phys. A142, 488(1970).

American Phys. Soc. Tucson Meeting, Nov. 1971

Renormalized Operators and Collective Particle-Hole Excitations in $^{40}$Ca and $^{48}$Ca.* H. MCMANUS and M. DWORZECKA, Mich. State Univ.—Collective particle-hole excitations in $^{40}$Ca and $^{48}$Ca are calculated with Sussex matrix elements in Tamm-Dancoff approximation. Calculations are done both with bare and renormalized operators. Renormalization is accomplished by including core polarization effects by perturbation in both the two-body interaction and transition moments. The results are similar to those obtained in random-phase approximation using realistic forces with core polarization screening.

A Study of $^{43}$Sc via the (p,α) Reaction.* Jerry A. NOLEN, Jr. and Paul ZEMANY, Mich. State Univ.—The direct (p,α) reaction has been measured with 30 MeV protons from the MSU Cyclotron. The alpha spectra were recorded on nuclear emulsions in a split-pole magnetic spectrograph with an over-all energy resolution of 15 keV. The states of $^{43}$Sc which are strongly populated by this reaction are $(f_{7/2})^3$ configurations, such as the ground state $(7/2^-)$ and the state at 1.83 MeV $(11/2^-)$ or proton-hole states, as in the cases of the 0.151 MeV $(3/2^+)$ and 0.856 MeV $(1/2^+)$ levels. There are several states of significant strength around 3 MeV excitation; one or more of these may be high spin states of $(f_{7/2})^3$ configuration. The $3/2^-$ state at 1.18 MeV which has large strength in stripping reactions is weakly populated in this reaction as are many other previously known levels of $^{43}$Sc. Spectroscopic strengths ex-tracted from DWBA calculations are compared with predictions based on shell-model wave functions. The effects of coherence in the (p,α) reaction will be discussed.

Fine Structure in Neutron-Gamma Ray Pulse Shape Discrimination.* R. St.ONGE,** T.M. AMOS, A. GALONSKY, and R.K. JOLLY, Mich. State Univ.—With a zero-crossover pulse-shape discrimination sys-tem we have examined pulses from an NE-213 liquid scintillator irradiated with neutrons and γ rays produced by bombardment of a thin $^7$Li target with 40-MeV protons. The 2-dimensional display of crossover time vs. pulse height shows the usual separation into neutron and γ-ray bands but with with three additional bands. By measuring the time-of-flight spectrum of each band separately we see that each additional band has a time spectrum of the neutrons. In order of decreasing separation from the γ-ray band the other bands are assigned: 1) carbon recoils, 2) alpha particles from carbon breakup, 3) the usual neutron band consisting of protons from $^{12}$C(n,p), and 4) high energy protons escaping from the liquid. The monotonic relation of the pulse shape effect to dE/dx is apparent.

Interpretation of $^{170}$Yb Levels Observed in the Decay of $^{170}$Lu.* F.M. BERNTHAL, Mich. State Univ. and D.C. CAMP, Lawrence Livermore Lab.—Analysis of Ge(Li) γ-ray and Si(Li) conversion electron data from decay of $^{170}$Lu has allowed spin and parity assignments to be proposed for 48 of the 70 excited states observed in $^{170}$Yb. Significant differences exist between our proposed level scheme and that reported elsewhere. The $^{170}$Lu β-decay displays essentially uniform feeding to the numerous low-spin states in $^{170}$Yb. Log(ft)'s derived from γ-ray intensity balances are generally ≳7.0 for beta feeding to all levels. Four $0^+$ excitations are observed within the pairing energy gap 2Δ. Of the four $2+0'$ states observed, only the $2+0_2$ (β-vibration?) band member has γ-ray branching to the ground band consistent with a single value of the $z_0$ mixing parameter. Other features of the $^{170}$Yb level scheme include (1) two low-lying 1-0 states at 1364.6 and 1512.4 keV, the expected 1-1 member of the "octupole" multiplet apparently being absent below 2 MeV; (2) the absence of a state 1+0 pre-viously thought to be identified[1] at 2533.1 keV; (3) an apparent dearth of states near the energy 2Δ.

Rotational Bands in $^{179}$W Excited in the $^{177}$Hf (α,2n) Reaction.* F.M. BERNTHAL and R.A. WARNER, Mich. State Univ.—The technique of in-beam γ-ray spectroscopy has been used to obtain γ-ray singles and γ-γ coincidence data on the rotational band structure of $^{179}$W. A metallic target of 92% en-riched $^{177}$Hf was bombarded with 27-MeV α-particles from the MSU sector-focused cyclotron. On the basis of energy, intensity, and coincidence re-lationships, and earlier published decay scheme work,[1] the structure of the $7/2^-$[514] ground and $9/2^+$[624] and $1/2^-$[521] excited rotational bands have been detailed to spins at least as high as 21/2. Analysis of the highly perturbed "parity unique" $9/2^+$ band in terms of Coriolis coupling will be discussed.

The Decay of $^{40}$Sc.* J.N. BLACK, Wm.C. McHARRIS, and W.H. KELLY, Mich. State Univ.—The decay of 0.18-sec. $^{40}$Sc to levels in $^{40}$Ca has been in-vestigated with large, high-resolution Ge(Li) γ-ray detectors using pulsed-beam methods. The activity was produced by bombarding a 2-mg/cm$^2$ 99.97% enriched $^{40}$Ca foil with 24-MeV protons from the MSU Cyclotron. Various beam-off ray spectra, together with a beam-on spectrum, were routed into the laboratory's Sigma-7 computer and accumulated for periods of up to 32 hr. Seven γ rays were identified and placed in a consistent decay scheme for $^{40}$Sc. Although the intensities of these γ rays are in agreement with the results of Armini, et al.,[1] the energies are not. How-ever the energies are generally in agreement with those reported by Kashy, et al.[1]

The Angular Distribution Study of the $^{159}$Tb(p,t) Reaction.* R.W. GOLES, R.A. WARNER, Wm.C. McHARRIS, and W.H. KELLY, Mich. State Univ.—30 MeV protons accelerated by the Michi-gan State University Sector-Focused Cyclotron were used to study this (p,t) reaction. Triton spectra taken between 10° and 75° at 5° intervals were momentum analyzed using an Enge split-pole magnetic spectrometer. Below the pairing gap, these spectra were dominated by β- and γ-vibra-tional and ground state rotational band members. The band members observed in our spectra are: ground band—GS($3/2^+$), 61($5/2^+$), 144($7/2^+$), 254($9/2^+$), 379($11/2^+$), 527($13/2^+$), and possibly 927 keV ($17/2^+$); γ band—598($1/2^-$), 640($3/2^+$), 699($5/2^+$), 795($7/2^+$), and 896 keV ($9/2^+$); β band—994($3/2^+$), 1048($5/2^+$), and 1120 keV ($7/2^+$). Angular distributions of the above listed states will be presented and compared with DWBA predictions.

**The Half-Life of the 628.6-keV State in $^{141}$Pm.*** R.A. WARNER, R.R. TODD, R.E. EPPLEY, W.H. KELLY, and Wm.C. McHARRIS, Mich. State Univ.——A 2-parameter (time vs. E) delayed-coincidence experiment using Ge(Li) and NaI(Tl) detectors has been performed to measure the half-life of the $11/2^-$ state at 628.6 keV in $^{141}$Pm. The result, $T_{1/2}=0.70\pm0.02$ $\mu$sec, leads to partial half-lives of 0.75 and 10.6 $\mu$sec for the 432-keV M2 and the 628.6-keV E3 transitions, respectively. The Moszkowski single-particle estimates for these transitions are 13 nsec and 17 $\mu$sec, respectively. The hindered M2 is typical and the slightly enhanced E3 is consistent with other E3 rates in this region.

---

**Inelastic Proton Scattering from $^{138}$Ba and $^{144}$Sm.*** Duane LARSON, Sam M. AUSTIN, B.H. WILDENTHAL, and S.H. Fox, Mich. State Univ.—— We have studied states of $^{138}$Ba and $^{144}$Sm via inelastic scattering of 30 MeV protons. The data was taken on plates using the technique of dispersion matching with the Enge spectrograph. Typical resolution of less than 10 keV has allowed us to make the following energy assignments in $^{138}$Ba (in keV); 1436(2), 1898(4), 2091(6), 2201, 2218(2), 2309(4), 2416, 2446, 2582, 2640(2), 2779(4), 2880(3), 3042, 3150, 3243, 3278, 3333(2), and 3363(2). In $^{144}$Sm we find levels at 1659(2), 1809(3), 2191(4), 2324(6), 2426(2), 2591(4), 2806, 2831, 2889(4), 3025, 3130, 3203, 3231, 3279, and 3317. The L transfers to the strong states are shown in parenthesis. Angular distributions have been obtained for all of the above states. Spin and parity predictions have been made based on the L transfers and are in agreement both with existing data and calculations. Microscopic DWA calculations including exchange will be shown.

---

**The Effective Two Nucleon Force in Nuclei.*** Sam M. AUSTIN, Mich. State Univ.—Many recent experiments on charge exchange and inelastic scattering initiated by nucleons in the 20-60 MeV range have been analyzed by their authors to yield a value of the effective two nucleon interaction, $V_{eff}$. We have reviewed these analyses and selected cases where a single term in $V_{eff}$ is dominant (see Equation) and where collective effects are fairly well understood. Where necessary corrections were made for contributions of exchange processes. Tensor forces were neglected. With a Yukawan radial dependence (r in Fermis)

$$V_{eff}=[V_0+V_\sigma\vec{\sigma}_1\cdot\vec{\sigma}_2+V_\tau\vec{\tau}_1\cdot\vec{\tau}_2+V_{\sigma\tau}(\vec{\sigma}_1\cdot\vec{\sigma}_2)(\vec{\tau}_1\cdot\vec{\tau}_2)]\frac{e^{-r}}{r}$$

we obtain $V_0=30\pm5$, $V_{\sigma\tau}=12\pm3$ MeV in reasonable agreement with estimates based on the free two-body force. There is very little available data on $V_\sigma$ and $V_\tau$ in this energy range.

---

**The ($^3$He,$^6$He) Reaction on Some Even-Even $f_{7/2}$ Shell-Nuclei.*** I.D. PROCTOR, J. DREISBACH, W. BENENSON, E. KASHY, Mich. State. Univ., G.F. TRENTELMAN, Northern Mich. Univ., and B.M. PREEDOM, Univ. of S. Carolina—A 74 MeV $^3$He beam has been used to investigate proton-rich nuclei via the ($^3$He,$^6$He) reaction on enriched targets of $^{46}$Ti, $^{48}$Ti, $^{50}$Cr, $^{54}$Fe, and $^{58}$Ni. The $^6$He particles were analyzed in a split-pole magnetic spectrograph and detected with photographic emulsions. Masses have been determined for the $T_z=-1/2$ nuclei $^{47}$Cr, $^{51}$Fe, and $^{55}$Ni by measurements relative to the known $^{43}$Ti and $^{45}$Ti masses. For $^{46}$Ti, the ($^3$He,$^6$He) reaction appears similar to the (p,$\alpha$) reaction on the same target.[1] The first hole state ($d_{3/2}$) in $^{43}$Ti was observed at 0.40 MeV and indicates the expected strong Coulomb shift relative to its analog in $^{43}$Sc at 0.15 MeV.[1] This data is currently being analyzed and the results will be presented.

---

**The ($^3$He,t) Reaction at 70 MeV to Isobaric Analog States of $^{50}$Cr, $^{62}$Ni, and $^{90}$Zr.*** R.A. HINRICHS and D.L. SHOW, Mich. State Univ.—The study of the energy dependence of the ($^3$He,t) reaction to isobaric analog states has been extended to an incident $^3$He energy of 70 MeV. Using the MSU Cyclotron and a stack of Si detectors, the analog state transition for the targets $^{50}$Cr, $^{62}$Ni, and $^{90}$Zr was studied with an overall resolution of 130 keV. Both microscopic and macroscopic DWBA calculations for these transitions yielded interaction strengths significantly less than those observed at 37 MeV, but consistent with the trend found at the lower energies.[1] Most fits were quite sensitive to the optical model parameter sets used, especially the microscopic calculations. The macroscopic form factors required different shapes for each nucleus for good fits, and were themselves different than the shapes found at lower energies.

---

**High Resolution Study of $^{59}$Co(p,d)$^{58}$Co.*** R.G.H ROBERTSON and J.A. NOLEN, Mich. State Univ.—The odd-odd nucleus $^{58}$Co has been studied experimentally via the (p,d) reaction at $E_p=30$ MeV. Outgoing deuterons were analyzed in an Enge split-pole spectrograph and detected on photographic plates. By optimizing beam quality using the system of Blosser et al.,[1] peak widths of 0.25 mm, corresponding to about 5 keV FWHM, were obtained. The 374 keV level was clearly resolved from the one at 366 keV and was shown to have a substantially higher $\ell_n=3$ component than had been assumed in a previous (d,t) study.[2] Many weak states above 1100 keV were seen for the first time in neutron pickup. Several stronger states, probably arising from $(\pi f_{7/2}^{-1})(\nu f_{7/2}^{-1})$, were seen at excitation energies around 2.7 MeV. Spectroscopic factors extracted via DWBA analysis will be presented.

---

Decay of $^{202m}$Pb.[*] Jean GUILE, R.E. DOEBLER, Wm.C.
MCHARRIS, and W.H. KELLY, Mich. State Univ. and
Lawrence Berkeley Laboratory—The decay of the
3.62-h 9$^-$ isomer, $^{202m}$Pb, has been investigated
using Ge(Li) detectors in a variety of con-
figurations. Combined with existing electron
data,[1] unambiguous multipolarity assignments
were made for 16 of its 18 transitions, and all
were placed in a decay scheme including seven
states in $^{202}$Tl (following the 9.5% $\epsilon$ branch) and
seven states in $^{202}$Pb itself (following the IT
branch). Specific $J^\pi$ assignments were made for
most of these states, and their structures are
discussed in shell-model terms. We also dis-
cuss the rising 2$^+$ state in the e-e Pb isotopes
as one moves away from N=126 as coming from an
increase in the pairing force.

In-Beam Study of the $\gamma$-rays Emitted in the
$^{48}$Ti(p,n$\gamma$)$^{48}$V Reaction.[*] L.E. SAMUELSON, R.A.
WARNER, and W.H. KELLY, Mich. State Univ.; E.M.
BERNSTEIN and R. SHAMU, Western Mich. Univ.—
The level structure of $^{48}$V up to 1530 keV in
excitation has been studied via the $^{48}$Ti(p,n$\gamma$)$^{48}$V
reaction. Excitation functions of the decay $\gamma$
rays and $\gamma\gamma$-coincidence measurements have al-
lowed the determination of the $^{48}$V $\gamma$-ray decay
scheme. Angular distributions of $^{48}$V de-
excitation $\gamma$ rays were also measured at five
proton bombarding energies. Comparisons of
relative cross-sections for the population
of each level, and of the $\gamma$-ray angular distri-
butions with the predictions of the compound
nuclear statistical model has led to possible
level spin assignments and $\gamma$-ray multipole-
mixing ratios. Tentative level energies (in
keV) and spins (in parentheses) for excitations
below 1 MeV are as follows: 308.4(2), 420.9(1),
423.5?(?), 427.9(5), 519.0(1), 613.4(4?),
745.4(2), and 765.6(3). A mixing ratio of
$-0.11 \leq \delta \leq -0.03$ is indicated for the 112.5 keV
$\gamma$-ray transition from the 420.9 keV level.

Shell Model Calculations for $^{22}$Na and $^{22}$Ne.[*]
B.H. WILDENTHAL, Mich. State Univ. and B.M.
PREEDOM, Univ. of South Carolina—Shell model
calculations have been performed for the nuclei
$^{22}$Na and $^{22}$Ne. These calculations include all
Pauli-allowed combinations of six particles in
the basis states $0d_{5/2}$-$1s_{1/2}$-$0d_{3/2}$ outside of
an inert $^{16}$O core. The two-body interaction is
an empirically modified version of one calcul-
ated by Kuo from the Hamada-Johnston n-n potential.
Excitation energies, E.M. transition rates, and
spectroscopic factors for single-nucleon trans-
fer are presented and compared with existing data.
Properties which are characteristic of rotations
of deformed nuclei are predicted in these shell
model calculations. These predictions agree well
for transitions and energy levels for which data
exists.

Separation of "Direct" Neutrons from Compound-
Nucleus Neutrons Produced by Protons with Energies
up to 40 MeV.[*] T.A. AMOS, A. GALONSKY, and R.K.
JOLLY,[**] Mich. State Univ.—With the time-of-flight
technique absolute neutron spectra were measured for
protons of 22, 30, and 40 MeV bombarding thick
targets of Cu, Ag, Ta, and Pb at 0°, 30°, 60°, 90°,
120°, and 150°. Starting with a peak at ∿1 MeV
each spectrum falls exponentially for at least a
few MeV before a lower decay rate sets in. At the
forward angles the change is quite distinct. In
the 0° Ta and Pb spectra at 40 MeV the decay rate
between 8 and 20 MeV is 1/10 its value between 1
and 5 MeV, the entire change occurring between 5
and 8 MeV. Energy and angular dependences of what
are apparently 2 groups of neutrons would indicate
that one is of compound-nucleus (CN) origin, the
other of non-CN, or "direct", origin. We have ex-
tracted the ratios.

Energy Levels of $^{25}$Si.[*] W. BENENSON, J.
DREISBACH, I.D. PROCTOR, F. TRENTELMAN,[**] and
B.M. PREEDOM,[***] Mich. State Univ.—The ($^3$He,$^6$He)
reaction at 70.4 MeV has been used to study the
level structure of $^{25}$Si up to 6.7 MeV excitation.
The $^6$He's were detected in low sensitivity photo-
graphic emulsions on the focal plane of a split-
pole spectrograph. A resolution of 28 keV permit-
ted resolving the ground and first-excited state
doublet. Levels of $^{25}$Si were found at 40, 815,
1963, 2373, 2606, 3285, 3818, 4993, 5417, and
5734 keV. The observation of the 40 keV state
leads to a new mass excess for the ground state
of $^{25}$Si of 3.824±0.010 MeV. A mass quartet based
on the first-excited state is fit well without a
cubic dependence of $T_z$ as is the ground state
multiplet. Some of the other states line-up well
with other known T=3/2,A=25 levels. Comparisons
to shell model calculations will be presented.

The $^{48}$Ca(p,t)$^{46}$Ca Reaction at $E_p$=39 MeV.[*]
G.M. CRAWLEY, P.S. MILLER, Mich. State Univ.
and G. IGO, J. KULLECK, Univ. of Calif.—A
number of 0$^+$ states have been observed around
5.5 MeV in $^{46}$Ca by the $^{44}$Ca(t,p) reaction.[1,2]
Because the previous results are not completely
consistent, and also since the observation of the
same states by both (t,p) and (p,t) is valuable in
removing ambiguities in the nuclear wave functions,
the reaction $^{48}$Ca(p,t) was carried out using
the MSU Cyclotron to examine these same states.
A total resolution of 11 keV FWHM was obtained.
Further interesting features of this experiment
were the strong excitation of the high spin states
associated with the $f_{7/2}^2$ configuration and the
observation of close doublets below 5 MeV.

Shell-Model Predictions for $^{27}$Mg, $^{28}$Al, $^{26}$Mg, and $^{29}$Al.* M.J.A. deVOIGT, and P.W.M. GLAUDEMANS, Rijksuniv., Utrecht, and B.H. WILDENTHAL, Mich. State Univ.—A surface-delta type Hamiltonian has been obtained in a fit to some of the level energies of $^{27}$Al, $^{28}$Si, and $^{29}$Si. A truncated model space, which allowed active particles in each of the three sd-shell orbits, was used. The resulting wave functions contained explanations for most of the observed features of the nuclear structure of these systems. We have used this identical Hamiltonian and model space, to predict energy levels and wave functions for the nuclei mentioned in the title, and have calculated the related single-nucleon S-factors, and beta-decay, and electromagnetic transition rates. The overall results might be termed surprisingly good.

Energy Calibration of a Split-pole Magnetic Spectrograph.* E. KASHY, I.D. PROCTOR, J.A. NOLEN, and S. EWALD, Mich. State Univ.—The (p,p') and (p,d) momentum matching technique[1] is used with photographic emulsions for an accurate determination of the proton beam energy. The location of well known levels, such as the lowest $2^+$ and $3^-$ levels of $^{12}$C and $^{16}$O, then gives a precise momentum calibration of the two dimensional space required to focus different reaction products. The resulting calibration allows measurements of excitation energies of 3 MeV to an accuracy of 1 keV at $E_p=34$ MeV. In this way we have found a significant error in the mass excess of the lowest $3/2^-$ state of $^{15}$O consistent with the results of Hensley.[2] Both the method and results will be discussed.

The Numerical Accuracy of Optical Model Calculations for 70 MeV $^3$He Elastic Scattering.* R.R. DOERING,** Mich. State Univ.—Differential cross sections for 70 MeV $^3$He elastic scattering from $^{60}$Ni calculated with the optical Model codes GENOA, SNOOPY3, and GIBELUMP and the DWBA code DWUCK, using identical parameters, differed by as much as 2-1/2 orders of magnitude at back angles. Angular distributions measured for 70 MeV He elastic scattering from several $f_{7/2}$ shell nuclei span over 9 orders of magnitude between $5°$ and $150°$. Thus, calculations of the small back angle cross sections require an extraordinary degree of cancellation in the partial wave sum. This necessitates unusually accurate individual amplitudes. Specifically, it was found necessary to employ a smaller integration step size, a larger matching radius, and more partial waves than suggested by criteria often used for calculations involving other projectiles and energies.

A High Resolution Study of the $^{209}$Bi(p,d)$^{208}$Bi Reaction.* W.A. LANFORD, G.M. CRAWLEY, H.G. BLOSSER, and E. KASHY, Mich. State Univ.—The $^{209}$Bi(p,d)$^{208}$Bi reaction has been studied using the 35 MeV proton beam from the MSU Cyclotron. Using dispersion matching techniques[1] a resolution of 5 keV (FWHM) has been obtained. Exposures were taken from $6°$ to $46°$ in $4°$ steps for excitation in $^{208}$Bi of 0-6 MeV. The present experiment examines the interaction of the $h_{9/2}$ proton (in the $^{209}$Bi g.s.) with the neutron holes up to $h_{9/2}$, thus extending the previous (d,t) work[2] to higher excitation and checks the previous spin assignments for lower lying states.

Study of Inelastic Proton Scattering from $^{90}$Zr at 40 MeV.* R.A. HINRICHS, D. LARSON, Mich. State Univ. and B.M. PREEDOM, Univ. of South Carolina—Angular distributions for inelastic proton scattering from $^{90}$Zr between $15°$ and $115°$ have been taken at 40 MeV using the MSU Cyclotron. Plates in an Enge split-pole spectrograph were used, which made it possible to observe the weakly excited ($\leq 1$ μb/sr) $0^+$ first excited state. Simple microscopic DWBA calculations including core polarization, with emphasis upon the $(g_{9/2})^2$ configuration, yielded good fits to the $2^+$, $4^+$, $6^+$, $8^+$ states. With the inclusion of other data at 18 and 61 MeV, no energy dependence in the core polarization parameters was seen. The $0^+$(1.75 MeV) state was not fit with these calculations.

Calculation of Allowed β-decay in the (0d-1s) Shell.* W.A. LANFORD and B.H. WILDENTHAL, Mich. State Univ.—Allowed β-decay transition rates and half-lives have been calculated for (0d-1s)-shell nuclei with A=17-23, 27-29, 30-35, and 35-39, using previously reported wave functions calculated with mass-independent Hamiltonians. For nuclei with A=17-22 and 34-39, for which complete (0d-1s) shell model calculations were available, the calculated and experimental log(ft)'s have a rms. deviation from experiment of about 5%. There are some serious discrepancies for the nuclei nearer the middle of the shell, for which only truncated shell model calculations were available. Predicted half-lives for several unobserved nuclei have been obtained. Relevance of the $^{37}$Ca decay to the solar neutrino experiment[1] will be discussed.

Shell-Model Predictions for Electromagnetic Transitions in $^{138}$Ba and $^{139}$La.* Duane LARSON and B.H. WILDENTHAL, Mich. State Univ.—Electromagnetic transition rates and ground state moments have been calculated for the N=82 nuclei $^{138}$Ba and $^{139}$La. Using shell model wave functions calculated in a four shell basis with a modified surface delta interaction and bare-nucleon charges and moments, we obtain a magnetic moment of 1.84 nm and a quadrupole moment of +13 efm$^2$ for the ground state of $^{139}$La. For $^{138}$Ba we obtain B(E2) values of 2↑-0↑(174 e$^2$fm$^4$), 4↑-2↑(2.32 e$^2$fm$^4$), and 6↑-4↑(7.61 e$^2$fm$^4$). Using an effective charge of E$_p$=1.5 and a suggested effective proton g$_\ell$ of 1.1 brings the calculations into good agreement with existing data.

A Comparison of $^{17}$O and $^{17}$F with Some Charged Particle Reactions.* I.D. PROCTOR, W. BENENSON, and D.L. BAYER,** Mich. State Univ.—Angular distributions for resolved states below 6 MeV were obtained for the reactions $^{16}$O(d,p)$^{17}$O at 20.9 MeV, $^{16}$O(h,d)$^{17}$F at 34.6 MeV, $^{16}$O(α,h)$^{17}$O and $^{16}$O(α,t)$^{17}$F at 46.2 MeV, $^{19}$F(p,h)$^{17}$O and $^{19}$F(p,t)$^{17}$F at 39.9 MeV. A level which has not been previously reported was observed in $^{17}$F at 5.215±.012 MeV. The FRNL DWA formalism is used to analyze these reactions. The DWA prediction for the mirror reactions (α,t), (α,h) and (p,t), (p,h) will be compared to the cross section ratios obtained for the 5/2$^+$ G.S. and 1/2$^+$ first excited state. Spectroscopic factors will be presented for the single nucleon transfer reactions.

Effects of Operator Renormalization on (e,e') and (p,p') Scattering in $^{40}$Ca.* H. MCMANUS, M. DWORZECKA, and R. HAMMERSTEIN, Mich. State Univ. Wave functions and transition densities have been calculated for the lowest 3$^-$ and 5$^-$ states in $^{40}$Ca using renormalized operators. Renormalization was accomplished by taking into account all second order perturbation corrections to the two-body interaction and the transition operator. Electron inelastic scattering form factors and proton inelastic scattering angular distributions were calculated using these transition densities and were compared with experiment.

Structure of $^{34}$Cl from Neutron Pickup.* J.A. RICE, B.H. WILDENTHAL, and B.M. PREEDOM,** Mich. State Univ.—The states of $^{34}$Cl have been studied by neutron pickup, via the (p,d) reaction, from targets of Li$^{35}$Cl and Na$^{35}$Cl at E$_p$=35 MeV. Data were recorded in photographic emulsions with energy resolutions of 6 to 14 keV FWHM. Angular distributions were measured between 3° and 48°. The small angle data yield a very sensitive test for $\ell$=0 components in the distributions and the factor of 40 between 4° and 40° cross sections for $\ell$=0 shapes allow an accurate measure of relative $\ell$=0 to $\ell$=2 spectroscopic factors. Many previously unknown levels in $^{34}$Cl are identified above 4 MeV excitation. The implications of the spectroscopic factors of the low-lying levels for nuclear structure studies in this region will be discussed.

Production Cross Sections of Masses 6 and 7 in Proton Spallation of $^{22}$Ne Between 30 and 42 MeV.* L.M. PANGGABEAN, H. LAUMER,** and Sam M. AUSTIN, Mich. State Univ.—Protons from the MSU sector focussed cyclotron bombarded an enriched (99.66%) $^{20}$Ne target contained in a gas cell with a total exit areal density of 110 to 200 μg/cm$^2$. Particles were detected in a Si surface barrier detector and their masses were measured using a time-of-flight technique. The angular distributions σ(θ) obtained for each mass were forward peaked. Total cross sections were obtained by integrating σ(θ) and were found to be a factor of 10 smaller than the spallation cross sections for $^{14}$N in this energy range, but comparable with those for $^{16}$O.[1] Available spallation cross sections were used to estimate the production rate of Li, Be, and B in the solar system.

A Study of $^{26}$Al via the $^{27}$Al(p,d) Reaction.* D.L. SHOW, J.A. NOLEN, E. KASHY, and B.H. WILDENTHAL, Mich. State Univ.—Angular distributions have been measured for states in $^{26}$Al up through 5.5 MeV excitation energy in the angular range 4° to 52°, with energy resolutions of approximately 6 keV, FWHM. Proton bombarding energies were 29 and 35 MeV. These data provide definitive $\ell$=0/$\ell$=2 relative spectroscopic factors for 2$^+$ and 3$^+$ levels, accurate excitation energies for the 4-6 MeV region of the spectrum and several new levels in the high excitation region. The magnitudes and distributions of the $\ell$=0 and $\ell$=2 spectroscopic factor strength will be discussed in comparison to the results of new d$_{5/2}$-s$_{1/2}$-d$_{3/2}$ shell model calculations for A=26.

Study of the $^{39}$K(p,d)$^{38}$K Reaction with High Resolution.* B.H. WILDENTHAL and J.A. RICE, Mich. State Univ.—This experiment was undertaken with the aim of studying the levels of $^{38}$K with good energy resolution in a mode which permitted good discrimination between ℓ=0 and ℓ=2 angular distribution patterns. Particle groups corresponding to levels up through 6 MeV excitation have been recorded with 8 keV resolution in emulsion plates at angles from 4° to 30°. Precise excitation energies are obtained for this region and several strong groups above 5.5 MeV excitation are resolved for the first time. States with T=1 are identified by comparison to previous $^{39}$K(d,$^{3}$He)$^{38}$Ar studies. The mixing between sd-shell states and core-excited states, first identified in the (d,$^{3}$He) work, will be examined in the light of new sd-fp shell model calculations.

The β Decay of $^{63}$Ga.* G.C. GIESLER,** Wm.C. McHARRIS, R.A. WARNER, and W.H. KELLY, Mich. State Univ.—The decay of 32.4 sec $^{63}$Ga to $^{63}$Zn has been studied with high resolution Ge(Li) spectrometers from sources produced by the $^{64}$Zn(p,2n)$^{63}$Ga reaction with natural Zn foils. A total of 16 γ transitions have been placed in a level scheme with levels (spin, parity) at 0(3/2$^-$), 193.0(5/2$^-$), 248.0(1/2$^-$), 627.1(1/2$^-$,3/2$^-$), 637.0(1/2$^-$,3/2$^-$), 650.1(3/2$^-$), 1065.2(3/2$^-$), 1395.4(3/2$^-$,1/2$^-$), and 1691.7(5/2$^-$) keV. The spins were determined from log(ft's) and γ transition intensities and are in agreement with results from various scattering reactions.

Levels in $^{171}$Hf from $^{171}$Ta Decay.* I. REZANKA, I.-M. LADENBAUER-BELLIS, F.M. BERNTHAL,** and J.O. RASMUSSEN, Yale University—The decay of $^{171}$Ta (T$_{1/2}$=25 min.) produced in $^{165}$Ho($^{12}$C,6n) and $^{159}$Tb($^{16}$O,4n) reactions on Yale HILAC was studied by means of γ-ray spectroscopy. Three low-lying bands were identified in $^{171}$Hf: 7/2$^+$[633] (ground state), 5/2$^-$[512] (49.6 band head), and 1/2[521] (band head position uncertain). These results are in good agreement with parallel in-beam studies. In addition to these lowest rotational levels, a number of higher-lying states were observed.

Levels in $^{62}$Cu Populated by the Decay of $^{62}$Zn.* G.C. GIESLER,** Wm.C. McHARRIS, R.A. WARNER, and W.H. KELLY, Mich. State Univ.—The decay of 9.3 hr $^{62}$Zn has been studied with high resolution Ge(Li) spectrometers. The sources were produced by the $^{63}$Cu(p,2n)$^{62}$Zn reaction and then chemically separated. A total of 19 γ transitions including new ones at 385.2, 489.1, 881.4, 915.6, 1142.5, 1280.8, 1389.1, and 1429.9 keV have been placed in a level scheme with levels (spin, parity) at 0(1$^+$), 40.94(2$^+$), 243.44(2$^+$), 287.98(2$^+$), 426.3(3$^+$), 548.4(1$^+$), 637.5(1$^+$), 915.6(1$^+$), 1142.5(0$^+$,1$^+$), 1280.8(0$^+$,1$^+$), and 1429.9(1$^+$) keV. The spins were determined from log(ft's) and γ transition intensities and are in agreement with the results of Davidson, et al.[1]

Rotational Bands in $^{181}$W Excited in the $^{180}$Hf(α,3n) Reaction.* F.M. BERNTHAL, R.A. WARNER, and R.W. GOLES, Mich. State Univ.—As part of a systematic investigation of the rotational band structure associated with the 9/2$^+$[624] Nilsson orbital in N=105 and 107 isotones, in-beam γ-ray spectroscopy has been used to deduce the band structure of $^{181}$W$_{107}$. Although still strongly mixed with the other members of the i$_{13/2}$ family of Nilsson orbitals, the 9/2$^+$[624] band in $^{181}$W is markedly less perturbed than the corresponding band in $^{179}$W reported earlier.[1] On the basis of γ-ray energies, intensities, and angular distributions, and γ-γ coincidence data, 9/2$^+$ band members in $^{181}$W are established up to spin 29/2 at 113.4, 251.2, 414.6, 599.7, 814.6, 1039.7, 1310.8, 1560.9, and probably 1899.8 and 2156.8 keV. Less complete data have been obtained for the negative parity bands in $^{181}$W. Analysis of the "parity unique" 9/2$^+$[624] band in terms of Coriolis coupling will be discussed.

γ-γ Coincidences from $^{56}$Fe(p,nγ)$^{56}$Co Below 2.8 MeV of Excitation.* L.E. SAMUELSON, R.A. WARNER, W.H. KELLY, and F.M. BERNTHAL, Mich. State Univ.—A Ge(Li)-Ge(Li) spectrometer was used to study γ-γ coincidences from the $^{56}$Fe(p,nγ)$^{56}$Co reaction at proton bombarding energies of 7.38 and 8.36 MeV. Based upon coincidence evidence and γ-ray energy sums, we have placed 32 γ-ray transitions from 19 excited states in $^{56}$Co. The energies in keV of states from which de-excitation γ rays are observed to be in coincidence are 158.4, 829.6, 970.2, 1114.5, 1450.6, 1720.1, 1930.2, 2059.7, 2224.5, 2288.3, 2289.8, 2304.7, 2357.2, 2464.8, 2610.0, 2635.3, 2647.2, 2665.3, and 2729.6. Errors in the level energies are ±0.2 keV up to and including the 1720.1 keV state and ±0.8 keV for higher lying states. These results incorporate the 21 γ rays previously reported by R. DelVecchio et al.,[1] from n-γ coincidence experiments using the same reaction.

Levels in $^{141}$Pm Populated by the Decay of $^{141g}$Sm.* R.R. TODD, R.A. WARNER, R.E. EPPLEY, W.H. KELLY, and Wm.C. McHARRIS, Mich. State Univ.—The decay of 11.3 m $^{141g}$Sm has been studied with high resolution Ge(Li) spectrometers. The sources were produced directly by the $^{142}$Nd($^3$He,4n)$^{141}$Sm reaction and indirectly by the reaction $^{141}$Sm(p,4n)$^{141}$En $\xrightarrow{\epsilon}$ $^{141}$Sm. On the basis of half-life determinations and identification in cross bombardments, 11 transitions have been identified as belonging to the decay of $^{141g}$Sm. Various coincidence experiments have resulted in the placement of levels at 403.9, 438.4, 728.0, 1292.7, 1495.7, 2004.5, 2037.7 keV in the daughter $^{141}$Pm. Comparisons are made with levels in other odd proton nuclei in the region.

Anomalous $\epsilon/\beta^+$ Decay Branching Ratios.* R.B. FIRESTONE and Wm.C. McHARRIS, Mich. State Univ. Relative positron feedings have been measured at the MSU Cyclotron by 511 keV-511 keV-γ triple coincidence experiments in which both halves of an 8x8 in NaI(Tl) split annulus are gated on the 511 keV γ$^{\pm}$ positron annihilation peak and a third coincidence (resolving time, 2τ≃100 nsec) is required among these and a Ge(Li) detector. $\epsilon/\beta^+$ decay branching ratios are then inferred from these relative feedings by normalizing to "good" transitions in which the theoretical branching ratios are thought to apply. Measurements of branching ratios have thus far been made for the decays of $^{143}$Sm, $^{143}$Eu, and $^{145}$Gd. Although the bulk of the data agrees with theoretical predictions within statistical significance, there are some striking instances in which the experimental branching ratios differ widely from theoretical predictions. Decay to the 1173.0 keV (1/2$^+$) and 1514.5 keV(3/2$^+$) levels in $^{143}$Pm and the 808.5 keV(1/2$^+$) level in $^{145}$Eu yield $\epsilon/\beta^+$ branching ratios 3.8, 1.8, and 13.0 times the theoretical values, respectively, indicating strong hindrance of the positron decay branch. Similarly, decay to the 1566.3 keV level in $^{143}$Sm gives a branching ratio 0.4 times the theoretical value indicating strong hindrance of the electron capture decay.

Section III

ABSTRACTS OF PAPERS IN PRESS

July 1972

## Study of the $^{173}$Hf Level Scheme from the Decay of $^{173}$Ta*

I. Rezanka, I.-M. Ladenbauer-Bellis, T. Tamura, and W.B. Jones

Heavy Ion Accelerator Laboratory,** Yale Univ. New Haven, Connecticut 06520

and

F.M. Bernthal

Dept. of Chemistry and Cyclotron Laboratory, Michigan State University and Heavy Ion Accelerator Laboratory, Yale University.

### ABSTRACT

The decay of $^{173}$Ta was studied using high resolution Ge(Li), Si(Li) and Si surface barrier detectors in singles and coincidence modes. The $^{173}$Ta activity was produced via the reaction $^{165}$Ho $(^{12}$C,4n$)^{173}$Ta, at a carbon beam energy of 63-69 keV per nucleon. All spectra were obtained from chemically separated Ta sources. Besides the previously known energy levels of $^{173}$Hf, the following levels in keV were determined: 255.5, 451.9, 508.9, 635.8, 775.5, 785.3, 811.7, 872.6, 927.5, 942.5, 1020.3, 111.4, 1127.0, 1192.8, 1248.3, 1450.0, 1574.2, 1655.6, 1667.1, 1694.3, 2263.3. Rotational bands based on the 1/2$^-$[521] (G.S.), 5/2$^-$[521] (107.2 keV), 7/2$^+$[633] (197.5 keV), and 5/2$^+$[642](9/2$^+$[624] Nilsson states were observed. The mass difference between $^{173}$Ta and $^{173}$Hf was determined to be 3670±150 keV from measurement of the $\beta^+$ end-point energy.

## States in $^{163}$Ho and $^{167}$Tm Populated Through the (p,t) Reaction on $^{165}$Ho and $^{169}$Tm*

R.W. Goles, R.A. Warner, Wm.C. McHarris, and W.H. Kelly

Dept. of Chemistry and Cyclotron Laboratory Michigan State University

### ABSTRACT

The (p,t) reaction at 30 MeV on the deformed nuclei, $^{165}$Ho and $^{169}$Tm, strongly populates collective states in the residual nuclei. Indirect multiple step processes evidently play an important role, and the reaction is a powerful tool for populating higher-lying rotational band members.

## Nuclear Spectroscopic Studies of $^{252}$Es

P.R. Fields, I. Ahmad, R.F. Barnes, and R.K. Sjoblom

Chemistry Div., Argonne National Laboratory and

Wm.C. McHarris

Chemistry Dept. and Cyclotron Laboratory Michigan State University

### ABSTRACT

The decay scheme of $^{252}$Es has been investigated with high-resolution semiconductor detectors in conjunction with coincidence techniques. The half-life of $^{252}$Es was measured by following the decay alpha count rate associated with $^{252}$Es decay and was found to be 350±50 d. The electron capture and alpha decay branchings were measured to be 22±2%, and 78±7%, respectively. The EC decay almost entirely populates a level at 969.8 keV in $^{252}$Cf with a log(ft) value of 8.7. This state has been identified as the two-neutron state (n[613]7/2$^+$; n[620]1/2$^+$)3$^+$. A $K^\pi$=2$^-$ band has been identified at 830.8 keV. A rotational band built on a 804.8-keV level has been interpreted as the γ-vibrational band ($K^\pi$=2$^+$). On the basis of the observed log(ft) value, the ground state of $^{252}$Es has been given as assignment of (n[613]7/2$^+$; p[521]3/2$^-$)5$^-$. The favored α transition of $^{252}$Es has been found to populate a level at 590 keV in $^{248}$Bk. The ground state of $^{248}$Bk has been given a spin-parity assignment of 6$^+$ with two-quasi-particle configuration (n[734]9/2$^-$; p[521]3/2$^-$).

Decays of $f_{7/2}$ Isomers, $^{53g}$Fe and $^{53m}$Fe[*]

J.N. Black, Wm.C. McHarris, B.H. Wildenthal,
W.H. Kelly

Department of Chemistry and Cyclotron Laboratory
Michigan State University

ABSTRACT

The decays of 8.5-min. $^{53g}$Fe and 2.5-min $^{53m}$Fe
have been studied with a variety of $\gamma$ and $\beta^+$ de-
tectors in many different singles and coincidence
configurations. States in $^{53}$Mn populated by $^{53g}$Fe
decay were found to lie at $0(J^\pi=7/2^-)$, 377.9($5/2^-$),
1288.0($[3/2^-]$), 1619.9($[9/2^-]$), 2273.5($[7/2]$),
2685.6($7/2$), 2946.6($[9/2]$), 3126.7($[9/2,7/2]$), and
3248.0 keV ($[9/2]$). States in $^{53}$Fe populated by
3040.6-keV ($19/2^-$) $^{53m}$Fe decay were confirmed at
$0(7/2^-)$, 1328.1($9/2^-$), and 2339.6 keV ($11/2^-$).
In addition, a 3040.6-keV E6 and a 1712.6-keV M5
transition were found to compete with the 701.1-keV
E4 isomeric transition in deexciting $^{53m}$Fe, this
being the first observation of such high multi-
polarities. The E6 has an intensity of $6.0 \times 10^{-4}$
and the M5 an intensity of $1.3 \times 10^{-2}$ relative to
the E4 transition. Shell-model calculations have
been performed for both $^{53}$Mn and $^{53}$Fe, using the
Oak Ridge Shell-Model Code, and these are compared
with the observed states and with other shell-
model calculations. We also calculate the transition
probabilities of the higher multipolarity
transitions and compare them with experiment.

Techniques for the Study of Short-Lived Nuclei

Ronald D. Macfarlane

Dept. of Chemistry and Cyclotron Institute
Texas A&M University
and
Wm.C. McHarris[*]

Dept. of Chemistry and the Cyclotron Laboratory
Michigan State University

I.    Introduction
      A.   The Study of Short-Lived Nuclei and Nuclei
           far from $\beta$ Stability
      B.   The Scope of this Chapter
II.   Rabbit Systems
      A.   General Features
      B.   Example
III.  Gas Transport Systems
      A.   Perspective
      B.   Transport of Species with Low Sticking
           Coefficients
      C.   Transport of Species with High Sticking
           Coefficients
IV.   Accelerator Pulsing Techniques
      A.   General Features
      B.   Examples
V.    Fast Chemical Techniques
      A.   Perspective
      B.   Examples
VI.   Current and Novel Approaches
      A.   RAMA
      B.   Electrostatic Particle Guide and MAGGIE
      C.   SASSY

The Numerical Accuracy of $^3$He Optical-Model
Calculations at 70 MeV[*]

R.R. Doering,[**] A.I. Galonsky, and R.A. Hinrichs
Cyclotron Laboratory, Michigan State University

ABSTRACT

Small differential cross sections, such as
those measured at back angles for 70 MeV $^3$He
elastic scattering (typically below $10^{-4}$ mb/sr
past 130°), are difficult to calculate ac-
curately when they result from considerable
cancellation in the partial-wave sum. The
codes GENOA, GIBELUMP, SNOOPY3, and DWUCK differ
by as much as 2-1/2 orders of magnitude on $\sigma(0)$
for an optical-model potential describing
$^{60}$Ni($^3$He,$^3$He)$^{60}$Ni scattering at 71 MeV. This
calculation is repeated with a modified version
of GIBELUMP for wide ranges of the parameters
affecting numerical accuracy. A study of errors
in scattering matrix elements and cross sections,
as functions of these parameters, reveals that
criteria commonly used to determine the matching
radius and number of partial waves employed in
optical-model calculations yield insufficient
values in this case.

Calculations of Allowed Beta-Decay in the (0d-1s)
Shell[*]

W.A. Lanford and B.H. Wildenthal
Cyclotron Laboratory, Michigan State University

ABSTRACT

Allowed $\beta$-decay transition rates and half-
lives have been calculated for (0d-1s) shell
nuclei with A=17-22, 23-24, 27-29, 30-34, and
35-39. For nuclei with A=17-22 and 34-39, the
calculated log(ft) values have a rms deviation
of 5% from experiment, with no discrepancies
greater than 12%. For nuclei nearer the middle
of the shell there are more significant discre-
pancies between experiment and theory. The cal-
culated log(ft) values are used to predict the
half-lives of some light elements. The predicted
half-lives for which there are no experimental
measurements are: $^{19}$Na (0.3 sec), $^{21}$O (2.9 sec),
and $^{22}$O (0.15 sec). The log(ft) values re-
levent to the solar neutrino experiment are dis-
cussed.

## Inelastic Proton Scattering from $^{138}$Ba and $^{144}$Sm at 30 MeV*

Duane Larson, Sam. M. Austin, and B.H. Wildenthal
Cyclotron Laboratory, Michigan State University

### ABSTRACT

Measurements of the inelastic scattering of 30 MeV protons from $^{138}$Ba and $^{144}$Sm have been carried out with better than 10 keV energy resolution. Differential cross sections were measured for levels up through 3.4 MeV excitation energy. Spin and parity assignments are suggested for most of these states on the basis of angular distributions distinctly characteristic of angular momentum transfer L=2, 3, 4, or 6.

## New Proton Rich Nuclei in the $1f_{7/2}$ Shell*

I.D. Proctor, W. Benenson, J. Dreisbach,** and
E. Kashy
Cyclotron Laboratory, Michigan State University
and
G.F. Trentelman
Dept. of Physics, Northern Michigan University
and
B.M. Preedom
Dept. of Physics, Univ. of South Carolina

### ABSTRACT

The masses of $^{43}$Ti and of the previously unknown nuclei $^{47}$Cr, $^{51}$Fe, and $^{55}$Ni have been measured. These proton-rich members of the $1f_{7/2}$-shell mirror pairs are important for extensions of nuclear mass relationships to the Z>N region.

## Proton Decay of the Isobaric Analogues of the Ground States of $^{206}$Pb, $^{207}$Pb, $^{208}$Pb, and $^{209}$Bi*

G.M. Crawley and P.S. Miller
Cyclotron Laboratory, Michigan State University

### ABSTRACT

The (p,np̄) reaction has been measured on the lead isotopes $^{206}$Pb, $^{207}$Pb, and $^{208}$Pb and on $^{209}$Bi. Coulomb energy differences are extracted from the positions of the p̄ peaks. Proton decay widths are also obtained and compared with values from resonance experiments and with a previous value from $^{209}$Bi(p,np̄).

## Study of ($^3$He,t) Reactions at 70 MeV to Isobaric Analog States of $^{50}$Cr, $^{62}$Ni, and $^{90}$Zr*

R.A. Hinrichs and D.L. Show
Cyclotron Laboratory, Michigan State University

### ABSTRACT

The analysis of ($^3$He,t) reactions at 70 MeV to isobaric analog states of $^{50}$Cr, $^{62}$Ni, and $^{90}$Zr have shown an energy dependence in the extracted isospin strengths consistent with results at lower energies; the interaction strengths are approximately 50% smaller than at lower bombarding energies. The shapes of the form factors in a macroscopic analysis are nuclei-dependent. A $^3$He optical potential with a real strength of about 110 MeV and a volume imaginary term is strongly preferred in the ($^3$He,t) calculations.

## The $^{48}$Ca(p,t)$^{46}$Ca Reaction at $E_p$=39 MeV*

G.M. Crawley and P.S. Miller
Cyclotron Laboratory, Michigan State University
and
G.J. Igo and J. Kulleck
University of California, Los Angeles

### ABSTRACT

There has been considerable interest in using a comparison of (p,t) and (t,p) reactions to the same final states, especially $0^+$ states, to compare wave functions for a series of nuclei.[1] Such a study in the calcium isotopes would benefit from a more thorough study of the $^{48}$Ca(p,t) reaction. The complementary $^{44}$Ca(t,p) reaction has been carried out in various laboratories[2,3] and strongly populates states of $J^\pi=0^+$ at excitation energies between 5 MeV and 7 MeV. The $^{48}$Ca(p,t) has also been studied previously but at fairly low energies[4,5] or with poor resolution[6] so that the states of interest could not be resolved. In addition discrepancies between the (t,p) experiments serves as an additional motivation for the (p,t) experiment. The present paper is a preliminary report of this work.

Investigation of the $^{32}$S($^3$He,p)$^{34}$Cl Reaction
at 24 MeV

H. Nann and L. Armbruster
Institut.für Kernphysik der Universität
Frankfurt am Main, GERMANY*
and
B.H. Wildenthal**
Cyclotron Laboratory, Michigan State University

ABSTRACT

The $^{32}$S($^3$He,p)$^{34}$Cl reaction has been studied
at an incident energy of 24 MeV. The proton spectra
were analyzed with a multi-angle magnetic spectro-
graph and angular distributions have been measured
for states in $^{34}$Cl up to 3.4 MeV of excitation
energy. Two sets of shell-model wave functions,
which use the same configuration space but different
treatments of the effective residual interaction,
are tested by comparing two-nucleon transfer DWBA-
calculations with the experimental angular dis-
tributions.

NUCLEAR REACTIONS $^{32}$S($^3$He,p), E=24 MeV;
measured $\sigma(\theta)$. Natural target.

Study of the $^{27}$Al($^3$He,p)$^{29}$Si Reaction

H. Nann, T. Mozgovoy, and R. Bass
Institut für Kernphysik der Universität*
Frankfurt am Main, GERMANY
and
B.H. Wildenthal**
Cyclotron Laboratory, Michigan State University

ABSTRACT

The $^{27}$Al($^3$He,p)$^{29}$Si reaction has been studied
at bombarding energies between 9 and 14 MeV.
Comparison of the experimental angular distri-
butions at 14 MeV incident energy with two-
nucleon transfer distorted-wave Born-approximation.
(DWBA) calculations is made to test shell-model
wave functions of the target ground state and
the residual ground and excited states.

E  NUCLEAR REACTIONS $^{27}$Al($^3$He,p), E=9-14 MeV;
measured $\sigma(\theta)$. Natural target.

3

Section IV

TITLE PAGE OF PUBLISHED PAPERS

July 1971-June 1972

# ULTRA-HIGH RESOLUTION SPECTROMETER SYSTEM FOR CHARGED PARTICLE STUDIES OF NUCLEI*

H. G. BLOSSER, G. M. CRAWLEY, R. DEFOREST, E. KASHY and B. H. WILDENTHAL

*Cyclotron Laboratory, Michigan State University, East Lansing, Michigan 48823, U.S.A.*

This paper describes an arrangement for introducing feedback into a charged particle magnetic analysis system for nuclear reaction studies. In initial tests of the system, a resolution of 5 keV has been obtained in (p,p') studies at 30 MeV with 70% of the cyclotron internal beam on target. This corresponds to a resolving power $p/\Delta p$ of 12000. Essential features of the system, in addition to the feedback, are a careful definition of the cyclotron source by means of internal slits and the use of dispersion matching to cancel the effect of coherent on-target energy spread.

## 1. Introduction

The crucial role of an intense source in determining the ultimate resolution of charged particle magnetic analysis systems has been discussed by Cohen[1], who concludes that the resolution in an optimized system is predominantly controlled by source luminosity. Generally, the effective source for such an analysis system consists of an object slit at the beginning of a beam preparation system. The accelerator is tuned to maximize the transmission through this slit and thus maximize the luminosity of this effective source. In such an arrangement the dispersive properties of the accelerator are normally ignored, which, for the case of a cyclotron, is a major error (as we explain in section 2). In the system described here this difficulty is avoided

by using the actual cyclotron ion source as the effective object for the system which, if all magnets are stable, is equivalent to an external slit with exactly correct "dispersion matching"[2] (also see sec. 2). For the system we describe the stable magnet requirement is effectively provided by a feedback circuit which acts to maintain the position of the optic axis at a fixed point on the focal plane of the magnetic spectrograph.

A second important feature of our system is a "resolution meter" based on fractional transmission through a small slit in the spectrograph focal plane. Such a meter, in conjunction with "separated function" magnets[3]), allows a quick empirical adjustment of quadrupoles and sextupoles to give the best linear focus, dispersion matching, cancellation of aberrations, etc.
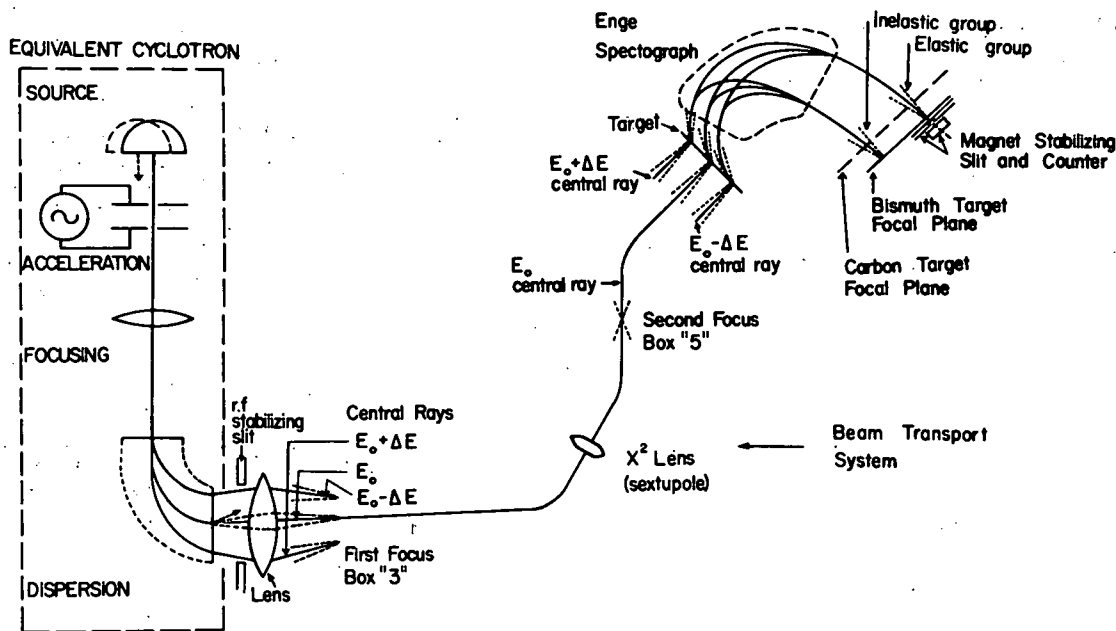


Fig. 1. "Equivalent circuit" of cyclotron and high resolution beam line.

# IMPROVING THE ENERGY RESOLUTION AND DUTY FACTOR OF ISOCHRONOUS CYCLOTRONS†

## M. M. GORDON

*Cyclotron Laboratory, Michigan State University, East Lansing, Michigan, USA*

A separated turn isochronous cyclotron can produce beams having a precise energy resolution together with a substantial duty factor if the effective voltage wave form is 'flat-topped'. Optimum flat-topping results are presented for five different harmonic combinations: $n = 1$ and $2$; $n = 1, 2,$ and $3$; $n = 1, 2, 3,$ and $4$; $n = 1$ and $3$; $n = 1, 3,$ and $5$. For a given energy resolution, the improvement in duty factor with each added harmonic is quite impressive. The success of this technique is limited by certain practical problems which are examined.

## 1. INTRODUCTION

If an isochronous cyclotron could be equipped with an rf system which provided a square wave voltage on the dees, then each ion pulse could extend for nearly half of the rf period, while the energy distribution within this pulse would remain quite homogeneous throughout the acceleration process. Assuming a small radial beam width, optimum conditions would then prevail for 'separated turn' operation with 100 per cent beam extraction.[1] The external beam would then possess exceptionally fine energy resolution together with a duty factor approaching 50 per cent. In addition, the transverse emittance of this beam would be directly correlated to that of the ion source or injector. In a certain sense, this cyclotron would operate like a pulsed dc accelerator.

The advantages of a square wave voltage for a classical cyclotron were first recognized by Rossi who devised a method for superimposing a third harmonic voltage on the dees, and who showed that when this voltage is one-ninth that of the main harmonic, the resultant flat-topped wave form partially fulfills the function of a square wave voltage.[2] This third harmonic flat-topping method was also investigated by Goodman as a means for improving both classical and isochronous cyclotrons.[3] Welton[4] and Blosser[5] considered voltage flat-topping as an important element in an isochronous cyclotron designed to yield superlative beam characteristics including a substantial duty factor.

† Work supported by the National Science Foundation.

The desirable effects of a flat-topped voltage wave form can be achieved by another method under certain circumstances. Since the energy gained at successive electric gap crossings is cumulative, and since only the resultant energy is significant, the voltages corresponding to different harmonics can be applied to separate sets of dees. This procedure is particularly suitable for ring cyclotrons where the ion injection energy is substantially greater than the energy gained at any one gap crossing.[1] Moreover, as pointed out by Rickey,[6] this procedure permits the utilization of even as well as odd harmonic voltages and such combinations always produce a superior flat-topping effect, and may produce duty factors exceeding 50 per cent. These considerations formed the basis for the design of the rf system of the Indiana Cyclotron now under construction.[7] Several other cyclotrons have been proposed recently which plan to utilize the flat-topping effect of either second or third harmonic voltages.[8,9]

The present paper explores the degree of energy homogeneity which can be achieved as a function of duty factor through the admixture of a small number of harmonic voltages, and discusses some of the practical problems which may limit the success of this technique. In a subsequent paper, we intend to discuss the limitation of energy resolution imposed by the longitudinal space-charge force in cyclotrons with a substantial duty factor.

## 2. FORMULATION

Using the azimuth $\theta$ as the independent variable,

# THE MASS OF $^{25}$Si AND THE ISOBARIC MULTIPLET MASS EQUATION*

G. F. TRENTELMAN and I. D. PROCTOR

*Cyclotron Laboratory, Michigan State University, East Lansing, Michigan*

The mass excess of $^{25}$Si has been measured as $3\,832 \pm 12$ keV via determination of the $Q$-value for the $^{28}$Si$(^{3}$He, $^{6}$He$)^{25}$Si reaction. The results are used to test the isobaric multiplet mass equation for $A = 25$.

Precise measurements of the masses of neutron deficient $T_z = -3/2$ nuclei are essential to test the isobaric multiplet mass equation [1], since these nuclei have generally been the least accurately measured members of $T = 3/2$ isobaric quartets. The isobaric multiplet mass equation (IMME), $M = a + bT_z + cT_z^2$, (where $T_z = \frac{1}{2}(N - Z)$) relates the masses of isobars under the assumptions that the specifically nuclear properties of all multiplet members are identical, and that all charge dependent forces are two-body in character.

Recent measurements of the $^{9}$C mass [2], and the $^{13}$O and $^{21}$Mg masses [3,4] have indicated that an additional term $dT_z^3$ ($d = 8.0 \pm 3.7$ keV)[2] is required for the IMME for $A = 9$, while for $A = 13$ and 21 the value of such a term is consistent with zero. This letter presents a new measurement of the mass of $^{25}$Si and subsequent application of the IMME to the $A = 25$ isobars.

The value of the mass of $^{25}$Si presented here was determined from the average of five individual measurements of the $Q$-value of the $^{28}$Si$(^{3}$He, $^{6}$He$)^{25}$Si reaction. This reaction was induced by 70 MeV $^{3}$He ions from the Michigan State University sector-focused cyclotron, and the $^{6}$He particles were momentum analysed in a split-pole magnetic spectrograph.

The $^{6}$He energies from $^{28}$Si$(^{3}$He, $^{6}$He$)^{25}$Si were measured by comparing their magnetic rigidity to that of $^{6}$He particles from the $^{12}$C$(^{3}$He, $^{6}$He$)^{9}$C (g.s.) reaction. The $Q$-value for the latter reaction is now well established [2]. A comparison was obtained by measuring the spectrograph magnetic fields necessary to get the $^{6}$He particles from each reaction at the same position on the focal plane. The spectro-

graph field behavior relative to the flat field value given by the NMR has been carefully calibrated for previous $(^{3}$He, $^{6}$He) work [5] with a momentum matching technique [6].

The scattering angle for each run was determined to an accuracy of $\pm 0.03°$ at $\theta_L \approx 10°$ by measuring the magnetic rigidity of $^{3}$He from $^{1}$H$(^{3}$He, $^{3}$He$)^{1}$H scattering from a very thin formvar target. The $^{3}$He beam energies were initially determined with the beam transport analysis system, and the final precise measurements made by comparing the magnetic rigidities of $^{6}$He from the $^{12}$C$(^{3}$He, $^{6}$He$)^{9}$C (g.s.) reaction to that of elastic scattering of $^{3}$He from $^{12}$C. Since the charge-to-mass ratio of these particles is different, the ratio of their magnetic rigidities is sensitive to the beam energy. Beam energies were thus determined to $\pm 35$ keV at $E \approx 70$ MeV.

Particle detection and identification at the spectrograph focal plane were accomplished with a 300 $\mu$m silicon surface barrier position sensitive detector operating in the d$E$/d$x$ mode for all particles of interest [7]. Serious background problems due to particle induced reactions in the position sensitive detector were nearly eliminated by mounting an ordinary silicon surface barrier detector behind the position detector and operating these two detectors in coincidence. Figs. 1 and 2 show $^{6}$He spectra from $^{28}$Si$(^{3}$He, $^{6}$He$)^{25}$Si with and without this coincidence requirement. Typical $^{6}$He resolution was target-thickness limited at $\approx 70$ keV FWHM.

The individual measurements of the $^{28}$Si$(^{3}$He, $^{6}$He$)^{25}$Si $Q$-value were $-28\,008 \pm 14$ keV, $-27\,985 \pm 8$ keV, $-27\,980 \pm 7$ keV, $27\,998 \pm 10$ keV, and $-27\,993 \pm 8$ keV. A weighted average of these values gives a $^{25}$Si mass excess of $3\,832 \pm 12$ keV. Uncertainties of $\pm 10$ keV, $\pm 4$ keV, and $\pm 3$ keV due to uncertainties in target thickness,

570

# Neutron-Hole-State Structure in $N = 81$ Nuclei. I. $^{144}$Sm and $^{142}$Nd $(p,d)$[†]

R. K. JOLLY and E. KASHY

*Cyclotron Laboratory, Michigan State University, East Lansing, Michigan 48823*

(Received 7 April 1971)

Angular distributions of deuterons from the $(p,d)$ reaction (energy resolution ~35 keV) on $^{144}$Sm and $^{142}$Nd at $E_p = 35$ MeV have been measured and compared with distorted-wave Born-approximation (DWBA) calculations. The DWBA calculations were performed both with and without the finite-range and nonlocality corrections. In some typical cases corrections were also included for the nuclear density dependence of the effective $pn$ interaction. The DWBA cross sections for $l = 5$ show an enhanced sensitivity to the inclusion of these corrections. Calculations including both the nonlocality and finite-range corrections yield acceptable spectroscopic factors. Considerable fractionation of the $(2d_{5/2})_n^{-1}$ and the $(1g_{7/2})_n^{-1}$ states is observed. No measurable population of neutron states in the $82 < N \leq 126$ major shell was observed. The single-neutron-hole energies (in MeV) are as follows: $d_{3/2}$, 0.0; $s_{1/2}$, 0.45; $h_{11/2}$, 1.22; $d_{5/2}$, 1.52; and $g_{7/2}$, 2.12 for $^{143}$Sm; and $d_{3/2}$, 0.0; $s_{1/2}$, 0.43; $h_{11/2}$, 1.07; $d_{5/2}$, 1.47; and $g_{7/2}$, 2.20 for $^{141}$Nd. Data on the systematics of splitting and movement of these single-neutron-hole states as a function of the proton number $(Z)$ in $^{143}$Sm, $^{141}$Nd, $^{139}$Ce, and $^{137}$Ba shall be presented in a subsequent paper.

## I. INTRODUCTION

Nuclei with 82 neutrons are expected to have a closed-neutron-shell structure. There is some evidence for this from previous $(d, p)$ measurements[1-3] on targets with 82 neutrons. Another way of checking shell closure at $N = 82$ would be by looking for small occupation probabilities of supposedly vacant shell-model orbits ($2f$ and $3p$ in the present case) via neutron pickup reactions on $N = 82$ nuclei. If shell closure is found to be good in these nuclei, then one may hope that neutron pickup reactions will be a satisfactory means of obtaining information on the neutron-hole states in $N = 81$ nuclei. There have been some $(p, d)$,[4] $(d, t)$[5, 6] and decay-scheme studies[7-9] on isolated cases, but the information obtained is very limited and not backed by enough systematic data to determine reasonably accurate spins and parities and values of single-neutron-hole energies in the $N = 81$ mass region. The present work is the first in a series of measurements to provide such systematic data on the structure of neutron-hole states in $N = 81$ nuclei.

Since the protons are filling some of the same orbits as the neutrons, the present work also provides an opportunity for observing the effect on the binding energy of neutrons owing to the $n$-$p$ interaction between protons and neutrons in the same shell-model orbits. Furthermore, since the protons in these nuclei do not form a closed or semi-closed shell, they can contribute to some low-lying collective core excitations. Such excitations however do not occur below 1.5 MeV of excitation energy in these nuclei, so that one expects the low-lying states in the $N = 81$ nuclei to be dominantly

neutron-hole states. States at higher excitation energies however, may be expected to have appreciable core excitation components mixed in them, resulting in splitting of the single-neutron-hole states.

The following section describes the experimental arrangement used in the present work. Section III describes details of three types of distorted-wave Born-approximation (DWBA) calculations performed to determine the effect of various corrections on the shape and the magnitude of the predicted differential cross sections. In Sec. IV we present the experimental results, the computed values of single-hole energies and strengths, etc., followed by a discussion of these results.

## II. EXPERIMENTAL PROCEDURE

35-MeV protons from the Michigan State University variable energy cyclotron bombarded targets of $^{144}$Sm and $^{142}$Nd and the reaction products were analyzed in a cooled and radiation shielded $\Delta E$-$E$ counter telescope. The counter telescope was also equipped with magnets for electron suppression so that with a combination of the aforesaid features and a proper choice of amplifier time constants, an over-all energy resolution of ~35 keV was achieved. Particle selection was accomplished by displaying $\Delta E$ vs $E$ in a two-parameter analysis mode where the reaction products were sorted out by drawing polynomial fits around their respective curved bands using a data acquisition program TOOTSIE.[10]

The targets (see Table I for target data and $(p, d)$ ground-state $Q$ values[11]) were prepared in the cyclotron laboratory by evaporating isotopically enriched inorganic compounds from a graphite boat

# Proposed Michigan State University trans-uranic accelerator facility

H. Blosser, M. M. Gordon, and D. A. Johnson
*Cyclotron Laboratory, Michigan State University,*
*East Lansing, Michigan 48823, U.S.A.*

Presented by H. Blosser

## ABSTRACT

This paper briefly describes the design of a versatile facility for accelerating ions of every element to energies sufficient to produce nuclear reactions on any target. The design utilises a large six-sector ring cyclotron with ~40 kG m average bending capability for the main acceleration. The present MSU cyclotron would be the light ion (p, d, $^3$He, $^4$He) injector. A number of possible heavy ion injectors are discussed, the field trimming problem is reviewed and initial studies of resonance transitions are described.

## 1. INTRODUCTION

The possible existence of 'islands' of nuclear stability well beyond the region of presently known nuclei is a topic of great current interest to physicists and chemists.[1] The most likely production processes for such super-heavy nuclei appear to be transfer reactions between a massive projectile and a massive target, such as $^{238}$U($^{238}$U, $^{178}$Yb)$^{298}$114, etc. Due to the large coulomb repulsion, such a reaction will only take place at bombarding energies in the range of 6–9 MeV/nucleon which is well beyond the capability of present accelerators (assuming realistic values for the ion charge state). A number of groups are hence currently planning accelerators to produce the desired energetic ions—several of these are described in other papers at this session.

The major difference between the proposed MSU facility and those envisaged by other cyclotron groups is the much larger final stage cyclotron (40·7 kGm vs 29·4, 27·0, 26·5, etc.). This large final stage cyclotron can produce the required energy using ions in a much lower charge state (for Uranium 24+ is adequate vs 33, 36, 45, etc.). The costly heavy ion injector can therefore be smaller leading to a system which we believe to be less expensive in total and with a very elegant light ion capability as an important bonus (protons up to 600 MeV, deuterons to 360 MeV, etc.). The MSU plans also to give very serious consideration

50

# The cyclotron and the computer: a look at the present and the future*

R. A. de Forest
*Cyclotron Laboratory and Department of Physics, Michigan State University, Michigan, U.S.A.*

## ABSTRACT

This paper shows that current approaches to computer control are philosophically the same and that there is a second approach which the author hopes to see implemented in the future, since it offers advantages in both cost and flexibility. Some details of computer hardware and software are described because they are of importance to persons making long range decisions. At this time, without sophisticated systems of logging and analysis which future cyclotron control systems will have, it is not possible to forecast in detail the changes computer control will bring to beam quality; however, computer control will dictate more careful attention to the engineering details of beam defining and measuring devices.

## 1. FUNDAMENTAL CONTROL CRITERIA

Two basic and obvious principles have dictated all control systems whether computerised or not. (1) All important settings of cyclotron parameters must be available to the human operator at all times. (2) The operator must be able to alter those settings without introducing undesirable step changes.

These two criteria have been responsible for the complexities of current systems in which the computer is an appendage rather than an integral part of control systems. We cannot do away with these criteria, but we can alter the method of control to eliminate complexity and duplication of hardware.

## 2. GENERALISATION OF THREE BASIC CONCEPTS

It is important to note that initial setting up of an accelerator (before knob twiddling) is a digital process as far as the operator is concerned.

141

# Optimisation of the cyclotron central region for the nuclear physics user*

H. G. Blosser
*Michigan State University, Michigan, U.S.A.*

## ABSTRACT

Beam requirements for high quality nuclear physics experiments are reviewed along with features of central region arrangements for preferentially transmitting particles satisfying the requirements. With such a central region, phase widths of. $1.5°$ can be achieved and such phase widths in conjunction with good stabilising circuits lead to highly monochromatic beams. (External beam energy spread $0.04\%$ *FWHM* at MSU.) Such systems also give $100\%$ extraction efficiency and high transmission through external analysis systems. (Total transmission of $20\%$ at MSU for 1 in 6000 energy resolution and emittance of less than 1 mm mrad.)

## 1. INTRODUCTION

Modern nuclear physics is a science of detail in which significant experiments are concerned in almost every case with careful determination of the individual properties of particular nuclear quantum states. Such experiments require very monochromatic beams in order to separate close lying quantum states, with good collimation in order to precisely study spatial details of the states. Desired beam currents are generally modest—usually in the range 50–500 nA on target—the limitation on current coming in most cases from the data processing system. Frequently the nuclear characteristics of greatest interest are rare phenomena and the cleanness of the setup is of great importance in separating the desired results from background phenomena.

Relative to these nuclear physics requirements, the cyclotron in its normal condition is a very intense, rather imprecise beam source. This mismatch is generally corrected by means of a beam analysis system which transmits a precisely defined sub-section of the beam to the user. The remaining beam (typically 90–99% of the total) is stopped and in so doing intense radiation and residual acitivity are produced along with intense thermal heating, all of which lead to substantial problems. Moreover these problems are all in principle unnecessary—the external analysis system is selecting a certain volume in phase space which (as a result of the character of the equations of motion) must have

# The longitudinal space charge effect and energy resolution*

M. M. Gordon
*Michigan State University, Michigan, U.S.A.*

## 1. INTRODUCTION

In the design of isochronous cyclotrons with distinctly separated turns at extraction, calculations of energy resolution are customarily based solely on considerations of the beam phase width, the rf voltage and its resultant wave form.[1] Machines of this type have been proposed which aim at 100 $\mu$A currents with an energy resolution of $10^{-3}$ or better, and it appears quite likely that the hitherto neglected longitudinal space charge effect will determine the actual current or energy resolution achievable in such cyclotrons.[2] The longitudinal space charge effect was first discussed by T. A. Welton who explained how this effect tends to destroy turn separation by increasing the energy spread within a turn.[3] Welton also pointed out that this effect could be alleviated by accelerating the beam off the peak of the rf wave.[4] More recently, W. B. Powell carried out approximate calculations which indicate that the longitudinal space charge effect could nevertheless still be very serious.[5] The present paper summarises an extensive analysis of the longitudinal space charge effect and provides formulas for calculating the resultant energy spread within a turn under certain conditions.

The MSU cyclotron has been operating successfully in a separated turn mode with 100% extraction for the past three years and therefore constitutes a real prototype for the 'separated turn isochronous cyclotron'. Recently, the phase selection technique used in this machine has been refined so that proton beams up to 10 $\mu$A can be obtained with a phase width of 1·4° *(FWHM)*.[6] This narrow phase width implies an energy resolution of: $\Delta E/E = 10^{-4}$ attainable under operating conditions computed to minimise this quantity at extraction.[7] However, the dee voltage has so far been regulated only to: $\Delta V/V = (2 \text{ to } 6) \times 10^{-4}$, so that this parameter restricts the energy resolution achievable in the external beam. Experimental measurements of the longitudinal space charge effect have recently been carried out for the first time in any cyclotron. Although these results are still preliminary, they demonstrate conclusively that the properly minimised energy resolution increases with beam current. The explicit calculations presented here are aimed toward accounting for these observations.

305

# Cyclotron beam pulser for particle time-of-flight experiments*

W. P. Johnson
*University of Maryland, Maryland, U.S.A.*

H. G. Blosser and P. Sigg
*Michigan State University, Michigan, U.S.A.*

Presented by W. P. Johnson

## ABSTRACT

The energy resolution in time-of-flight experiments performed on a cyclotron is limited by the reaction product flight times of approximately 60 ns associated with the beam microstructure. A scheme for eliminating $N-1$ out of every $N$ micropulses from the external beam has been developed for the Michigan State University Cyclotron. The internal beam is stopped on a collimator on the first one-half turn by applying a d.c. voltage to a radially deflecting plate located in the dee between the ion source and collimator. A 60 ns wide pulse, synchronised with the dee voltage, but with $1/N^{th}$ the repetition rate cancels the d.c. deflection voltage allowing single micropulses through the collimator. Beam currents of 1 $\mu A$ time-average have been obtained with pulse widths of 0·4 ns at one-tenth the rf repetition rate. By removing a set of phase selecting slits inside the cyclotron, time-average currents of 10 $\mu A$ have been obtained at 10% duty cycle with pulse-widths of approximately 1·5 ns.

## 1. INTRODUCTION

Time-of-flight experiments require very short bursts of particles with long waiting periods between bursts. Cyclotrons produce such short beam pulses, but the repetition rates, typically of the order of 50–100 ns, are often too high. It is possible to eliminate some of the bursts by sweeping the beam across a collimator synchronously with the orbital frequency in such a manner that only one out of $N$ micropulses pass through the collimator and reach the experimenter's target. This can be done in two ways: by blocking the external beam or by stopping the beam near the ion source. The former has the great disadvantage that the beam thrown away activates whatever it hits and

# High resolution nuclear studies using cyclotron beams*

E. Kashy, G. F. Trentelman and R. K. Jolly
*Michigan State University, Michigan, U.S.A.*

Presented by E. Kashy

## ABSTRACT

Various types of nuclear experiments which require high resolution particle beams are described. Examples of the performance of the MSU Cyclotron in providing such beams are given. Proton beam currents of approximately 200 nA for $\Delta E/E = 1/6000$ resolution are easily obtained at $E_p \geq 25$ MeV with internal beam currents of only 3 $\mu$A. The role of dispersion matching is discussed and preliminary results using the laboratory broad range magnetic spectrograph are shown.

## 1. INTRODUCTION

The importance of high resolution beams and detection systems in the study of the nucleus has been apparent for many years, especially in nuclear spectroscopy, i.e. the classification of nuclear levels, their excitation energies, decay properties, spin, parity, etc. More recently high resolution beams have proved to be essential in certain aspects of the study of isobaric analogue levels. Up to now these studies have been the exclusive domain of electrostatic accelerators, mostly the Van de Graaff type, which have in many ways the most desirable beam properties. In this paper it is shown that cyclotrons like the MSU sector focused cyclotron when used with a highly dispersive beam analyser such as the one presently in use in the MSU Cyclotron Laboratory[1] can compete successfully in a field previously reserved to electrostatic machines, and in some instances improve upon such machines.

## 2. TYPES OF EXPERIMENT

We can divide the high resolution experiments into two broad types: (a) where energy resolution is required on target and (b) where energy resolution of reaction products is desired. An example of the first requirement is the reaction:

380

# THE ISOBARIC MASS EQUATION IN $A = 4n+1$ NUCLEI

N. AUERBACH and A. LEV

*Department of Physics and Astronomy, Tel-Aviv University, Tel-Aviv, Israel*

and

E. KASHY *

*The Niels Bohr Institute, University of Copenhagen, Copenhagen, Denmark*

The parameters of the isobaric mass equation are calculated for the $T=3/2$ multiplets in $A=4n+1$ nuclei, for $n=2$ to $n=10$.

In first order perturbation theory the masses of an isobaric multiplet with isospin $T$ are given by an equation quadratic in $T_z$ [1,2,3]

$$M(\alpha, T, T_z) = a(\alpha, T) + b(\alpha, T)T_z + c(\alpha, T)T_z^2 \qquad (1)$$

where $\alpha$ includes all charge independent quantities.

The difference in the masses of the lowest two members of the multiplet gives the so-called Coulomb displacement energy $-E_d$.

$$E_d = -(b(\alpha, T) - c(\alpha, T)) \times (N-Z-1) + \Delta_{np} \qquad (2)$$

where $N$ and $Z$ are the number of protons and neutrons in the lowest member of the multiplet, and $\Delta_{np}$ is the neutron proton mass difference.

A great deal of effort has been put into measuring Coulomb displacement energies from Isobaric Analog Resonance experiments. The main contribution to $E_d$ is linear in the excess neutron distribution [4,5] $\rho^{exc}(r) = \rho^n(r) - \rho^p(r)$ and therefore $E_d$ is a source of information concerning neutron density distribution in nuclei. However, the investigation of the excess neutron distributions in medium and heavy mass nuclei via Coulomb displacement energies is hampered by the fact that only the energy of the first two members of the multiplet is determined. So far no experiment has been performed which located a third member of an isomultiplet in nuclei with $A > 40$.

In light mass nuclei ($A < 40$) several high precision experiments have been performed in which more than two members of a multiplet

* John Simon Guggenheim Fellow. On leave from: Department of Physics, Michigan State University East Lansing, Michigan.

were found [3,6]. In particular, all four members of several $T = 3/2$ multiplets have been observed and their masses measures [3,6-11]. One of the important results of these experiments is that the mass equation (1) is very well obeyed and terms proportional to $T_z^3$ are smaller than experimental uncertainties [8,10]. Only the $A=9$ quartet shows deviations from eq.(1) greater than the experimental uncertainties, and there the coefficient of the $T_z^3$ term is very small, only $8.0 \pm 3.7$ keV [9].

Another consequence of measuring the masses of the entire $T = 3/2$ multiplet is the determination of the parameter $c$. In addition to $b$ (or $E_d$) we have now to our disposal a second parameter which can be used to study density distributions in nuclei. For example, one may ask the question whether it is possible to reproduce the values of both $b$ (or $E_d$) and $c$ using the same set of wave functions for nucleons outside an $N = Z$ core.

In the present work an attempt is made to calculate $b$ and $c$ using for both the same set of wave functions. We consider the $T = 3/2$ multiplets in nuclei with mass $A = 4n+1$, for $n=2$ to 10. The masses of the four members of the quartets for $A=9$, 13,17,21,25 and 37 have been measured [3,6-11]; and the parameters $a$, $b$ and $c$ determined. In table 1 the experimental results for $b$ and $c$ are summarised. For $A=29,33$ and 41 only the displacement energies are known experimentally [6,12].

The calculation of the displacement energies is performed using the methods outlined in ref. [5]. The main contribution to $E_d$ is the so-called direct term [4,5] given by:

# Calculations with a 1s,0d Shell Model for $A$ = 34–38 Nuclei*

B. H. Wildenthal

*Michigan State University, East Lansing, Michigan 48823
and Oak Ridge National Laboratory, Oak Ridge, Tennessee 37830*

and

E. C. Halbert and J. B. McGrory

*Oak Ridge National Laboratory, Oak Ridge, Tennessee 37830*

and

T. T. S. Kuo

*Oak Ridge National Laboratory, Oak Ridge, Tennessee 37830
and State University of New York, Stony Brook, New York 11790*

Results are presented of calculations made in the full space of 1-shell-model wave functions for positive-parity states in the nuclei with $A$ = 34–38. We employed in this work several different effective Hamiltonians, some of which had two-body parts obtained by reaction-matrix techniques from the Hamada-Johnston scattering potential. The observables calculated were energy-level spectra, single-nucleon spectroscopic factors, and $E2$ and $M1$ moments and transition strengths. These calculations yield fair-to-good agreement with many of the observed nuclear-structure data in this mass region.

## I. INTRODUCTION

This paper presents the results of shell-model calculations for positive-parity states of nuclei with mass numbers $A$ = 34 through 38. The model vector space is defined by a complete set of many-particle basis states for $A - 16$ nucleons distributed among the three single-particle orbits $0d_{5/2}$, $1s_{1/2}$, and $0d_{3/2}$. The model core is $(0s)^4(0p)^{12}$. The two-body parts of most of the Hamiltonians which we use in this space are derived by reaction-matrix techniques[1] from the Hamada-Johnston nucleon-nucleon scattering potential.[2] Following the current terminology, we shall refer to such Hamiltonians as "realistic."

One purpose of our work was to test how well the experimentally determined properties of $A$ = 34–38 nuclei could be reproduced by using currently available realistic interactions. Our present $A$ = 34–38 study is the natural extension of a similar study made earlier for $A$ = 18–22.[3,4] As tests of a realistic interaction, the $A$ = 18–22 and $A$ = 34–38 projects differ in that they emphasize different aspects of the interaction. For $A$ = 18–22, the model nuclear wave functions tend to be dominated by components in which all active nucleons occupy the $0d_{5/2}$ and $1s_{1/2}$ orbits. Thus for $A$ = 18–22, the one- and two-body matrix elements of the effective Hamiltonian which are most important (and most severely tested) are those involving only the $0d_{5/2}$ and $1s_{1/2}$ orbits, while matrix elements involving only the $0d_{3/2}$ orbit are less important. But in the $A$ = 34–38 region, where the $0d_{5/2}$ orbit is "effectively" filled for most low-lying states, matrix elements which involve the $0d_{3/2}$ and $1s_{1/2}$ orbits are the most important. Thus, studies of the $A$ = 18–22 and $A$ = 34–38 regions complement each other as tests of realistic interactions designed for use in $(1s, 0d)^{4-16}$ shell-model calculations.

Techniques for calculating realistic shell-model effective interactions are far from perfect[5,6]; but they have improved since the time we calculated realistic interactions for this $A$ = 34–38 study, and presumably they will be improved further in the future. We realized at the start of this project that there would be uncertainties and imperfections in any particular realistic Hamiltonian that we could obtain, and for that reason we decided to examine the shell-model results from several alternative Hamiltonians. We have used four different realistic effective interactions, calculated in four slightly different ways, and with each of these realistic interactions we have tried two alternative sets of single-particle energies. In addition, we have used some two-body interactions of a considerably different character, i.e., interactions derived from considerations other than nucleon-nucleon scattering data. All in all, we have calculated shell-model results from 10 different $(1+2)$-body effective Hamiltonians.

In this paper we shall compare these alternative sets of shell-model results with each other and with experimental data. These comparisons offer some information about the probable characteris-

# Neutron-Hole-State Structure in $N = 81$ Nuclei. II. $^{140}$Ce and $^{138}$Ba$(p, d)$[†]

R. K. Jolly and E. Kashy

*Cyclotron Laboratory, Michigan State University, East Lansing, Michigan 48823*

(Received 5 May 1971)

In continuation of our program of neutron-hole-state studies in $N = 81$ nuclei, angular distributions of deuterons from $(p, d)$ reactions (energy resolution ~35 keV) on $^{140}$Ce and $^{138}$Ba at $E_p = 35$ MeV have been measured and compared with distorted-wave Born-approximation calculations including finite-range and nonlocality corrections. These calculations yield acceptable spectroscopic factors and are in fair agreement with the shapes of the experimental angular distributions. The neutron-single-hole energies have been determined. These energies (in MeV) are $d_{3/2}$, 0.0; $s_{1/2}$, 0.33; $h_{11/2}$, 1.07; $d_{5/2}$, 1.72; and $g_{7/2}$, 2.90 for $^{139}$Ce; and $d_{3/2}$, 0.0; $s_{1/2}$, 0.54; $h_{11/2}$, 1.07; $d_{5/2}$, 1.71; and $g_{7/2}$, 2.93 for $^{137}$Ba.

Considerable fractionation of the $(2d_{5/2})_\nu^{-1}$ and the $(1g_{7/2})_\nu^{-1}$ states is observed while the $(1h_{11/2})_\nu^{-1}$ and the $(3s_{1/2})_\nu^{-1}$ states are each observed to split mostly into two components. Systematics of the energies and strengths of the various neutron-single-hole states and their components are presented for all $N = 81$ nuclei from $^{137}$Ba through $^{143}$Sm and the significance of the systematics discussed. No measurable population of any neutron state in the $82 < N \leq 126$ major shell has been observed.

## I. INTRODUCTION

In a previous paper[1] (henceforth referred to as Paper I) we reported our results on the analysis of $(p, d)$ measurements on the $N = 82$ nuclei of $^{144}$Sm

and $^{142}$Nd[1] together with a study of the effects of different values of lower cutoff, finite-range and nonlocality (FRNL) corrections, and density dependence of the effective $pn$ interaction on the shapes and magnitudes of distorted-wave Born-approxima-

# THE STRUCTURE OF THE LIGHTER $N = 82$ NUCLEI[*]

B. H. WILDENTHAL and Duane LARSON

*Cyclotron Laboratory and Physics Department,*
*Michigan State University, East Lansing, Michigan 48823, USA*

Shell-model predictions for nuclei which can be characterized as 1, 2 and 3 protons outside the doubly-magic $N = 82$, $Z = 50$ core give a good accounting for recently discovered features of $^{133}$Sb, $^{134}$Te and $^{135}$I.

Recent advances in experimental techniques have made possible the quantitative study of the lighter-mass nuclei having 82 neutrons [1-4]. Spectra have been obtained for $^{133}$Sb, $^{134}$Te and $^{135}$I; these nuclei correspond respectively to one, two and three protons outside the $Z = 50$, $N = 82$ doubly-magic $^{132}$Sn core. The properties of these systems are interesting because their presumed simplicity should permit a relatively unambiguous delineation of the various facets involved in nuclear structure phenomena. The nuclei around $^{208}$Pb have been extensively studied in this same spirit in order to extract such quantities as effective charges and effective $g$-factors. Next to the $^{208}$Pb neighborhood, the $N = 82$ region may well exhibit the best "closed shell" behavior available to us. In addition, the $N = 82$ region provides what the lead region does not, namely a long string of nuclei (14 have been studied at present) built by adding protons to the doubly-magic core. Thus for $N = 82$ we will have the opportunity to pursue the consequences of our deductions based on the simple, "few" nucleon systems through a series of "many" nucleon systems.

Actually, of course, because of the accidents of nuclear stability, the situation has been reversed in the $N = 82$ region. The naturally stable, many-proton, systems have been extensively investigated, both experimentally and theoretically, for some time, while the few-proton nuclei have just begun to be studied. In this note we present theoretical predictions for the structure of the $Z = (50 + 1, 2, 3$ and $4)$, $N = 82$ nuclei and compare these results to the presently available experimental data.

Our predictions for $^{133}$Sb, $^{134}$Te and $^{135}$I are based on previous shell-model calculations for heavier $N = 82$ nuclei [5]. These calculations employed an MSDI residual interaction [6,7] and a model space comprised of all $0g_{7/2} - 1d_{5/2}$ configurations plus all configurations formed by exciting one particle from the $0g_{7/2} - 1d_{5/2}$ subspace to either a $2s_{1/2}$ or $1d_{3/2}$ orbit. In our initial work [5] we chose values for the SDI strength and for the single-particle-energy (SPE) splittings which optimized agreement between model and experimental excitation energies for all known positive-parity $N = 82$ states in $A = 136 - 146$ inclusive. Subsequently, because the model space is most appropriate for the lighter $N = 82$ nuclei, we readjusted the SDI strength and the SPE splittings to optimize agreement only for $A = 136 - 140$. The significant change which results from the new approach is an increase, from 0.48 MeV to 0.88 MeV, of the $0g_{7/2} - 1d_{5/2}$ SPE splitting. (In all of this work we have employed the shell model computer codes described by French, Halbert, McGrory and Wong [8]).
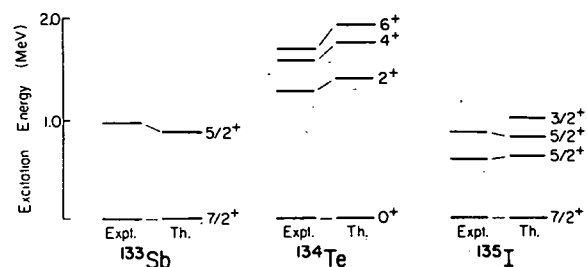


Fig. 1. Calculated and experimentally inferred spectra of the nuclei $^{133}$Sb, $^{134}$Te and $^{135}$I.

266

# Structure of Nuclei with Masses $A$ = 30–35, as Calculated in the Shell Model

B. H. Wildenthal

*Department of Physics and Cyclotron Laboratory,\* Michigan State University, East Lansing, Michigan 48823*

and

J. B. McGrory and E. C. Halbert

*Oak Ridge National Laboratory,† Oak Ridge, Tennessee 37830*

and

H. D. Graber

*Cornell College, Mt. Vernon, Iowa 52314*

(Received 19 May 1971)

Properties of positive-parity states of nuclei with $A$ = 30–35 have been calculated in a shell-model space which encompasses all Pauli-allowed basis vectors of all configurations $(0s)^4(0p)^{12}(0d_{5/2})^{n_1}(1s_{1/2})^{n_2}(0d_{3/2})^{n_3}$ for which $n_1 \geq 10$. Two different empirical Hamiltonians, one of a $\delta$-function form, were used. Calculated energies and spectroscopic factors are in good agreement with an extensive body of experimental data. The model wave functions also yield satisfactory agreement with many available experimental data on electric quadrupole observables if effective charges of $0.5e$ are added to the proton and neutron. The model predictions for magnetic dipole observables are generally in qualitative agreement with experimental observations, but inconsistencies between theory and experiment are more noticeable in this area.

## I. INTRODUCTION

This paper describes the results of a series of shell-model calculations which have been carried out in an attempt to understand the structure of energy levels in nuclei of $A$ = 30–35. The properties of these nuclei present an attractive challenge to theoretical interpretation in that experimental information[1] about spins and parities of observed levels in this mass region is extensive and there are also many data on lifetimes, spectroscopic factors, and the like. Thus, any theory for these nuclei can be critically examined with unusual thoroughness.

Despite all this experimental activity, there have been relatively few theoretical investigations of these nuclei. This probably results from the fact that experimental phenomena typical of the region do not readily yield to analysis by the simplest forms of any of the popular models for describing nuclear structure. The level structures of $A$ = 30–35 do not exhibit obvious rotational features to the extent found, for example, in $A$ = 20–25. Thus, the most straightforward Nilsson-type calculations for nuclei with $A \geq 30$ are not as successful as for the lighter nuclei of the $sd$ shell.[2] However, more involved calculations of this kind have successfully accounted for some properties of individual nuclei.[3] Similarly the simplest kind of weak-coupling vibrational calculation meets with little success in this region,[4] although recent, more

sophisticated intermediate-coupling calculations[5] appear promising.

A detailed shell-model calculation of the structure of these nuclei was first made by Glaudemans and his co-workers[6] in a study which assumed an inert $^{28}$Si core and active $1s_{1/2}$ and $0d_{3/2}$ orbits. They treated all nuclei from $A$ = 29–40, but the results obtained for the lighter nuclei were obviously impaired in some respects by the omission of an active $d_{5/2}$ orbit. This region was also studied via shell-model methods as part of a general survey of the $sd$ shell by Bouten, Elliot, and Pullen.[7] By making simplifying assumptions about the Hamiltonians and the wave functions, they were able to include effects of some excitations out of the $d_{5/2}$ orbit. However, they presented and discussed only energy-level spectra.

The results of previous calculations, and examination of the experimental data, strongly suggest that any conventional shell-model calculation for the $A$ = 30–35 region should allow some excitation out of the $d_{5/2}$ orbit. As we shall discuss further below, there are no obvious indications from experiment that the orbits of the $0f$-$1p$ shell are necessary for an adequate description of the properties of the low-lying positive-parity states in the $A$ = 30–35 region. We have accordingly studied the properties of these nuclei by means of a conventional shell-model calculation in a vector space which includes basis states with particles in the $d_{5/2}$, $s_{1/2}$, and $d_{3/2}$ orbits. We shall show that a

# PREPARATION OF THIN FILM DEPOSITS FROM BIOLOGICAL, ENVIRONMENTAL AND OTHER MATTER*

R. K. JOLLY and H. B. WHITE, Jr.

*Cyclotron Laboratory, Michigan State University, East Lansing, Michigan 48823, U.S.A.*

A technique for preparing uniform thin film deposits (10–1000 $\mu g/cm^2$) of practically all materials of biological, environmental and nuclear physics interest is proposed. The technique involves preparing a solution or colloidal suspension of micron size particles of the substance of interest, generating a nebulized (practically invisible) mist from this liquid and condensing the mist on a rotating substrate. The cost in time and money for several materials is minimal.

## 1. Introduction

In the elemental analysis of materials employing nuclear reaction and scattering techniques[1-3], it is necessary to prepare the sample in the form of a thin film (10–1000 $\mu g/cm^2$). For metallic samples and some of their inorganic compounds the technique of vacuum evaporation is commonly employed. However, for biological and environmental samples a new technique is needed. In the section below we describe a technique that enables one to prepare thin film deposits from such diverse materials as mineral and rock samples, animal tissue, blood and soluble salts using relatively inexpensive equipment. In certain materials like a whole fish, the uniformity of the deposit depends on the uniformity and size of the particles in the colloidal suspension that is prepared.

## 2. Preparation and deposition

Any material to be deposited must be first reduced to a solution or a suspension of microscopic particles ($\approx 1$–$10\,\mu m$) in an inert solvent (pure water is best for most materials). Table 1 gives a listing of the techniques used by the authors towards accomplishing this objective. The suspended or the dissolved material is placed in the container shown in the apparatus, called a nebulizer[5], in fig. 1. The compressed gas (preferably inert) forces the liquid through a small hole (at the top of the tube partially immersed in the liquid) in the form of a high-speed spray which in turn impinges on an obstruction and thus breaks up into droplets of various sizes. The finest of these droplets are swept along by the gas escaping out of the nozzle. These droplets are so fine that they are not visible to the unaided eye. Illuminating the mouth of the nozzle reveals a cloudy mist (hence the name nebulizer) but the individual

* Supported by the National Science Foundation.

droplets are still not seen. The nebulized mist is then allowed to deposit on a rotating substrate. By mounting the nebulizer bottle on a stand that performs a slow up and down (or sideways) oscillatory motion such that all parts of the substrate receive the mist for the same length of time, a very uniform deposit can be obtained. The microscopic size of these droplets is crucial to the success of this method in obtaining a thin uniform

TABLE 1
Reduction of biological, environmental and other matter to a solution or colloidal suspension.

| Class of materials | Technique for reduction |
|---|---|
| 1. Animal tissue, plants, etc. | Slow freezing to rupture the cells followed by 1) reduction to a liquidized form by a high-speed blender (e.g. Waring Scientific Blender, 15 000 rpm model), and 2) immersion of an ultrasonic probe in the liquidized sample for several minutes (length depending on the quantity and type of material). |
| 2. Blood, milk, etc. | Sonication with an ultrasonic probe if necessary to break up the individual cells (25–50 $\mu m$). In some applications (proton scattering, X-ray fluorescence) these substances may be deposited without any sonication. |
| 3. Rock, dry wood, etc. | Grinding in a tungsten carbide mortar and pestle or a micronising mill[4] and subjecting a paste of the material to sonication (with an ultrasonic source) if necessary. |
| 4. Beverages and soluble materials, etc. | May be simply dissolved or diluted in pure water before deposition. |

# SPREADING OF THE GIANT DIPOLE: A SIMPLE ESTIMATE*

G. F. BERTSCH

*Department of Physics, Michigan State University, East Lansing, Mich. 48823, USA*

The spreading width of the nuclear giant dipole state is related to the damping width of single-particle states, using the long-wavelength approximation. We find $\Gamma_{\text{dipole}} = \frac{4}{9}\Gamma_{\text{single-particle}}$.

One of the interesting parameters of the nuclear giant dipole resonance is the width of the state. In heavy nuclei, the width is due primarily to the mixing of the state with other configurations; particle and gamma decay widths are relatively small. Estimates of the spreading width have generally involved complicated microscopic calculations [1]. These yield detailed strength functions, but do not indicate the qualitative trends or give a gross description of the spreading.

Since the dipole state is well described by a particle-hole wavefunction, why is not the width given by the single-particle spreading widths of the particle and the hole? The answer is that there is a coherence between particle and hole which reduces the off-diagonal matrix elements responsible for the spreading.

This is a well-known phenomenon in the theory of the electron gas, occurring in the theory of the plasmon excitation [2]. The plasmon is a collective particle-hole excitation which can decay by two mechanisms:

(1) If some uncorrelated particle-hole states are degenerate with the plasmon, it will spread into these (Landau damping).

(2) The state can always decay into 2p-2h states, but the probability is proportional to the square of the momentum carried by the plasmon [3]. In the long wavelength limit, particle and hole contribute an equal and opposite amplitude to the decay to any given 2p-2h state.

We will estimate the spreading of the nuclear giant dipole state into 2p-2h states in the corresponding limit. The assumption of a long wavelength for the dipole excitation implies that there will be a perfect correlation between particle and

hole matrix elements. The accuracy of this is to order $(a/R)^2$, where $a$ is the range of the effective interaction and $R$ is the size of the nucleus. Because of the differing isospin structure of the particle and hole matrix elements, there will be some decay into 2p-2h states even in the long wavelength limit. We also need to assume that the excitation energy of the giant dipole is large compared to single-particle energies, in order to neglect phase-space considerations in the intermediate states. We also neglect the spreading due to the single-particle structure. This has been shown to play a large role in light nuclei [4] and in deformed nuclei [5], but does not seem to be important in heavy spherical nuclei.

We first derive an expression for the damping of a single-particle state, then derive the corresponding expression for the damping of the correlated particle-hole state. Taking the ratio of the two dampings, all the details of the nuclear structure will cancel out. The principle assumption in calculating the single-particle spreading is that it damps by creating $S = 0$, $T = 0$ particle-hole pairs. Only for these quantum numbers is the energy of the particle-hole state low enough to give a high density of 2p-1h states degenerate with the single-particle state. The matrix element connecting these states is

$$\langle p \,|\, V \,|\, p(ph^{-1})^{S=0}_{T=0} \rangle =$$

$$= \sum_{s,t} \sqrt{\frac{2s+1}{2}} \sqrt{\frac{2t+1}{2}} \, U(\tfrac{1}{2}\tfrac{1}{2}\tfrac{1}{2}\tfrac{1}{2};s\,0) \, U(\tfrac{1}{2}\tfrac{1}{2}\tfrac{1}{2}\tfrac{1}{2};t\,0) \, V_{st}$$

$$= \tfrac{1}{8}(V_{00}+3V_{10}+3V_{01}+9V_{11}) \tag{1}$$

where $V_{st}$ labels the spin and isospin quantum numbers of the interaction in particle-particle coupling. The giant dipole state we treat as a $T = 1$, $S = 0$ particle-hole excitation. The 2p-2h states important for damping would thus have a

# Shapes of Angular Distributions in the Reaction $^{89}$Y($^{3}$He,$t$)$^{89}$Zr to Antianalog and Other $T_<$ States*

R. A. Hinrichs and G. F. Trentelman†

*Cyclotron Laboratory, Michigan State University, East Lansing, Michigan 48823*

(Received 24 June 1971; revised manuscript received 10 September 1971)

The reaction $^{89}$Y($^{3}$He,$t$)$^{89}$Zr to $T_<$ states in $^{89}$Zr shows that the angular distributions have shapes characteristic of nonallowed $L$ transfers and are in disagreement with microscopic predictions. The antianalog states appear not to be unique in possessing this feature.

## I. INTRODUCTION

The ($^{3}$He, $t$) charge-exchange reaction has served in recent years as a useful spectroscopic tool in determining the spins and parities of states in many odd-odd nuclei. Since angular distributions with transitions to states of the same $J^\pi$ seemed to be nearly identical,[1] values of $J^\pi$ in the residual nucleus were assigned by comparing the shapes of the experimental angular distributions with those of transitions to known states. Also, distorted-wave Born-approximation (DWBA) calculations, with the inclusion of a tensor term[2] in the effective interaction to account for transitions to unnatural-parity states, have appeared to be quite successful in fitting the data. This agreement between calculations and data has also been obtained in cases where there is a difference in the angular-distribution shapes for transitions to different states having the same spin and parity within the same nucleus.[3] Recently, however, ambiguities have been noted[4] in ($^{3}$He, $t$) reactions with the observation that angular distributions for $0^+$ to $0^+$ transitions to antianalog states in $^{40}$K and $^{64,66}$Ga were not fitted by the calculated $L=0$ angular momentum transfer shape as expected, but by $L=1$. Transitions to $0^+$ isobaric analog states in these nuclei, however, were well fitted by an $L=0$ shape. Recent examinations of other charge-exchange results[5] for transitions to $T_<$ states (states with iso-

CORE POLARIZATION EFFECTS IN (p,p') REACTIONS*

H. McManus

Michigan State University, East Lansing, Michigan

Let me remark first of all that, regardless of the status of its theoretical description at any moment, core polarization is a well established experimental phenomenon, or rather is well established in the interpretation of experimental phenomena in terms of a microscopic model, i.e. the shell model, in an extended version or otherwise. A typical example is the interpretation of electromagnetic transitions, in terms of effective charge. The effective charge is the bare charge of a nucleon, +1 for a proton, 0 for a neutron, plus the polarization charge. Typically for an E2 transition, as the shell model basis becomes larger, and the calculation increases in complexity, the polarization charge needed to fit experiment decreases but usually more and more slowly, until when the limits of present computing are reached, it still remains at ~0.5e. Figure 1 shows such an example taken from calculations in the s-d shell.[1]

Here the polarization charge $\Delta e$ required to match experimentally observed E2 transitions in $^{33}S$ is shown as a function of the average number of basis states, N, in the wave functions corresponding to three models III, II and I in which the shell model basis is successively enlarged (A). Figures B and C show the same effect in a different representation. Curve 1 plots the polarization charge $\Delta e$ versus neglect of components in the wave function with amplitudes less than x and curve 3 plots the average number of configurations corresponding to this neglect. It is seen that with only a few basis states, with a corresponding neglect of components with amplitudes less than 0.1, the polarization charge is ~1-1.2. Increasing the number of basis states to ~100 brings down the polarization charge required to 0.4, with the corresponding inclusion of a large number of amplitudes of the order ~1%.

265

THE EFFECTIVE TWO-NUCLEON INTERACTION FROM INELASTIC PROTON

SCATTERING*

Sam M. Austin

Michigan State University

Since inelastic scattering cross-sections depend on a nuclear matrix element containing both the wave functions of the nuclear states involved and the effective interaction $V_{eff}$ between the projectile and the target nucleons,[1] it is necessary to have an a priori value for $V_{eff}$ before one can use inelastic scattering as a tool for nuclear spectroscopy. An approach to determining $V_{eff}$ which I will explore in detail in this paper, is entirely empirical in nature. One examines transitions where the wave functions are well known and adjusts the strength of the two-body interaction to fit the observed cross-sections. If the results for a representative sample of cases are consistent one has obtained a workable interaction for spectroscopic studies.

This approach was tried by Satchler[2] in his early studies of inelastic scattering, but was unsuccessful for reasons which we now understand fairly well. The major difficulty was that the states involved were collective in nature so that the cross sections were greatly enhanced. On the other hand, only simple wave functions were used in the theoretical calculations, so single-particle-size cross sections were predicted, and when the two-body potential was adjusted to fit the measured cross sections, the resulting potential was unphysically large. Since the collective enhancement depends on the nucleus, the state involved, and the angular-momentum transfer (L) of the transition, the effective interaction obtained was also nucleus, state and L dependent. In addition the calculations neglected exchange contributions which depend on L and the bombarding energy,[1] and again the empirical $V_{eff}$ mirrored this dependence. For these reasons it was not possible to find a consistent effective-interaction for the strong, spin independent part of the force. Studies[2-9] of L=0 transitions involving spin-flip or isospin-flip were more successful

285

131

# PERTURBATIVE TREATMENT OF COLLECTIVE
# PARTICLE-HOLE STATES IN $^{40}$Ca AND $^{48}$Ca *

## M. DWORZECKA and H. McMANUS

*Cyclotron Laboratory, Michigan State University, East Lansing, Michigan 48823, USA*

The effects of ground state correlations and core polarization have been included in the effective particle-hole interaction and transition moments by second order perturbation theory. Energy levels and transition probabilities of 3⁻ collective states in $^{40}$Ca and $^{48}$Ca were calculated in Tamn-Dancoff approximation and compared with the results obtained by using the random phase approximation.

Considerable success has been achieved by Gillet et al. [1] in describing negative parity collective excitations in closed shell nuclei by means of a simple particle-hole model with ground state correlations taken into account via the RPA. The ground state correlations so treated consist of multiple excitations within the single particle and hole configurations originally picked for the description of the state (model space), and give, compared with the TDA calculations in the original model space, a large energy shift and an increase in collectivity as measured, for instance, by the BE3 of a 3⁻ state. However, the calculations used a force whose parameters were fixed by comparing calculations with experiment. On the other hand, if one wants to use a realistic force, then other types of correlation have to be taken into account, i.e. core polarization. The effect of core polarization has been found to be very important [2-4] for the particle-particle nuclear effective interaction. Kuo [5] did similar calculations for the particle-hole case using RPA and including core-polarization by perturbation. The results of the calculations were very sensitive to the way the core-polarization effects were taken into account, though some of the variations were due to an incorrect choice of backward
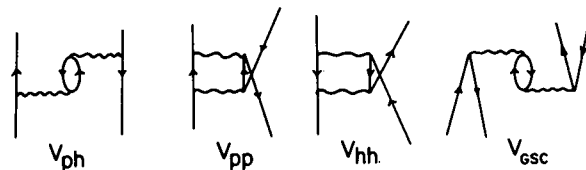
fig.2.

going graphs in RPA. Similar calculations have been done by Dieperink [6]. This method treats one type of correlation - core polarization, by perturbation theory, and another - ground state correlations, by a different approximation, the RPA.

The present calculation compares the results of treating both effects perturbatively with the results of RPA, taking the collective 3⁻ states at $^{40}$Ca and $^{48}$Ca as an example. In perturbation theory both the effective interaction and effective transition operator have to be calculated. The effective interaction is calculated from the diagrams of fig. 2. $V$ is the bare force, in this case Sussex matrix elements [7], $V_{2p-2h} = V_{ph} + V_{pp} + V_{hh}$ the lowest order core polarization contributions involving energy dominators $2\hbar\omega$. $V_{GSC}$ gives the effect on the interaction of ground state correlations via 3p-3h intermediate
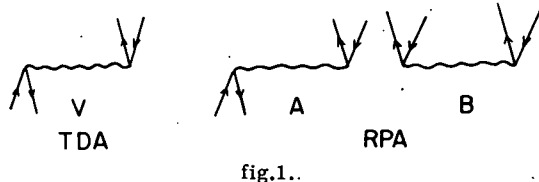


fig.1.
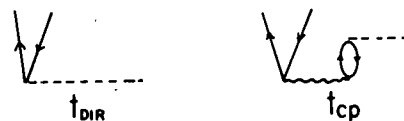


fig.3.

# CALCULATION OF THE $^{12}$C+$\alpha$ CAPTURE CROSS SECTION AT STELLAR ENERGIES*

### By F. C. Barker†

*Abstract*

The $^{12}$C$(\alpha, \gamma)^{16}$O cross section is calculated at stellar energies, using $R$-matrix parameters obtained by fitting consistently the $^{12}$C+$\alpha$ scattering phase shifts and the $\alpha$-spectrum from $^{16}$N $\beta$-decay. This limits the $^{12}$C+$\alpha$ channel radius to the range 5–7 fm. The $S$-factor at $E_\alpha = 400$ keV is calculated to lie in the range 0·05–0·33 MeV.b.

## I. INTRODUCTION

The cross section of the $^{12}$C$(\alpha, \gamma)^{16}$O reaction at $\alpha$-particle energies of the order of a few hundred keV is of interest for theories of nucleosynthesis in stars. Direct experimental measurement of the cross section is not feasible below a few MeV, so that an indirect determination is necessary. The assumption usually made is that the main contributions are from the known 1$^-$ levels of $^{16}$O at 7·12 MeV (46 keV below the $^{12}$C+$\alpha$ threshold) and 9·59 MeV, and the greatest uncertainty comes from the value of the $\alpha$-particle dimensionless reduced width $\theta_\alpha^2$ of the 7·12 MeV level.

Previous estimates of $\theta_\alpha^2$ have differed widely. A theoretical estimate by Stephenson (1966) based on models for the 1$^-$ and 3$^-$ levels of $^{16}$O gave $\theta_\alpha^2 = 0·08\pm0·04$.‡ Experimental estimates have been made by various methods:

(1) Stripping reactions. From the $^6$Li$(^{12}$C, d$)^{16}$O reaction Loebenstein *et al.* (1967) obtained $\theta_\alpha^2 = 0·06$–0·14,‡ while from $^{12}$C$(^7$Li, t$)^{16}$O, Pühlhofer *et al.* (1970) gave $\theta_\alpha^2 = 0·025$‡ with the suggestion that this may be too low by a factor of 1·5 or 2. Dolinsky, Turovtsev, and Yarmukhamedov (1970) have pointed out some difficulties in obtaining reliable estimates in this way.

(2) Analysis of the $^{12}$C+$\alpha$ elastic scattering p-wave phase shift. With the energy dependence of the phase shift represented by a many-level $R$-matrix formalism, Clark (1969) obtained $\theta_\alpha^2 = 0·71^{+0·37}_{-0·18}$, while a Caltech group (Weisser, Morgan, and Thompson 1970) found for $\theta_\alpha^2$ a very small value (Thompson, personal communication) with a large uncertainty. This is because $\theta_\alpha^2$ is involved in both the incoming and outgoing channels so that the 7·12 MeV level contributes little to the phase shift.

# THE PICKUP-STRIPPING MECHANISM FOR
## INELASTIC AND QUASI-INELASTIC SCATTERING

R. SCHAEFFER [‡]

*Service de Physique Théorique, Centre d'Etudes Nucléaires de Saclay, 91 Gif-sur-Yvette, France*

and

G. F. BERTSCH

*Cyclotron Laboratory, Michigan State University, East Lansing, Michigan 48823, USA*

The (h, t) reaction can be dominated by the formation of an intermediate alpha-particle cluster. This process accounts for the relatively large cross sections for high spin transfer and the $L = 1$ shape of some $0^+ \to 0^+$ transitions.

The general assumption for the (h, t) reaction mechanism is that the reaction proceeds through the charge-exchange part of the two-body nucleon-nucleon interaction [1]. However, serious discrepancies [2,3] have been seen when comparing the predictions of this model with experiment. The calculated [2] cross sections are too weak by factors from 2 to 500, the difference increasing almost exponentially with increasing spin transfer. The most striking discrepancy is the breakdown of commonly accepted selection rules for inelastic or quasi-inelastic scattering: Hinrichs et al. [3] observed an $L = 1$ shape instead of $L = 0$ for some $0^+ \to 0^+$ transitions to antianalogue states.

As proposed earlier [4] these reactions should be described by an additional mechanism which is the pickup of a particle, forming an intermediate alpha cluster, followed by stripping. In second order perturbation theory, the corresponding transition matrix is:

$$T^{(2)} = \frac{1}{(2\pi)^3} \int dk \quad \sum_n \langle t^{(-)} A^* | V | \alpha (A-1)_n \rangle$$
$$\times \frac{1}{E - E_n^{A-1} - E_\alpha + i\epsilon} \langle \alpha (A-1)_n | V | h^{(+)} A \rangle \quad (1)$$

where $A$ and $(A-1)_n$ denote the nuclear states with $A$ and $A-1$ particles, and t, h, and $\alpha$ de-

note the internal and optical wavefunctions of the projectile. If in addition we assume that all the states $(A-1)_n$ containing large components of a hole in the $j$-shell coupled to $A$ have about the same energy $E_n^{A-1}$, $T^{(2)}$ becomes:

$$T^{(2)} = D_0^2 \sum_{jj'} \langle A^* | a_{j'}^+ a_j | A \rangle \langle t^{(-)} \varphi_{j'} | G | h^{(+)} \varphi_j \rangle \quad (2)$$

where $G$ is the $\alpha$-particle Green function, and $D_0$ is the one-particle transfer strength [5].

It may be seen from eq. (2) that the second order $(h\alpha)$, $(\alpha t)$ process is sensitive to exactly the same correlations between the ground and excited states as the direct (h, t) process, and may therefore be expected each time a direct (h, t) transition occurs. However, the effective interaction, $D_0^2 G$, has a nonlocality characteristic of the alpha propagation, which is much longer than the nonlocality inherent in the two-body interaction. Similar arguments could be used in favor of the formation of an intermediate deuteron. However, the coupling constant $D_0$ is substantially smaller in this case. We neglected the (hd), (dt) process in the computation below, although further investigations in this direction are planned.

To understand the origin of the $L = 1$ angular distribution to antianalogue states, consider the transition density for exciting the analogue state (IAS) and the antianalogue state (AAS) from the parent ground state. In $^{40}$Ar, these two states are described as $[d_{3/2}^{-2} f_{7/2}^2]_{T=2}$ and $[d_{3/2}^{-2} f_{7/2}^2]_{T=1}$, respectively. Two single-particle transition den-

# $(p, t)$ Reaction on Even-Even $N = Z$ Nuclei in the $2s1d$ Shell[*]

R. A. Paddock†

*Cyclotron Laboratory and Physics Department, Michigan State University, East Lansing, Michigan 48823*

(Received 21 June 1971)

The $(p,t)$ reaction on the even-even $N=Z$ nuclei in the $2s1d$ shell has been used to study the energy levels of $^{18}$Ne, $^{22}$Mg, $^{26}$Si, $^{30}$S, $^{34}$Ar, and $^{38}$Ca. The energies of the excited states observed are reported along with spin and parity assignments when possible. Two-nucleon-transfer distorted-wave calculations were carried out. Comparisons are made with the shapes of the experimental angular distributions. It is found that the calculated shapes are primarily dependent upon the $L$ transfer and the optical-model parameters. The magnitudes of the calculated cross sections are found to depend strongly not only on the optical-model parameters, but also the bound-state parameters and the configuration mixing in the initial and final nuclear wave functions.

## I. INTRODUCTION

The $(p, t)$ two-nucleon-transfer reaction has been studied for even-even $N = Z$ targets in the $2s1d$ shell. In particular, the targets were $^{20}$Ne, $^{24}$Mg, $^{28}$Si, $^{32}$S, $^{36}$Ar, and $^{40}$Ca, which all have $J^{\pi} = 0^{+}$ ground states. These $(p, t)$ reactions reach states in nuclei which are two nucleons away from stability. The only other way of reaching the same nuclei by a two-body final-state reaction is the $(^{3}\text{He}, n)$ reaction. Until recently these nuclei have not been studied to any great extent although the $(p, t)$ reaction has been used extensively to study nuclei in the light-mass region[1-3] and in the medium-to-heavy-mass region.[4-8] These studies have shown that the shapes of the angular distributions are characteristic of the $L$ transfer.

We denote the reaction by

$$A(p, t)B,$$

and the transferred quantum numbers by $L$, $S$, $J$, and $T$. Since the targets are all $J_A = 0$, $T_A = 0$, and since $T = 1$ is a requirement of the $(p, t)$ reaction, it follows that $J_B = J$ and $T_B = 1$. The two neutrons bound in the triton are mostly ($\sim$95%)[9] in a state of relative spatial symmetry which requires that $S = 0$. This leads to $J_B = L$ as an approximate restriction. If it is further assumed that the neutrons in the triton are in a relative $s$ state, then the parity change is restricted to $\Delta \pi = (-1)^{L}$. These restrictions make the spin-parity assignments to the final nuclear states quite unambiguous once the $L$ transfer has been established.

## II. THEORY

The conventional distorted-wave method for di-

rect reactions such as set forth by Satchler[10] was used to calculate the shapes of the angular distributions. The details of the reaction mechanism are calculated by a spin-dependent distorted-wave computer code in a zero-range approximation. Glendenning[11] developed the form factor needed in this calculation by using harmonic-oscillator wave functions for the two bound neutrons and a Gaussian wave function for the triton. It has been shown by Drisko and Rybicki[12] that the use of finite-well wave functions alters considerably the predicted cross section. We choose to follow the finite-well wave-function approach as expressed in detail in a paper by Jaffe and Gerace.[13]

The bound-state wave functions of the two neutrons are taken to be those of a particle bound in a well of the form

$$U(r) = -V_0 f(r) + \left(\frac{\hbar}{m_\pi c}\right)^2 V_s \frac{1}{r} \frac{d}{dr} f(r) \vec{l} \cdot \vec{\sigma},$$

where $f(r)$ is taken to be the standard Woods-Saxon shape with $r_0 = 1.25$ fm and $a = 0.65$ fm as suggested by Bayman and Hintz,[8] and $V_s$ was taken as 6 MeV, which is typical of single-nucleon spin-orbit strengths. The real well depth was adjusted so that the individual neutrons were bound by one-half the two-neutron separation energy as suggested in Refs. 6 and 12. These wave functions were expanded in terms of harmonic-oscillator wave functions with typically five to eight terms needed to fit the Woods-Saxon wave function to better than 2% out to twice the nuclear radius. The calculations of the individual form factors were carried out by the computer code TWOFRM (written by W. Gerace, Princeton University). The distorted-wave calculations were carried out with the code JULIE.[14] The distorted waves were obtained from an optical-model po-

# EXCHANGE CURRENTS IN PARITY NON CONSERVING ELECTROMAGNETIC TRANSITIONS*

B. H. J. McKELLAR**

*Cyclotron Laboratory, Michigan State University, East Lansing, Michigan 48823, USA*

It is shown that exchange currents do not contribute significantly to parity non-conserving transitions of the electric multipole type.

There has been some discussion in the literature of the role which the exchange currents necessary for gauge invariance play in parity non conserving electromagnetic transitions. Gari and Huffman [1] have considered the various processes likely to be importance and conclude that the Feynman diagram of fig. 1 dominates the conventional process of fig. 2. Eman and Tadic [2] however consider that Siegert's theorem [3] indicates that exchange currents will not contribute to electric multipole transitions.

In this letter we generalize the arguments leading to Siegert's theorem and show that they do apply to parity nonconserving transitions, leading to the result of Eman and Tadic. This conclusion depends on assumptions about the weak photoproduction terms of fig. 3, namely that they do not modify Siegert's assumption that the charges can be regarded as being localized on the nucleons. We support this assumption by showing that these terms contribute only to order $k^2$ relative to the leading terms as a consequence of Low's low energy theorem [4]. Part of the reason for the interest in such terms is that they provide a mechanism for one pion exchange terms which are not surpressed in Cabibbo theory by the factor $\sin^2\theta$. In case terms of order $k^2\cot^2\theta$ are regarded as significant we show using PCAC and current algebra that such terms could be derived phenomenologically from data on radiative hyperon decays. Although such data are not available we find that these terms arise only from the 27 parts of the weak Hamiltonian and are sur-
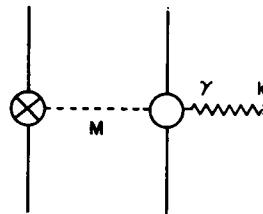
Fig. 1. The strong photoproduction exchange current found to be large by Gari and Huffman. In this and all other figures a crossed circle represent the weak parity violating interaction.

pressed by the octet enhancement mechanism. Our conclusion is therefore that parity non conserving electric multipole transitions can be calculated without considering exchange effects provided good wave functions are used. The discrepancy between present calculations [5] and experiments [6] for the tantalum transition could however lie in the crude calculation of the strength of the $\rho$ exchange parity violating potential [7] or in deficiencies in the nuclear wave function rather than be a demonstration of the inadequacy of the Cabibbo Hamiltonian.

We now proceed to demonstrate each of our points in turn:

(i) *Siegert's theorem.* The derivation of Siegert's theorem for parity conserving transitions makes essential use of Siegert's assumption that the charge distribution in the nucleus depends solely on the nuclear coordinates; even though the exchange of mesons between the nucleons gives rise to currents in the nucleus they move so rapidly that the static charge distribution is localized on the nucleons. It only remains to demonstrate that matrix elements for electric multipole transi-

401

# COMPUTER COMPATIBLE SERVO SYSTEM FOR CYCLOTRON RF *

P. SIGG

*Cyclotron Laboratory, Michigan State University, East Lansing, Michigan 48823, U.S.A.*

A new servo control system, which allows computer as well as manual setup of the rf-system of the MSU-cyclotron has been built and tested. It features automatic switching to phase detectors when the desired positions are reached in order to fine-tune the system if the rf-drive goes on.

## 1. Introduction

The new rf-servo system allows simultaneous setup either from thumbweel switches on the console of the cyclotron or from a computer.

Since the system contains seven tunable elements,

this saves a considerable amount of time, since the old system required the operator to set each element to the desired position by a manual control switch. The operator no longer is required to pay any attention to the tuning process, though it still could be done manually if so desired. Separate two-speed clocks for each servo allow a high setting speed and a matched
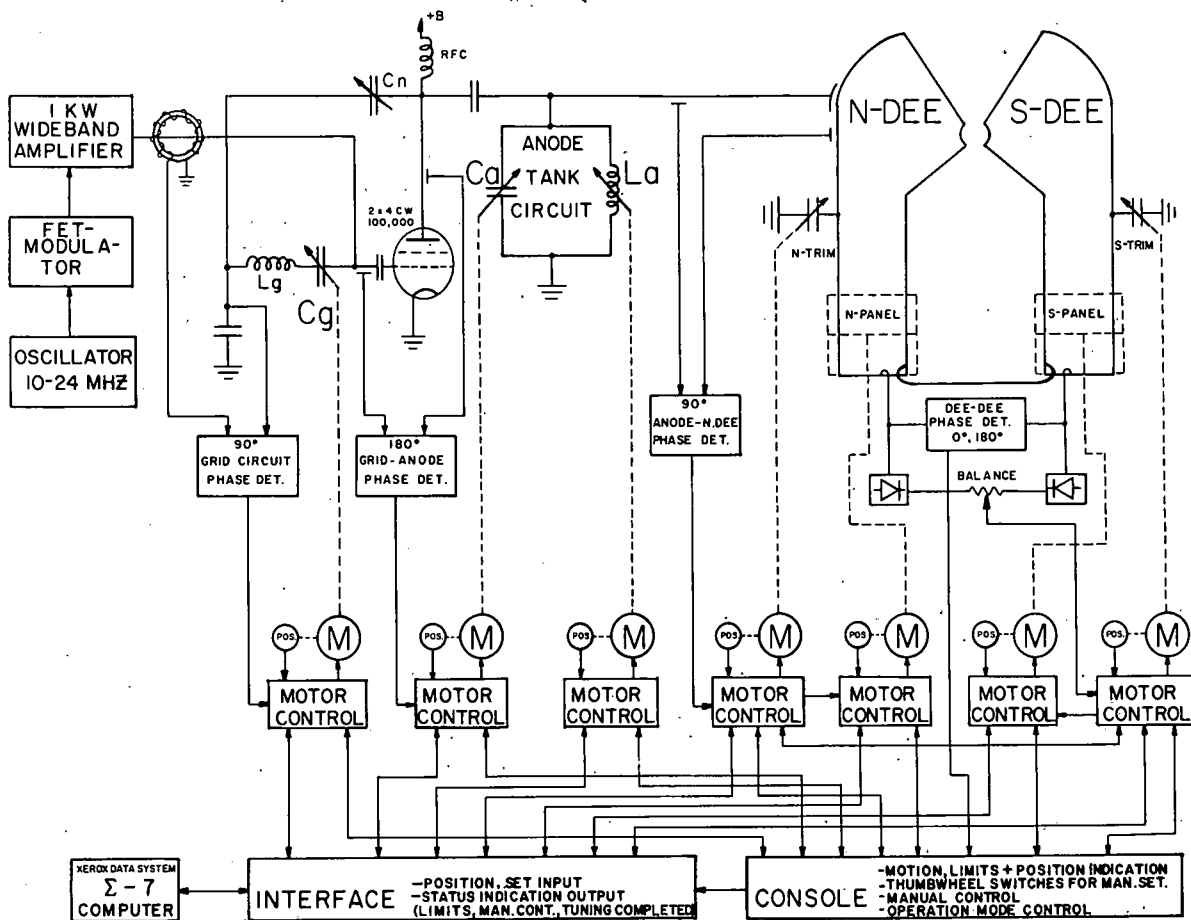


Fig. 1. Block diagram of the rf system.

# Decay of $^{141m}$Sm — A Three-Quasiparticle Multiplet in $^{141}$Pm

R. E. Eppley*

*Department of Chemistry†‡ and Cyclotron Laboratory,‡ Department of Physics,
Michigan State University, East Lansing, Michigan 48823*

and

R. R. Todd

*Cyclotron Laboratory,‡ Department of Physics, Michigan State University, East Lansing, Michigan 48823*

and

R. A. Warner and Wm. C. McHarris

*Department of Chemistry† and Cyclotron Laboratory,‡ Department of Physics,
Michigan State University, East Lansing, Michigan 48823*

and

W. H. Kelly

*Cyclotron Laboratory,‡ Department of Physics, Michigan State University, East Lansing, Michigan 48823*

(Received 13 July 1971)

We have studied the $\gamma$ rays emitted following the decay of 22.1-min $^{141m}$Sm with Ge(Li) and NaI(Tl) detectors in various singles, coincidence, and anticoincidence configurations, including Ge(Li)-Ge(Li) two-dimensional "megachannel" coincidence experiments. Of the 47 $\gamma$ rays definitely established as belonging to $^{141m}$Sm decay, all but six very weak ones have been placed in a consistent decay scheme. The energies in keV [and $J^\pi$ assignments] of the states in $^{141}$Pm populated by the decay of $^{141m}$Sm are 0 [$\frac{5}{2}^+$], 196.6 [$\frac{7}{2}^+$], 628.6 [$\frac{11}{2}^-$], 804.5 [$\frac{11}{2}^+$, $\frac{9}{2}^+$], (837.1) [$\frac{9}{2}^+$], 974.0 [$\frac{9}{2}^+$], 1108.1 [$\frac{7}{2}^+$, $\frac{9}{2}^+$, ($\frac{5}{2}^+$)], 1167.2 [$\frac{13}{2}^{-(+)}$, $\frac{11}{2}^{-(+)}$, $\frac{9}{2}^{-(+)}$], 1313.2 [$\frac{13}{2}^{-(+)}$, $\frac{11}{2}^{-(+)}$, $\frac{9}{2}^{-(+)}$], 1414.8 [$\frac{11}{2}^-$, $\frac{9}{2}^-$], (1834.0) [$\frac{11}{2}^-$, $\frac{9}{2}^-$], 1983.1 [$\frac{9}{2}^-$], 2063.5 [$\frac{11}{2}^-$, $\frac{9}{2}^-$], 2091.6 [$\frac{11}{2}^-$, $\frac{9}{2}^-$], 2119.0 [$\frac{11}{2}^-$, $\frac{9}{2}^-$], and 2702.4 [$\frac{13}{2}^-$, $\frac{11}{2}^-$, $\frac{9}{2}^-$]. Less than 0.2% of the decay of $\frac{11}{2}^-$ $^{141m}$Sm proceeds via an $M4$ isomeric transition to 11.3-min $\frac{3}{2}^+$ $^{141g}$Sm. Two-thirds of the $^{141m}$Sm electron-capture decay goes to the six (possibly seven) highest-lying states in $^{141}$Pm, another example analogous to $^{139m}$Nd decay of the population of a well-defined three-quasiparticle multiplet by an $N=79$ nuclide. In simple shell-model terms this can be written as $(\pi d_{5/2})^2(\nu d_{3/2})^{-2}(\nu h_{11/2})^{-1} \rightarrow (\pi d_{5/2})(\nu d_{3/2})^{-1}(\nu h_{11/2})^{-1}$. Most of the remaining states can be characterized quite satisfactorily as specific single-particle and core-coupled states. The behavior of these states allows us to add considerably to the systematics of shell-model orbits and their occupations in this region below $N=82$.

## I. INTRODUCTION

These results of our study of the decay of $^{141m}_{62}$Sm$_{79}$ supplement the similar work done on the decay of $^{139m}_{60}$Nd$_{79}$ by Beery, Kelly, and McHarris.[1] The decay of $\frac{11}{2}^-$ $^{139m}$Nd selectively populates six high-spin states at relatively high energies in $^{139}$Pr. These states were characterized as three-quasiparticle states having the configuration, $(\pi d_{5/2})(\nu d_{3/2})^{-1}(\nu h_{11/2})^{-1}$, and the preferred electron-capture ($\epsilon$) decay of $^{139m}$Nd could be written as $(\pi d_{5/2})^2(\nu d_{3/2})^{-2}(\nu h_{11/2})^{-1} \rightarrow (\pi d_{5/2})(\nu d_{3/2})^{-1}(\nu h_{11/2})^{-1}$.

The work on $^{139m}$Nd decay led to the prediction by McHarris, Beery, and Kelly[2] that other $N=79$ or $N=77$ nuclides might possess the requisite configurations for similar $\epsilon$ or $\beta^+$ decay into three-quasiparticle multiplets. In addition to the configuration such a nuclide must also have sufficient

decay energy to populate states above the pairing gap in its daughter, and it must have relatively low probability for other modes of decay — for example, if it is a metastable state the energy for the isomeric transition must be low enough to make that transition quite slow.

Working his way out from $\beta$ stability, one finds that $^{141m}$Sm and $^{137m}$Nd are the next likely candidates. For example, the addition of two protons to the $^{139m}$Nd configuration produces the very similar configuration for $^{141m}$Sm, $(\pi d_{5/2})^4(\nu d_{3/2})^{-2}(\nu h_{11/2})^{-1}$. The calculated $Q_\epsilon$ is more than 5 MeV, allowing it to populate high-lying states in $^{141}$Pm. Finally, as in the other $N=79$ odd-mass isotones, the $h_{11/2} - d_{3/2}$ (metastable → ground state) separation is small ($\approx 171$ keV), making the $M4$ isomeric transition very slow. The results that we present in this paper do indeed confirm these predictions — a

# CALCULATION OF $T=2 \rightarrow T=1 \rightarrow T=0$ M1 DECAYS IN $A=20$ AND $A=32$ NUCLEI

S. MARIPUU *

*Aerospace Research Laboratories, Wright-Patterson Air Force Base, Ohio 45433, USA*

and

B. H. EILDENTHAL**

*Cyclotron Laboratory, Dept. of Physics, Michigan State University,
East Lansing, Michigan 48823, USA*

Absolute strengths and branching ratios are calculated for M1 transitions between states of different isospin in two $A = 4n$ nuclei of the sd-shell.

The gamma decay of the lowest $T = 2$ levels in self-conjugate $A = 4n$ nuclei offers a unique possibility of studying $T = 2,1$ and 0 levels within a single system. From studies of once- and twice-forbidden capture reactions in the 2s1d-shell, strong gamma-ray cascades from $(J^\pi, T) = (0^+, 2)$ states have been reported in $A = 20, 24, 28$ and 32 nuclei [1]. The characteristic gamma decay proceeds with one or more cascades of M1 character where the $(J^\pi, T)$ combinations are $(0^+, 2) \rightarrow (1^+, 1) \rightarrow (0^+, 0)$ or $(2^+, 0)$. Information on the $(1^+, 1) \leftarrow (0^+, 0)$ M1 transition strengths has been obtained from measurements of 180° inelastic electron scattering [2,3].

In this paper we report a shell model calculation of $\Delta T = 1$, M1 transition strength for the gamma-ray cascades from $(J^+, T) = (0^+, 2)$ levels in $A = 20$ and 32. A realistic effective two-body interaction, deduced from the Sussex relative oscillator matrix elements and corrected for core-polarization and other space-truncation effects, has been employed [4]. An inert $^{16}$O core has been assumed. Diagonalization of the energy matrices has been performed in full sd space for $A = 20$. For the mass 32 calculation only up to two $d_{5/2}$ particles have been allowed to be excited to $s_{1/2}$ and $d_{3/2}$ orbits. The shell model energy matrices were constructed with the codes described by French et al. [5]. The single-particle energies have been taken from the $^{17}$O experimental spectrum. Except for the harmonic oscillator size, $\hbar\omega = 14.4$ MeV, no parameters

* NRC-AFSC Senior Resident Research Associate.
** Research supported in part by the National Science Foundation.

have been used. No variation of $\hbar\omega$ has been made in order to obtain accurate predictions of absolute binding energies for different mass numbers. The theoretical energies, as presented in fig. 1 and table 1 together with experimental information, have been "normalized" such that the lowest $(J^\pi, T) = 1^+, 1)$ state is equal to the experimental value. The excitation energies in table 1 are the experimental ones. (The values marked with asterisks are predicted values for experimentally unknown levels.) The predicted transition strengths have been calculated with the assumption of pure M1 transitions and bare nucleon $g$-factors.

For $^{20}$Ne, the predicted absolute strengths for the transitions through the lowest $(1^+, 1)$ level, $[(0^+, 2) \rightarrow (1^+, 1)$ and $(1^+, 1) \leftarrow (0^+, 0)]$,
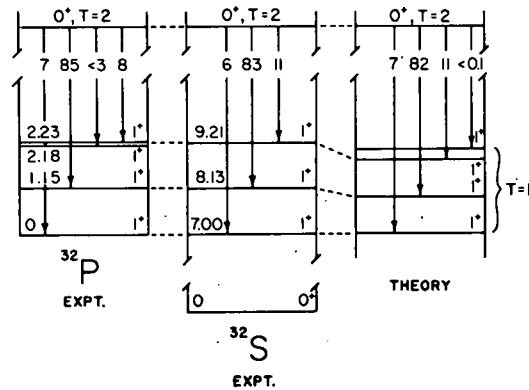


Fig. 1 The experimental and theoretical branching ratios of the $J^\pi = 0^+$, $T = 2$ levels in $A = 32$.

464

# INELASTIC ELECTRON SCATTERING FORM-FACTORS CALCULATED
## FROM SHELL-MODEL WAVE FUNCTIONS *

G. R. HAMMERSTEIN, Duane LARSON and B. H. WILDENTHAL

*Cyclotron Laboratory, Physics Department.*
*Michigan State University, East Lansing, Michigan 48823, USA*

From-factors measured for (e, e') on $^{20}$Ne, $^{24}$Mg, $^{28}$Si and $^{32}$S are well reproduced by calculations which use shell-model wave functions and scaling factors consistent with the usual effective charge assumptions.

Recent measurements [1] have yielded form-factors for inelastic electron scattering leading to the lowest 2$^+$ and 4$^+$ states of $^{20}$Ne, $^{24}$Mg and $^{28}$Si. Older data [2] are available for $^{32}$S. In this note we present results of analyses of these data which use shell-model wave functions to generate the relevant transition densities. It has been shown [3-6] that presently available data on E2 transition strengths and electric quadrupole moments in the sd-shell can be understood in terms of these same wave functions if protons and neutrons are each assumed to carry an additional charge of 0.5e, an assumption not at variance with data available from the "single particle" nuclei $^{17}$O and $^{17}$F. The question of interest here is whether the more detailed information contained in the experimental (e, e') form-factors can also be explained in the same terms.

The shell-model wave functions we use here have been obtained from calculations made in $0d_{5/2}$-$1s_{1/2}$-$0d_{3/2}$ basis spaces. The $^{20}$Ne calculations employed the full set of states available in this space, but in the other calculations limits were placed on the numbers of allowable $d_{5/2}$ holes and $d_{3/2}$ particles so as to keep dimensions within practical bounds. The Ne and Mg shell-model calculations employed as a model Hamiltonian a (slightly) modifies [7] version of Kuo's matrix elements [8]. The $^{28}$Si and $^{32}$S calculations were made with versions of the modified surface-delta interaction. Details of these calculations are available elsewhere [3-5].

In the present work, these shell-model wave functions are used to generate the expectation values of the operators $(a_j^+ a_{j'})_J$ between the initial

and final states of the target nucleus, where $j, j'$ refer to the orbits of the active model space and $J$ to the multipolarity of the transition. A specially adapted version [9] of the computer cod codes described by French et al. [10] is used for this procedure. These results are then appropriately combined with radial wave functions of the model orbits in order to construct transition densities $\rho_J(r)$. The form-factors for inelastic electrons scattering then follow from the expression

$$|F(q)|^2 = \frac{4\pi}{Z^2} \frac{2J_f + 1}{2J_i + 1} \left| \int_0^\infty \rho_j(qr)\rho_J(r)r^2 dr \right|^2. \quad (1)$$

We note that, since $j_J(qr) \to q^J r^J/(2J+1)!!$ as $q \to 0$, the expression for the form factor becomes in the limit of $q \to 0$, equal to the definition of the $B(EJ)$ of an electric transition of multipolarity :

$$\frac{Z^2[(2J+1)!!]^2}{4\pi} \lim_{q \to 0} \frac{|F(q)|^2}{q^{2J}} =$$

$$= \frac{2J_f + 1}{2J_i + 1} \left| \int_0^\infty \rho_J(r)r^J \, dr \right|^2 \equiv B(EJ) . \quad (2)$$

However, the complete (e, e') form factors provide a more detailed test of the transition density than is available from just the $B(EJ)$, since $\rho$ is sampled for varying values of $r$ as $q$ varies. Provided the calculated and observed shapes of $|F(q)|^2$ are in reasonable agreement, the square of the isoscalar effective charge $e(\text{eff}) = e_p(\text{eff}) + e_n(\text{eff})$ (all the present transitions are $\Delta T = 0$) may be defined as the number which normalizes the form factor calculated with $e_p = 1.0$, $e_n = 0.0$ to the experimental dis-

176

# Electromagnetic Transition Rates in $^{28}$Al[†]

J. V. Maher,[*] G. B. Beard,[‡] and G. H. Wedberg[§]
*Argonne National Laboratory, Argonne, Illinois 60439*

and

E. Sprenkel-Segel and A. Yousef
*Illinois Institute of Technology, Chicago, Illinois 60616,*
*and Argonne National Laboratory, Argonne, Illinois 60439*

and

B. H. Wildenthal[¶]
*Michigan State University, East Lansing, Michigan 48823*

and

R. E. Segel[¶]
*Northwestern University, Evanston, Illinois 60201,*
*and Argonne National Laboratory, Argonne, Illinois 60439*
(Received 15 November 1971)

Lifetimes for the 2nd through 12th excited states in $^{28}$Al have been obtained by use of the attenuated-Doppler-shift technique. Combining these results with previous information on this nucleus makes it possible to assign spins to all of the states that have been studied. All of the information is then compared with a shell-model calculation and with other theoretical descriptions that have been advanced.

## I. INTRODUCTION

In the simplest shell-model picture, the $1d_{5/2}$ subshell closes at $^{28}$Si. While the closeness of the $1d_{5/2}$, $2s_{1/2}$, and $1d_{3/2}$ subshells indicates that this simplest picture can only be a rough approximation to the true situation for the nuclei in the mass-28 region, the level scheme of $^{28}$Al does give substantial support to the simple picture. This level scheme is relatively simple for an odd-odd nucleus; it has only seven levels below 2 MeV, and the two lowest states are as predicted by the $(d_{5/2})^{-1}s_{1/2}$ assignment. In order to determine how well a simple picture holds up when the stringent test of predicting electromagnetic transition rates is applied, the present work of measuring the lifetimes of the low-lying states in $^{28}$Al was undertaken.

The attenuated-Doppler-shift method was much the same as in earlier Argonne work[1,2]; i.e., the spectra of $\gamma$ rays in coincidence with each of two proton detectors were recorded. Figure 1 is a schematic diagram of the experimental arrangement. The pulses were processed by conventional electronics, and for each event the proton and $\gamma$-ray pulse heights in digitized form were recorded on magnetic tape. The available memory capacity was sufficient for on-line recording of some of the $\gamma$-ray spectra of interest, though others had to be obtained by sorting the data stored on the tapes. The Doppler shifts were extracted for those transitions deemed to be most useful in de-

# Energy Levels of $^{25}$Si from the Reaction $^{28}$Si($^{3}$He, $^{6}$He)$^{25}$Si at 70.4 MeV*

W. Benenson, J. Driesbach,† I. D. Proctor, and G. F. Trentelman‡

*Cyclotron Laboratory and Physics Department, Michigan State University, East Lansing, Michigan 48823*

and

B. M. Preedom

*Physics Department, University of South Carolina, Columbia, South Carolina 29208,*
*and Cyclotron Laboratory, Michigan State University, East Lansing, Michigan 48823*

(Received 6 December 1971)

The energy levels of $^{25}$Si have been measured by detecting $^{6}$He particles from the reaction $^{28}$Si($^{3}$He, $^{6}$He)$^{25}$Si in photographic plates on the focal plane of a spectrometer. 12 excited states were observed. The observation of a weak state at 40-keV excitation leads to a new $^{25}$Si ground-state mass excess, 3.824 ± 0.010 MeV. The observed levels are discussed in terms of the isobaric multiplet mass equation and the shell model.

The ($^{3}$He, $^{6}$He) reaction has been used previously to study the ground-state masses of proton-rich nuclei.[1-3] Six $T = \frac{3}{2}$ mass quartets have been completed this way and the results have been used to determine the coefficients of the isobaric multiplet mass equations (IMME). In principle this same equation should link the mass excesses of the excited $T = \frac{3}{2}$ states as well. The dependence of the various coefficients of the equation on excitation energy and spin can therefore be observed at a fixed value of $A$. The present experiment deals with the energy level scheme of $^{25}$Si, which up to present was completely unknown.

Even the ground-state transitions in the ($^{3}$He,$^{6}$He) reaction are difficult to observe because of the very small cross sections (typically 1 μb/sr at the peak). Previous measurements employed a position-sensitive detector on the focal plane of a spectrometer[1,2] or a three-detector telescope.[3] When these methods are employed, the background due to neutrons and other charged particles obscures weakly populated states. In the case of the reaction $^{28}$Si($^{3}$He,$^{6}$He)$^{25}$Si, the resolution (70 keV) was not good enough to observe the ground state as a doublet (as predicted by the IMME), and hence the assumption was made that the peak observed was the ground state only.[2] In the present experiment relatively insensitive photographic plates were used in the focal plane of the spectrometer. The large solid angle, kinematic compensation, and dispersion matching of the spectrometer, coupled with the insensitivity of the plates to neutrons, γ rays, and lower-mass charged particles of the same magnetic rigidity, permitted the observation of the ground state and 12 excited states in $^{25}$Si.

Ilford K(−1) plates were used with absorbers

stepped in thickness to keep the $^{6}$He particles between 12 and 18 MeV at the surface of the emulsion. This puts the α particles at 50 to 60 MeV, typically. At this energy they leave barely observable tracks, which in the present experiment did not obscure any region of the plate in spite of the large number of α particles compared to $^{6}$He particles. The elastic $^{3}$He particles, however, are so numerous at the forward angles used that they blacken the plate. Fortunately they fall at the same place as $^{6}$He particles corresponding to a fairly high excitation energy (about 6.7 MeV) in $^{25}$Si. In general, the present method is limited to $^{6}$He particles of energy greater than about $\frac{1}{2}$ the beam energy.

Data were taken at 9, 12, and 16° (lab) with a 600-μg/cm² natural Si target and at 9 and 12° with a 200-μg/cm² SiO target. The beam energy was 70.4 MeV in all cases. The energy resolution was limited mainly by target thickness to 50 keV for the natural Si target and 28 keV for the SiO target. The spectrum taken on natural Si at 9° is shown in Fig. 1. The higher-resolution SiO runs were used to attempt to resolve the first-excited-state-ground-state doublet which is shown in Fig. 2. These results show that mass measurement of $^{25}$Si was predominantly of the ground state, as was assumed by the authors,[2] but that the mass should be shifted downward by 8 keV, which is within the error of their measurements. The new mass excess of $^{25}$Si is 3.824 ± 0.010 MeV.

The new mass of $^{25}$Si changes the coefficients of the IMME only slightly. The form of the IMME used is

$$M = a + bT_z + cT_z^2 + dT_z^3 .$$

The coefficients of the equation are sensitive to

# SHELL-MODEL CALCULATIONS FOR MASSES 27, 28 AND 29:
# ELECTROMAGNETIC TRANSITION RATES AND MULTIPOLE MOMENTS

M. J. A. DE VOIGT, P. W. M. GLAUDEMANS and J. DE BOER

*Fysisch Laboratorium, Rijksuniversiteit, Utrecht, The Netherlands*

and

B. H. WILDENTHAL

*Michigan State University, East Lansing, Michigan 48823*

Abstract: Electromagnetic transition probabilities, multipole moments and log $ft$ values have been calculated from many-particle shell-model wave functions in a truncated $1d_{\frac{5}{2}} 2s_{\frac{1}{2}} 1d_{\frac{3}{2}}$ configuration space, with a maximum of four holes in the $1d_{\frac{5}{2}}$ subshell. The electric quadrupole transition strengths and moments are reproduced very well in a least-squares fit to 74 experimental data with one parameter, for the isoscalar effective charge, yielding the values $e_p = 1.6\,e$ and $e_n = 0.6\,e$. The results for magnetic dipole transition strengths and moments follow from adjusting two effective reduced single-particle matrix elements in separate least-squares fits to 17 experimental data in $A = 27$ nuclei and 21 data in $A = 29$ nuclei. The average absolute deviations between theory and experiment for E2 and M1 transition strengths are 3.0 and 0.05 W.u., while the average measured strengths are 7.7 and 0.08 W.u., respectively. Transitions from excited states above $E_x = 4.8$ MeV in $^{27}$Al and from some low-lying states in $^{27}$Al and $^{28}$Si are poorly reproduced by the present model. Calculated strengths of transitions from analogue states are given. Previous conclusions about the single-particle character of M1 transitions and the collective behaviour of E2 transitions are confirmed. The experimental data of seven $A = 27$–29 nuclei are well reproduced in one general treatment with an appreciably lower number of free parameters than are required to obtain comparable results in collective model calculations.

## 1. Introduction

A possible rotational-like structure of the nuclei around mass 28 has been discussed by several authors [1-6]. Since many-particle shell-model calculations in the mass region $A = 30$–34 have met with considerable success [7,8], it was thought worthwhile to extend these calculations to the slightly lighter $A = 27$–29 nuclei. The electromagnetic properties are reported here. The excitation energies and spectroscopic factors are discussed in another paper [9]. The electric quadrupole moments of $^{27}$Al and $^{28}$Si as found in a previous calculation have already been published [10]. Similar calculations for $A = 23$–27 nuclei of which some have an established deformed character are in progress [11].

These calculations are feasible since a wealth of experimental information on $A = 27$–29 nuclei became available recently (see table 1). The wave functions have been calculated [9] with the Oak Ridge-Rochester shell-model computer programs [12]. The configuration space is given by: $(1s)^4(1p)^{12}(1d_{\frac{5}{2}})^{n_1}(2s_{\frac{1}{2}})^{n_2}(1d_{\frac{3}{2}})^{n_3}$ with $n_1+n_2+n_3$

365

# Decays of the Even-Even Lead Isomers: $^{202m}$Pb and $^{204m}$Pb

Jean Guile,* R. E. Doebler,† and Wm. C. McHarris

*Department of Chemistry‡ and Cyclotron Laboratory,§ Department of Physics,
Michigan State University, East Lansing, Michigan 48823*

and

W. H. Kelly

*Cyclotron Laboratory,§ Department of Physics, Michigan State University, East Lansing, Michigan 48823*

(Received 17 February 1972)

The decays of the 9⁻ isomers, $^{202m}$Pb and $^{204m}$Pb, have been investigated using Ge(Li) detectors in a variety of singles and coincidence configurations. Improved conversion coefficients were obtained for two of the transitions following the decay of $^{204m}$Pb, but no new, weak transitions were seen. Considerable improvement and enlargement of the $^{202m}$Pb decay scheme was possible. We have been able to make unambiguous multipolarity assignments for 15 of the 18 transitions following its decay and to place all 18 in a consistent decay scheme. States in $^{202}$Pb were established (following the 90.5% isomeric-transition decay) at 0 ($J^\pi = 0^+$), 960.70 (2$^+$), and 1382.82 (4$^+$), 1623.1 (4$^+$), 1915.2 (4$^+$), 2040.3 (5$^-$), and 2169.8 keV (9$^-$). Those in $^{202}$Tl (following the 9.5% electron-capture decay) lie at 0 (2$^-$), 490.47 (4$^-$), 950.19 (7$^+$), 1098.7 (6$^+$, 7$^+$, 8$^+$), 1340.1 (8$^+$), 1552.1 (8$^+$.[9$^+$]), and 1675.6 keV (9$^+$, 8$^+$). Interpretation is made concerning the nature of the states in $^{202}$Pb and even-even Pb isotopes and also in $^{202}$Tl and odd-odd Tl isotopes on the basis of the simple shell-model plus pairing forces.

## I. INTRODUCTION

The Pb isomers were the first case of even-even isomerism to be observed. Besides being interesting in their own right, they also provided (and still provide) an advance opportunity to study some of the lower-lying states in the Pb isotopes, states that presumably should be amenable to explanation in simple shell-model terms. $^{204m}$Pb and $^{202m}$Pb, especially, have proven useful for building up skeletal level schemes for $^{204}$Pb and $^{202}$Pb before these could be studied by transfer reactions or the much more complicated decays of $^{204}$Bi and $^{202}$Bi. In the present work we reexamine the decays of $^{204m}$Pb and $^{202m}$Pb, using Ge(Li) γ-ray detectors for the first time. We then correlate our findings with those from other types of experiments when possible and examine the trends in the even-even Pb isotopes not too far from stability. We are also able to make arguments concerning

the structures of some of the odd-odd $^{202}$Tl states populated by the electron-capture (ε) decay branch of $^{202m}$Pb.

The decay scheme of 66.9-min $^{204m}$Pb has been the subject of many previous studies, beginning with Sunyar et al. in 1950.[1] An excellent summary of the intervening work is to be found in Hyde, Perlman, and Seaborg[2] and thus will not be repeated. It should be mentioned, however, that the decay scheme remains essentially that proposed by Fritsch in 1956.[3] Our study was aimed chiefly at finding weak, previously unobserved transitions. None was found, but we were able to obtain better values for some of the internal-conversion coefficients, using a unique single-crystal Ge(Li) "conversion-coefficient spectrometer" developed in this laboratory.[4]

The existence of an isomer associated with $^{202}$Pb was first reported by Maeder and Wapstra in 1954.[5] They produced this isomer by bombarding

2.L

# ELASTIC AND INELASTIC SCATTERING OF PROTONS FROM 6Li BETWEEN 25 AND 45 MeV

K. H. BRAY [t], MAHAVIR JAIN [tt], K. S. JAYARAMAN, G. LOBIANCO,
G. A. MOSS [t], W. T. H. VAN OERS and D. O. WELLS

*Cyclotron Laboratory and Department of Physics, University of Manitoba, Winnipeg 19, Canada*

and

F. PETROVICH

*Department of Physics, Michigan State University, East Lansing, Michigan 48823* [‡]

Abstract: The elastic and inelastic scattering of protons from 6Li has been studied at incident energies of 25.9, 29.9, 35.0, 40.1 and 45.4 MeV. The 2.18 MeV ($3^+$, $T = 0$) first excited state of 6Li was found to be strongly excited, but the 3.56 MeV ($0^+$, $T = 1$) second excited state was quite weakly excited. Angular distributions for excitation of the 2.18 MeV level were measured at all five energies, while angular distributions for excitation of the 3.56 MeV level were extracted only at 25.9 and 45.4 MeV. To test the applicability of the optical model for the scattering of protons from such a light nucleus the elastic scattering angular distributions have been analyzed using the eleven-parameter search code SEEK. Available polarization angular distributions were included in the analysis. Reasonable fits to the data have been obtained with an average geometry potential. Theoretical estimates of the real part of the optical potential and the inelastic scattering differential cross sections have been made using the microscopic model for proton-nucleus scattering. Both phenomenological and realistic forces have been considered and the necessary nuclear transition densities have been extracted from experimental elastic and inelastic electron scattering data. An estimate of a possible spin-spin term in the optical potential has also been made.

## 1. Introduction

Various groups have previously reported measurements of elastic and inelastic cross sections for proton scattering from 6Li in the energy region 25–50 MeV [refs. [1−4])]. One of the purposes of the present experiment was to improve the knowledge of the energy dependence of the 6Li+p elastic cross sections. This is important in the case of such a light nucleus as there may be contributions from resonances in the compound system at some energies and information about the optical potential extracted at a single energy could prove to be misleading. An analysis of the elastic data has been made using a conventional phenomenological optical potential. Existing polarization

35

# $^{19}$F$(d, p)^{20}$F and the Nuclear Structure of $^{20}$F[†]

H. T. Fortune*

*Argonne National Laboratory, Argonne, Illinois 60439,*
*and Physics Department, University of Pennsylvania, Philadelphia, Pennsylvania 19104*

and

G. C. Morrison, R. C. Bearse,‡ and J. L. Yntema
*Argonne National Laboratory, Argonne, Illinois 60439*

and

B. H. Wildenthal
*Physics Department, Michigan State University, East Lansing, Michigan 48823*
(Received 6 December 1971)

The reaction $^{19}$F$(d, p)^{20}$F has been studied with 16-MeV deuterons. Outgoing protons were detected in photographic emulsions in a magnetic spectrograph. Spectroscopic factors were extracted and combined with previous information and compared with results of shell-model calculations performed in a complete $sd$-shell basis. Of the previously known 25 states below $E_x = 4.5$ MeV, angular distributions measured at 14 angles were obtained for all but the 5 at $E_x = 1.824$, 2.871, 3.761, 4.20, and 4.21 MeV. Strong stripping angular distributions were observed for 10 states – 6 dominated by $l = 2$, and 4 by $l = 0$. These 10 states agree reasonably well in position and strength with the 10 lowest shell-model states predicted to have appreciable amounts of the configuration [$^{19}$F(g.s.) $\otimes 1d_{5/2}$ or $2s_{1/2}$ neutron)].

## I. INTRODUCTION

The spectroscopy of $^{20}$F is typical of non-self-conjugate odd-odd nuclei; the knowledge about it is extremely scant in view of the effort that has been expended. The most notable early work on its structure was that of El Bedewi[1] in 1956. Using an 8.9-MeV deuteron beam and one of the first heavy-particle spectrographs, he was able to obtain excitation energies and angular distributions for a great many of the states in $^{20}$F. His analysis of the angular distributions was limited by the use of the plane-wave Born approximation (PWBA). However, as we shall see below, his results for the few strong states were qualitatively correct.

Accurate excitation energies have been mea-

sured[2] up to $E_x = 6.043$ MeV by use of the reactions $^{18}$O$(^3$He, $p)^{20}$F and $^{19}$F$(d, p)^{20}$F at low bombarding energies. Information on the $\gamma$ decay of levels of $^{20}$F has been obtained in studies of the reactions $^{18}$O$(^3$He, $p\gamma)^{20}$F,[3-7] $^{19}$F$(d, p\gamma)^{20}$F,[3, 8] $^{19}$F$(n, \gamma)^{20}$F,[9-12] and $^{18}$O$(t, n\gamma)^{20}$F.[13] Further studies include measurements of lifetimes[13-16] of excited $^{20}$F levels, angular-distribution measurements of the reaction $^{19}$F$(d, p)^{20}$F obtained with a polarized deuteron beam,[17] and a study of the reaction $^{22}$Ne$(p, ^3$He)-$^{20}$F.[18] Studies of the reactions $^{18}$O$(^3$He, $p)^{20}$F and $^{22}$Ne$(d, \alpha)^{20}$F have also been reported recently.[19] The experimental results concerning $^{20}$F are excellently summarized in the review by Ajzenberg-Selove.[20]

Directional-correlation measurements[7] in the re-

# A SEARCH FOR QUARKS AT THE CERN INTERSECTING STORAGE RINGS

M. BOTT-BODENHAUSEN, D. O. CALDWELL*, C. W. FABJAN,
C. R. GRUHN**, L. S. PEAK***, L. S. ROCHESTER,
F. SAULI, U. STIERLIN, R. TIRLER, B. WINSTEIN and D. ZAHNISER

*CERN, Geneva, Switzerland*
*and Max-Planck-Institut für Physik und Astrophysik, Munich, Germany*

No quark candidates have been seen among $0.6 \times 10^9$ charged particles at the ISR. The corresponding cross-section limit for charge $\frac{1}{3}$ ($\frac{2}{3}$) is $\lesssim 3(6) \times 10^{-34}$ cm$^2$ for quark masses up to 22(13) GeV, assuming $\langle P_T \rangle = 0.4$ GeV/c.

The Intersecting Storage Rings provide, for the first time, the possibility of producing in a controlled way pairs of heavy objects of masses up to ~25 GeV each. Thus the range of the search for heavy, stable, "fundamental" particles has been considerably extended beyond the ~5 GeV Serpukhov limit [1]. We report in this letter first results[+] from a search for quarks now in progress at the ISR. We give here flux limits on charge $\frac{1}{3}$ and charge $\frac{2}{3}$ quarks relative to the flux of normal charged particles, and we derive cross-section limits on the basis of a simple production model.

The detector layout is shown in fig. 1. Six scintillation counter telescopes, interlaced with proportional chambers, sample laboratory production angles between 10 mrad and 75°. These telescopes accumulate data simultaneously and independently. Also shown are some of the counters used to monitor the luminosity and background conditions of the beams.

Each telescope consists of nine plastic scintillation counters, one plastic Čerenkov counter, and two or more anticounters (not shown in the figure). Six multi-

wire proportional chamber planes cover the solid angle of each telescope.

The scintillation counters provide nine independent samples of energy loss for each event. They are 2 cm thick and are designed to give between 20 and 50 photoelectrons for a relativistic charge $\frac{1}{3}$ quark. As a result, our pulse-height spectra for ordinary particles are dominated by fluctuations in energy loss rather than by photoelectron statistics.

Care must be taken to avoid simulation of the low pulse heights expected from a fractionally charged quark. For instance, the nine counters of each telescope are aligned in such a way that no more than three scintillator edges line up from any direction. Also, the light guides are made of scintillator material, to avoid production of low pulse heights from Čerenkov radiation in conventional plexiglas light guides.

The Čerenkov counter for each telescope is made of 5 cm thick Pilot 425 plastic. Its pulse height has a velocity dependence different from that of the scintillators, and this it gives independent information in the search for anomalous charge values.

The anticounters detect any particles which could generate a signal directly in the telescope photomultipliers (56 DVP's). In addition, they tag any particles traversing the telescope light guides.

Multiwire proportional chambers [3] with a total of 5000 wires spaced at 2 mm, cover the solid angle subtended by the telescopes. The chambers are run with a 300 nsec strobe width for maximum quark detection efficiency. For relativistic particles, their efficiency is greater than 99.98%, as measured at the ISR. The chambers provide a means of track recognition and background suppression.

---

693

# Some Comments on the Cross Section of $^{37}$Cl for Solar Neutrino Absorption*

W. A. Lanford and B. H. Wildenthal

*Cyclotron Laboratory and Physics Department, Michigan State University, East Lansing, Michigan 48823*

Nuclear wave functions from recent shell-model calculations are used to evaluate the
log($ft$) values relevant to the neutrino absorption cross section of $^{37}$Cl.

In order to understand better the causes and/or consequences of the unexpectedly low yield of the solar neutrino experiment,[1] we have re-examined some of the assumptions which underlie the calculation of the neutrino absorption cross section of $^{37}$Cl. As has been pointed out,[2,3] there is very little uncertainty in the calculated absorption cross section for low-energy neutrinos ($E_\nu < 2.22$ MeV) in the reaction $\nu + ^{37}$Cl $\rightarrow ^{37}$Ar $+e^-$ since this calculation depends only upon the measured electron capture rate of $^{37}$Ar and other known quantities. However, there are unmeasured quantities which enter into the calculation of absorption cross sections for neutrinos with energies greater than 2.22 MeV.

These uncertainties result from the lack of experimental $\beta$-decay log($ft$) values for some of the transitions which connect the $^{37}$Cl ground state with excited states of $^{37}$Ar. Under the standard assumption that isospin is a good quantum number, the measurement of the delayed proton spectrum from the $\beta$ decay of $^{37}$Ca provides log($ft$) values for transitions to the excited states of $^{37}$Ar above 3 MeV[4] relative to the superallowed transition to the $J=\frac{3}{2}$, $T=\frac{3}{2}$ state at 4.993 MeV in $^{37}$Ar. (This latter state is the isobaric analog of the $^{37}$Cl ground state.) Transitions to excited states below 3 MeV have not been observed and the absolute rate for the 4.993-MeV isobaric analog state has not been measured. Hence, estimates for their contributions to the neutrino capture cross section must be based on nuclear structure calculations.

When the solar neutrino experiment was first proposed, Bahcall made simple shell-model estimates of these log($ft$) values based on the assumption that the relevant low-lying states of $^{37}$Ar and $^{37}$Cl could be described by couplings of three nucleon holes in the $0d_{3/2}$ shell-model orbit.[2] In this note we report values for these transitions based on the most complete nuclear wave functions presently available. These wave functions span the full $0d_{5/2}$-$1s_{1/2}$-$0d_{3/2}$ space. Single-nucleon transfer and $E2$ and $M1$ strengths calculated with these wave functions agree well with experimen-

tal results from the $A = 35$–$38$ region.[5] In particular, the wave functions yield predictions for stripping and pickup to $^{37}$Ar that are consistent with recent experimental results.[6,7] These same experimental results point up the inadequacy of Bachcall's simple model for the lowest $\frac{1}{2}^+$ and $\frac{5}{2}^+$ states. The transitions which are in question proceed to the levels in $^{37}$Ar at 1409 keV ($J^\pi = \frac{1}{2}^+$), at 2797 keV ($J^\pi = \frac{5}{2}^+$), and at 4993 keV ($J^\pi = \frac{3}{2}$, $T = \frac{3}{2}$). We have calculated the log($ft$) values for the corresponding shell-model states with both the "11.0h + ASPE" and "12.5p + $^{17}$O" wave functions of Ref. 5. The results are substantially the same. We discuss the results from "11.0h + ASPE" because there is some indication that this set gives a slightly better accounting for $A = 37$ and 38 data than does "12.5p + $^{17}$O." The predicted log($ft$) values for the $^{37}$Ar transitions are shown in Table I and Fig. 1. These numbers were obtained as part of a general study of $\beta$ decay in this region of the nuclear chart.[8] We have calculated all the $\beta$ decays for which experimental data exist in the mass ranges $A = 17$–$23$ and $34$–$39$ and the overall percentage rms deviation between calculated and experimental log($ft$) values in these nuclei was 5%.

We show in Fig. 1 the calculated and experimental energies and log($ft$) values for the states of $^{37}$Ar ($^{37}$K). By examining this figure, one sees

TABLE I. The calculated log($ft$) values for transitions which connect the ground state of $^{37}$Cl with excited states in $^{37}$Ar. These log($ft$) values are needed to predict the solar neutrino absorption cross section.

| | | | log($ft$) | |
| $J_f$ | $T_f$ | $E_x$ (keV) | Bahcall | Present calculation |
|---|---|---|---|---|
| 3/2 | 1/2 | 0 | (5.06)[a] | 5.14 |
| 1/2 | 1/2 | 1409 | 4.48 | 5.44 |
| 5/2 | 1/2 | 2797 | 4.34 | 4.36 |
| 3/2 | 3/2 | 4993 | 3.28 | 3.30 |

[a]This is an experimental number, based on the electron capture of $^{37}$Ar.

148

## Collective Effects Shown by the (p, t) Reaction on the Closed-Shell Nucleus, $^{141}$Pr

R. W. Goles, R. A. Warner, and Wm. C. McHarris*

*Department of Chemistry† and Cyclotron Laboratory,‡ Department of Physics, Michigan State University, East Lansing, Michigan 48823*

and

W. H. Kelly

*Cyclotron Laboratory,‡ Department of Physics, Michigan State University, East Lansing, Michigan 48823*

(Received 18 February 1972)

The reaction $^{141}$Pr$(p, t)^{139}$Pr at 40 MeV strongly populates collective states in the residual nucleus. The shapes of the angular distributions, taken at 5° intervals between 15 and 65°, show the inadequacies even of finite-range, two-nucleon-pickup distorted-wave Born-approximation calculations and the need for inclusion of higher-order effects.

The (p, t) reaction on $^{141}$Pr has been studied as part of a general investigation of the systematics of the (p, t) reaction on spherical and deformed rare-earth nuclei. The residual nucleus of this reaction, $^{139}$Pr, has been extensively studied through the $\epsilon/\beta^+$ decays of the ground and meta-stable states of $^{139}$Nd.[1] Because of the large number of very dissimilar states established in this decay scheme, 23 below 2.2 MeV, it was thought that here would be an excellent place to begin this general investigation.

In the present work, ≈800-μg/cm² $^{141}$Pr targets prepared by vacuum evaporation on 25-μg/cm² carbon backings were bombarded with 500-nA beams of 40-MeV protons from the Michigan State University sector-focused cyclotron. A $dE/dX$, $E$ counter telescope consisting of two cooled Si surface-barrier detectors was used to identify and measure the energies of the outgoing scattered particles. Triton spectra were taken between 15 and 65° at 5° intervals. Figure 1 contains triton spectra taken at the laboratory scattering angles of 25 and 35°. The over-all experimental resolution was 50 keV full width at half maximum. The excitation energies corresponding to the various triton peaks were determined internally by making a correspondence between some of the more obvious triton groups and the previously determined states in $^{139}$Pr. In addition, an independent energy measurement of some of the more intense triton groups was conducted using a broad-range magnetic spectrometer, utilizing a 3-cm Si position-sensitive detector.

The experimental angular distributions, together with distorted-wave Born-approximation (DWBA) predictions, are displayed in Fig. 2. The distorted-wave predictions for various $l$ transfers were cal-

culated using a zero-range, cluster-transfer approach[2] as well as a more rigorous finite-range, two-nucleon-pickup formalism.[3] These are denoted by broken and continuous curves, respectively. Optical-model and bound-state parameters used in generating these theoretical curves appear in Table I.

The angular distribution corresponding to the $\frac{5}{2}^+ - \frac{5}{2}^+$ ground-state transition corresponds to an ap-
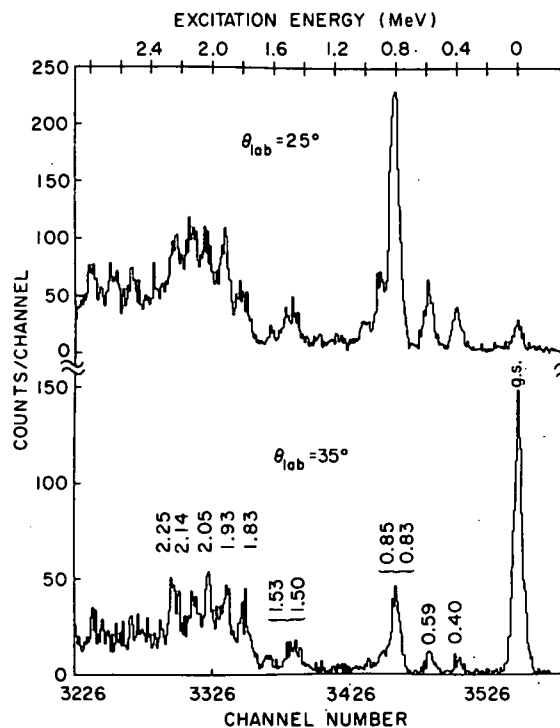


FIG. 1. Two spectra ($\theta_{lab} = 25$ and 35°) of tritons from the $^{141}$Pr$(p,t)$ reaction at 40 MeV.

# DATA ACQUISITION FROM SIMULTANEOUS EXPERIMENTS USING THE MSU SIGMA-7 COMPUTER*

## WM. C. McHARRIS, R. F. AU, D. L. BAYER, W. BENENSON, R. A. DeFOREST, W. H. KELLY, AND W. E. MERRITT

MICHIGAN STATE UNIVERSITY
EAST LANSING, MICHIGAN 48823

The large size of the nuclear spectroscopy group at Michigan State University and the relative ease and efficiency with which experiments can be performed using the MSU Sector-Focused Cyclotron make it imperative that simultaneous data acquisition and analysis be possible. The Sigma-7 computer at the MSU Cyclotron Laboratory forms the basis of a flexible real-time, time-sharing system that meets the requirements for performing simultaneous spectroscopic experiments or spectroscopic experiments simultaneously with nuclear scattering experiments, all the while allowing data analyses to be performed.

The computer consists of $32K$ of 32-bit core memory plus a 1.5-megabyte (8 bits = 1 byte) RAD (rapid access disk) for file storage and a 3.0-megabyte RAD for memory swapping during computation. [During this fall a 5.3-megabyte RAD (transfer rate = 3 megabytes/sec) will be added for memory swapping and both current RAD's (transfer rate = 0.19 megabytes/sec) will be used for file storage.] It has standard peripherals such as teletypes (with and without paper tape), card reader, card punch, 600 lines/sec line printer, two 9-track magnetic tape units, and a CalComp plotter.

323

150

# A NaI(T1) SPLIT ANNULUS FOR COINCIDENCE, ANTICOINCI-
# DENCE, TRIPLE COINCIDENCE, AND PAIR SPECTROMETRY—

W. H. KELLY —CYCLOTRON LABORATORY,* DEPARTMENT OF PHYSICS AND
Wm. C. McHARRIS —DEPARTMENT OF CHEMISTRY[†] AND CYCLOTRON
LABORATORY,* DEPARTMENT OF PHYSICS, MICHIGAN STATE UNIVERSITY
EAST LANSING, MICHIGAN 48823

During the last three years we have been using an 8 x8-in. NaI
(T1) split annulus more or less routinely as a counterpart to Ge(Li)
detectors in various coincidence and anticoincidence configurations.[1]
Its most common use has been for Compton suppression (external,
collimited source) and simple anticoincidence experiments (internal
source), most often with the insertion of an additional 3 x3-in. NaI
(T1) detector at the end of its tunnel opposite the Ge(Li) detector in
order to reduce Compton edges further. In fact, we have found it
advisable to perform such experiments at the very outset of study of
a new decay scheme so as to pinpoint immediately any delayed transi-
tions or primarily $\beta$-fed ground-state transitions. The split feature of
the annulus has made it very useful for other, more exotic experiments
as well. Among these have been triple coincidence experiments in-
volving short-lived nuclides or weak transitions, made possible only
because of the high efficiency of the annulus. It has also been used
as part of an efficient pair spectrometer for obtaining $\beta^+$ feedings and
/or double-escape spectra, and it has been used to enhance the back-
ground reduction of a "Compton" or "duode" spectrometer.[2] As
examples of its use in coincidence and triple coincidence experiments
are straightforward and already appear in the literature;[1,3] here we

1435

# Collective and Higher-Order Effects Shown by the $(p, t)$ Reaction on the Deformed Nucleus $^{159}$Tb

R. W. Goles, R. A. Warner, and Wm. C. McHarris*

*Department of Chemistry† and Cyclotron Laboratory,‡ Department of Physics, Michigan State University, East Lansing, Michigan 48823*

and

W. H. Kelly

*Cyclotron Laboratory,‡ Department of Physics, Michigan State University, East Lansing, Michigan 48823*

(Received 26 May 1972)

The reaction $^{159}$Tb$(p,t)^{157}$Tb at 30 MeV strongly populates collective states in the residual nucleus. Angular distributions of $\beta$ and $\gamma$ vibrational and ground-state rotational band members are presented and compared with distorted-wave Born-approximation predictions. We also include evidence supporting the importance of indirect multiple-step processes accompanying the $(p,t)$ reaction. The $(p,t)$ reaction is shown to be a powerful spectroscopic tool for populating higher-lying rotational band members in odd-mass deformed nuclei.

The $(p,t)$ reaction on $^{159}$Tb continues a general study of the characteristics of the $(p,t)$ reaction on odd-mass rare-earth elements. From a previously completed investigation[1] of the $(p,t)$ reaction on the closed-shell nucleus $^{141}$Pr, it was found that this reaction proceeds predominantly through a direct mechanism at the bombarding energies used in this study, and that large cross sections exist for the population of collective vibrational states within the residual nucleus $^{139}$Pr. However, unlike the previous study, the present investigation involves permanently deformed target and residual nuclei. These provide a very suitable system for studying and further testing the collective characteristics previously associated with the $(p,t)$ reaction. The $(p,t)$ reaction is shown to be a powerful spectroscopic tool for populating higher-lying rotational band members in odd-mass deformed nuclei.

In this study an $\approx 300$-$\mu$g/cm$^2$ metallic target of $^{159}$Tb was bombarded with 30-MeV protons accelerated by the Michigan State University sector-focused cyclotron. The scattered tritons were analyzed with an Enge split-pole magnetic spectrometer and collected on photographic plates. Spectra were taken between 10° and 75° at 5° intervals in the lab system with an overall energy resolution of 15–20 keV, although higher-resolution spectra (10 keV full width at half-maximum) have also been obtained at some angles.

From previous radioactivity studies,[2,3] rotational bands built upon the ground state and a $\beta$ vibrational excitation of the ground state have been identified in the $^{157}$Tb nucleus. In addition, the presence of a $K = \frac{1}{2}$ band based at 598 keV of

excitation was also indicated. There are two possibilities for the origin of such a $K = \frac{1}{2}$ band in this nucleus. It can be explained as a rotational band superimposed either on the $\frac{1}{2}^+[411]$ single proton state expected in this region, or on a $\gamma$ vibrational state based on the $\frac{3}{2}^+[411]$ ground state. The vibrational origin of these states is strongly suggested both from systematics and from the very small decoupling parameter associated with this band. The empirical value of this decoupling parameter is $\approx \frac{1}{20}$ of the calculated value[2] for a $\frac{1}{2}^+[411]$ band based on a nuclear deformation of $\eta = 5$, and it is of opposite sign. However, experimentally determined $K$-conversion coefficients imply significant $M1$ admixtures in transitions de-exciting this band to the ground band; these should be formally forbidden for states having a vibrational origin, although band mixing could easily account for this phenomenon.

The $^{159}$Tb$(p,t)$ triton spectrum taken at the lab scattering angle of 20° appears in Fig. 1. The most striking feature of this spectrum is the strong population of the ground-state rotational band, with members certainly up to $\frac{13}{2}^+$ and possibly as high as $\frac{17}{2}^+$ being excited. At 598 keV one finds three states that, within experimental uncertainty, correspond to the first three members of the previously discussed $K^\pi = \frac{1}{2}^+$ rotational band. In addition, if one generates the $\frac{7}{2}^+$ and $\frac{9}{2}^+$ members of this band by parametrizing the simple rotational energy relationship, one finds two additional states populated by this reaction which appear to be the next two members of this ($\gamma$ vibrational) band. In light of the established tendency of the $(p,t)$ reaction to populate collec-

# Energy Dependence of Proton Inelastic Scattering from $^{40}$Ca[†]

C. R. Gruhn,[*] T. Y. T. Kuo,[‡] C. J. Maggiore,[§] H. McManus, F. Petrovich,[¶] and B. M. Preedom[||]

*Department of Physics and Cyclotron Laboratory, Michigan State University, East Lansing, Michigan 48823*

(Received 30 December 1971)

Inelastic proton scattering from $^{40}$Ca has been measured at beam energies of 24.93, 30.04, 34.78, 34.78, and 39.83 MeV. Angular distributions from 13 to 97° for about 40 inelastic states were obtained. Analyses with both microscopic and macroscopic theories are presented.

## I. INTRODUCTION

The double magic nuclei, such as $^{40}$Ca, have been studied in great detail both experimentally and theoretically. The degree of deviation from a simple double-closed-shell structure is of great interest. Recent advances in the theories of nuclear shell models [random-phase approximation (RPA) and deformed], the effective nucleon-nucleon force, and the distorted-wave treatment of direct reaction enable one to formulate a microscopic description of the inelastic scattering of protons by nuclei.[1-6] The $^{40}$Ca nucleus was chosen as a target to test the $(p, p')$ reaction as a probe of nuclear structure because of the following points: First, it is a target which allows the $(p, p')$ reaction to examine all the components of the proton-nucleus force. Second, it is a target in which the eigenvectors describing the excited states are relatively well established both experimentally and theoretically. Third, it is a target for which good optical-model parameters exist.

The structure of $^{40}$Ca has also been investigated in other experiments such as $(\alpha, \alpha')$,[7,8] $(e, e')$,[9,10] $(^3He, d)$,[11] $(d, n)$,[12] and $(p, p'\gamma)$.[13] The $(\alpha, \alpha')$ reaction is a predominantly surface-dominated reaction and it leads to diffraction scattering. It measures $L$ transfer for the excited normal-parity states, and the isoscalar component of the projectile-nucleon force. The $(e, e')$ reaction gives reduced electromagnetic transition probabilities and multipolarities. The $(^3He, d)$ and $(d, n)$ proton stripping reactions allow one to study individual components of the vectors of the excited states. The $(p, p'\gamma)$ reactions have been used primarily to determine the spins and parities of the excited states; whereas, the $(p, p')$ reaction is useful in probing various components of the effective interaction and testing microscopic wave function.

By studying the energy dependence of the reaction, in many cases, one is able to remove ambiguities due to reaction mechanism problems. The present experiment studies proton inelastic scattering from $^{40}$Ca at bombarding energies of 24.93,

30.04, 34.78, and 39.83 MeV. Spectra were taken simultaneously by two surface-barrier Ge(Li) detectors with an over-all resolution of 30 keV [full width at half maximum (FWHM)]. Angular distributions for inelastic scattering to approximately 50 excited states were obtained over the angular range from 13 to 97° (lab). The data were analyzed using both a collective model to extract $L$ transfers and nuclear deformations and a microscopic model employing a realistic force, RPA wave functions, and approximate exchange.

## II. EXPERIMENTAL APPARATUS AND PROCEDURES

The data were obtained using protons from the Michigan State University sector-focused cyclotron.[14-16] The beam was energy-analyzed using two 45° bending magnets with image and object slits set to pass beam with fractional energy spread of $\pm 1.25 \times 10^{-4}$. Detailed discussions of the optical properties of the beam and of the energy-analysis system are given elsewhere.[17-19] The absolute energies of the proton beams were obtained from nuclear-magnetic-resonance calibrations of the magnets. The uncertainty in this absolute scale was $\pm 0.1\%$.[17] The absolute beam energies for this experiment were $24.93 \pm 0.03$, $30.04 \pm 0.03$, $34.78 \pm 0.04$, and $39.83 \pm 0.04$ MeV.

The beam on the target was monitored using both a Faraday cup and a Ge(Li) proton detector placed at 45° with respect to the beam. The scattering chamber[20] used in this experiment consisted of a target chamber which was viewed through ports in a sliding seal. Two ports separated by 14.7° were coupled such that a pair of Ge(Li) proton detectors could be used. The solid angles of the two detectors were $1.38 \pm 0.04 \times 10^{-4}$ and $0.786 \pm 0.024 \times 10^{-4}$ sr for detectors 1 and 2, respectively. The angular range of detection was from 12 to 97° in 5° steps. Data were taken twice at 27 and 72° by each detector for the relative normalization. Details concerning these detectors are given in a previous publication.[21] The target was a rolled, self-supported 2-mg/cm$^2$

# Proton Inelastic Scattering from $^{48}$Ca[†]

C. R. Gruhn,[*] T. Y. T. Kuo,[‡] C. J. Maggiore,[§] and B. M. Preedom[¶]

*Department of Physics and Cyclotron Laboratory, Michigan State University, East Lansing, Michigan 48823*

(Received 29 December 1971)

Inelastic proton scattering from $^{48}$Ca has been measured at beam energies 25, 30, 35, and 40 MeV. Angular distributions from 13 to 97° for 22 inelastic states were obtained. Analyses with the collective distorted-wave Born approximation are presented. A direct comparison of the excitation of the $^{48}$Ca 3.830-MeV $2^+$ and 6.342-MeV $4^+$ states is made with the low-lying excited $2^+$ and $4^+$ states of $^{50}$Ti and $^{52}$Co.

## I. INTRODUCTION

Doubly magic nuclei, in general, have been studied in great detail both experimentally and theoretically. Perhaps the exception to this statement is $^{48}$Ca. From the experimental standpoint only a few of the low-lying states of $^{48}$Ca have well established spin and parity. From the theoretical point of view $^{48}$Ca is of interest because of the purity of its double-closed-shell structure. Jaffrin and Ripka[1] have tested the occupation numbers and find that the $1f_{7/2}$ shell and the inner neutron shells are at least 97% closed. It is because of the strong theoretical motivation and of our interest in developing the $(p, p')$ reaction as a probe in microscopic structure that we undertook the present $(p, p')$ experiment on $^{48}$Ca.

The level structure of $^{48}$Ca has also been investigated in other experiments such as $(\alpha, \alpha')$,[2,3] $(e, e')$,[4] $(t, p)$,[5] $(p, p')$,[6] and $(p, p'\gamma)$.[7] The $(\alpha, \alpha')$ and $(e, e')$ experiments probably should be repeated with the now available better resolutions. In principle, then, at least some of the ambiguities in the present assignments of the low-lying levels could be removed.

## II. DESCRIPTION OF EXPERIMENT

The experiment was carried out using the proton beam from the Michigan State University sector-focused cyclotron. Figure 1 shows the cyclotron and beam-handling system. The two horizontal bending magnets M3 and M4 are used to momentum analyze the beam and M5 deflects the beam into the goniometer.[8] More complete descriptions of the properties of the energy analysis system have been published elsewhere.[9,10] During this experiment the slits S1 and S3 were set at 15 mils for beam energy resolution of ±5 keV. S2 was set at 100 mils to yield a beam divergence of ±2 mrad. The Faraday cup is located in a shielded beam dump 12 ft beyond the goniometer.

The scattered protons were detected with two surface-barrier Ge(Li) detectors designed specifically for this experiment.[11] The two detectors were separated by 14.7° and were located outside the 16-in. scattering chamber. The detectors coupled to the scattering chamber vacuum via a sliding seal. A monitor counter at a fixed angle viewed the scattered beam through a 1-mil Kapton window.

The target was a commercially prepared self-supporting foil of $^{48}$Ca approximately 1.08 mg/cm$^2$ thick. The composition of the target as determined by the Isotopes Division of Oak Ridge National Laboratory is listed in Table I. The target was stored in vacuum when not in use and transferred to the scattering chamber in vacuum via a target-transfer system.[8]

Inelastic proton spectra were taken every 5° from 13 to 97°. The over-all energy resolution was 25–30 keV full width at half maximum. Each counter subtended an angle of about 0.5° in the scattering plane. The scattering angle was checked by comparing the positions of the H and $^{12}$C contaminant peaks relative to the $^{48}$Ca ground state and found to be accurate to within 0.1°. The energy of the incident protons determined by mea-

# Decay of $^{170}$Lu to Levels in $^{170}$Yb[†]

David C. Camp*

*Lawrence Livermore Laboratory, University of California, Livermore, California 94550*

and

Fred M. Bernthal

*Departments of Chemistry and Physics, Michigan State University, East Lansing, Michigan 48823*

(Received 24 November 1971)

The locations of 70 energy levels in $^{170}$Yb were deduced from Compton-suppressed $\gamma$-ray singles, three-crystal $\gamma$-ray pair, conversion-electron, and Ge(Li)-Ge(Li) $\gamma$-$\gamma$ coincidence measurements on the electron-capture-$\beta^+$ decay of $^{170}$Lu. Both chemically separated and isotopically separated sources of $^{170}$Lu were used in collecting the data. A total of 550 $\gamma$-ray transitions have been observed in the $^{170}$Lu decay spectrum, 220 of which are definitely assigned to the $^{170}$Yb level scheme from 112 coincidence spectra. These definitive transitions account for 93% of the total observed $\gamma$-ray intensity. An additional 118 $\gamma$-ray transitions were placed on the basis of excited-state energy differences. Eight $E0$ transitions were observed in the conversion-electron data. Each of four excited $0^+$ states identified has less than 1% $\beta$ decay feeding from the $0^+$ parent. Spin and parity assignments are proposed for 46 levels in addition to the ground-state rotational band members. The $^{170}$Yb level structure is compared with available theoretical calculations, and a preliminary interpretation of several features of the decay scheme is presented.

## I. INTRODUCTION

The most complicated radioactive decay yet studied is the electron-capture (EC)-$\beta^+$ decay of 2.15-day $^{170}$Lu to the levels of $^{170}$Yb. Early attempts to interpret the complex $\gamma$-ray spectrum from NaI(Tl) data were largely unsuccessful, and until recently, the best available data consisted primarily of conversion-electron spectra.[1-3] With the advent of germanium detectors, however, several groups[4-8] renewed their efforts at unraveling this very complex decay. Hansen and co-workers[9] established 0+ as the ground-state spin and parity of $^{170}$Lu. Paperiello et al.[10] carried out directional-correlation measurements on several of the more intense transition cascades in this decay and have definitely established the spins of 10 levels in $^{170}$Yb. Concurrent with the work reported here were the recent studies reported by Bonch-Osmolovskaya and co-workers[11, 12] who employed Ge(Li) detectors, electron-$\gamma$, $\gamma$-$\gamma$, and electron-electron coincidences, in an effort to define the decay scheme. They placed some 177 transitions of 280 seen in the decay, thus accounting for almost 87% of the total $\gamma$-ray intensity.

In this work we report the results of extensive $\gamma$-ray singles, $\gamma$-$\gamma$ coincidence, and conversion-electron measurements. Compton suppression and three-crystal pair-spectrometer techniques were used to accurately define the energies and intensities of the $^{170}$Lu $\gamma$-ray transitions. Measurements at lower energies (<1.2 MeV) were carried

out with isotopically separated sources. An on-line computer and multiparameter data acquisition system were used in conjunction with two Ge(Li) detectors and an isotopically separated $^{170}$Lu source to carry out a detailed study of the $\gamma$-$\gamma$ coincidence spectra. Conversion-electron studies were carried out using chemically separated lutetium sources and a Si(Li) detector. On the basis of these data, we have constructed a level scheme for $^{170}$Yb consisting of 70 excited states. Of 550 $\gamma$-ray transitions identified, over 200 have been placed on the basis of $\gamma$-$\gamma$ coincidence data and another 118 were placed on the basis of energy differences; these two groups of $\gamma$ rays account for 93 and 3% of the total $\gamma$-ray intensity, respectively. Significant differences exist between our decay scheme and that of Bonch-Osmolovskaya et al.,[12] and slight differences distinguish our decay scheme from the less complete level scheme of Mihelich.[13]

## II. EXPERIMENTAL

### A. Target and Source Preparation

Sources of $^{170}$Lu were prepared by the $^{169}$Tm-$(\alpha, 3n)^{170}$Lu reaction by irradiating 40-mg samples of $Tm_2O_3$ at the Lawrence Berkeley Laboratory 88-in. cyclotron with 40-MeV $\alpha$ particles. 3-h irradiations at about 20-$\mu$A beam current produced about 1 mCi of $^{170}$Lu activity for each experiment.

The lutetium activity was separated from other

# The $^{48}Ca(p,t)^{46}Ca$ Reaction at Ep=39 MeV[*]

G.M. Crawley and P.S. Miller
Michigan State University

and

G.J. Igo and J. Kulleck
University of California, Los Angeles

## 1. INTRODUCTION

There has been considerable interest in using a comparison of (p,t) and (t,p) reactions to the same final states, especially $0^+$ states, to compare wave functions for a series of nuclei.[1] Such a study in the calcium isotopes would benefit from a more thorough study of the $^{48}Ca(p,t)$ reaction. The complementary $^{44}Ca(t,p)$ reaction has been carried out in various laboratories[2,3] and strongly populates states of $J^\pi=0^+$ at excitation energies between 5 MeV and 7 MeV. The $^{48}Ca(p,t)$ has also been studied previously but at fairly low energies[4,5] or with poor resolution[6] so that the states of interest could not be resolved. In addition discrepancies between the (t,p) experiments serves as an additional motivation for the (p,t) experiment. The present paper is a preliminary report of this work.

## 2. EXPERIMENTAL

The experiment was carried out in two stages using the Michigan State University Cyclotron at a proton beam energy of 39 MeV. A high resolution study was carried out using the Enge split-pole spectrograph and the resolution was peaked using the focal plane speculator system.[7] A resolution of 11 keV FWHM was obtained where these data were recorded on photographic emulsions. The second stage was run with intermediate resolution ($\sim$50 keV) using a pair of single wire proportional counters in the focal plane of the spectrograph. Angular distributions were

---

# THE (p,t) REACTION ON $^{24}$Mg AND $^{26}$Mg[*]

J.A. Nolen, W. Benenson, Duane Larson
I.D. Proctor and B.H. Wildenthal
Cyclotron Laboratory, Physics Department
Michigan State University, East Lansing, Michigan   48823

## ABSTRACT

The $^{24}$Mg(p,t)$^{22}$Mg and $^{26}$Mg(p,t)$^{24}$Mg reactions have been studied at proton energies of 42.0 and 40.0 MeV respectively. Angular distributions were obtained for the ground and first excited states of $^{22}$Mg and for the ground and five lowest excited states in $^{24}$Mg. Measured reaction strengths are compared to predictions of the DWBA made with shell-model wave functions.

## 1. INTRODUCTION

Shell model calculations of nuclear structure[1,2] can now successfully account for many of the characteristics of the low-lying energy levels of sd-shell nuclei. Phenomena such as excitation energy spectra, single nucleon transfer strengths, electromagnetic decay rates and beta decay have been treated in some detail. In addition, several studies in the last few years have used shell model wave functions to analyze two-nucleon transfer between sd-shell nuclei.[3-7] These studies offer the possibility of examining the nuclear wave functions from a viewpoint quite different from those that are available in other kinds of observations.[8] Hence, if the experimental data are amenable to an unambiguous analysis with respect to the reaction process, conclusions from two-nucleon transfer experiments should be vital to extending our comprehension of nuclear structure in this region. In the present work we study $^{22}$Mg and $^{24}$Mg, nuclei for which wave functions successful in essentially all other areas of phenomena are available,[9] via the (p,t) reaction from $^{24}$Mg and $^{26}$Mg.

381

2.F

# EFFECT OF COMPLEX COUPLING
# IN INELASTIC CROSS SECTIONS,
# ASYMMETRIES AND SPIN FLIP IN THE DWA

R. H. HOWELL † and G. R. HAMMERSTEIN

*Cyclotron Laboratory, Physics Department, Michigan State University, East Lansing,
Michigan, 48823* ††

Abstract: The effects of adding an effective imaginary part to real inelastic microscopic form factors in DWA are investigated. Calculations are compared to data for the proton differential cross sections and asymmetries of the lowest-lying states of $^{120}$Sn, $^{58}$Ni, and $^{208}$Pb. Proton spin flip is calculated for $^{120}$Sn. Both collective imaginary and effective microscopic imaginary contributions were considered. The most substantial improvements were in fits to asymmetry data. Collective-model calculations indicate the effects of complex coupling are comparable to those of the deformed spin-orbit well.

## 1. Introduction

A number of authors have pointed out that when the collective model is applied to inelastic proton-nucleus scattering it is important to deform the imaginary and spin-orbit wells in addition to deforming the real well [1]. Satchler recently proposed a semi-phenomenological model for the imaginary form factor in microscopic (p, p') calculations [2]. Also, it is now possible to include a two-body spin-orbit term in microscopic calculations [3,4].

In view of this it is useful to study the effects of complex coupling on cross sections and asymmetries and to compare the results with those of similar calculations which include a spin-orbit term.

We performed calculations for the lowest-lying excited states in $^{58}$Ni, $^{120}$Sn, and $^{208}$Pb using in each case a microscopic real form factor and each of two models for the imaginary form factor. Spin-orbit contributions were calculated with the collective model.

The calculations were done in DWA for 30 MeV incident protons using the optical parameters of ref. [5]. Exchange effects were included using a zero-range pseudopotential [6]. Angular distribution and asymmetry data are from ref. [7], the spin-flip data from ref. [8].

651

# V. Ph.D. Thesis Titles (July 1971-June 1972)

## Department of Physics

Howell, Richard

Proton Spin-Flip Probability in Inelastic Scattering on $^{120}$Sn and $^{124}$Sn at 30 MeV

Laumer, Helmut

Proton Induced Reactions on $^{14}$N and $^{16}$O and the Creaction of Elements Lithium, Beryllium, and Boron

Todd, Richard

Gamma-Ray Spectroscopic Studies of Members of the A=141 Decay Chain

## Department of Chemistry

Black, Jerry

Nuclear Spectroscopic Studies of Members of the A=141 Decay Chain

Giesler, Gregg

Nuclear Spectroscopic Studies of Some Short-Lived and Neutron Deficient Ga and Zn Isotopes

Goles, Ronald

The (p,t) Reactions on Rare Earth Nuclei